STUDY OF MULTIMETALLIC GERMANIUM AND TIN COMPOUNDS IN THEIR LOW OXIDATION STATE

A THESIS

SUBMITTED TO PARTIAL FULFILMENT OF THE DEGREE OF

DOCTOR OF PHILOSOPHY IN CHEMISTRY

BY

PADMINI SAHOO

ID: 20163467

UNDER THE GUIDANCE OF

DR. MOUMITA MAJUMDAR

INDIAN INSTITUTE OF SCIENCE EDUCATION AND RESEARCH, PUNE

2023

Contents

CERTIFICATE

Certified that the work incorporated in the thesis entitled, "*Study of Multimetallic Germanium and Tin Compounds in their Low Oxidation States*" Submitted by **Ms. Padmini Sahoo** was carried out by the candidate, under my supervision. The work presented here or any part of it has not been included in any other thesis submitted previously for the award of any degree or diploma from any other University or Institution.
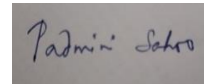
Supervisor

23.08.2023
DATE

Moumita Majumdar
Associate Professor
IISER Pune

DECLARATION

I hereby declare that; this written submission represents my ideas in my own words and where other's ideas have been included; I have adequately cited and referenced the original sources. I also declare that I have adhered to all principles of academic honesty and integrity and have not misrepresented or fabricated or falsified any idea/data/fact/source in my submission. I understand that violation of the above will be cause for disciplinary action by the institute. It can also evoke penal action from the sources which have thus not been appropriately cited or from whom proper permission has not been taken when needed.

<div align="right">

Padmini Sahoo

Padmini Sahoo
Registration Number: 20163467
IISER Pune

</div>

Date: 04/05/2023

ACKNOWLEDGEMENT

Dedicated to my Parents

Abbreviations

Chemical Abbreviation

ACN	Acetonitrile	CAAC	Cyclic Alkyl Amino Carbene
Ad	Adamantyl	FLP	Frustrated Lewis Pair
Ar	Aryl	Ph	Phenyl
C_6D_6	Dueterated benzene	TMSCl	Trimethylsilylchloride
$CDCl_3$	Deuterated chloroform	TMSOTf	Trimethylsilyl trifluoromethanesulphonate
Cp	Cyclopentadienyl		
DCM	Dichloromethane	NaH	Sodium hydride
Dipp	2,6-Diisopropylphenyl	THF	Tetrahydrofuran
DMSO	Dimethyl sulfoxide	*t*Bu	Tertiary butyl
EtOAc	Ethyl Acetate	*t*BuNC	Teriarybutyl Isocyanide
*i*Pr	Isopropyl	py	Pyridine
MeOH	Methanol	Trip	2,4,6-Triisopropylphenyl
Me	Methyl		

Mes	2, 4, 6 –trimethylbenzene
Mes*	2,4,6-tri-tertbutylphenyl
n-BuLi	*n*-butyllithium
NHC	*N*-Heterocyclic Carbene
NHSi	*N*-Heterocyclic Silylene
NHGe	*N*-Heterocyclic Germylene
OTf	Trifluromethanesulphonate
PMe_3	Trimethyl Phosphine
PhLi	Phenyllithium

Units, Standard terms and general notations

J	Coupling constant in NMR	Anal.	Analysis
Equiv.	Equivalents	Calcd.	Calculated
HRMS	High Resolution Mass Spectrometry	λ	Wavelength
NMR	Nuclear Magnetic Resonance	CCDC	Cambridge Crystallographic Data Centre
g	gram(s)	CIF	Crystallographic Information file
mmol	milimol	°C	Degree Centigrade
VT	Variable temperature	mg	Milligram
mL	Mili Litre	h	Hour
DFT	Density Functional Theory	Hz	Hertz
NMR	Nuclear Magnetic Resonance	min.	Minute
SC-XRD	Single Crystal X-Ray Diffraction	M.P.	Melting Point
		NBO	Natural Bond Order
Decomp	Decomposition	WBI	Wiberg Bond Indices
δ	Chemical shift		
%	Percentage	NPA	Natural Population Analysis
MHz	Mega Hertz		

Synopsis

Study of multimetallic Germanium and Tin compounds in their Low oxidation states

Carbenes have been explored in various applicatory fields such as organocatalysts, as components of FLPs (Frustrated Lewis Acid-Base Pair), in metallopharmaceuticals, homogeneous catalysis, activation of small molecules, organometallic materials and so on. Following the same trend heavier analogues of silicon, germanium and tin have been synthesized over the last few decades and have been utilized as FLPs, as ligands to transition metals, in catalysis and small molecule activation. Furthermore, the bistetrylenes have been explored to study the cooperative effect of two terylenes in the same molecular framework and they have been found to be very useful in small molecule activation, catalysis, and coordination with main group as well as transition metals. To further explore such cooperative properties, we have synthesized various multi metallic systems with different oxidation states.

The first chapter explores the synthesis and characterization of bis(chlorogermyliumylidene) in a 2N2P ligand system where it is found to be unstable at room temperature in the presence of base and hence rearranged products are identified and characterized. So, the ligand is converted to its saturated counterparts and further used in synthesis of new bis(chlorogermyliumylidene)s which were found to be stable at room temperature. On addition of bases like DMAP (4-dimethylaminopyridine) and PMe$_3$, the complexes coordinated with them and the reactions were studied using NMR techniques.
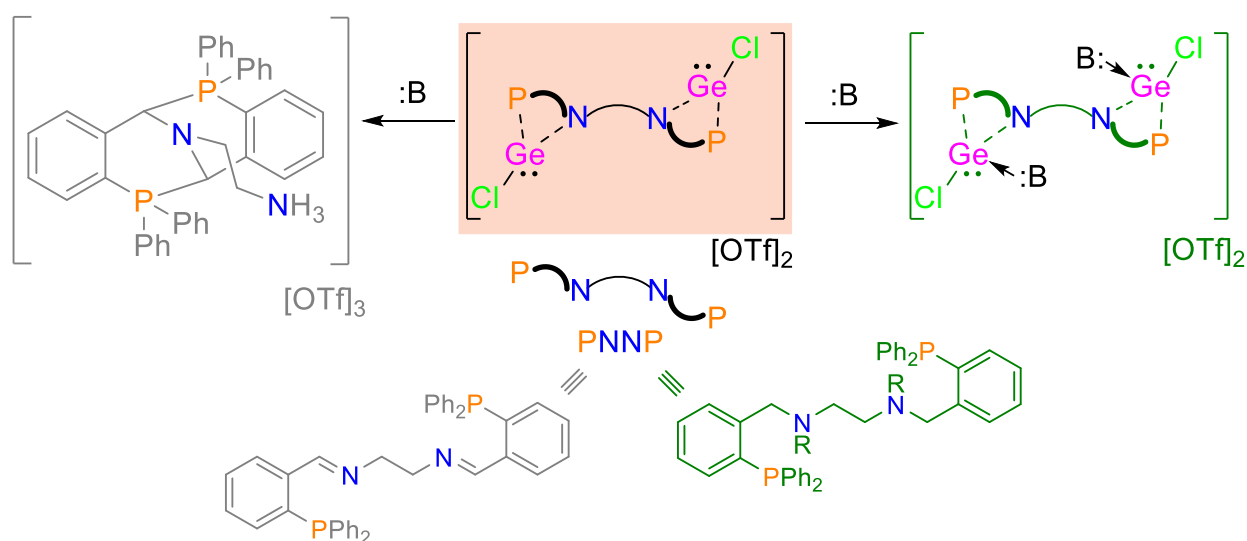
The second chapter explores the synthesis of Au(I)-Au(I) aurophilic complex. On reaction of the previous ligand system with Gold(I) chloride in one and two equivalents, monometallic and bimetallic complexes are synthesized respectively. The monometallic gold complex was reacted with GeCl$_2$.Dioxane in the anticipation of formation of Z-Ligand like system. However, the germanium center was found to undergo an addition reaction with the gold chloride bond rather than coordinating with the ligand. So, the monometallic gold complex was reacted with PPh$_2$Li followed by GeCl$_2$.Dioxane to form the targeted aurophilic complex.
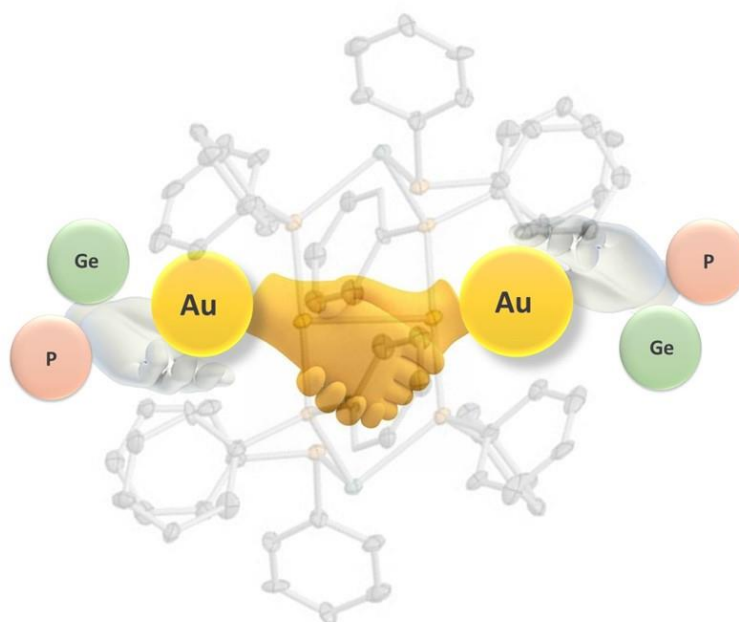
The third chapter explores the synthesis, characterization, and computational study of multimetallic tin complexes. On reaction of N-(2,6-diisopropylphenyl)imidazole with Bis[bis(trimethylsilylamino)] tin(II) as a base, a dimeric tin complex was formed. Further, Bis[bis(trimethylsilylamino)] tin(II) was reacted with bis(imidazolyl)methane to form a crown shaped tetrametallic tin complex. Both the complexes were characterized by SCXRD and NMR techniques. Computational study of the tetrametallic complex showed the presence of electron density at the center of the ring with the two of tin centers being stannides and the other two

centers being stannyliumylidenes.
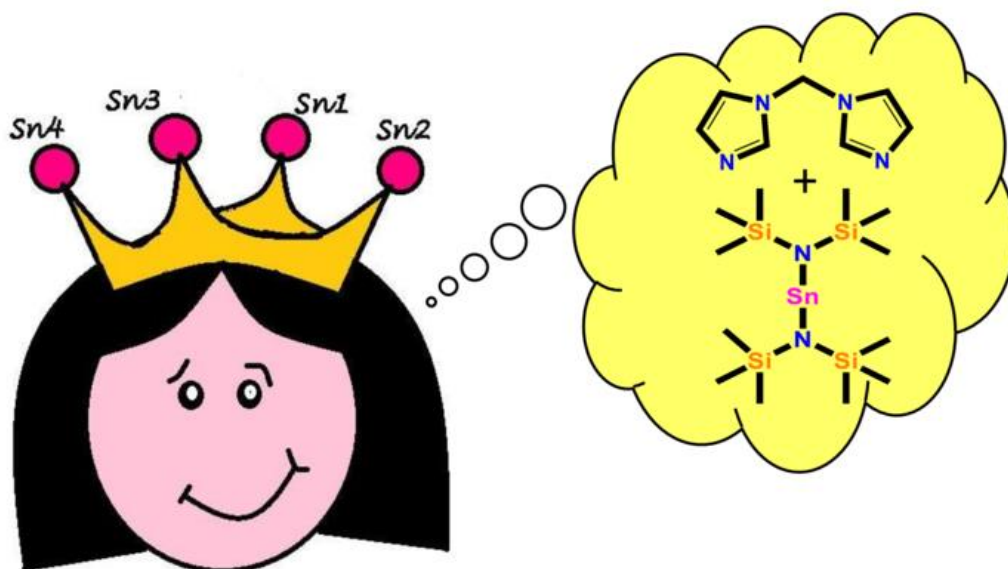
List of Publications

- Sahoo, P.; Chibde, P.; Banerjee, S.; Mali, B. P.; Vanka, K.; Gonnade, R.G.; Yilidz, C. B.; Majumdar, M.; A zwitterionic Tetrastanna(II) Cyclic Crown, *Eur. J. Inorg. Chem.*, **2023**. (Manuscript accepted)

- Sahoo P.; Majumdar, M.; Reductively disilylated N-heterocycles as versatile organosilicon reagents, *Dalton trans.* **2021**, *51*, 1281 (Perspective article).

- Maurya, D.; Karmakar, J.; Sahoo, P.; Raut, R.; Majumdar, M.; Versatile bridging modes of Acyclic N2X2 (X= O, S and P) Ligands towards [GeCl]+ and AuCl units, *Inorg. Chim. Acta*, **2020**, 119380.

- Raut, R. K.; Sahoo, P.; Chimnapure, D.; Majumdar,M.; Versatile coordinating abilities of acyclic N4 and N2P2 ligand frameworks in conjunction with $Sn[N(SiMe_3)_2]_2$, *Dalton Trans.* **2019**, *48*, 10953.

- Sahoo, P.; Raut, R.; Maurya, D.; Kumar, V.; Rani, P.; Gonnade, R. G.; Majumdar, M.; Stabilisation of bis(chlorogermyliumylidene)s within bifunctional PNNP ligand frameworks and their reactivity studies, *Dalton trans.* **2019**, *48*, 7344.

- Majumdar, M.; Raut, R. K.; Sahoo, P.; Kumar, V.; Bis(chlorogermyliumylidene) and its Significant Role in an Elusive Reductive Cyclization, *Chem. Commun.* **2018**, *54*, 10839.

- Raut, R. K.; Amin, S, A.; Sahoo, P.; Kumar, V.; Majumdar. M.; One-pot Synthesis of Heavier Group 14 N-Heterocyclic Carbene Using Organosilicon Reductant, *Inorganics*, **2018**, *6*, 69.

CHAPTER 1

Introduction

1.1. A Brief Introduction to Main group Chemistry

Last few decades have seen tremendous growth in the chemistry of low valent main group complexes. The heavier congeners of the main group elements show different properties as compared to their lighter counterparts where the latter already have a well-established chemistry of their own. And these difference in properties are the center of these evolutionary reports where the heavier congeners are compared with transition metals. These comparisons arise as the result of small energy difference between the frontier orbitals of these elements which makes them resemble transition metal complexes.[1] The various frontiers that have been in highlight in these recent years are 1) multiple bonded heavier congeners,[2] 2) low valent or subvalent derivative stabilization,[3] 3) elements in frustrated Lewis acid-base pair system[4] and 4) radical systems.[5]

1.2. Carbenes

The onset of low valent group 14 chemistry was marked with the discovery of stable bottleable singlet N-heterocyclic carbenes by Arduengo *et. al.* in 1991(Figure 1.1).[6] Although being neutral they have a divalent carbon with six valence electrons making them highly reactive due to their incomplete octet. But when stabilized with σ-electron withdrawing and π-electron donating adjacent nitrogen atoms the carbenic center is stable and can act as a nucleophilic center. The cyclic nature forces the singlet state of the carbon making it a sp^2 hybridized with the lone pair on the carbon center as HOMO and an empty p-orbital on the carbon center as LUMO.

Ad= Adamantyl
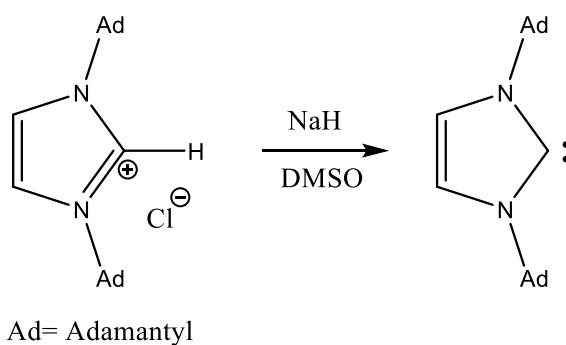
Figure 1.2.1. Synthesis of Imidazolylidene

However, by changing the aromaticity, the substituents, or the adjacent atom a lot of properties

of these molecules have been altered.[7] The steric bulk of the carbene can be decreased by changing the substituents on the flanking nitrogen atoms into methyl groups (1.2.A).[8] Non-aromatic cyclic carbenes are also reported by Arduengo *et.al* (1.2.B) .[9] The nitrogen atoms in the cycle can be replaced by other heteroatoms as well (1.2.C).[10] Bertrand *et.al.* introduced another kind of carbene called cyclic alkyl amino carbenes with a carbon center instead of nitrogen (1.2.D).[11] Another type of carbene reported are the one with the carbene centers situated other than central carbon and they are name as mesionic or 'abnormal' carbenes (1.2.E).[12] Finally, six-membered carbenes called N, N'-Diamidocarbenes have also been reported (1.2.F).[13] In 2017, Bertrand and co-workers synthesized another ambiphilic singlet carbene called bicyclic (alkyl)(amino)carbene BICAAC with high σ-donating and π-accepting properties.[14]

Imidazolylidene R=Ad, Me, Mes, IPr, tBu **1.2.A**	Imidazolinylidene **1.2.B**	X= S, O Thioazolylidene Oxaazolylidene **1.2.C**
Pyrrolinylidene **1.2.D**	Mesionic carbene **1.2.E**	N,N'-Diamidocarbene **1.2.F**

BiCAAC

1.2.G
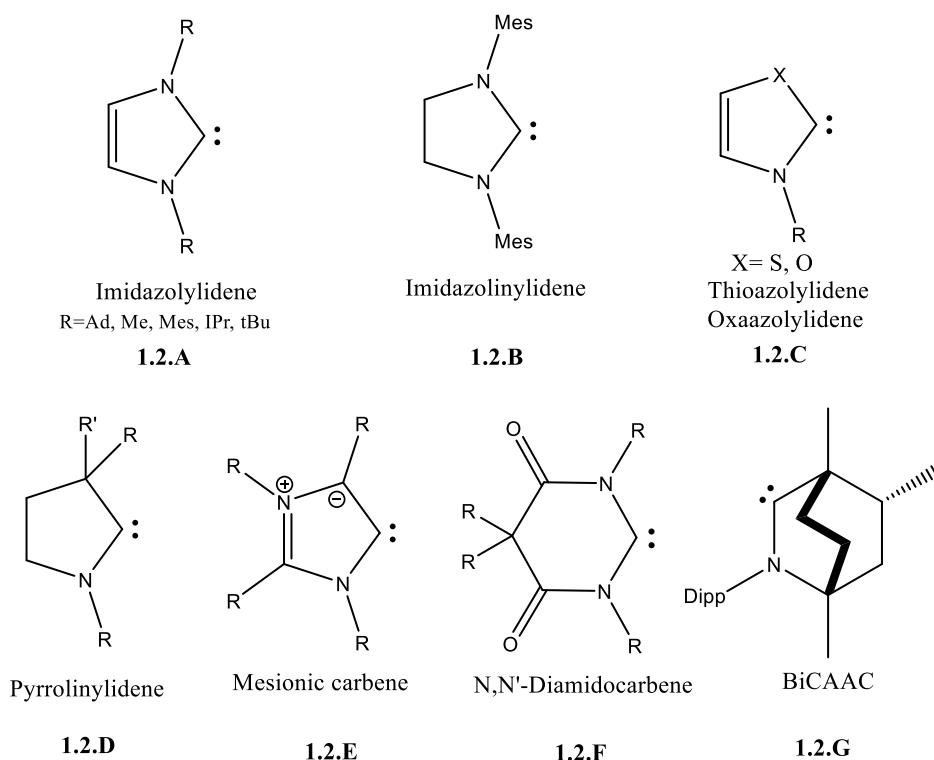
Figure 1.2.2. Types of carbenes

These carbenes have been applied in various fields broadly classified into coordination to transition metals, coordination to main group elements and as organocatalysts depending on the HOMO-LUMO gap they have to offer. The coordination complexes are further applied in the fields of metal-organic frameworks, metallopharmaceuticals, organometallic materials, surface coordinnations, homogeneous catalysis, activation of small molecules, as frustrated

Lewis acid base pairs, as reagents in organic synthesis and so on.[7]

The preceding applications encouraged the exploration of heavier congeners like tetrylenes and cationic terylenes. Terylenes like silylenes, germylenes, stannylenes and plumbylenes were synthesized and explored in next decade.

1.3. Germylenes and Stannylenes

Since the chemistry of carbene and silylenes have been well explored, the synthesis and application of the heavier congeners were expanded. The stabilization of tetrylenes is comparatively easier as the inert pair effect is more pronounced as we move down the group. However, their isolation at ambient conditions is slightly difficult due to their high electrophilic nature. So, they are stabilized kinetically by providing bulk around the tetrylene center.[15] The tunable properties of these tetrylenes make them an excellent candidate as ligands and in small molecule activation. Germylenes and Stannylenes are divalent species with the central atom in sp^2 hybridization with a lone pair and an empty p-orbital. They are larger in size which makes the separation between *sp* orbitals wider rendering them comparatively less reactive as compared to their lighter congeners.[16]

The very first acyclic germylene was reported by Lappert *et.al.* in 1974 which was syntheised by reacting $GeCl_2$.Dioxane and lithium hexametyldisilazane. The molecule remained a monomer in gas and solution phase but converts into the dimeric form in the solid state (1.3.A).[17] The cyclic germylene was first stabilized by Veith *et.al.* by stabilizing the the germylene thermodynamically(1.3.B).[18] Again Okazaki *et.al.* stabilized an acyclic germylene by increasing the bulk on the substituents (1.3.C).[19] The cyclic counterpart of Lappert's germylene was synthesized by Kira in 1999 (1.3.D).[20] Further N-hetrocyclic germylene was stabilized by Wagner *et.al.* in 1992. This germylene is thermodynamically stabilized by the two flanking nitrogen centers like the carbene center previously discussed (1.3.E).[21] In 2008, Roesky *et.al.* reported a chlorogermylene which is supported by an amidinate ligand where one of the nitrogen center coordinates to the germylene center and the other is covalently bonded to it(1.3.F).[22]

1.3.A   **1.3.B**   **1.3.C**

1.3.D   **1.3.E**   **1.3.F**
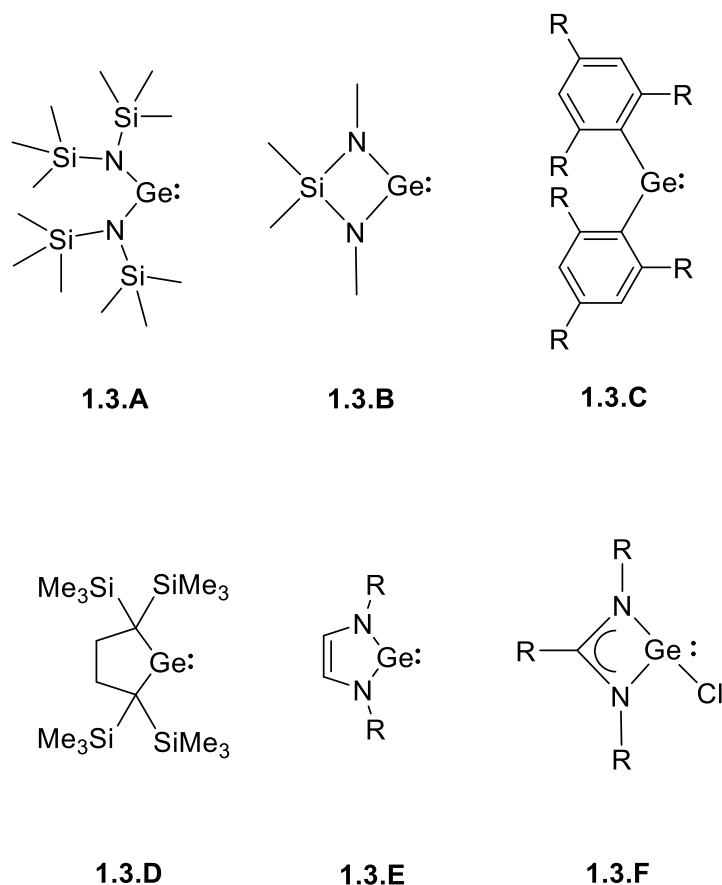
Figure 1.3.1. Selected examples of germylenes

Stannylene are divalent congeners of germylene are more stable than them. So, they exist in divalent halo salts in polymeric form or ion pair form. To stabilize the monomeric form various substituents have been used from time to time. These substituents are instrumental in determining the donation properties of the stannylene and hence determining their ability to coordinate or activate small molecules. The first acyclic stannylene was reported by Lappert *et.al.* in 1970, which was stable in solution phase (1.3.G).[23] The first cyclic stannylene was stabilized by Kira *et.al.* which was the stable dialkyl monomeric stannylene(1.3.H).[24] The stable monomeric acyclic diaryl stannylene were reported by Weidenbruch in 1994. However, they were found to undergo intramolecular cyclization in solution to afford a different stannylene(1.3.I).[25] Other stable acyclic monomeric diaryl substituted stannylene were reported later which were stable towards such intramolecular cyclization (1.3.J).[26]
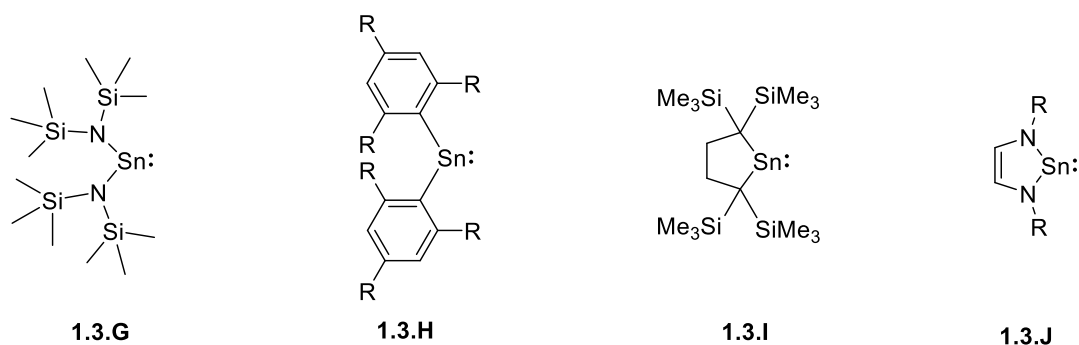
Figure 1.3.2 Selected examples of stannylenes

1.4. Germyliumylidenes and Stannyliumylidenes

Germyliumylidenes and stannyliumylidenes are species, also known as cationic germylenes or stannylenes, with the central atom sp[2] hybridized and a cationic charge on it. The central atom also possesses two empty orbitals and a covalent bond. These species are highly unstable due to their charged state and high electrophilic nature. So, they are usually stabilized kinetically using a lot steric bulk around the charged atom which protects the species from reacting otherwise. So, usually bulky donor groups are used to donate electrons into one or both the empty orbitals to stabilize them.

The very first report of a cationic germylene and stannylene species was reported by Jutzi *et al*. Both the species have a teryliumylidene center stabilized by a cyclopentadiene (Cp[*]) group with BF$_4^-$, AlCl$_4^-$ and CF$_3$SO$_4^-$ anion as counter anion. The synthesis of the tetryliumylidene was carried out by reacting dicyclopentadienyl tetrylene with an electrophile which was further attacks the Cp[*] ring. Alternatively, the synthesis can be carried out by reaction of cyclopentadienyl germanium (II)/ tin (II) chloride with a chloride abstracting agent like AlCl$_3$ to obtain the targeted cationic species (1.4.A).[27] Following the above-mentioned report, several sandwich complexes coordinated to the cationic germylene/stannylene were reported. However, in 1996, a different ligand system was used by Dias *et. al.*to stabilize germyliumylidene/Stannyliumylidene. They used aminotropominate which is a 10π electron ligand system to stabilize these species where the imine nitrogen center donates into the empty p-orbital of the tetryliumylidene (1.4.B).[28] Again Schmidbaur and coworkers reported the use of [2.2.2]cyclophane ligand to trap the germyliumylidene/stannyliumylidene species where the three aryl rings show η[6] coordination to charged center (1.4.C).[29] In 2012, Roesky and co-worker used 2,6-diacetylpyridinebis-(2,6-isopropylanil) as ligands and when reacted with germanium (II)/tin(II) halides to obtain the respective cationic complexes (1.4.D).[30] Inoue *et. al.* reported the formation of germylene/stannylene complexes by reacting E[(NSiMe$_3$)$_2$]$_2$ (E=

Ge/Sn) with bis(diisopropylphenyl)imidazoline-2-amino ligand which on reacting further with $B(C_6F_5)_3$ leads to the formation of the desired cation species (1.4.E).[31] In 2020, the same group reported the discovery of a NHC stabilized germyliumylidene species which was isolated by treating chlorogermylene with two equivalents of 1,3,4,5-tetramethylimidazol-2-ylidene (1.4.F).[32]

1.4.A   **1.4.B**   **1.4.C**

1.4.D   **1.4.E**   **1.4.F**

E= Ge, Sn
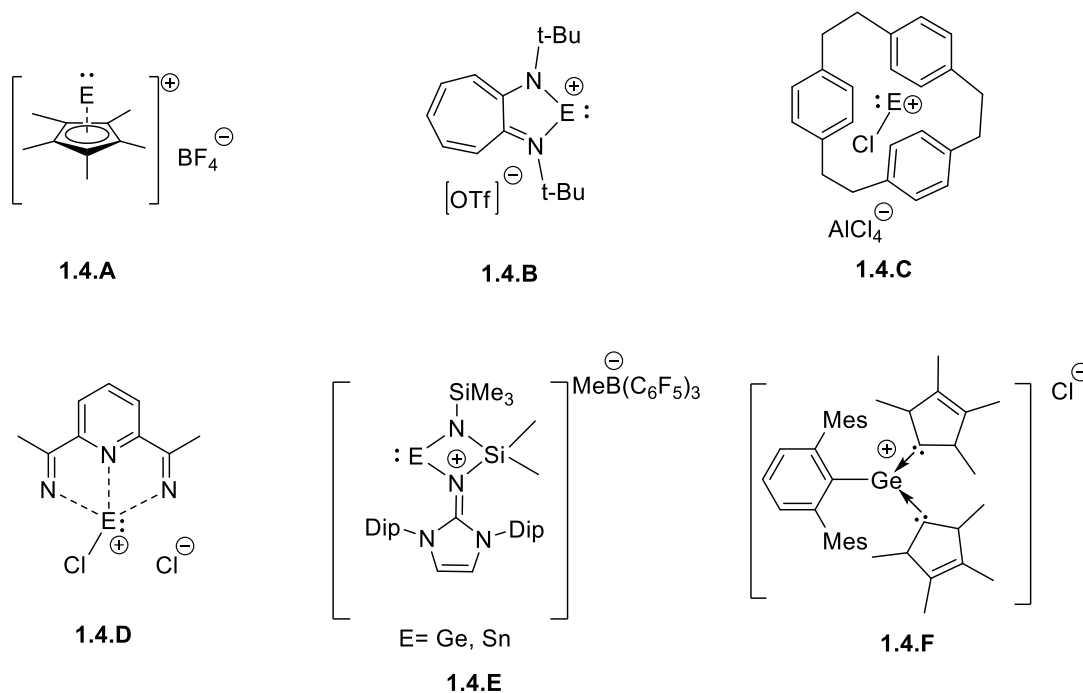
Figure 1.4.1. Selected examples of germyliumylidene/stannyliumylidene

1.5. Application of Ge (II)/Sn (II) neutral and cation complexes

Neutral and cationic Germanium (II) and tin (II) complexes have a lone pair and an empty p-orbital. Depending on the type of substituents they can act as a Lewis acid or base and can have several applications which are briefly highlighted here.

Because of the lone pair and the empty p-orbital on the germylene center, it can activate small molecules. It can donate as well as accept electrons simultaneously and can break bonds heterolytically. The first ever report of activation of a hydrogen molecule was made by Power *et al.* using a bulky dimesitylphenyl group substituted di-coordinated germylene. The bulkier germylene with diisopropylphenyl group substitution showed the formation of substituted trihydrogermane with the elimination of 1,3-diisopropylbenzene. Theoretical calculations elucidated the interaction of the σ-orbital with the empty orbital of germylene and the lone pair of the germylene interacting with the σ* orbital of the dihydrogen.[33] Again, the analogous diisopropylphenyl group substituted di-coordinated stannylene on reaction with dihydrogen

lead to the formation of a hydride bridged stannylene. However, the dimesitylphenyl group substituted stannylene did not react with dihydrogen (Fig 1.5.1).[34]
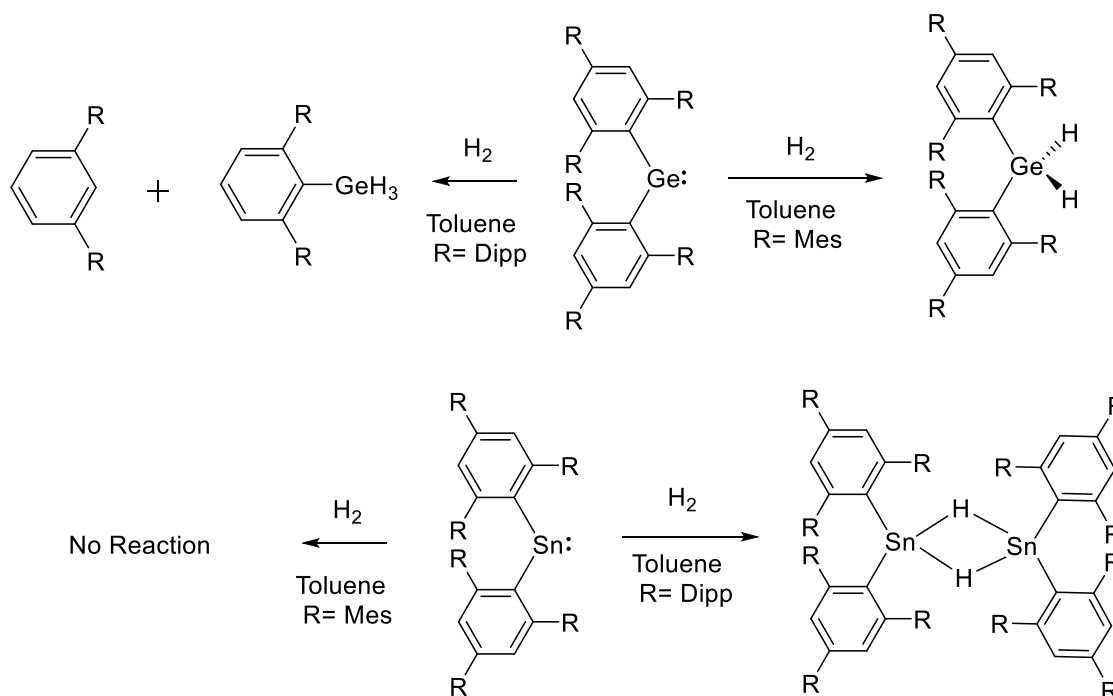
Figure 1.5.1. Activation of hydrogen by germylenes and stannylenes

As germylenes have a lone pair they can act as Lewis bases and coordinate with Lewis acids to form adducts and can be used for activation of small molecules. This notion was applied by Roesky and co-workers in the synthesis of and intramolecular Germylene-borane adduct **X** that reacted with 4-methoxyacetophenone to form a Ge centered spiroheterocycle. Further the adduct reacts with isopropyl isocyanate to give two different spiroheterocycles (Fig.1.5.2).[35]
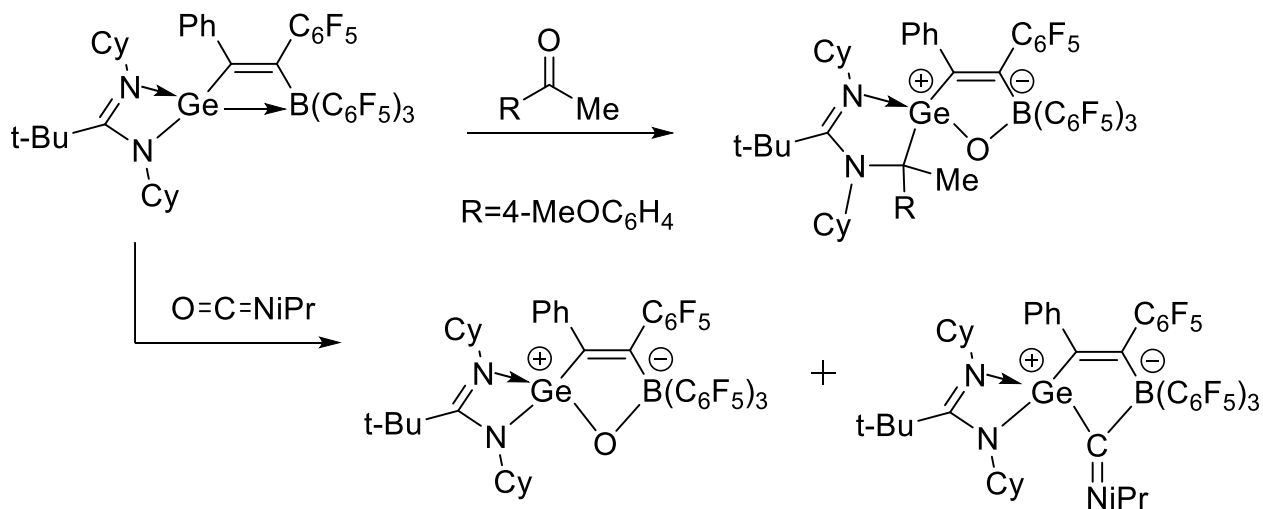
Figure 1.5.2. Reactivity of Germylene-borane adduct

Similarly, *Kato et al.* developed a Lewis acid base-pair system using germylene **X** along with $B(C_6F_5)_3$ as the Lewis acid, which activated various silanes (Fig. 1.5.3).[36]
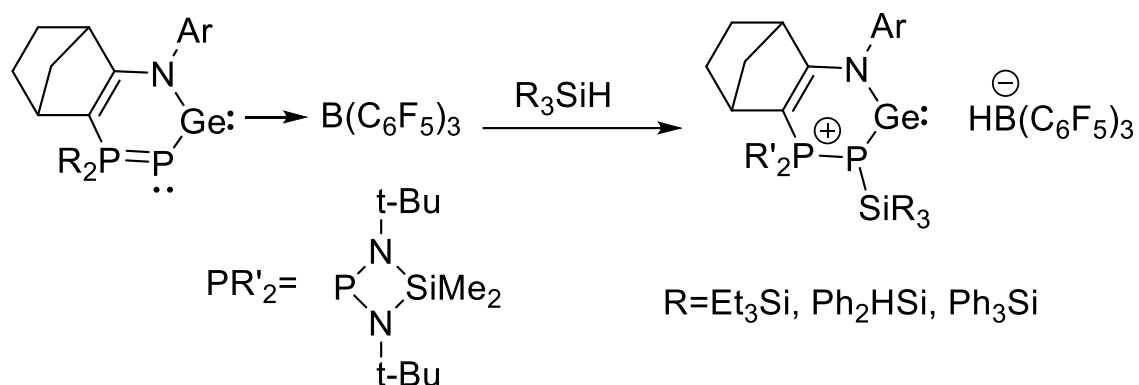
Figure 1.5.3. Activation of silanes by Germylene-borane adduct

The germyliumylidene complex stabilized by Inoue *et al.* in 2020 reacts with N_2O to form a germaacylium ion which activates CO_2 reversibly and have been used in catalytic conversions (Fig. 1.5.4).[32]
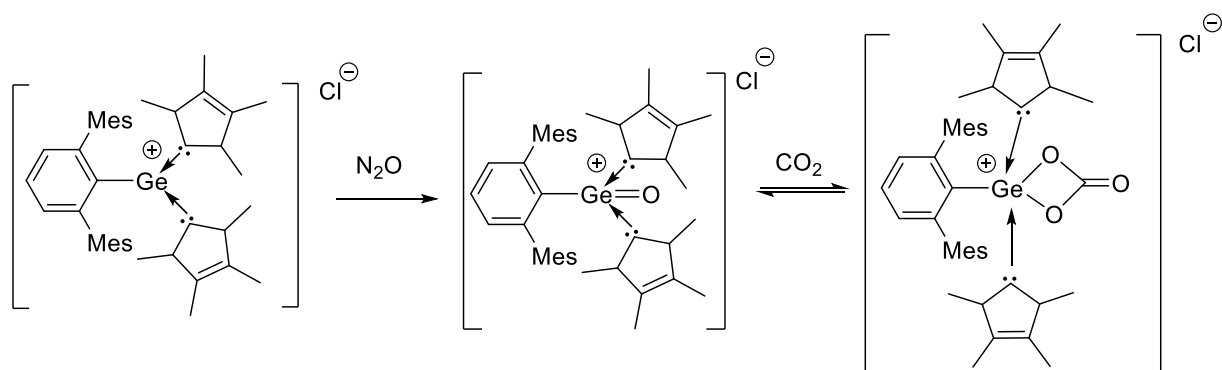
Figure 1.5.4. CO₂ Activation by germaacylium ion

The same germyliumylidene complex has been utilized in catalytic cyanosilylation and hydroboration of aldehyde and ketones under mild conditions and have produced good yields of the reduced targeted products. These conversions are a result of the Lewis acidity of the Ge-C^{NHC} σ^* bond orbital (Fig. 1.5.5).[37]
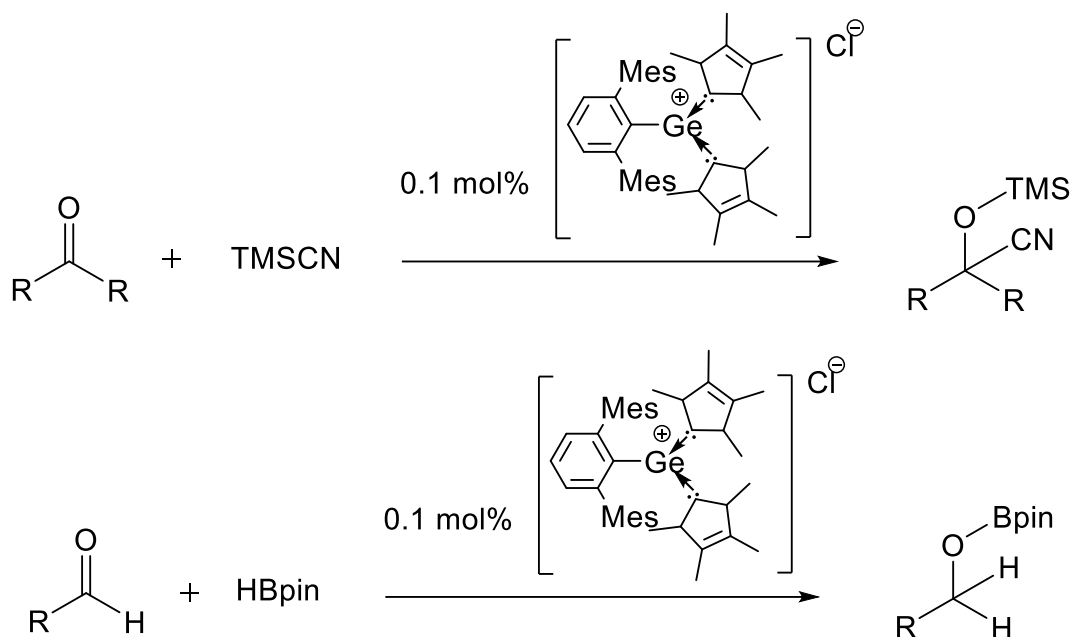
Figure 1.5.5. Reduction of carbonyl compounds by germyliumylidene

1.6. Bistetrylenes

Keeping in mind, the applications of neutral and cationic Ge(II) and Sn(II) complexes, the usage of two tetrylene moiety in the same ligand is a better alternate and so designing bistetrylenes was quintessential. Hence, they have been synthesized and studied over the past decade. There are several reports of bistetrylenes donating to a single transition metal center. But the first report of bistetrylene bridged by an oxygen atom was made by Driess's group in 2010.[38]

The above mentioned ligand was synthesized by Driess and coworkers by adding Lithium amidinate LLi [L= PhC(NtBu)$_2$] with 1,1,3,3,terachlorodisiloxane to yield the disiloxane **1.6.1** in 53% yield. Further the reaction of **1.6.1** with 2 molar LiN(SiMe$_3$)$_2$ in toluene led to the formation of the anticipitated bis-silylene oxide **1.6.2** by dehydrochlorination. Formation of both complexes **1.6.1** and **1.6.2** was confirmed by single crystal X-ray diffraction as well NMR spectroscopy. The bis-silylene oxide **1.6.2** was found to be comprising of two silylene moieties with lone pair electrons, joined by the oxide bridge. The ^{1}H and ^{13}C NMR spectrum showed a single set of peaks for the ligand. The ^{29}Si spectrum showed a singlet peak at -16.1 ppm which is downfield shifted in comparison to the ^{29}Si peak of disiloxane **1.6.1** (δ = -111.1 ppm). The molecular structure of **1.6.2** confirmed the Si-O bond distance to be 1.641(2) and 1.652(2) Å which is comparable to the typical bond distances for Si-O bond in other disiloxanes.[39]

Figure 1.6.1. Synthesis of ligand 1.6.2

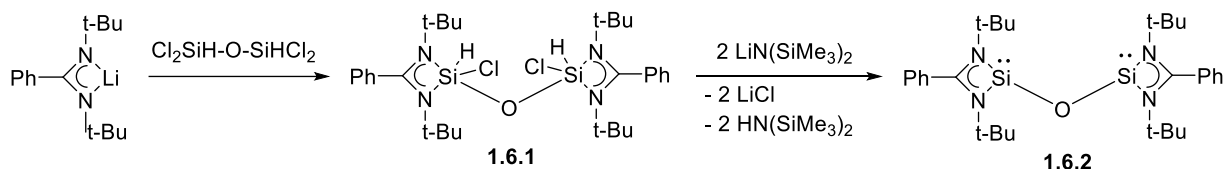The Si-O-Si bond angle is 159.88(15)° and is larger than the bond angle of C-O-C in corresponding ethers. On reacting Ni(COD)$_2$ with the bis-silylene oxide **1.6.2** in toluene at room temperature there was a sudden appearance of an intense red colour. The crystals of the complex were obtained by recrystallisation of the crude product in hexane at -30°C in 91% yield. The complex 1.6.**3** was characterized by single crystal X-ray diffraction and NMR techniques. The ^{1}H and ^{13}C NMR spectrum showed a single set of peaks for the *t*-Bu group, the COD molecule and the -Ph groups of amidinate ligand. The ^{29}Si spectrum was found to be downfield shifted to the "free ligand" **1.6.2**. The X-ray data showed the coordination of Ni center to the two silylene centers and to one COD molecule. The Si-O bond lengths are longer than the bis-silylene oxide **1.6.2** [1.7011(15) and 1.7081(17) Å]. The Si-O-Si bond angle [93.44(8)°] was found to be smaller in comparison to that of the bis-silylene oxide **1.6.2**. The Ni-Si bond lengths are longer than the ylide like silylene-nickel complexes [2.0369(6) and 2.0597(10) Å].[40] However, the shorter than the Ni-C bond of Ni(COD)$_2$ [2.11-2.15 Å]. This indicates a stronger back-donation from Ni center to the silylene centers.
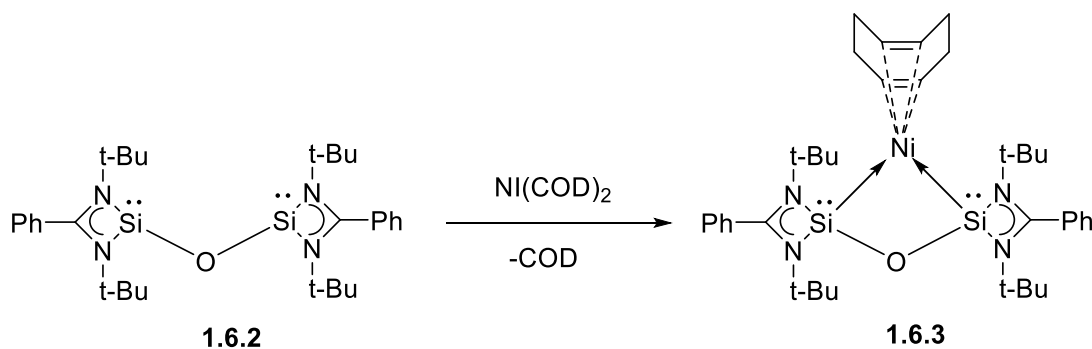
Figure 1.6.2. Nickel(0) complex 1.6.3 Stabilised by ligand 1.6.2

The bis-silylene oxide **1.6.2** was also used to stabilize two Cu(I) centers to form a dinuclear metallacyclooctane salt complex **1.6.4**. On reacting the ligand **2** with [Cu(CH$_3$CN)$_4$][OTf] led to the formation of complex **1.6.4**. ^{1}H NMR spectrum shows signal for the *t*-Bu groups of the amidinato group of the ligand and the ^{29}Si NMR spectrum has the signal of the donating silylene groups at -16.1 ppm confirming the formation of the complex.

The solid-state structure confirms the formation of the dinuclear complex with each silylene of the two different set of ligands donating to a single copper (I) center.[41]
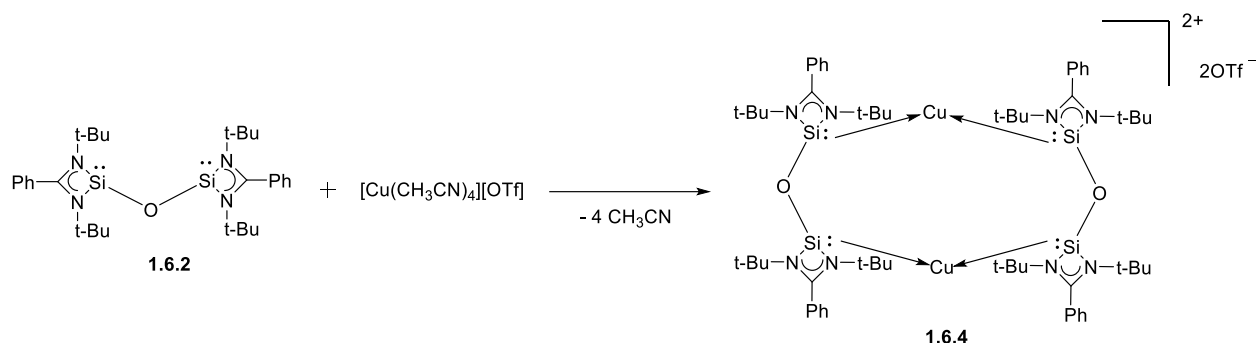
Figure 1.6.3. Dinuclear metallacyclooctane salt complex 1.6.4 stabilised by ligand 1.6.2

Further, bis-silylenes were synthesized by the same group with a bridging phenyl ring which makes the chemistry further interesting as it provides a route for the activation of the C-H bond at the 2-position of the benzene ring. The SiCSi pincer ligand **1.6.5** was synthesized by dilithiating 4,6-di-*tert*-butylresorcinol with *n*Buli to give 1,3-dilithium resorcinolate. By salt metathesis with N-stabilized chloro silylene LSiCl [L(amidinate)= PhC(N*t*Bu)$_2$] in molar ratio of 1:2 the desired pincer ligand **1.6.5** was obtained. Ligand **1.6.5** was characterized by NMR spectroscopy and Single X-ray diffraction technique. ^{1}H NMR spectrum shows one set of signals for the *t*-Bu and one set of signals for Ph- groups of the amidinate group. On doing a VTNMR not much change is observed in the signals indicating the low rotation barriers of the Si-O bond. The ^{29}Si NMR spectrum shows a single peak at -24.0 ppm for the silylene centers. The Si-O bonds are longer than that of bis-silylene oxide **1.6.2** [1.7056 and 1.7190 Å] because of the steric congestion in the molecule. One of the Si-O-C bond angle is larger than the other Si-O-C bond angle making the molecule asymmetric [141.79° and 132.17°].

4,6-di-tert-butyl resorcinol　　**1,3-dilithium resorcinolate**　　　　　　　　**1.6.5**

Figure 1.6.3. Synthesis of ligand 1.6.5

Using DFT the symmetric counterpart has been found to be 1.8kcal/mol higher in energy than the asymmetric molecule. The two imidinate stabilized silylene molecules are strong σ-donor but poor π-acceptors. To confirm their donor abilities the ligand was reacted with Pd(PPh$_3$)$_4$ in the molar ratio of 2:1 to obtain bis-silylenesilyl(phenyl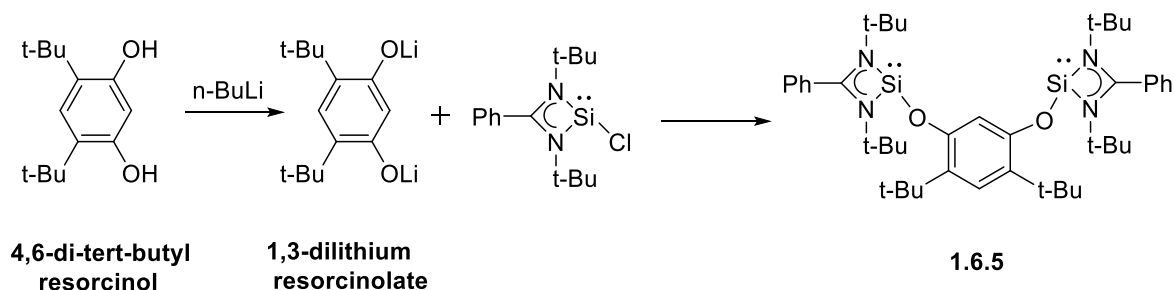)palladium(II) complex **1.6.6** as sole product in 81% yield. Changing the molar ratio from 2:1 to 1:1 reduced the yield of the product to <40% but no other product or intermediate was detected by ^{1}H NMR spectroscopy. The complex **1.6.6** was characterized both by NMR Spectroscopy and SCXRD technique. Complex **1.6.6** crystallises in a racemic mixture of its R and S enantiomers. The molecular structure of the S-enantiomer depicts the presence of Pd(II) centre coordinated to two silylenes from different ligand molecule **1.6.5** and covalently bonded to one Si(IV) centre and the C-2 of the central aryl ring of the ligand. So, the Pd(II) centre is placed in a distorted square planar coordination sphere. The Si-N bond of the ligand is disrupted during the complexation due to the 1,2-shift of the hydrogen from the Pd centre to the Si centre forming the silyl group. Due to the saturation of coordination around the Pd centre one of the silylene centres remain free. The silylene Si-Pd and Silyl Si-Pd bond distances are different owing to the difference in bond types. The two silylene Si-Pd bond distances are comparable to the previously reported bond distances.[42] The Pd-C bond is longer than the previously reported complex presumably due to steric congestion.[43] ^{1}H and ^{13}C NMR spectrum shows the twelve sets of *t*-Bu groups of the ligand systems which is consistent with the SCXRD data. The Si-*H* proton resonates at -6.59 ppm. The ^{29}Si NMR spectrum of the complex in C$_6$D$_6$ gives four signals at δ= -8.7, 39.7, 62.3 and 65.8 ppm. Also, the infrared spectrum shows an Si-H bond stretching band at 2135 cm^{-1}.[44]
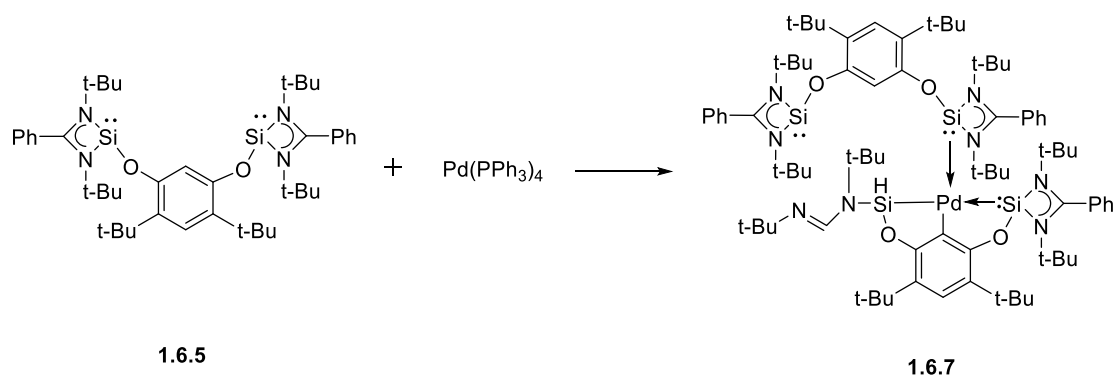

Figure 1.6.4. Synthesis of complex 1.6.7

Ligand 3 was further used to stabilise Iridium complexes. On addition of [{IrCl(coe)$_2$}$_2$] to a solution of ligand **1.6.5** in C$_6$D$_6$ leads to the formation of complex **1.6.8** immediately in quantitative amount. The ^{1}H NMR spectrum showed the clean indication of

hydride containing complex having a signal at δ= 25.6 ppm. The ^{13}C NMR spectrum showed the peaks for the t-butyl groups, phenyl grous and the coordinated cyclooctene. Also, the ^{29}Si NMR spectrum showed a single peak at δ= 54.9 ppm. Single crystal X-ray diffraction data revealed that the bond length of Si-Ir bond was found to be 2.305(1) and 2.301(1) Å which falls between Ir^{III}-Si^{IV} bond lengths and Ir^{III}-silylene bond lengths.[45] Similarly the corresponding germanium complex **1.6.9** was synthesized using the reported analogous bis(germylene) ligand **1.6.10** and [{IrCl(coe)$_2$}$_2$].[46]
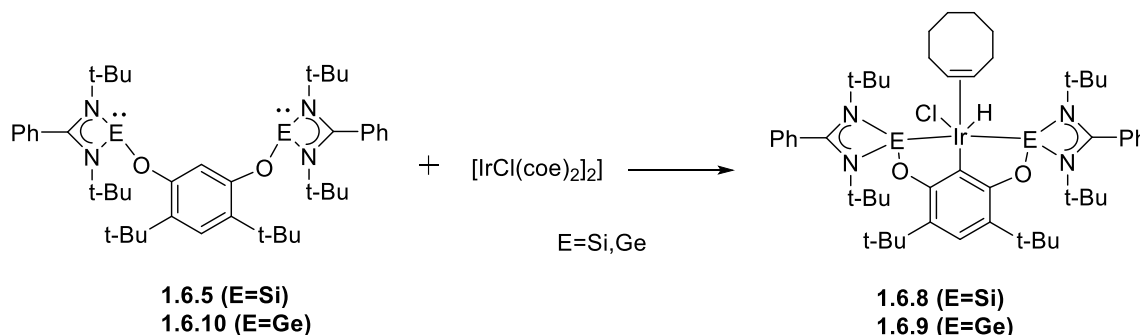
Figure 1.6.5. Synthesis of complexes 1.6.8 and 1.6.9

Further the coordination of these ligands was screened with several rhodium precursors. It was found that on heating the bis(silylene) ligand with [IrH(CO)(PPh$_3$)] at 100°C led to the formation of dihydride complex **1.6.11**. The ^1H NMR spectrum showed a clean signal for the hydride at δ= -10.2 ppm. Also, the ^{31}P NMR showed the presence of free PPh$_3$ group. The IR spectrum showed two signals, one for CO stretching frequency at v= 1968 cm^{-1} and a weak band for hydride at v= 2251 cm^{-1}. Reaction of the bis(silylene) ligand with Wilkinson's dimer [{RhCl(PPh$_3$)$_2$}$_2$] led to the formation of complex **1.6.12**. It was characterised by NMR spectroscopy. The ^1H NMR spectrum showed the signal for the hydride at δ=17.2 ppm. ^{31}P NMR spectrum showed the presence of the coordinated PPh$_3$ at δ= 36.6ppm and the ^{29}Si NMR revealed a peak at δ= 66.4 ppm. But when similar reactions were attempted using the bis(germylene) ligand no complex formation was observed. The probable cause was attributed to the weak donation properties of the bis(germylene) ligands compared to the bis(silylene) ligand. Further, the catalytic activities of the Iridium complexes **1.6.8** and **1.6.9** were explored. In presence of COE borylation of benzene using HBpin was carried out in excellent yields.[47]
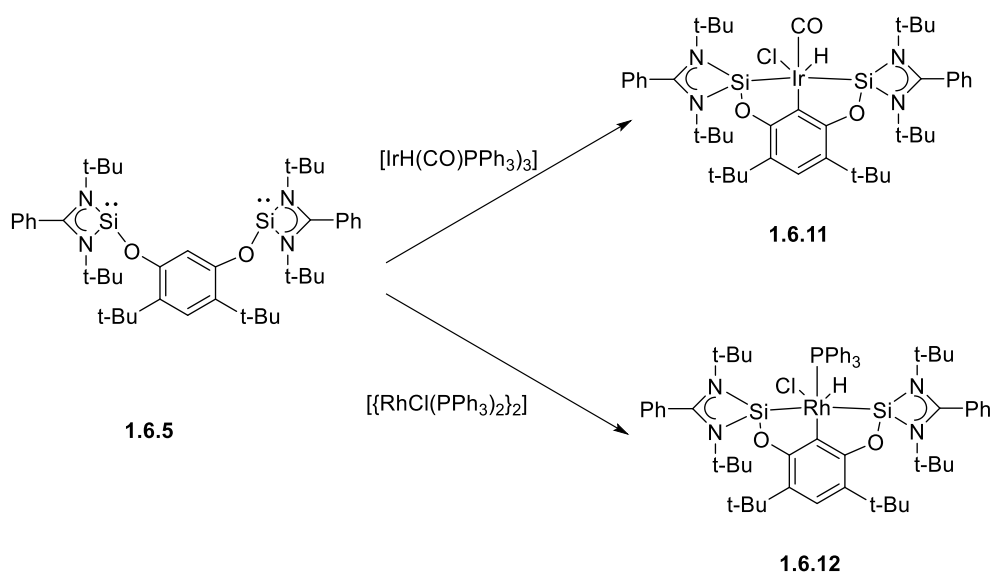
Figure 1.6.5. Synthesis of complexes 1.6.11 and 1.6.12

A new bis(silyene) and a bis(germylene) was synthesised by the same group using ferrocenyl group as the linker which resulted in unique results. Similar to ligand **1.6.5** reported previously, ligands **1.6.13** and **1.6.14** were synthesised by salt metathesis between 1,1'-dilithioferrocene and N-stabilized chloro silylene and germylene LECl [L(amidinate)= PhC(N*t*Bu)$_2$, E= Si, Ge] in 70% and 77% yield respectively. Both the complexes were characterized by Single Crystal X-ray diffraction and NMR spectroscopy techniques. Ligand **1.6.13** and **1.6.14** exhibit three peaks in ^{13}C NMR spectrum namely at δ= 70.9, 72.7 and 84.6 ppm and δ= 70.1, 72.3 and 92.0 ppm) respectively. All the peaks correspond to the ferrocendiyl moiety. Ligand **1.6.13** exhibits a singlet at δ= 43.3 ppm in ^{29}Si NMR spectrum. The Solid-state structure of **1.6.14** shows the presence of two conformational isomers. The germylene moieties were found to be attached to the C1 and C8 centers of the ferrocene with the germanium centers adopting a pyramidal geometry. The Ge-N bonds were found to be shorter than the precursor germylene. The structure of ligand **1.6.13** was found to be like ligand **1.6.14** however the data was insufficient for discussion.

Figure 1.6.6. Synthesis of Ligands 1.6.13 and 1.6.14

Further, transition metal coordination was tried using cobalt precursors. One of the suitable precursors was found to be CpCo(I) which was *in-situ* generated by reaction of NaCp, CoBr$_2$ and KC$_8$ in toluene or THF. This was reacted with both the bis(silylene) as well as bis(germylene) to afford the chelated complexes **1.6.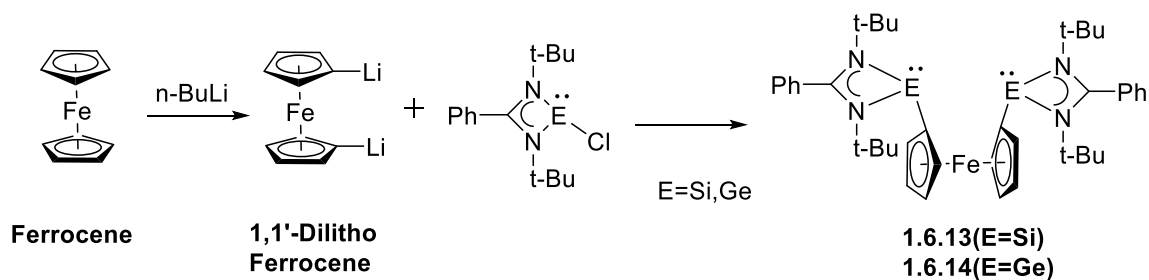15** and **1.6.16** in 30% and 61% yield respectively. The ^{29}Si NMR spectrum shows a peak at δ= 82.0 ppm which is downfield shifted in comparison to **1.6.13**. When **1.6.13** was allowed to react with two equivalents of [CpCo(CO)$_2$], bis(silylene)-Co complex **1.6.17** was obtained in 87% yield. The ^{29}Si NMR spectrum shows a peak at δ= 85.7 ppm for complex **1.6.17** and ^{13}C NMR depicts the presence of CO group in the complex by showing the characteristic peak at -207.8 ppm. The solid-state structures of complex **1.6.15** and **1.6.16** shows a four coordinated silicon and germanium centers with tetrahedral geometries. The Co-Si and Co-Ge bonds in the complex **1.6.15** and **1.6.16** indicat the strong σ-donation from the ligands **1.6.13** and **1.6.14**. Further the catalytic abilities of the complexes **1.6.15** and **1.6.16** were explored. It was found that complex **1.6.15** acts a precatalyst in trimerization of phenylacetylene into **1.6.18** and **1.6.19** in 72% and 28% yield. However, complex **1.6.16** did not show any catalytic activity due to strong coordination of Ge (II) to Co moiety. Complex **1.6.15** was able to catalyze the [2+2+2] cycloaddition of phenylacetylene with an excess of acetonitrile in low yields but again complex **1.6.16** failed to catalyze the reaction.[48]
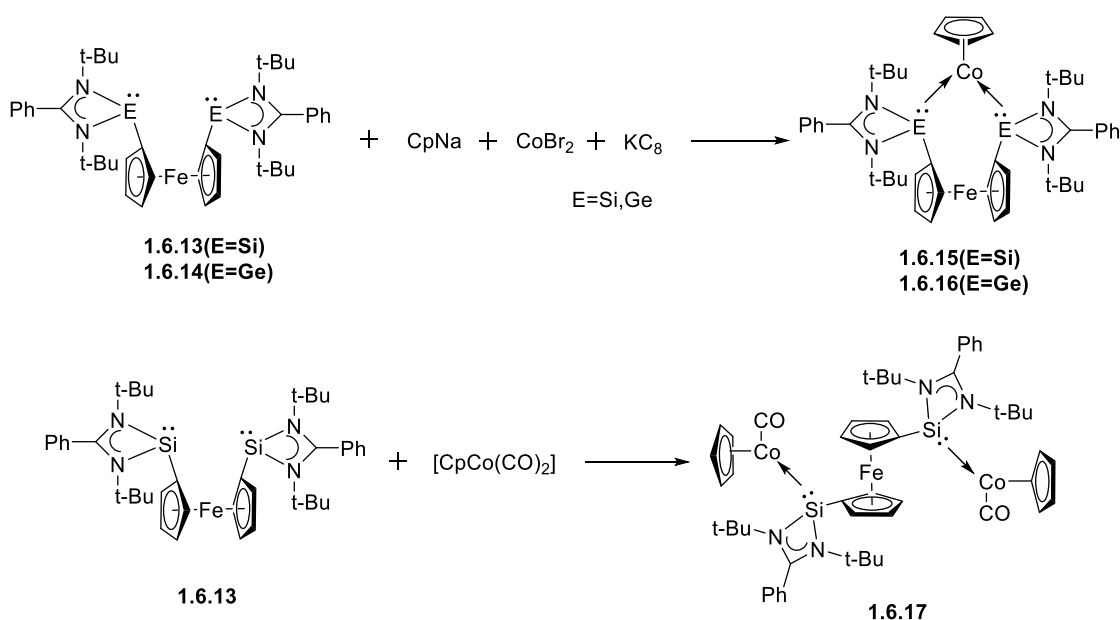

Figure 1.6.6. Synthesis of complexes 1.6.15, 1.6.16 and 1.6.17

The bis(silylene) ligand **1.6.5** and the analogous bis(germylene) ligand **1.6.10** were used to stabilize Ni complexes. However, there was an attempt made to synthesize the

complexes from the bromo derivatives rather than the hydride derivatives previously used. So, subsequently the bromo derivative were synthesized by slow addition of LHMDS to a mixture of 2-bromo-4,6-di-tert-butylresorcinol and *N*, *N′*-di-tertbutylchloro(phenylamidinate)germanium (II) to obtain ligands **1.6.18**. The ligand was fully characterized by NMR spectroscopy, mass spectrometry and single crystal X-ray diffraction. The structural features of the complex were found to be like that of the ligand **1.6.10**. An attempt to make the similar bromo derivatives of the bis(silylene) ligand were not successful. The reaction of Ni(cod)$_2$ and ligand **1.6.18** lead to the formation of complex **1.6.19**. The analogous silylene-nickel complex **1.6.20** was prepared by reacting ligand **1.6.5** and NiBr$_2$(dme). Complex **1.6.21** was alternately synthesized by reacting NiBr$_2$(dme) with ligand **1.6.10**. Both the complexes **1.6.20** and **1.6.21** were characterized by NMR spectroscopy and Single crystal X-Ray diffraction. The absence of peak of phenyl C-H of the ligand **1.6.5** from the ^{1}H NMR spectrum and appearance of a signal δ= 20.2 ppm in the ^{29}Si NMR spectrum confirmed the formation of complex **1.6.20**. The solid-state structure confirmed the square planar Ni (II) sites positioned in the molecular structure. Both the complexes were found to be catalysing the Sonogashira coupling between phenylacetylene and (E)-1-iodo-1-octene to form (E)-dec-3-en-1-ynylbenzene in moderate yields.[49]
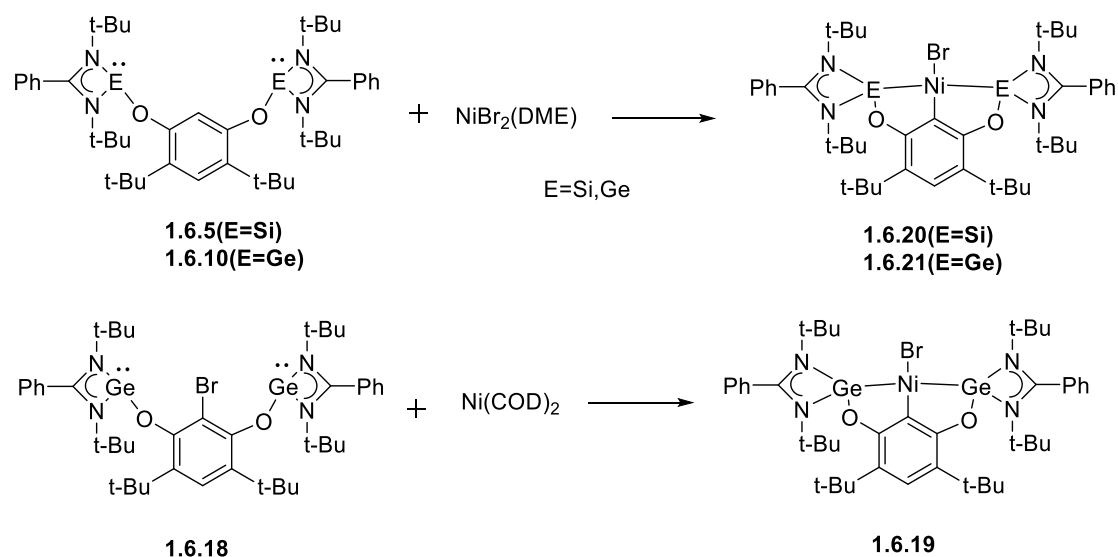
Figure 1.6.7. Synthesis of complexes 1.6.19, 1.6.20 and 1.6.21

A new set of pincer bis(metallylene) ligands were established by the same group. Tridented pyridine-based ligands **1.6.22** and **1.6.23** were synthesized by deprotonating *N*, *N′*-diethylpyridine using *n*-BuLi followed by addition of *N, N′*-di-tertbutyl(phenylamidinato) chlorosilylene or -germylene in toluene respectively. Both the ligands show a singlet signal for

the *t*-butyl, a triplet for the methyl and a quartet for the methylene groups in their ^{1}H NMR spectra. Further the ligands were characterized by ^{13}C and ^{29}Si NMR spectra, high-resolution mass spectrometry and elemental analyses. The ^{29}Si NMR of ligand **1.6.22** revealed the non-equivalence of the silylene centers as they are free to rotate. However, for the solid-state structures only ligand **1.6.22** was crystallised and studied as ligand **1.6.23** was found to be highly soluble in all organic solvents. The molecular structure revealed that the silylene are leaning outwards from the pyridine moiety.
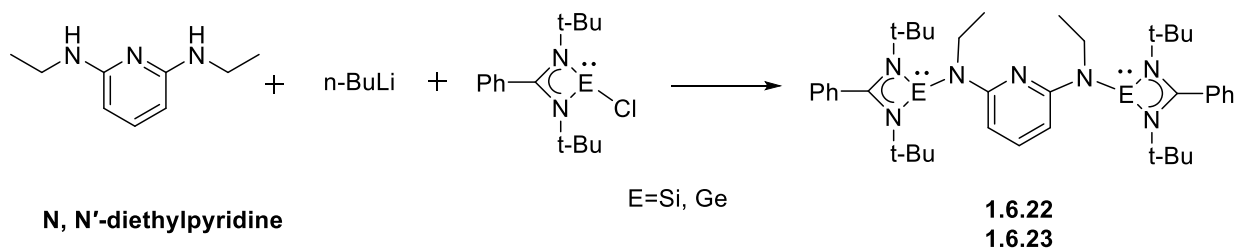
Figure 1.6.8. Synthesis of ligands 1.6.22 and 1.6.23

Reaction of the ligands with *in-situ* prepared FeCl$_2$.(thf)$_{1.5}$ led to the formation of yellow coloured complexes **1.6.24** and **1.6.25**. The solid-state structure shows the formation of a tetrahedral complex between Fe(II) and the metallylene centres. No coordination was found between the pyridine and the Fe(II) centre. This was attributed to the strong donation from the metallylene moieties. Due to the strong donation the Fe-Cl bond lengths were found to be elongated than usual. The complexes were further characterized by NMR spectroscopy and high-resolution mass spectrometry. The electronic structure was studied by Mössbauer spectroscopy.
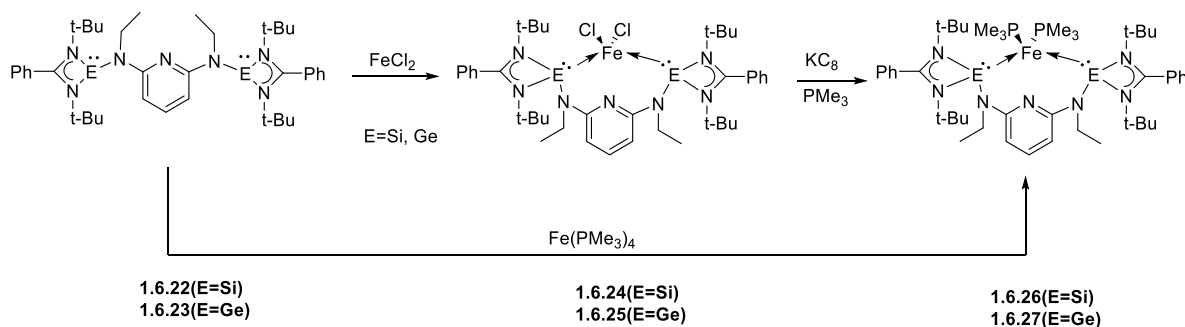
Figure 1.6.9. Synthesis of complexes 1.6.26 and 1.6.27

Reduction of both the complexes was carried out in presence of coligands. Complex **1.6.24** was reduced with KC$_8$ in presence of excess PMe$_3$ to obtain a red coloured complex **1.6.26** with the iron centre reduced from +2 to zero oxidation state. The reduction of complex 6.4 in presence

of PMe$_3$ led to the formation of side products only. So, the reaction of Fe(PMe$_3$)$_4$ with ligand **1.6.23** led to the formation of the analogous germylene-Fe(0) complex **1.6.27**. ^{1}H, ^{29}Si and ^{31}P NMR spectra of complex **1.6.26** showed inequivalency of the two phosphorus atoms coordinated to the Fe centre. Both the silylene centers were found to be equivalent but having different metric coupling constants to each phopshane. The Single crystal X-Ray diffraction data showed a slightly distorted pseudo-square pyramidal structure with the two coligand phosphines at the apical positions. Also, the bond distance of Fe-Si was found to be comparable to a double bond due to the backdonation of electrons from the Fe centre to the silylene centre.[49] The DFT calculations further confirms the above fact. The HOMO and HOMO-1 showed the π-back donation of electrons from d$_x^2$-$_y^2$ and d$_{yz}$ orbitals of the Fe centre to the 3p orbitals of Si(II) centre. However, complex **1.6.27** was only characterised by NMR spectroscopy as the complex was found to be highly soluble in most of the organic solvents. So, the crystals of the complex were never obtained. The NMR spectra were very close to those observed for complex **1.6.26** except the ^{31}P NMR spectrum showed two doublets at δ= 10.2 and 27.2 ppm indicating the Berry pseudorotation rate of the phosphanes on the Fe centre. Stirring solution of complex **1.6.26** in CO atmosphere produced a mixture of disubstituted and trisubstituted complex **1.6.28** and **1.6.29** respectively. Single crystal X-ray diffraction of both the structures showed that the Fe centre exists in a trigonal bipyramidal structure. Also, the strong donation of the metallylenes led to the easy substitution of PMe$_3$ by the CO groups. The IR spectrum showed the C-O frequency were quite lower and the C-O bond lengths were quite elongated. This indicates strong σ-donation from the silylene and germylene moieties. Finally, complex **1.6.26** showed excellent catalytic activity in the hydrosilylation of acetphenones showing good yields in mild conditions.[51] The catalyst showed excellent tolerance for both electron donating as well as electron accepting groups present as substituents in the aryl group. Only for the ortho substituents the catalyst shows lower activity due to steric hindrances. The elaborate study for the reaction mechanism shows that the Fe(0) centre undergoes oxidative addition to Fe(II) centre. The silyl group attached to the Fe(II) centre acts as the reactive centre and the Fe(II) centre does not play any direct role in the catalysis. The silyl group act as the Lewis acid centre which catalyses the reaction by activating the carbonyl group.[52]
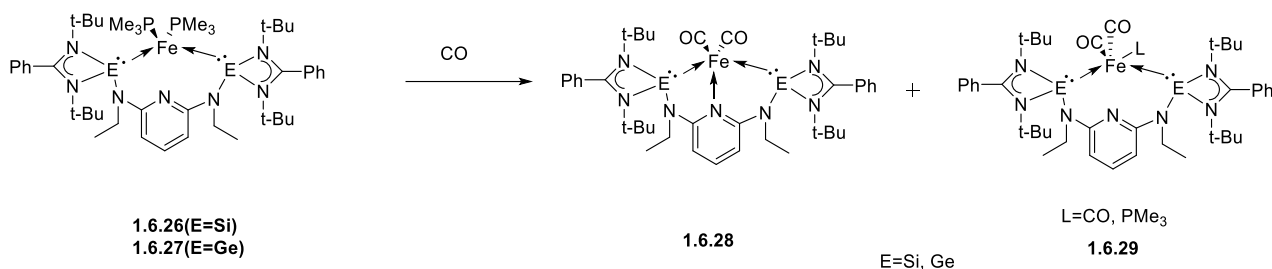
Figure 1.6.8. Synthesis of complexes 1.6.28 and 1.6.29

A new bis(silylene) ligand **1.6.30** with an *ortho*-carborane backbone was synthesised by the same group. The ligand was synthesised by salt metathesis reaction between $(LiC)_2B_{10}H_{10}$ and *N, N'*-di-tertbutyl(phenylamidinato)chlorosilylene. The Single Crystal X-ray Data showed two silylene moieties pointing towards each other with 3.267 Å distance, which formed a chelating cavity for the transition metal centre. On reacting the ligand with $(DME)_2NiBr_2$, a new complex **1.6.31** with the silylene chelating $NiBr_2$ centre was obtained. The ^{29}Si NMR spectrum of the complex gives a signal at $\delta = 58.7$ ppm which was downfield in comparison to the free ligand. Single crystal X-Ray diffraction analysis showed the square planar environment of the Nickel (II) centre. Reduction of complex **1.6.31** with KC_8 in presence of CO resulted in the Ni (0) complex **1.6.32**. The IR Spectrum depicted strong σ-donation capacity of the ligand **1.6.32** in comparison to the previously reported bis(silylene) ligands. This fact was further strengthened by DFT calculations. To study the catalytic activity of complex **1.6.31**, Buchwald-Hartwig reaction was tried with phenyl chloride and morpholine in presence of 0.5 mol% of 7.2 as catalyst, catalytic amount of $AgBPh_4$ and 1.2 molar equivalents of KO*t*Bu as base. The reaction resulted in 93% yield. However, using only $Ni(dme)Br_2$ as catalyst resulted in poor yield. Also, poor leaving groups led to lesser yield. Similarly, electron withdrawing groups at para positions increased the overall rate of reaction in comparison to electron donating groups. Also, sterics played a significant role in the reaction dynamics as aryl groups with substituents in *para* position resulted in better yields than the aryl groups with substituents at *meta* and *ortho* positions. The proposed reaction mechanism was the generation of Ni(0) species which undergoes oxidative addition with the aryl halide followed by replacement of the halide with the amide group. The C-N coupling leads to reductive elimination of the product regenerating the Ni(0) species.[53]
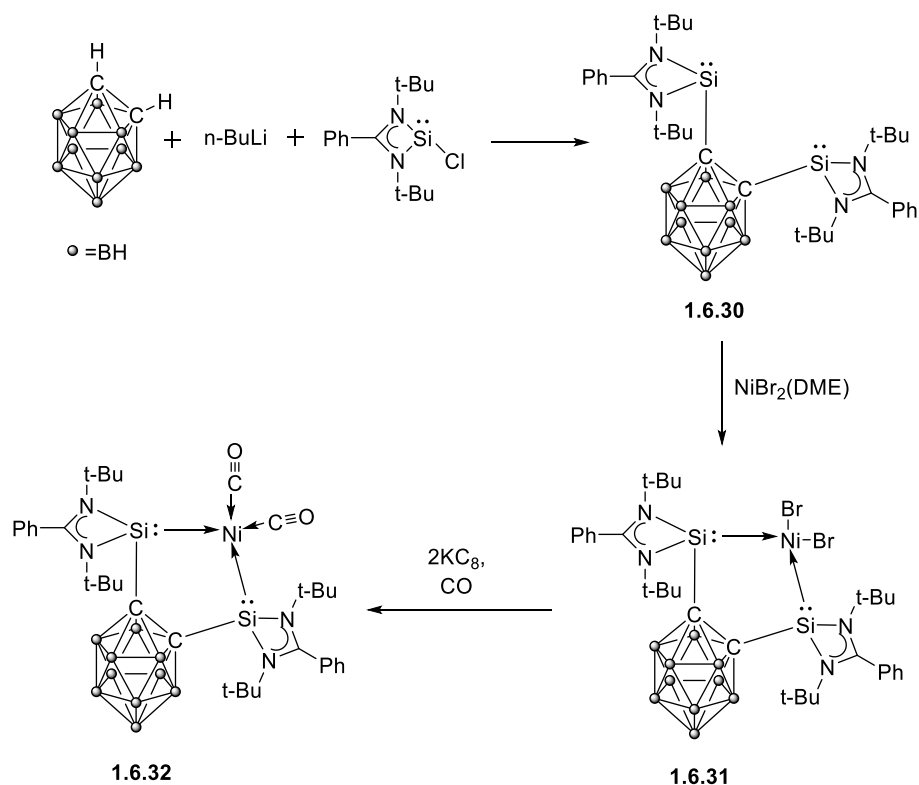
Figure 1.6.8. Synthesis of complexes 1.6.31 and 1.6.32

Again, the ligand **1.6.13** was used to stabilise an Fe(II) center. Reaction of ligand 4.1 with $FeX_2(thf)_n$ (X=Cl, Br) resulted in two yellow complexes **1.6.33** and **1.6.34**. Both the complexes were found to be silylene coordinated FeX_2 complexes. Both the complexes were extremely air sensitive and were found to be decomposing in air in a few minutes. The composition of both the complexes were confirmed by elemental analyses. The [57]Mössbauer spectra indicated the formation of a high-spin complex in a tetrahedral environment. Complex **1.6.33** crystallises in orthorhombic space group *Pbca* and complex **8.2** crystallises in triclinic space *P-1*. Both the structures have the Fe centre coordinated to the two silylene centres and two halides. Reduction of complexes **1.6.33** and **1.6.34** with KC_8 in presence of benzene or toluene led to the formation of 18 electron η^6-arene Fe(0) complexes **1.6.35** and **1.6.36** supported by the two silylenes. The formation of both the complexes was confirmed by ^{1}H NMR spectroscopy, elemental analyses, ESI-MS spectrometry, and Single crystal X-ray diffraction studies. The ^{1}H NMR spectrum of **1.6.35** revealed the singlet peak of η^6 coordinated benzene at δ= 5.16 ppm which is downfield shifted in comparison to other Fe(0) complexes.[54] ^{13}C and ^{29}Si NMR spectra were not recorded due to the lower solubility of both these complexes in C_6D_6 or THF-d_8. The SCXRD data shows that the arene molecule is perpendicular to the Fe centre. Also, the Fe-Si bond lengths of complexes **1.6.35** and **1.6.36** are shorter than those of

complexes **1.6.33** and **1.6.34**indicating the presence of a π-back donation of electrons from Fe(0) centre to the Si(II) centres. Cyclic voltammogram studies revealed that there is reversible redox event at $E^{1/2}$ = -1.56 V for complex **1.6.35** and $E^{1/2}$ = -1.58V for complex **1.6.36** which are assigned to Fe^0/Fe^{+1}. The [57]Mössbauer spectra indicated the presence of pentacoordinate Fe(0) centre in a pseudo-trigonal bipyramidal coordination environment. DFT studies were carried out to further elaborate the electronic properties of the complexes. The LUMO and LUMO+1 were found to be located on the phenyl group of the ligand whereas the HOMO was found to be located on the π-backdonation from Fe(0) centre to the 3p orbital Si(II) centre. The HOMO-1 is represented by the π interaction between arene moiety and the Fe(0) centre. The HOMO-LUMO gap is found to be 2.599 and 2.584 eV for complexes **1.6.35** and **1.6.36** respectively.
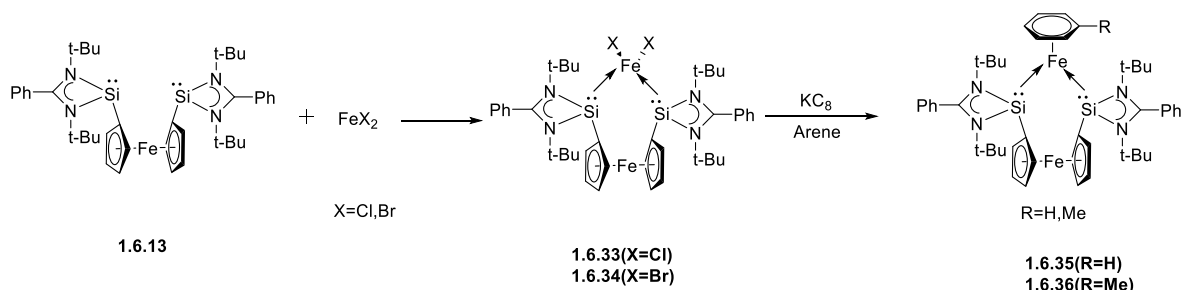
Figure 1.6.8. Synthesis of complexes 1.6.33, 1.6.34, 1.6.35 and 1.6.36

Complex **1.6.37** was synthesised by reacting complex 8.3 and 8.4 in an atmosphere of CO. Alternatively, it can be synthesised by reducing complexes 8.1 and 8.2 in the presence of CO gas. The IR spectrum showed a strong coordination of the silylene centres to Fe(0) centre. Complex **1.6.37** was characterised by NMR spectroscopy and ESI-MS spectrometry however no crystals were successfully obtained for the complex. Complex **1.6.35** showed excellent catalytic activity for the hydrogenation of various ketones. The catalyst was tolerant towards both electron donating and electron withdrawing groups as substituents. However, bulkier groups lower the yield of the reaction.[55]
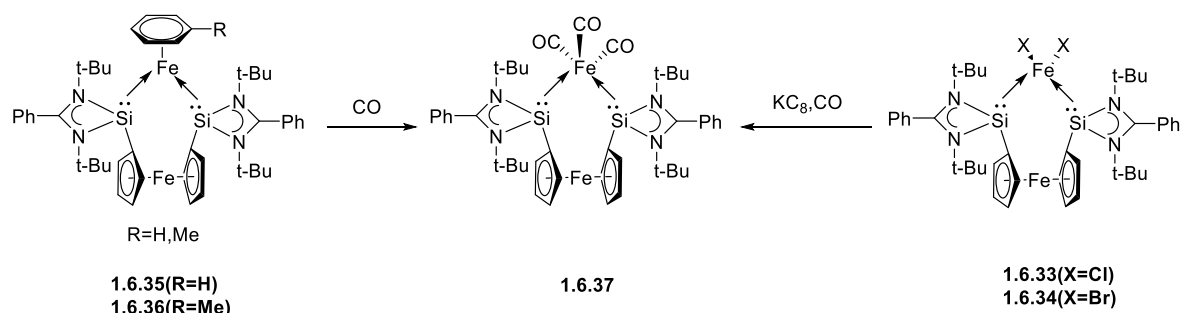
Figure 1.6.8. Synthesis of complex 1.6.37

The same ligand **1.6.13** was used to stabilise Rh centred complex to catalyse hydroformylation reaction of styrene. Initially, commercially available HRh(CO)(PPh$_3$)$_3$ was reacted with [{PhC(NtBu)2}(NMe2)Si:](**R1**)[56] and [{C2H2(NtBu)2}Si:](**R2**)[57] to obtain complexes HRh(CO)(R1)$_3$ and HRh(CO)(R2)$_3$. Both the complexes were identified by NMR spectroscopy. The ^{1}H NMR spectra showed an absence of ^{31}P-coupling for the hydride signal at δ=-10.45 ppm and δ = 9.68ppm respectively. The ^{31}P NMR spectrum showed signals for "free" PPh$_3$ ligand. A clean doublet at δ= 62.8 ppm and δ= 106.0ppm for both the complexes were obtained in the ^{29}Si NMR spectra. This indicates equatorial substitution of **R1** and **R2** in a trigonal bipyramidal geometry. No crystals were obtained because of the residual PPh$_3$ in the solution. Both the complexes showed poor catalytic performance when used for hydroformylation of styrene which was attributed to the strong σ-donation from the silylene moieties which lowered the coordination of the substrate. So, bis(silylene) and bis(germylene) ligands **1.6.13** and **1.6.14** were used to substitute the PPh$_3$ groups in HRh(CO)(PPh$_3$)$_3$ to obtain complexes **1.6.38** and **1.6.39**. Both complexes showed a doublet peak in the ^{31}P NMR for the coordinated PPh$_3$. Also, ^{1}H NMR spectra of both the complexes showed a phosphine-coupled signal for the hydride. However, the solid-state structures of the complexes were not obtained as the crystals were not obtained due to the residual PPh$_3$ in the solution. Complex **1.6.38** was found to be excellent as the catalyst for the hydroformylation reaction. This was attributed to its very strong σ-donation that led to the easy dissociation of PPh$_3$ and leave an active site for the substrate to attack. However, complex **1.6.39** was not able to catalyse the hydroformylation reaction.[58]

1.6.13(E=Si)
1.6.14(E=Ge)

1.6.38(E=Si)
1.6.39(E=Ge)

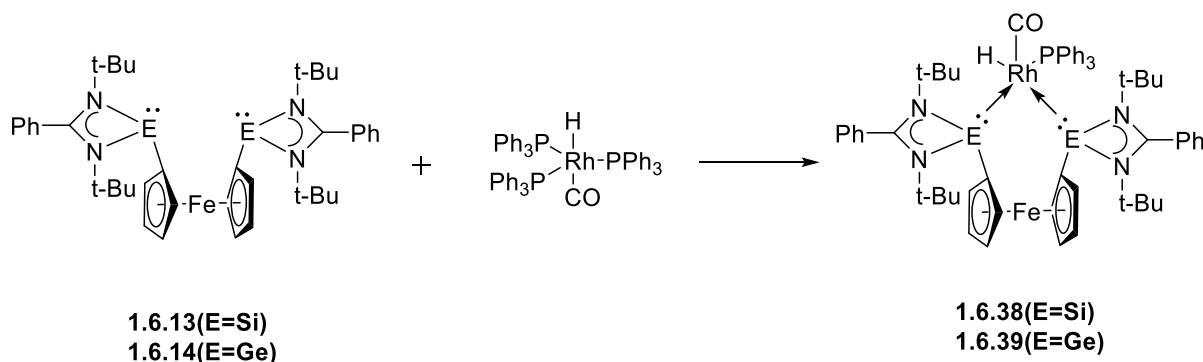**Figure 1.6.8. Synthesis of complexes 1.6.38 and 1.6.39**

A new ligand **1.6.40** was reported again by the same group with bis(silylene) supported by xanthene backbone. Ligand 10.1 was synthesized by dilithiating 4,5-dibromo-9,9-dimethylxanthene followed by salt metathesis with chlorosilylene [PhC(N*t*Bu)$_2$]SiCl. The ligand was characterised by NMR spectroscopy and X-ray diffraction analysis. Further, ligand

1.6.40 was reacted to Ni(COD)$_2$ to obtain complex **1.6.41**. Complex **1.6.41** shows a downfield signal in comparison to the ligand in the ^{29}Si NMR spectra. Single crystal X-ray diffraction studies depicts a trigonal planar Ni center and was found to be disordered because of the rapid exchange between the two C=C bond of coordinated cyclooctadiene molecule. Complex **1.6.41** was reacted with PMe$_3$ to obtain complex **1.6.42** which has the COD molecule substituted with two PMe$_3$ molecule. Complex **1.6.42** was characterised by NMR spectroscopy and single crystal X-ray diffraction studies.
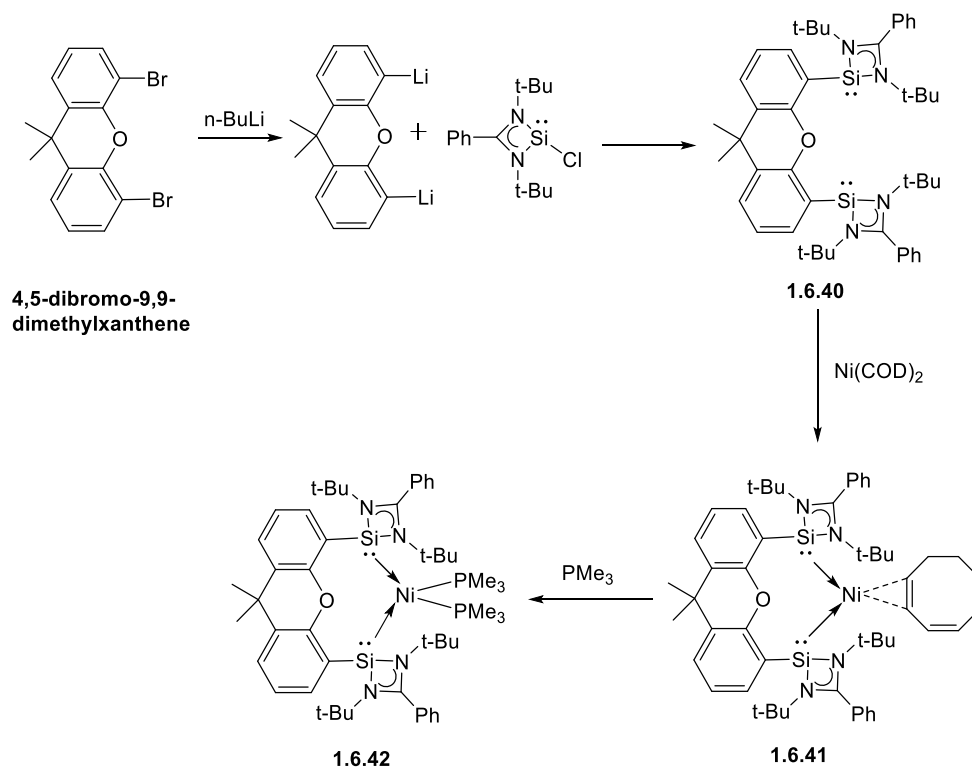
Figure 1.6.8. Synthesis of complexes 1.6.41 and 1.6.42

Further, complex **1.6.41** was able to activate H$_2$ to produce complex **1.6.43**. The solid-state structure of the complex **1.6.43** depicts a four membered planar Ni$_2$Si$_2$ core supported by the bis(silylene) ligand. The ^{1}H NMR spectrum depicts unsymmetrical tBu groups of the ligand. The ^{29}Si NMR spectra revealed two signals for two different silicon centres: One for the silylene centre and the other for the Ni-H-Si moiety. ^{1}H NMR study of H$_2$ activation showed the initial monohydrogenation of the COD molecule to COE (cyclooctene) molecule.
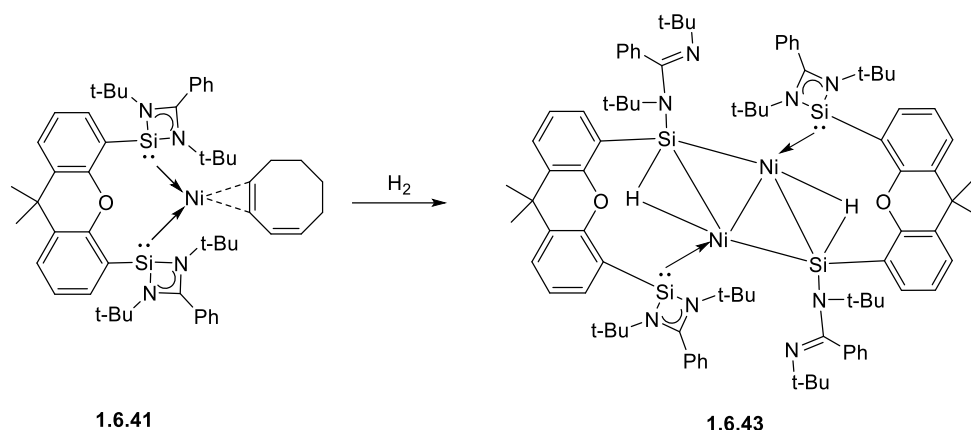
Figure 1.6.8. Synthesis of complex 1.6.43

Complex **1.6.42** also activates hydrogen reversibly to give complex **1.6.44**. NMR spectroscopy revealed formation of dihydrido Ni complex along with "free" PMe₃, 10% of 10.3 and traces of Ni(PMe₃)₄. ^{1}H NMR spectrum of complex **1.6.44** displays a doublet at δ= -1.51 ppm corresponds to the Ni-H centres. ^{31}P NMR spectra showed a peak at δ= -28.3 ppm corresponding to the coordinated PMe₃ molecule. The ^{29}Si NMR spectrum showed a doublet signal at δ= 9.7 ppm for both the silicon centres which are chemically distinct. This confirms the fast exchange between the two silicon centres. This was further studied by isotope labelling techniques. X-ray diffraction studies revealed that the Ni centre adopts a distorted square pyramidal geometry with H₂ added to one of the Ni-Si bonds. Both complexes **1.6.41** and **1.6.42** were screened for hydrogenation of olefins. However, only **1.6.41** was found to be the efficient catalyst for hydrogenation of olefins under very mild conditions.[59]

Figure 1.6.8. Synthesis of complex 1.6.44

24

A new ligand **1.6.45** was synthesised by reacting 1,4-bis(2-bromophenyl)benzene with two equivalents of *s*-BuLi and the lithiated product was further reacted with [PhC(N*t*Bu)$_2$]SiCl. The ^{29}Si NMR Spectrum showed a signal at δ= 16.8 ppm which is similar to the previously reported ligand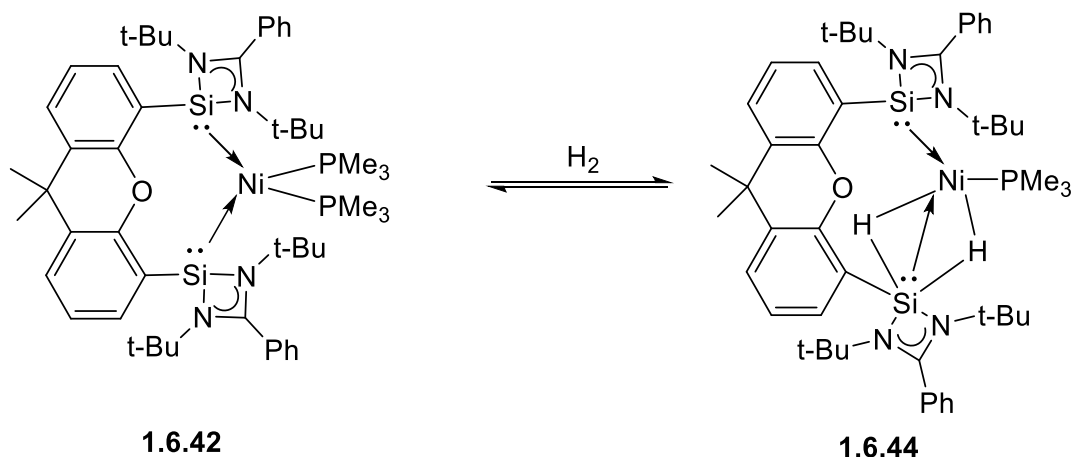s. Reacting ligand **1.6.45** with Ni(COD)$_2$ led to the formation of complex **1.6.46**. The molecular structure revealed that the two silylene moieties donating to the Ni centre which is further coordinated in η^2 coordination mode to the central phenyl ring. The ^{29}Si NMR spectrum showed a downfield shifted signal in comparison to that of the ligand.
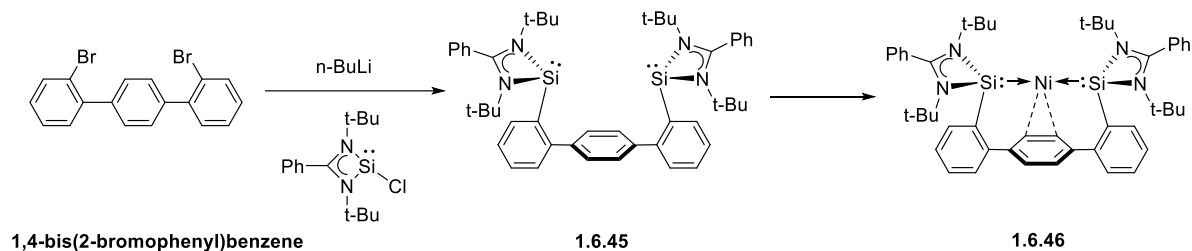
Figure 1.6.8. Synthesis of complexes 1.6.45 and 1.6.46

Treatment of Complex **1.6.46** with PMe$_3$ or excess acetonitrile did not lead to the formation of any new complexes. However, reaction with CO resulted in the formation of the complex with two CO molecule coordinated to the Nickel centre. The IR stretching frequencies showed that the ligand is a strong σ-donor in comparison the similar ligands reported previously like ligand **1.6.5** and **1.6.13**. Complex **1.6.46** was used as a pre catalyst for the olefin hydrogenation. It was found to show good functional group tolerance with good yield and selectivity. To look further into the details of mechanism of the catalytic reaction the complex **1.6.46** was reacted with H$_2$ at room temperature led to the reversible formation of complex **1.6.47**. The molecular structure of the complex showed that the dihydrogen adds across the Si-Ni bond and on applying vacuum the dihydrogen releases, keeping the complex **1.6.46** intact. The activated dihydrogen transfers to the olefin leading to high TON of the olefin hydrogenation reaction. Further the mechanism is studied in detail experimentally and computationally.[60]
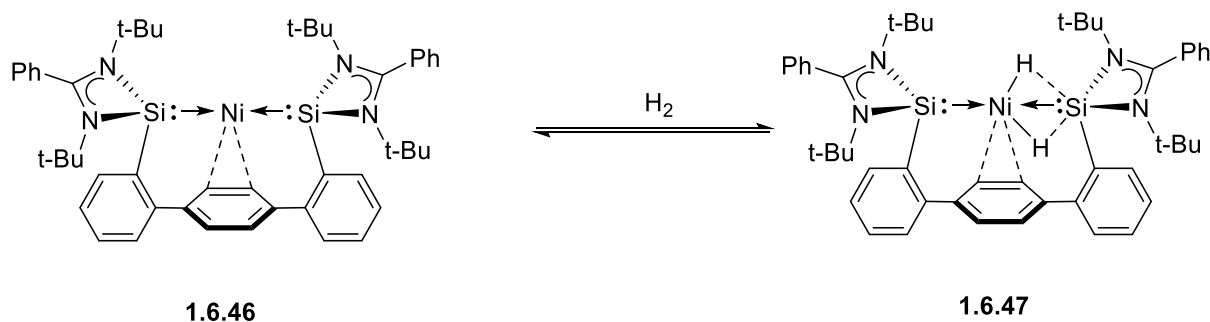
Figure 1.6.8. Synthesis of complex 1.6.47

Another ligand **1.6.48** was synthesised by lithiating 4,5-dibromo-2,7,9,9-tetramethyl-9,10-dihydroacridine and reacting it further with chlorosilylene [PhC(N*t*Bu)$_2$SiCl]. Reacting ligand **1.6.48** with [FeCl$_2$(Py)$_4$] led to the formation of [FeCl(Py)(SiNSi)] (**1.6.49**). Treating **1.6.49** with [Li(NSiMe$_3$)$_2$] led to the formation of amido Iron complex **1.6.50**. The molecular structure of all the three complexes were confirmed by X-ray diffraction analysis.
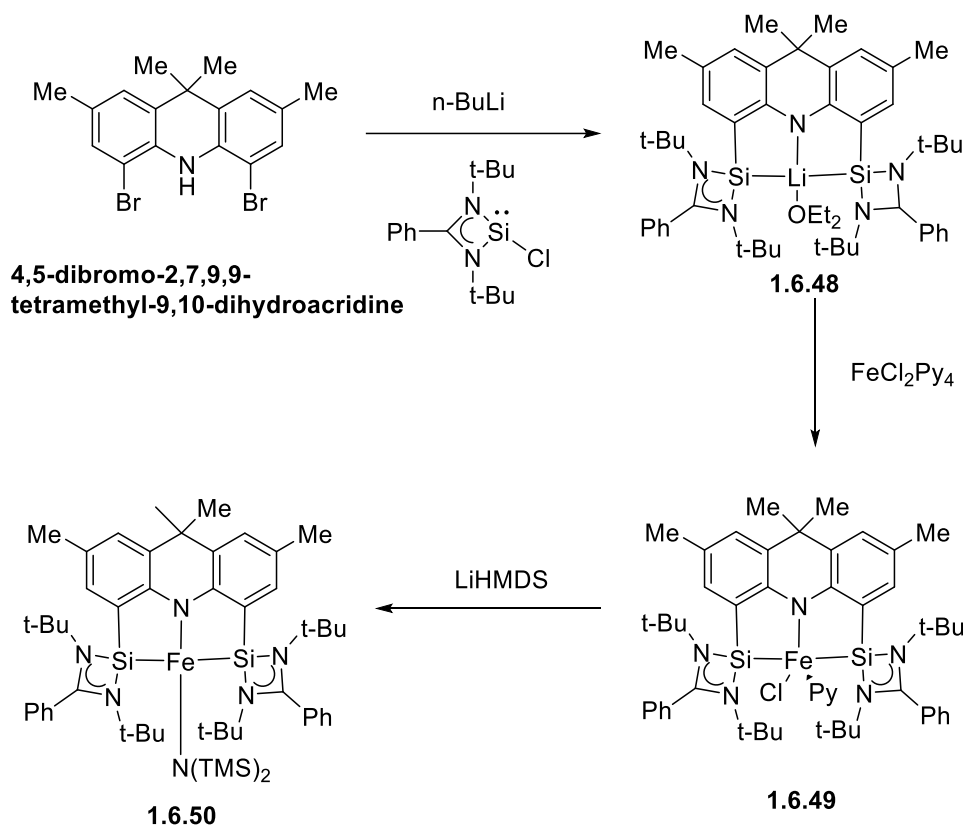
Figure 1.6.8. Synthesis of complexes 1.6.49 and 1.6.50

Exposing complex **1.6.50** to N$_2$O gas resulted in the formation of iron-silanone complex **1.6.51**. The molecular structure of complex **1.6.51**showed that the silanone moiety is four coordinated and the O atom donates to the Fe centre. The deoxygenation of N$_2$O in presence of HBpin and catalytic amount of Complex **1.6.50** and **1.6.51**led to smooth formation of N$_2$, H$_2$ and (pinB)$_2$O. The high reactivity of these complexes in the reduction of N$_2$O led to the screening of their potential to deoxygenate nitro compounds. It was found that complex 3 is a suitable catalyst which reduced nitro compounds to their corresponding ammonium derivatives in quantitative yield. The catalyst showed good tolerance for wide variety of functional groups and showed good selectivity. DFT studies confirmed the cooperative nature of silylene and Fe centre led to the excellent activity of the catalyst. [61]
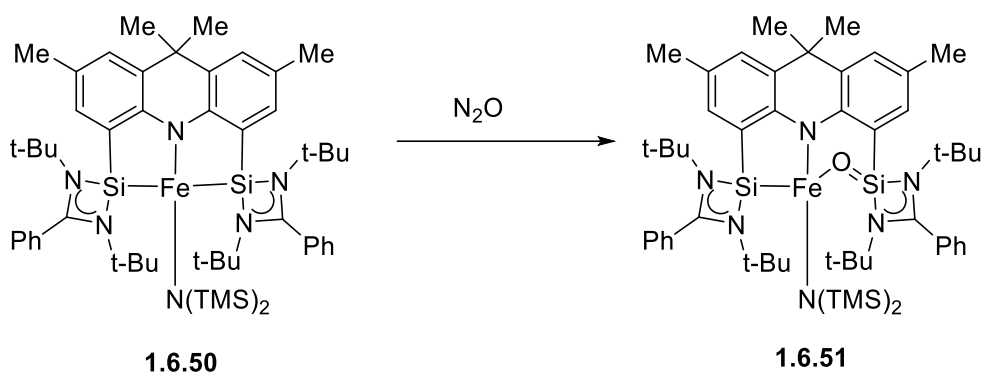
Figure 1.6.8. Synthesis of complex 1.6.51

Main group moieties

Ligand **1.6.22** was used to stabilize a germylone species. The reaction of GeCl$_2$.Dioxane with ligand **1.6.22** led to the formation of the chlorogermyliumylidene species stabilised by the two silylene moieties leading to the formation of the complex **1.6.52**. The ^{29}Si NMR spectrum depicted a downfield signal in comparison to that of the ligand indicating the formation of complex **1.6.52**. The single crystal x-ray diffraction data showed a longer Ge-Cl bond due to the strong σ-donation from the silylene groups.[62] The pyridine N centre was found to be barely coordinated to the Ge centre. Reduction of complex 11.1 with KC$_8$ or sodium naphthalenide did not lead to the formation of Ge(0) complex. It was presumed that the Ge(0) species is too labile because of the strong σ-donation from the silylene groups. DFT studies confirmed this presumption. It was found that the lone pair on the Ge centre is predominantly s-type with some double bond character between the Ge-Si bond. Because of the excessive electron density on the Ge centre it was assumed that the Ge(0) species could be stabilised by ligand **1.6.22** with the help a strong electron acceptor. So, on reacting complex **1.6.52** with collman's reagent K$_2$Fe(CO)$_4$ led to the formation of the complex **1.6.53**. X-ray diffraction studies showed that the pyridine N-centre was coordinated to one of the silylene group rather than the Ge centre. The Ge centre adopts a trigonal pyramidal geometry. The IR stretching frequencies showed that the CO ligands act as strong electron acceptors at the Fe centre. DFT studies shows that Ge-Fe bond is a donor-acceptor bond rather than a covalent bond. On reacting complex **1.6.53** with GeCl$_2$.Dioxane led to the insertion of GeCl$_2$ moiety in between Ge-Fe bond leading to the formation of complex **1.6.54**. X-ray diffraction studies revealed the formation of Ge-Ge single bond with the GeCl$_2$ moiety adopting a pyramidal geometry.[63]
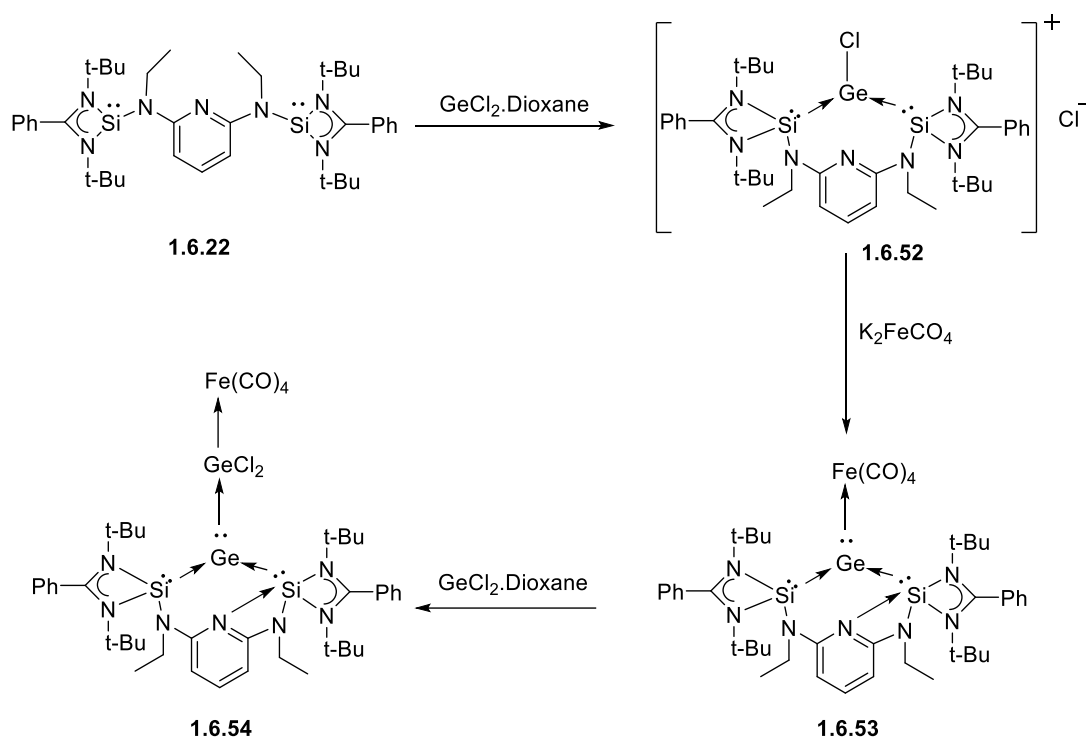
Figure 1.6.8. Synthesis of complexes 1.6.52, 1.6.53 and 1.6.54

Again ligand **1.6.40** was used to stabilise a Ge(0) moiety. On reacting ligand **1.6.40** with GeCl$_2$.Dioxane led to the formation of the germyliumylidene complex **1.6.55**. Complex **1.6.55** has the germanium atom in trigonal pyramidal geometry. The chloride ion serves as the counter anion and remains in weak interaction with one of the silylene moieties. NMR studies shows that the chloride ion exchanges coordination rapidly between the two silylene centres. Reduction of complex **1.6.55** with KC$_8$ led to the formation very sensitive Ge(0) complex **1.6.56**. The complex was characterised by Single crystal X-ray diffraction, NMR spectroscopy, High resolution mass spectrometry, elemental analysis and UV-Vis spectroscopy. The UV-Vis spectroscopy shows a band at λ$_{max}$= 596 nm. ^{1}H NMR spectrum reveals a highly symmetrical molecule. ^{29}Si NMR spectrum shows a downfield shifted signal in comparison to ligand **1.6.40** and complex **1.6.55** showing strong σ-donation from the two silylene moieties. DFT studies revealed a partial double bond between the silylene and Ge(0) centres. Natural bond analysis shows the presence of two perpendicular lone pair on the Ge centre. One of them consists of s-orbital with some contribution from the p-orbital. The other lone pair consists of the 3p orbital of Ge atom. The second lone pair is partially donated into the empty p-orbitals of the silylene moieties.
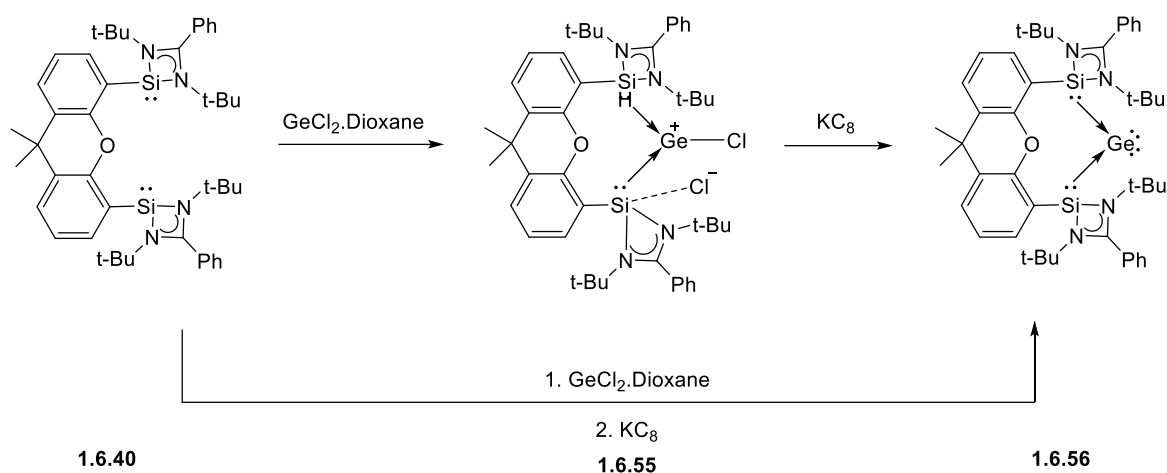
Figure 1.6.8. Synthesis of complexes 1.6.55 and 1.6.56

Reaction of complex **1.6.56** with one equivalent of AlBr$_3$ lead to the formation of the Lewis acid adduct complex **1.6.57**. In presence of coordinating solvents another equivalent of AlBr$_3$ was not coordinated but in benzene another equivalent of AlBr$_3$ was added to the complex **1.6.57** to form complex **1.6.58**.
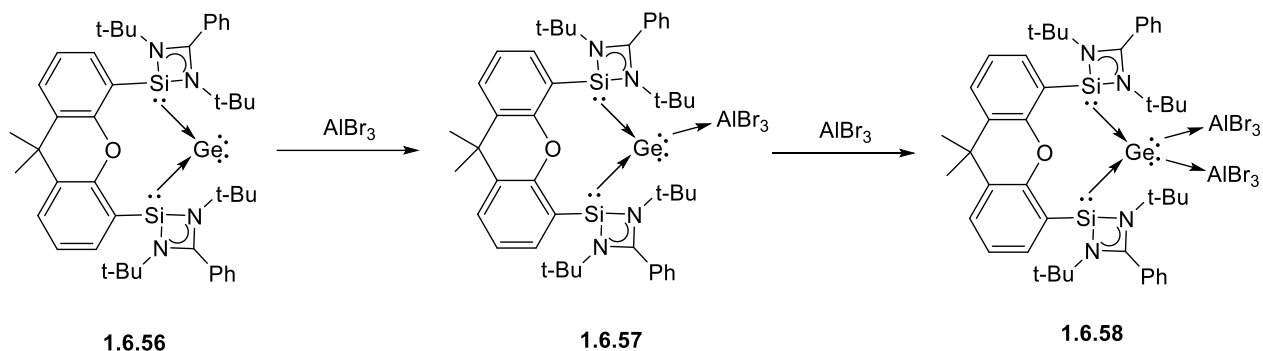
Figure 1.6.8. Synthesis of complexes 1.6.57 and 1.6.58

Further, complex **1.6.56** was reacted with Lewis acid 9-borabicyclo[3.3.1]nonane (9-BBN) to form an asymmetric complex **1.6.59**. One of the silylene group adds up a hydrogen from the 9-BBN to form a silyl group and the boryl group attaches to the germylene group.

29
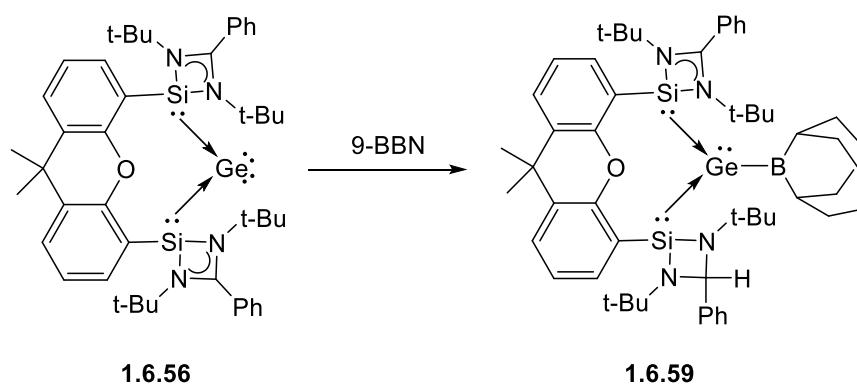
Figure 1.6.8. Synthesis of complex 1.6.59

The asymmetric complex was characterised by X-ray diffraction studies and NMR studies. DFT studies showed that the complex has 2 electron-3 centre B…Ge…Si heteroallylic π-bond interaction.
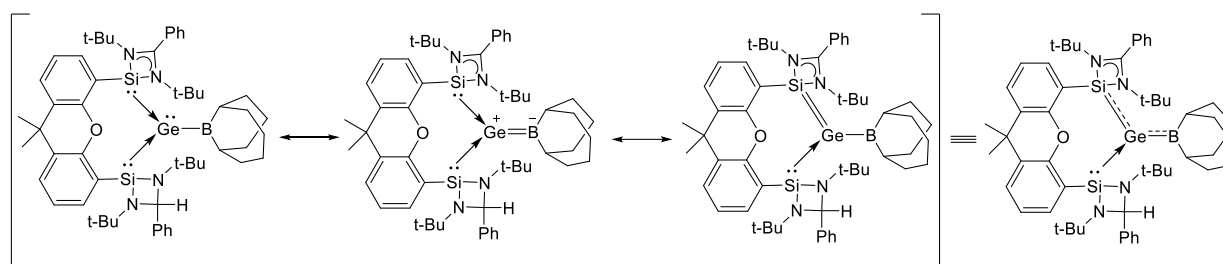
Figure 1.6.8. Resonating Structures of complex 1.6.59

Complex **1.6.56** further reacted with Ni(COD)$_2$ gave a novel diamagnetic complex **1.6.60**. Complex **1.6.60** is a three membered complex of Ge$_2$Ni^{II} core. NMR spectroscopy depicts that two silylene moieties of two different ligands coordinate to the Ni^{II} centre and the other two silylene moieties coordinate to the Ge atoms. X-ray diffraction studies reveal that the Ni(II) centre remains in the square planar geometry and the germanium centres adopt distorted tetrahedral geometry with one lone pair left at the vertex. Complex **1.6.60** can be described as Ge^{I}-Ni^{II}-Ge^{I} metallacycle.
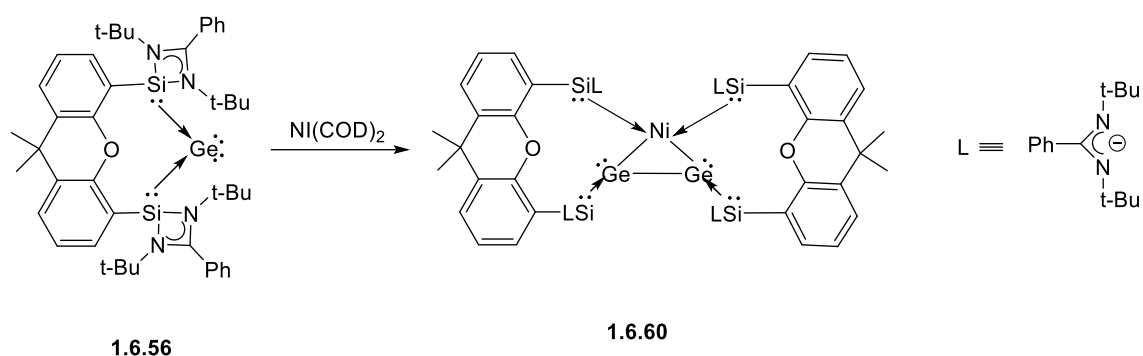
Figure 1.6.8. Synthesis of complex 1.6.60

Further, activation of H$_2$ was tried with complex **1.6.56** but it was found that in the presence of a bulky Lewis acid like BPh$_3$ it acts as a frustrated lewis acid-base pair and activates H$_2$ to form complex **1.6.61**. To further confirm this activation, D$_2$ molecule was used for the reactivity studies showing the attachment of one of the D atoms to the germylone centre and another to the BPh$_3$ moiety.[64]
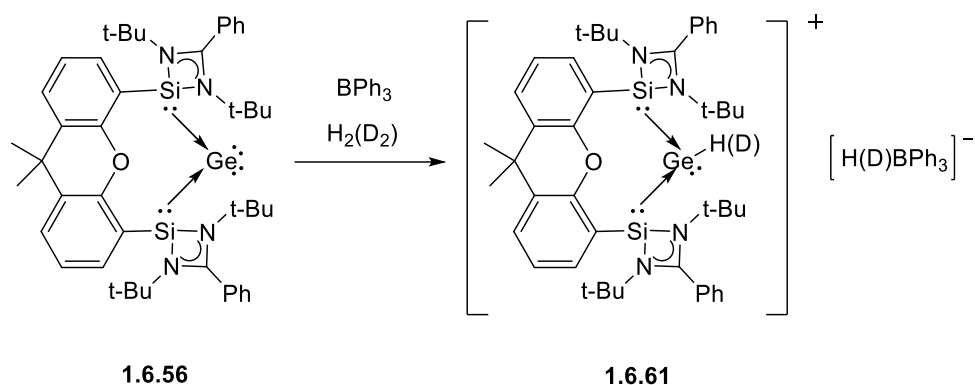
Figure 1.6.8. Synthesis of complex 1.6.61

Ligand **1.6.40** was reacted with one equivalent of NHC-SiCl$_2$ to form a silyliumylidene complex **1.6.62**. When reacted with two equivalents of NHC-SiCl$_2$, it forms complex **1.6.63**. Complex **1.6.63** can otherwise be formed by reacting complex **1.6.62** with one equivalent of NHC-SiCl$_2$. Both the complex adopts a trigonal pyramidal geometry with a lone pair at the apex. The counter anion Cl$^-$ is not in the coordination of silicon for complex **1.6.62** however for complex **1.6.63** the counter anion Cl$^-$ is directly in interaction with one of the silylene centres. Two signals are obtained for complex **1.6.62** and three signals are obtained for complex **1.6.63** in ^{29}Si NMR spectra.
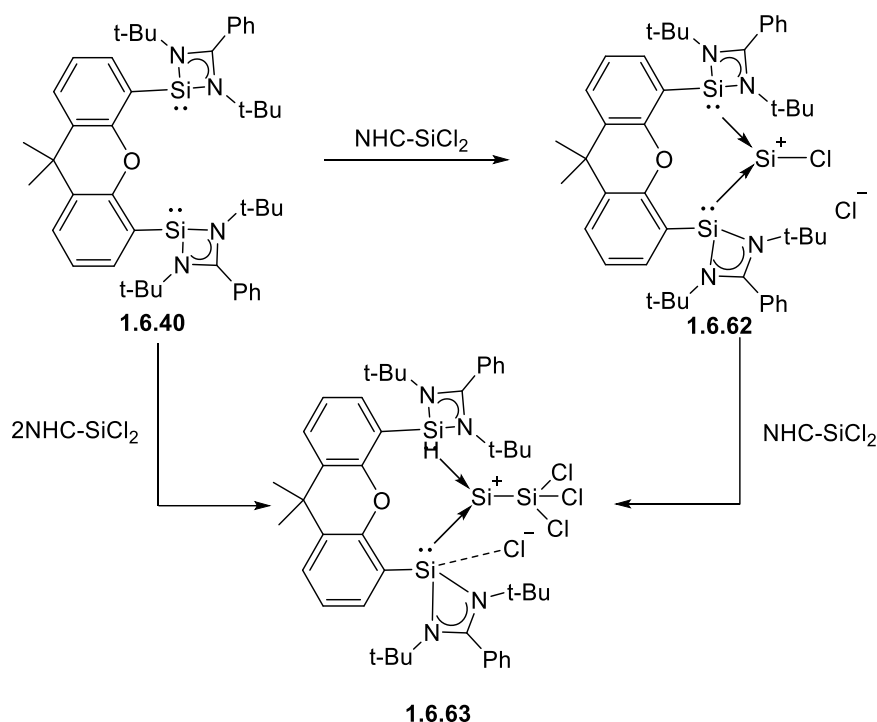
Figure 1.6.8. Synthesis of complex 1.6.62 and 1.6.63

When complex **1.6.62** is reduced with KC$_8$ the expected Si(0) complex **1.6.64** is obtained. NMR spectroscopy of complex **1.6.64** reveals highly symmetric structure of the complex and the strong σ-donation of the silylene ligands. The X-ray diffraction analysis of complex **1.6.64** revealed that the complex has long Si-Si bond due to the poor π-accepting property of the NHSi groups.[65] The O-centre of the xanthene moiety is not in contact with the central Si atom. However, DFT studies shows that the Si-Si bond length is significantly shorter than Si-Si single bond showing some double bond contribution. The Si(0) centre has one lone pair which is s-type lone pair with some p-orbital contribution. The Si-Si-Si bond is shown to be 3 centre- 2 electron bond with π-delocalisation of electrons.

1.6.62   **1.6.64**
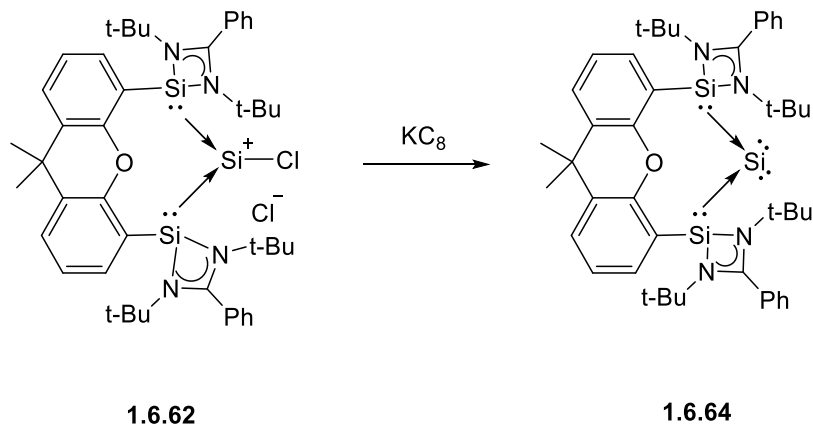
Figure 1.6.8. Synthesis of complex 1.6.64

When complex **1.6.64** was exposed to CO_2 and O_2 it decomposes but when exposed to two equivalents of N_2O it leads to the formation of complex **1.6.65**. In presence of one equivalent N_2O complex **1.6.66** is formed. Reacting complex **1.6.64** to one more equivalent of N_2O led to the decomposition of the complex proving that it is not an intermediate for the formation of complex **1.6.66**.
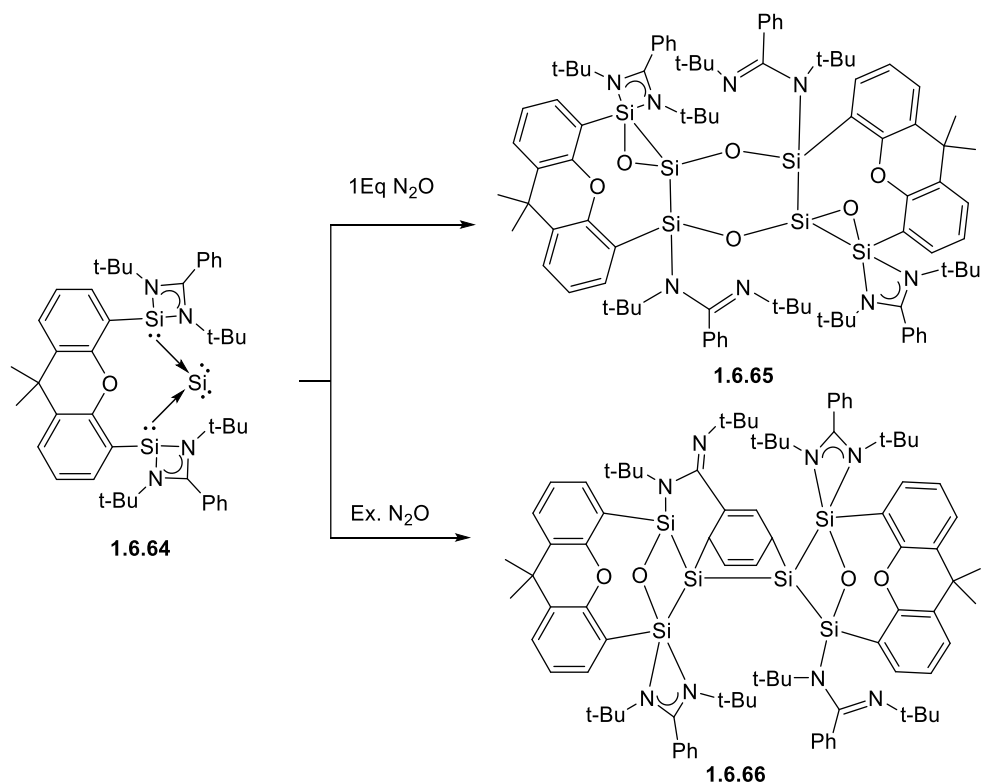
Figure 1.6.8. Synthesis of complexes 1.6.65 and 1.6.66

Further complex **1.6.64** was exposed to two equivalents of NH_3 to obtain complex **1.6.67** at room temperature. Complex **1.6.67** is a 1,3-diaminotrisilane molecule supported by a xanthene backbone. Each ammonia molecule gets activated with protons attaching to the central Si centre and the $-NH_2$ moiety attaching to the flanking Si centres.
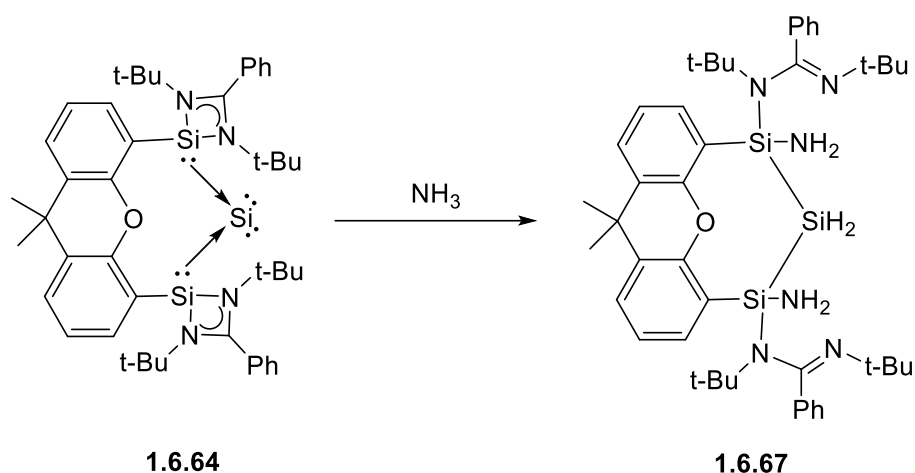
Figure 1.6.8. Synthesis of complex 1.6.67

Complex **1.6.64** was reacted with H_2 and ethylene but was found inert towards both the gases. However, in presence of BPh_3 the complex activates H_2 and ethylene to form complexes **1.6.68** and **1.6.69**. DFT studies reveal that the mechanism of activation of both the molecules involves frustrated Lewis acid-base pair activation pattern.[66]
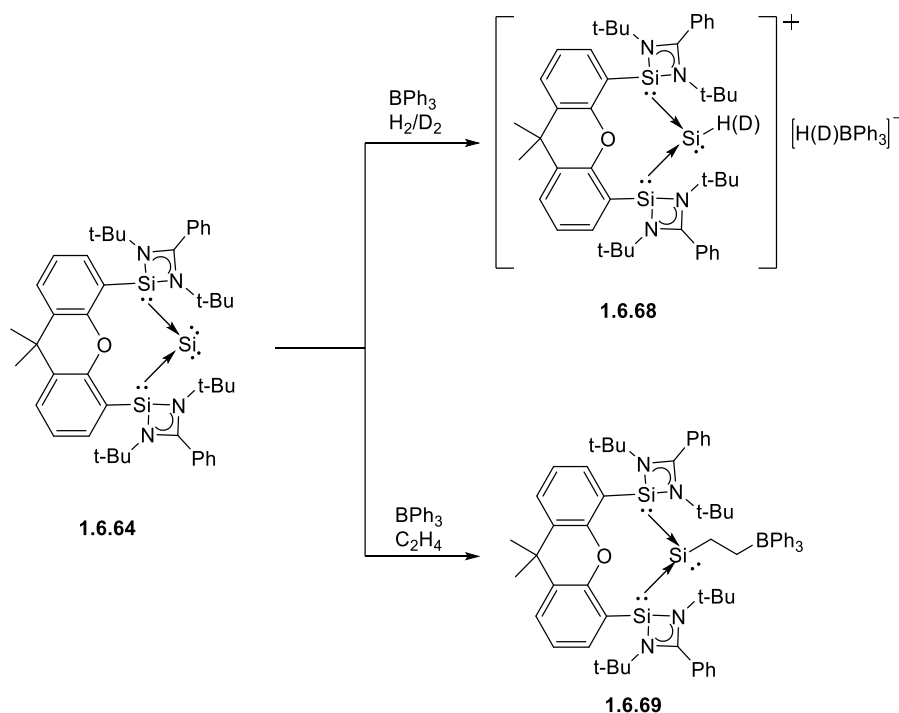
Figure 1.6.8. Synthesis of complexes 1.6.68 and 1.6.69

Ligand **1.6.30** was used for stabilising nitreones. Treatment of ligand **1.6.30** with one equivalent adamantyl azide led to the formation of neutral bis(silylium) carborane complex **1.6.70** with the adamantyl azide ligated to both the silicon centre in an end-on μ_2-bridging

mode. For the formation of complex **1.6.70** there is an intramolecular two electron transfer from silylene centres to carborane backbone converting it from neutral closo-C_2B_{10} to dianionic nido- C_2B_{10}. Due to the zwitterionic nature of the complex **1.6.70**, it is soluble in dichloromethane. The ^{29}Si NMR shows a single signal which is high field shifted in comparison to the ligand. The solid-state structure of the complex revealed a nido carborane structure with a C…C distance of 2.777 Å and has shorter Si-C bonds in comparison to that of the ligands. The Si-N bonds lie in the single bond region and the azide nitrogen bonds are found in the range of FLP-azide moieties.[67] The oxidation of both the silylene centres to Si(IV) centres occur as soon as the terminal N-atom of the azide adds to the ligand **1.6.30**.
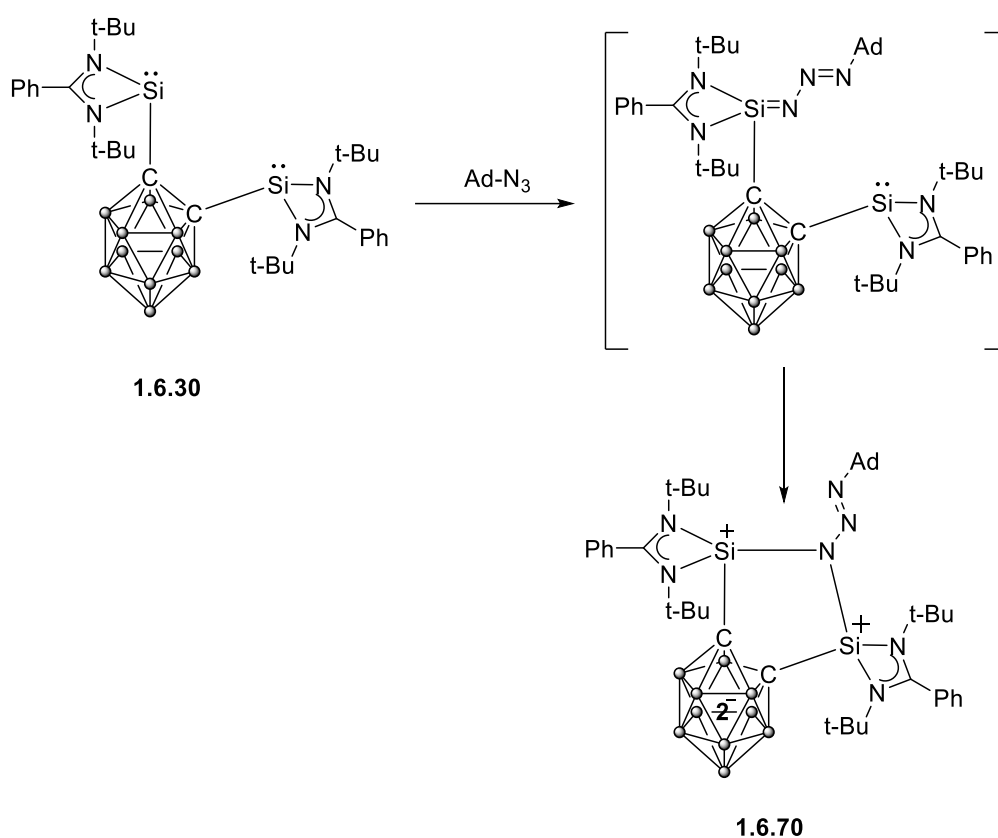
Figure 1.6.8. Synthesis of complex 1.6.70

On reduction of the complex **1.6.70** with KC_8 in presence of 18-crown-6 ether, the anionic complex **1.6.71** is formed along with the release of adamantane and dinitrogen. Most of the features of the complex **1.6.71** is similar to the complex **1.6.70**. It is found to be a charge separated complex in which the anion comprises of an anionic nido-C_2B_{10} moiety supporting a positively charged Si-N-Si moiety. Oxidation of complex **1.6.70** with AgOTf led to the formation of the cationic complex **1.6.72** with the simultaneous release of adamantane as side

product. Isotope labelling studies led to the conclusion that the carborane backbone provides for the hydrogens for the formation of adamantane. ^{1}H NMR spectrum shows a signal low field shifted in comparison to that of the complex **1.6.72** however ^{29}Si NMR shows a signal upfield shifted. The solid-state structure reveals that the carborane backbone resembles that of the ligand **1.6.30** as it converts back into a closo-carborane backbone but the SiNSi moiety resembles that of complex **1.6.71**. On mixing complexes **1.6.71** and **1.6.72** a radical complex **1.6.73**. During the salt metathesis one electron transfer occurs from complex **1.6.71** to complex **1.6.72**. This fact is supported the cyclic voltammogram studies which reveal that the oxidation of complex **1.6.71** leads to the formation of the complex **1.6.73** and finally gets oxidised to the cationic complex **1.6.72**. Further DFT studies were carried out to study the above reaction.[68]
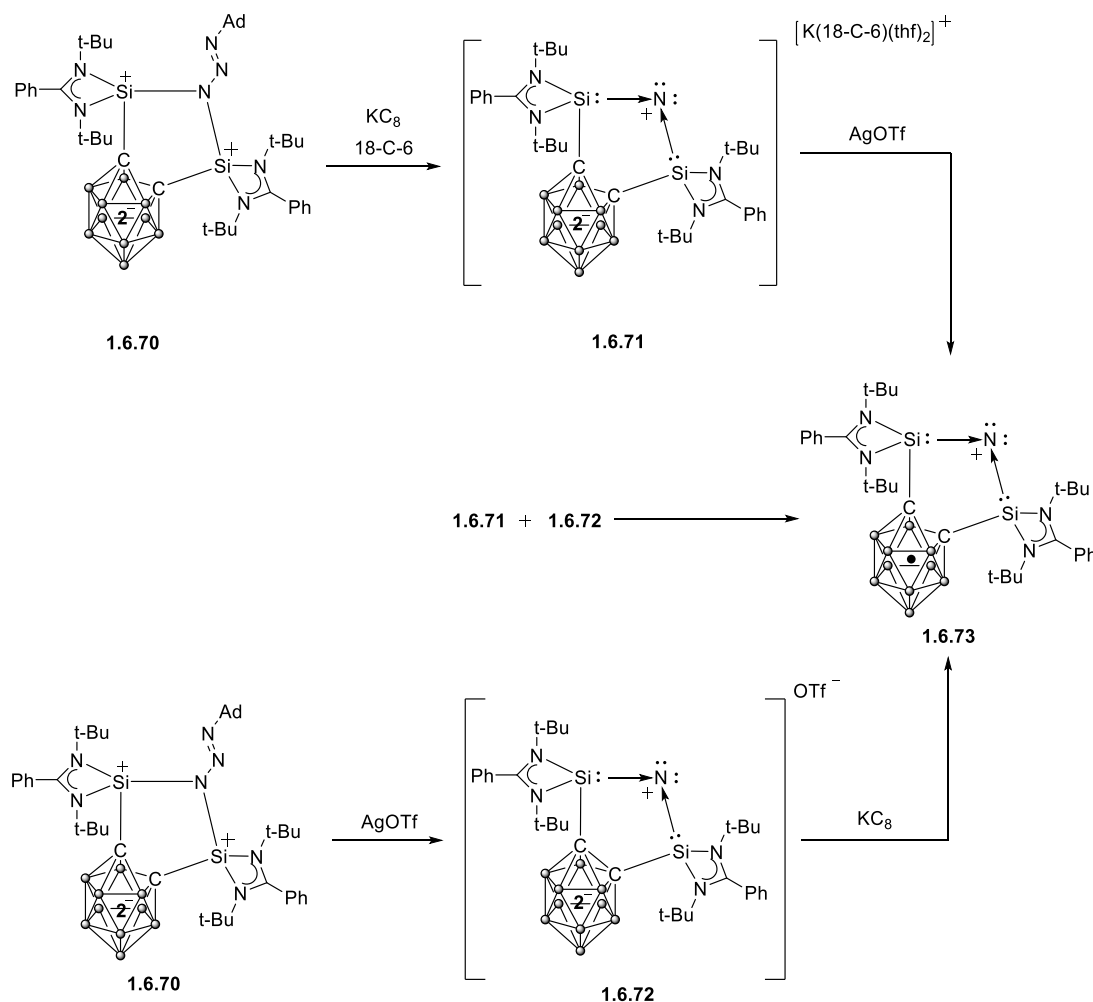
Figure 1.6.8. Synthesis of complex 1.6.73

The same ligand **1.6.30** was used to stabilise Si(0) species. The synthesis of SiCl$_2$ stabilised by ligand **1.6.30** on reacting with NHC-SiCl$_2$ failed and led to the formation of

mixture of products. So, ligand **1.6.30** was reduced first with KC_8 forming the dipotassium 1,2-bis(silylenyl)-nido-carborane dianion salt **1.6.74**. X-ray diffraction revealed the preliminary 1-D polymeric chain structure. On reacting **1.6.74** with $NHC-SiCl_2$ the desired Si(0) complex **1.6.75** supported by the bis(silenyl)-closo-carborane ligand was formed. The two electrons from the salt **1.6.74** were transferred to the Si centre leading to its reduction to Si(0) centre. The ^{29}Si NMR spectrum showed three signals for the three silicon centres. The C-C bond distance of the carborane gets reduced in comparison that of the ligand **1.6.30** confirming the formation of closo-carborane from the nidocarborane. On reducing the complex **1.6.75** with lithium naphthalenide led to the homocoupling product **1.6.76**. The X-ray diffraction analysis showed the formation of a one dimension polymeric chain of bis(silylenyl)-nido-carborane supported silyliumylidene centres forming a Si-Si bond and further these cages are connected by two $[K(THF)_2]^+$ ions. The silyliumylidene centres adopt trigonal pyramidal geometry with a lone pair at each silicon centre. The DFT studies shows that the HOMO and HOMO-1 is represented by the σ and π-lone pairs on the silicon centres. NBO analysis shows that the π-lone pair undergoes for donor-acceptor interaction with the low-valent 3p orbital of the silylene centre and the σ-lone pair interacts with the low valent sp^3 orbitals of the silylene centre. Further a detailed study of the mechanism for the formation of the complex **1.6.76** has been done.[69]
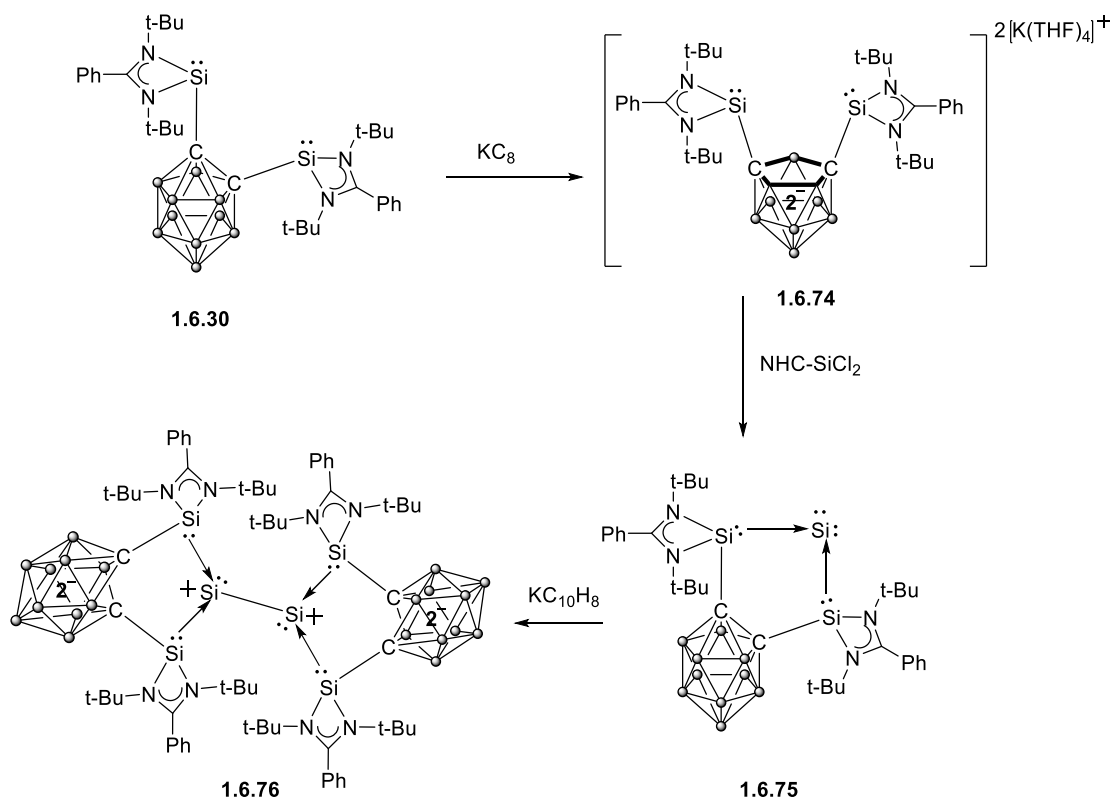
Figure 1.6.8. Synthesis of complexes 1.6.75 and 1.6.76

Ligand **1.6.40** was used to stabilise P$_2$ species formed by degrading P$_4$ molecule. On reacting ligand **1.6.40** with P$_4$ molecule led to the formation of P$_2$ complex **1.6.77**. The ^{31}P NMR spectrum shows a peak at δ= -282.4 ppm which is upfield as compared to the previously reported complexes, indicating a very strong σ-donation of the ligand **1.6.40**.[70] The ^{29}Si NMR spectrum shows a triplet at δ= 3.7 ppm with a coupling pattern due to the P-centres. The X-ray diffraction analysis reveals that the Si-P bonds are perpendicular to the P-P bonds. The P-P bond length was found the longest reported till date again showing the strong σ-donation of the ligand. DFT studies shows that the complex **1.6.77** can be represented mostly bis(silylene) supported P$_2$ moiety. Additionally negative charges were observed on the P$_2$ moiety confirming the strong electron donation of the ligand.
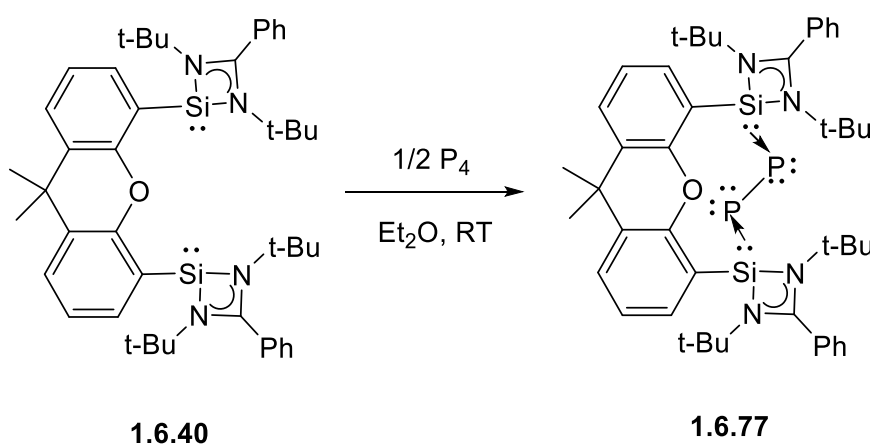
Figure 1.6.8. Synthesis of complex 1.6.77

On reacting complex **1.6.77** with CO$_2$ in 1:2 ratio complex **1.6.78** is obtained. Complex **1.6.78** exhibits a central motif having two five membered rings of Si$_2$PCO sharing a common P-P bond. The CO$_2$ molecule adds on to Si-P moiety. Controlled exposure of complex **16.1** to water vapour led to the oxidation of complex **1.6.77** to complex **1.6.79**. Complex **1.6.79** comprises of a five membered Si$_2$P$_2$O ring with a PH-PH moiety. Also, one of the Si centres of the ligand is five coordinated and the other is four coordinated leading to an unsymmetrical structure. Further Complex **1.6.77** was reacted with 9-BBN to obtain complex **1.6.80**. Complex **1.6.80** is a phosphinoborane with P→B coordination bond. The B-H hydrogen atom adds to the PhC moiety of one of the [PhC(NtBu)$_2$]Si group. On reacting with Cr(CO)$_6$ complex **1.6.77** affords cationic complex **1.6.81**and [Cr(CO)$_5$(PCO)] as counter anion. Complex **1.6.81**is a P(I) cation stabilised by the ligand **1.6.40**. P$^-$ inserts into Cr-CO bond to form the counter anion with a PCO moiety.
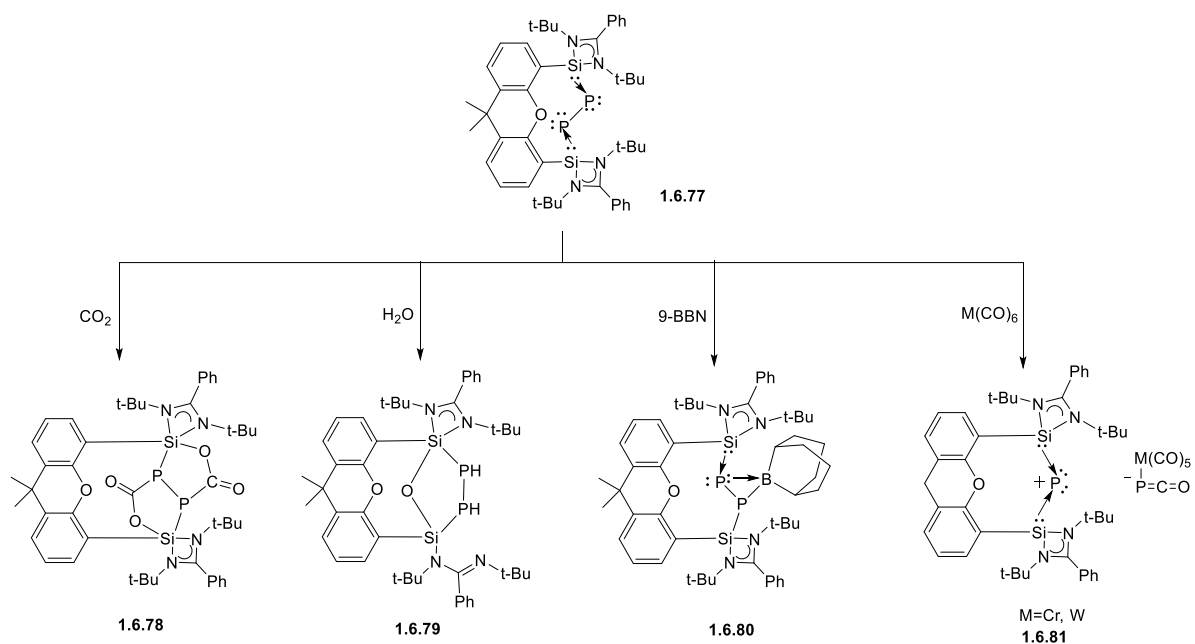
Figure 1.6.8. Reactivity Study of complex 1.6.77

To further elucidate the mechanism of the previous reaction, complex **1.6.77** was reacted with CO. However, the complex decomposed as the PCO moiety generated was not stabilised by the reaction conditions. So, it was reacted with 1,3,4,5-tetramethylimidazol-2-ylidene to obtain complex **1.6.82**. To induce cleavage of the Si-P bond and subsequent phosphorus transfer it was reacted with [PhC(N*t*Bu)₂]GeCl for the Cl/P exchange reaction. The reaction led to the formation of bis(silylene) supported P⁺Cl⁻ complex **1.6.83** and NHC-supported germylidenylphosphinidene complex **1.6.84**. Thus, the heterolytic cleavage of the P_2 moiety by NHC is the key step to the mechanism of the PCO transfer reaction.[71]
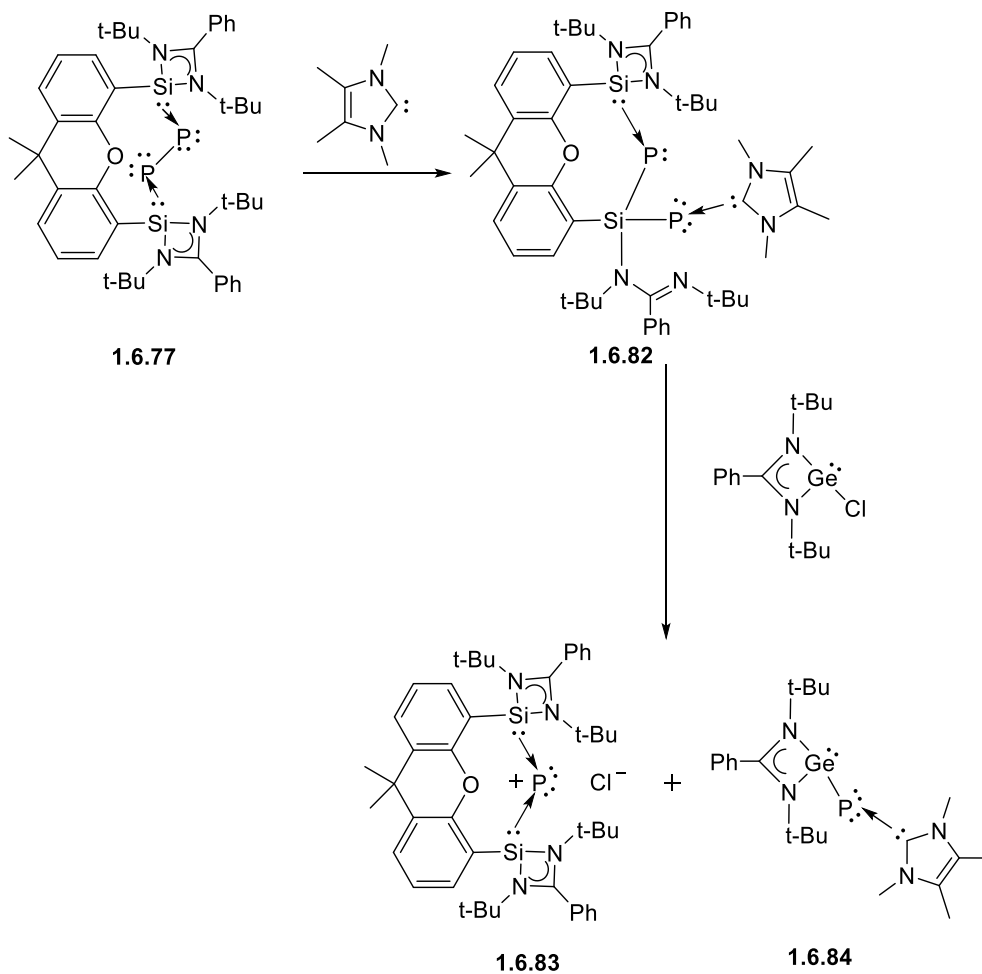
Figure 1.6.8. Stabilisation of P(I) complex 1.6.84

Again ligand **1.6.40** was used to stabilise a Sn(0) complex. When reacted with one equivalent of $SnCl_2$.Dioxane and $SnBr_2$.Dioxane it led to the formation of complexes **1.6.85** and **1.6.86** respectively. The ^{29}Si NMR spectrum depicts that the signal for both the complexes is downfield shifted as compared to that of the ligand. In case of complex **1.6.85,** the Sn(II) centre remains in trigonal pyramidal coordination geometry with the chloride counter anion attached to one of the silylene centre of the ligand. However, in complex **1.6.86** the Sn(II) centre remains four coordinated adopting a see-saw geometry for the bromine centres and the Sn centre in the apical position.
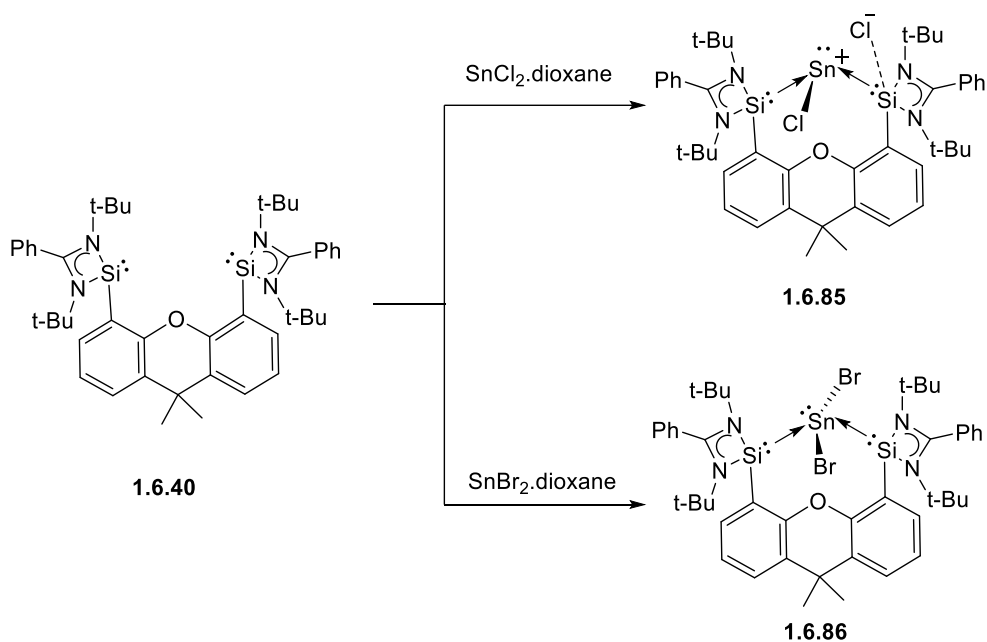
Figure 1.6.8. Synthesis of complexes 1.6.85 and 1.6.86

Reducing both the complexes with KC_8 or $Na(C_{10}H_8)$ were attempted but led to no significant products. Hence, the reduction of complex **1.6.85** was performed in presence of Collman's reagent $K_2[Fe(CO)_4]$ to afford complex **1.6.87**. The molecular structure of complex **1.6.87** reveals a bis(silylene) supporting an Sn(0) centre which further coordinates to two independent $Fe(CO)_4$ moieties.
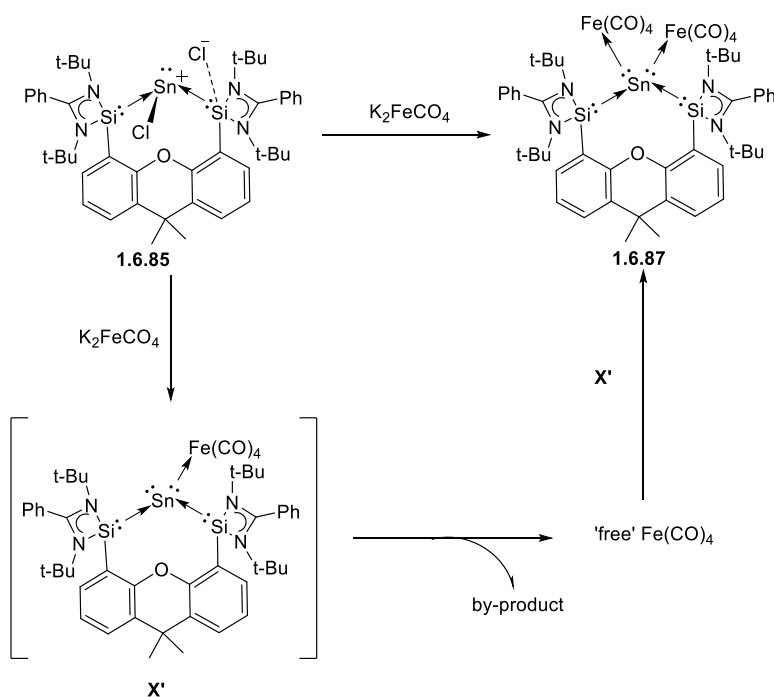
Figure 1.6.8. Synthesis of complex 1.6.87

Complex **1.6.87** was further reduced with KC$_8$ to afford the anticipated stannylone complex **1.6.88**. The signals of ^{29}Si NMR spectrum of complex **1.6.88** was found to be downfield shifted in comparison to that of complexes **1.6.87** and ligand **1.6.40**. Complex **1.6.88** was found to be decomposing in solution on standing. However, it can be converted back to complex **1.6.87** by reacting it with Fe$_2$(CO)$_9$. The solid-state structure of the complex reveals that the Si-Sn bond lengths are intermediate between Si-Sn single and Si-Sn double bond. DFT studies confirmed this fact as it was found that HOMO and HOMO-1 correspond to a σ-lone pair and a π-lone pair on the Sn(0) centre. The π-lone pair delocalize into the adjacent Si(II) vacant orbitals and the σ-lone pair remains on the Sn(0) centre.[72]
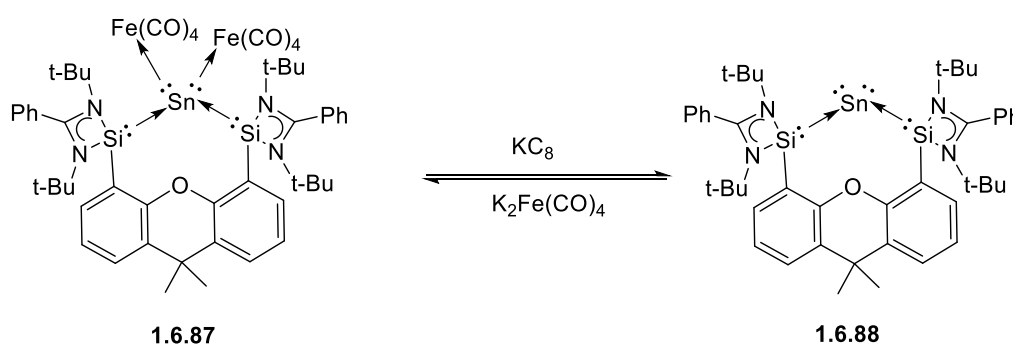
Figure 1.6.8. Synthesis of complex 1.6.88

Activation of small molecules

Ligand **1.6.13** and **1.6.40** were used to activate CO molecule to reductive couple them into corresponding ketene molecule. On reacting **1.6.13** and **1.6.40** with CO at room temperature led to the formation of the corresponding ketene molecules **1.6.89** and **1.6.90** in good yields. Both the complexes were fully characterised by Single crystal X-ray diffraction and NMR studies. The ^{29}Si NMR spectrum of complex **1.6.90** shows upfield shifted signals in comparison to that of the ligand **1.6.40** revealing the change of Si(II) centres to Si(IV) centres for the formation of ketenes. The IR spectrum shows a strong absorption band υ= 2069 cm^{-1} confirming the presence of C=C=O species. The solid-state structure of complex **1.6.90** showed that there is formation of a planar four membered ring of Si$_2$OC where the two Si centres are five coordinated and closer than the ligand **1.6.40** distorting the planar xanthene ring. Similar to the ligand **1.6.40**, bis(NHSi)benzofuran was synthesized and reacted with CO gas but it was found unreactive towards the CO gas. This was due to the longer Si…Si distance that does not facilitates the activation of CO molecule. Ligand molecules **1.6.13** and **1.6.40** provided the

appropriate distance for the activation of CO molecule. Further, isotopically labelled CO molecules were used to study the reductive coupling reaction. When both the ligands were exposed to ^{13}C labelled CO molecules, the respective ^{13}C labelled complexes **1.6.89** and **1.6.90** were obtained with [13]C=[13]C=O moiety. DFT calculations were done to further elucidate the mechanism. It was found that the HOMO and HOMO-1 which resides on the silylene centres attacks the π^* orbitals of CO molecule as lewis base which activates the molecule.
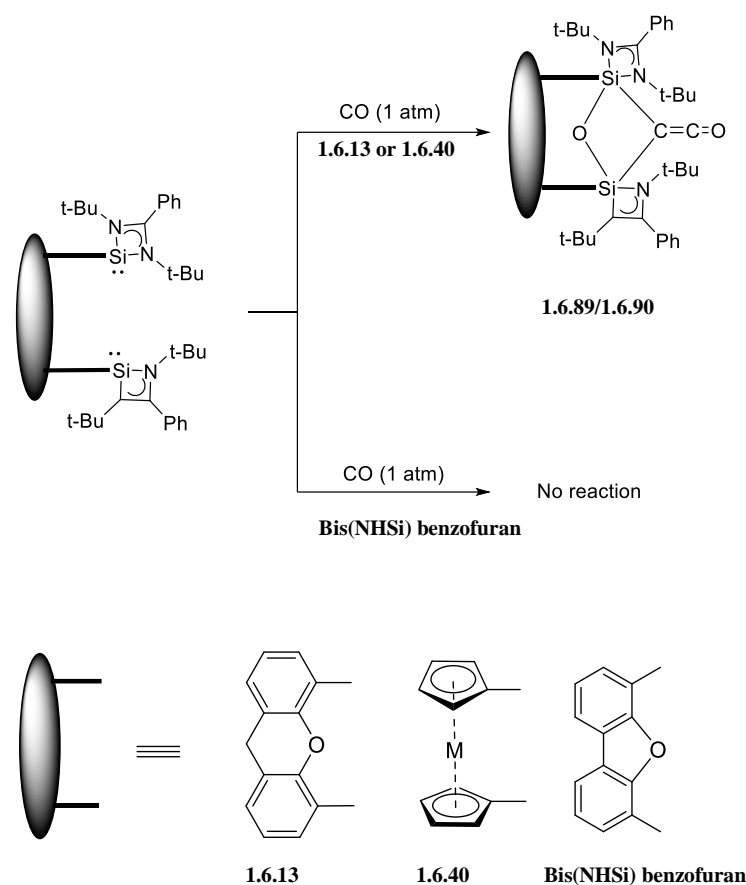
Figure 1.6.8. Synthesis of complex 1.6.89 and 1.6.90

Further reaction of ligand **1.6.40** with Xyl-NC (Xyl= 2,6-Me$_2$C$_6$H$_3$) led to the reversible formation of complex **1.6.91**. ^{1}H NMR spectrum of complex **1.6.91** revealed that the two methyl groups of the isocyanide are not magnetically equivalent anymore. Also, the aromatic hydrogens of the isocyanide are shifted upfield indicating the aromaticity of the molecule is lost, activating the aromatic ring. ^{29}Si NMR depicts that the two silicon centres have different shifts. Molecular structure reveals that complex **1.6.91** is a highly conjugated (silyl)(imido)silene derivative which is identified to have an intermediate **1.6.91'**. Reaction of intermediate **1.6.91'** with one more equivalent of XylNC led to the rearomatization of the isocyanide leading to formation of complex **1.6.93** and a small amount of complex **1.6.92**.

43
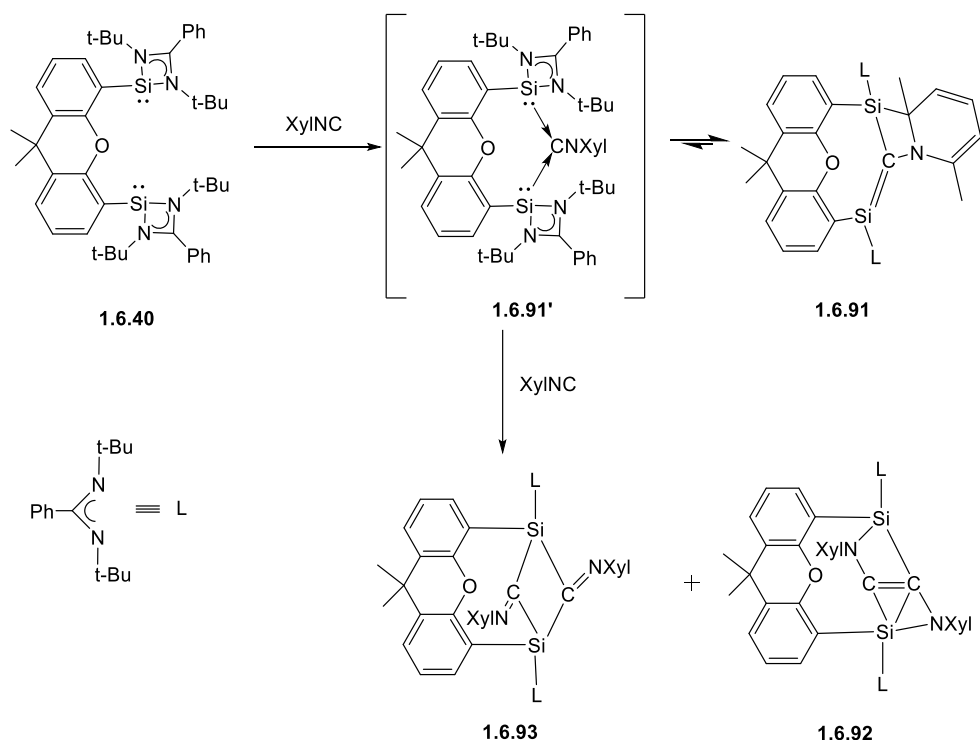
Figure 1.6.8. Synthesis of complex 1.6.91, 1.6.92 and 1.6.93

However, complex **1.6.93** does not react further with CO to form the compound analogous to ketene due to steric hindrance. Exposing complex **1.6.91** to CO led to the formation of complex **1.6.94** which is a ketenimine analogue of complex **1.6.90**. The complex showed a single signal in the ^{29}Si NMR spectrum proving a very symmetrical molecule. Molecular structure revealed that the single O atom bridges the two silicon centres forming a disilaketenimine. Reaction with ^{13}CO led to the formation of ^{13}C=C=N and C=^{13}C=N moieties containing complex **1.6.94** indicating no coupling occurs. So, in conclusion scrambling of carbon atoms happen during the formation of disilaketenimine **1.6.94** however no such scrambling was observed for the formation of complex **1.6.90**.[73]
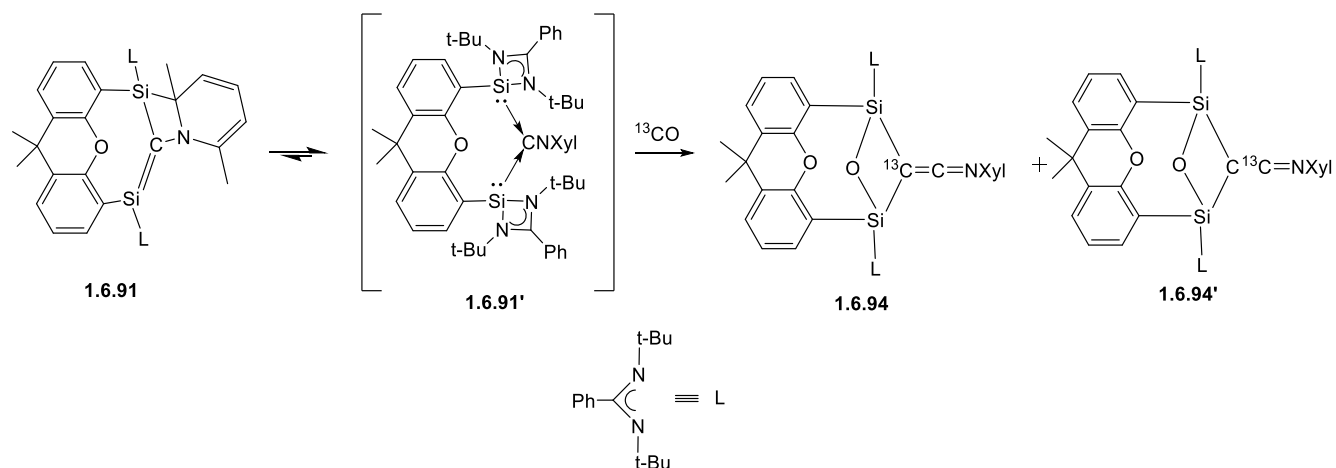
Figure 1.6.8. Synthesis of complex 1.6.94

Complex **1.6.89** reacted with ammonia and amines to give corresponding acetamides along with Fc-disiloxanediamines. So, when reacted with ammonia it yielded the acetamide and corresponding Fc-disiloxanediamine. With N-benzylamine, it yielded acetamide and disilyldiamine. All the molecules were fully characterised by SCXRD, NMR spectroscopy, IR spectroscopy and ESI mass spectrometry and DFT studies were carried out to study the mechanism.[74]
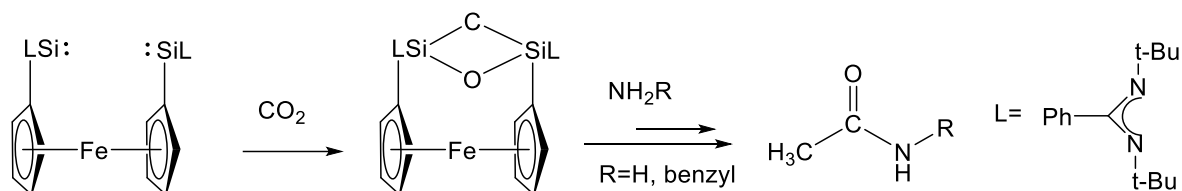
Figure 1.6.8. Homocoupling of CO₂ and Ammonia/primary amines

Ligand **1.6.30** was used to activate CO and 2,6-dimethylphenyl isocyanide and was found that it is more reactive than the previously reported ligands. However, due to the rigidity of the ligand **1.6.30** it was found to show different reactivity in comparison to the previous report. When reacted with CO, no silaketene intermediate was found to form due to the rigidity of the carborane backbone. However, complex **1.6.95** was formed which is head-to-head homocoupling product of CO with the ligand **1.6.30**. The complex crystallises in P-1 triclinic space group. The molecular structure depicts to have three rings, One eight-membered $Si_2C_4O_2$ ring and two four membered SiOSiC rings. Both the Si centres are pentacoordinate and remain in a distorted trigonal bipyramidal geometry. However, the ^{29}Si NMR revealed two different peaks indicating the presence of two different silicon centres. On reacting ligand

1.6.30 with 2,6-dimethylphenyl isocyanide, it was homocoupling in a head-to-tail fashion to produce complex **1.6.96**. Irrespective of the chosen molar ratio of the ligand and 2,6-dimethylphenyl isocyanide, complex **1.6.96** is obtained in every case. NMR studies shows that there are two different silicon centres. Solid state structure revealed that one of the silicon is tetracoordinate featuring a distorted tetrahedral coordination environment and the other silicon centre is pentacoordinate with a distorted trigonal bipyramidal geometry. It crystallises in P2$_{1/n}$ space group and it shows the homocoupling of two molecules of isocyanide to form N=C-N-C and concomitantly forms Si-C bond. All the attempts to separate or identify an intermediate failed. So, DFT studies were carried out to elucidate the mechanism.[75]
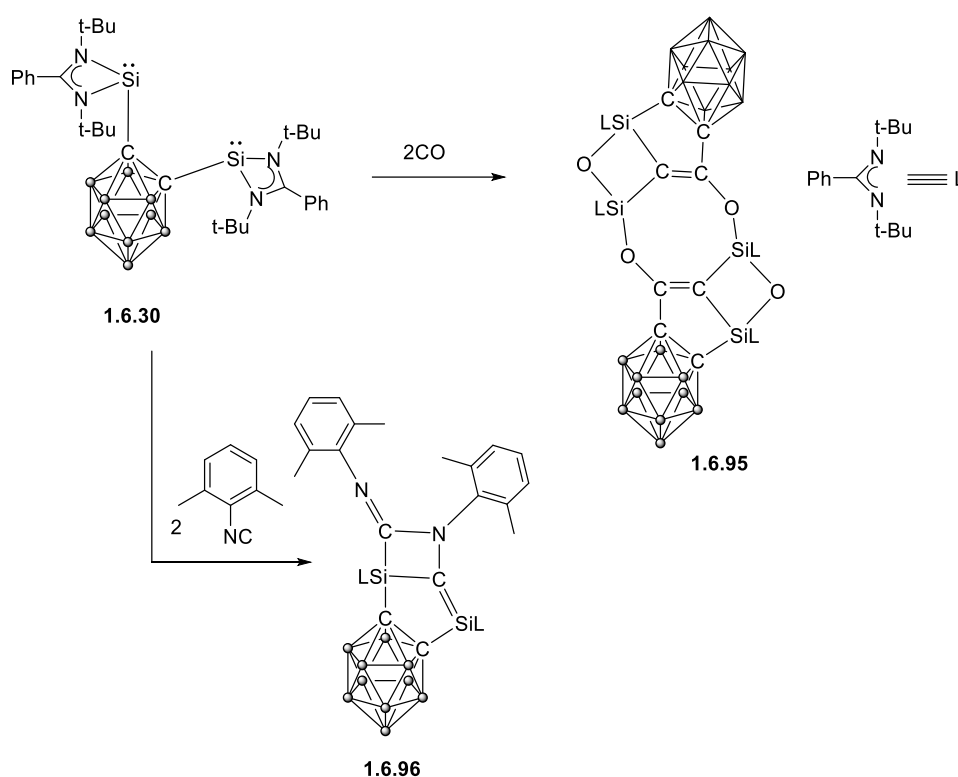
Figure 1.6.8. Synthesis of complex 1.6.95 and 1.6.96

Ligand **1.6.13** was reacted with BPh$_3$ led to the formation of bis(silylene-borane) adduct **1.6.97**. Compound **1.6.97** crystallised in P12$_1$/c1 space group in which both the silicon centres adopt a distorted tetrahedral geometry. ^{29}Si NMR signals shows that it is downfield shifted in comparison to that of the ligand **1.6.13** confirming the formation of compound **1.6.97**. Compound **1.6.97** was reacted with CO$_2$ to obtain compound **1.6.98**. X-ray diffraction analysis revealed the formation of borane stabilized bis(silanone). It was found to be stable in solution up to 60°C. The ^{29}Si NMR showed that the silanone has a high field signal in comparison to

that of the compound **1.6.97**. To remove BPh_3 and to form an isolated bis(silanone), compound **1.6.98** was reacted with PMe_3. The reaction led to the formation of $BPh_3.PMe_3$ adduct and 1,3,2,4-cyclodisiloxane complex **1.6.99**. The ^{29}Si NMR showed a drastically high-field signal. The reaction of ligand **1.6.13** with 1 bar of CO_2 led to the formation of compound **1.6.99**.[76]
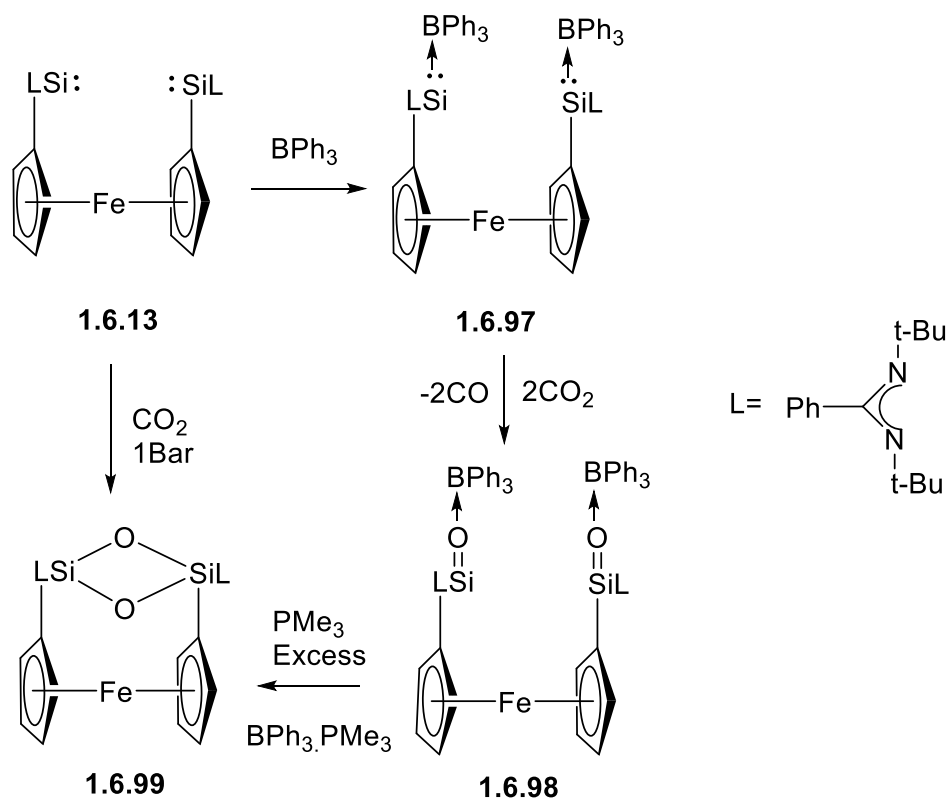
Figure 1.6.8. Synthesis of complex 1.6.97, 1.6.98 and 1.6.99

A new ligand bis(silylene)terphenylene **1.6.45** was reacted with CS_2 molecule affording an unusual compound which is the dearomatized product **1.6.100**. It forms due to the cycloaddition of a reactive silene intermediate to the phenylene ring. Two different bis(silylene) **1.6.45^{Ph}** and **1.6.45^{Mes}** were used and the corresponding product obtained were characterised by HR-ESI mass spectrometry, NMR spectroscopy and X-ray diffraction analysis. The mechanism of the formation was also studied by DFT calculations.[77]
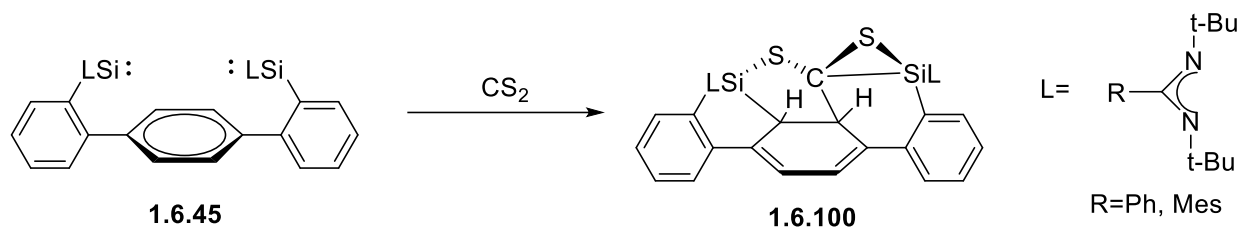
Figure 1.6.8. Synthesis of complex 1.6.100

1.7. References

1. a) Power, P.P. *Nature*; **2010**, *463*, 171-176. b) Yadav, S.; Saha, S.; Sen, S.S. *ChemCatChem*, **2016**, *8*, 486 – 501.

2. Power, P. P. *Chem. Rev*., **1999**, *99*, 3463–3503.

3. a. Gaspar, P. P.; West, R.; Silylene Chemistry of Organic Silicon Compounds 2, Part 3 (eds Rappoport, Z. & Apeloig, Y.) 2463–2568 (Wiley, 1998). b) Mizuhata, Y.; Sasamori, T.; Tokitoh, N. *Chem. Rev*., **2009**, *109*, 3479–3511.

c. Linti, G.; Schnöckel, H. *Coord. Chem. Rev*., **2000**, *206–207*, 285–319.

4. Stephan, D. W. Dalton Trans., **2009**, 3129–3136.

5. Power, P. P. *Chem. Rev*., **2003**, *103*, 739–809.

6. Arduengo III, A. J.; Harlow, R. L.; Kline, M. *J. Am. Chem. Soc*., **1991**, *113*, 361–363.

7. Hopkinson, M. N.; Richter, C; Schedler, M.; Glorius, F. *Nature*, **2014**, *501*, 485-496.

8. a) Heinemann, C.; Müller, T.; Apeloig, Y.; Schwarz, H. *J. Am. Chem. Soc*., **1996**, *118*, 2023–2038. b) Arduengo III, A. J.; Rasika Dias, H. V.; Harlow, R. L.; Kline, M. *J.Am. Chem. Soc*., **1992**, *114*, 5530–5534. c) Herrmann, W. A. Köcher, C.; *Angew. Chem. Int. Ed.*, **1997**, *36*, 2162–2187. d) de Frémont, P.; Marion, N.; Nolan, S. P. *Coord. Chem. Rev*., **2009**, *253*, 862–892. e) Bourissou, D.; Guerret, O.; Gabbaï, F. P.; Bertrand, G. *Chem. Rev*., **2000**, *100*, 39–92.

9. Arduengo III, A. J.; Goerlich, J. R.; Marshall, W. J.; *J. Am. Chem. Soc*., 1995, **117**, 11027–11028.

10. Melaimi, M.; Soleilhavoup, M.; Bertrand, G. *Angew. Chem. Int. Ed*., **2010**, *49*, 8810–8849.

11. Lavallo, V.; Canac, Y.; Präsang, C.; Donnadieu, B.; Bertrand, G. *Angew. Chem. Int. Ed*., **2005**, *44*, 5705–5709.

12. Aldeco-Perez, E. et al. *Science*, **2009**, *326*, 556–559.

13. Schuster, O.; Yang, L.; Raubenheimer, H. G.; Albrecht, M.; *Chem. Rev*., **2009**, *109*, 3445–3478.

14. Tomás-Mendivil. E.; Hansmann, M. M.; Weinstein, C. M.; Jazzar, R.; Melaimi, M. Bertrand, G. *J. Am. Chem. Soc.* **2017**, *139*, 7753-7756.

15. Hadlington, T. J.; Driess, M.; Jones, C. *Chem. Soc. Rev.* **2018**, *47*, 4176-4197.

16. a) Jutzi, P.; Hoffmann, H. J.; Brauer, D. J.; Krueger, C. *Angew. Chem.* **1973**, *85*, 1116-1117. b)Stobart, S. R. *J. Chem. Soc., Chem. Commun.* **1979**, 911-912.

17. Harris, D. H.; Lappert, M. F. *J. Chem. Soc., Chem. Commun.* **1974**, 895-896.

18. Veith, M. *Angew. Chem. Int. Ed. Eng.* **1987**, *26*, 1-14.

19. a) Tokitoh, N.; Manmaru, K.; Okazaki R. *Organometallics* **1994**, *13*, 167-171. b) Tokitoh,

N.; Matsumoto, T.; Manmaru, K.; Okazaki, R.; *J. Am. Chem. Soc.* **1993**, *115,* 8855-8856. c) Tokitoh, N.; Kishikawa, K.; Matsumoto, T.; Okazaki, R. *Chem. Lett.*, **1995**, 827-828.

20. Kira, M. I.; S.; Iwamoto, T.; Ichinohe, M.; Kabuto, C.; Ignatovich, L.; Sakurai, H. *Chem.Lett.* **1999**, 263-264.

21. a) Herrmann, W. A.; Denk, M.; Behm, J.; Scherer, W.; Klingan, F.-R.; Bock, H.; Solouki, B.; Wagner, M. *Angew. Chem., Int. Ed. Engl.* **1992**, *104*, 1489-1492; b) Kuehl, O.; Loennecke, P.; Heinicke, J. *Polyhedron* **2001**, *20*, 2215-2222; c) Baker, R. J.; Jones, C.; Mills, D. P.; Pierce, G. A.; Waugh, M. *Inorg. Chim. Acta* **2008**, *361*, 427-435; d) Raut, R.K.; Amin, S, F.; Sahoo, P.; Kumar, V.; Majumdar, M. *Inorganics* **2018**, *6*, 69-75.

22. Jones, C.; Rose, R. P.; Stasch, A. *Dalton Trans.* **2008**, 2871-2878; b) Foley, S. R.; Bensimon, C.; Richeson, D. S. *J. Am. Chem. Soc*. **1997**, *119*, 10359-10363; c) Nagendran, S.; Sen, S. S.; Roesky, H. W.; Koley, D.; Grubmüller, H.; Pal, A.; Herbst-Irmer, R. *Organometallics* **2008**, *27*, 5459-5463.

23. Harris, D. H.; Lappert, M. F. *J. Chem. Soc., Chem. Commun.* **1974**, 895-896; b) Davidson, P. J.; Lappert, M. F. *J. Chem. Soc. Chem. Commun.* **1973**, 317-318.

24. Kira, M.; Yauchibara, R.; Hirano, R.; Kabuto, C.; Sakurai, H. *J. Am. Chem. Soc.* **1991**, *113*, 7785-7787.

25. Weidenbruch, M.; Schlaefke, J.; Schafer, A.; Peters, K.; Vonschnering, H. G.; Marsmann, H. *Angew. Chem., Int. Ed. Engl.* **1994**, *33*, 1846-1848. b) Yang, X. J.; Wang, Y. Z.; Wei, P. R.; Quillian, B.; Robinson, G. H. *Chem. Commun.* **2006**, 403-405. c) Tajima, T.; Takeda, N.; Sasamori, T.; Tokitoh, N. *Organometallics* **2006**, *25*, 3552-3553. d) Simons, R. S.; Pu, L. H.; Olmstead, M. M.; Power, P. P. *Organometallics* **1997**, *16*, 1920-1925. e) Spikes, G. H.; Peng, Y.; Fettinger, J. C.; Power, P. P. *Z. Anorg. Allg. Chem.* **2006**, *632*, 1005-1010. f) Kano, N.; Shibata, K.; Tokitoh, N.; Okazaki, R. *Organometallics* **1999**, *18*, 2999-3007.

26. Gans-Eichler, T.; Gudat, D.; Nieger, M.; *Angew. Chem. Int. Ed*., 2002, **41**, 1889-1891.

27. Jutzi, P.; Kohl, F.; Hofmann, P.; Krüger, C.; Tsay, Y.-H. *Chem. Ber.***1980**, *113*, 757-758.

28. Dias, H. V. R.; Wang, Z. *J. Am. Chem. Soc.* **1997**, *119*, 4650-4655; (b) Dias, H. V. R.; Jin, W. J. Am. Chem. Soc. 1996, 118, 9123-9126.29. Probst, T.; Steigelmann, O.; Riede, J.; Schmidbaur, H. *Angew. Chem., Int. Ed. Engl.* **1990**, *29*, 1397-1398.

30. Singh, A. P.; Roesky, H. W.; Carl, E.; Stalke, D.; Demers, J.-P. Lange, A. *J. Am. Chem. Soc.* **2012**, *134*, 4998-5003.

31. Ochai, T.; Franz, D.; Wu, X.; Inoue, S.; *Dalton. Trans,* **2015,** *44*, 10952-10956.

32. Sarkar, D.; Weetman, C.; Dutta, S.; Schubert, E.; Jandl, C.; Kolet, D.; Inoue, S.; J. *Am.*

Chem. Soc., **2020,** *142,* 15403-15411.

33. Peng, Y.; Guo, J.-D.; Ellis, B. D.; Zhu, Z.; Fettinger, J. C.; Nagase, S.; Power, P. P. *J. Am. Chem. Soc.* **2009,** *131,* 16272

34. Peng, Y.; Ellis, B. D.; Wang, X.; Power, P. P. *J. Am. Chem. Soc.* **2008,** *130,* 12268.

35. Li, J.; Li, B.; Liu, R.; Jiang, L.; Zhu, H.; Roesky, H.W.; Dutta, S.; Koley, D.; Liu, W.; Ye, Q.; *Chem.Eur.J.,* **2016,** *22,* 14499–14503.

36. Del Rio, N.; Lopez-Reyes, M.; Baceiredo, A.; Saffon-Merceron, N.; Lutters, D.; Muller, T.; Kato, T.; *Angew.Chem.Int.Ed.,* **2017,** *56,* 1365–1370.

37. Sarkar, D.; Dutta. S.; Weetman, C.; Schubert, E.; Kolet, D.; Inoue, S.; *Chem. Eur. J.* **2021,** *27,* 13072–13078.

38. Wang, W. Inoue, S.; Yao, S.; Driess, M.; *J. Am. Chem. Soc.* **2010,** *132,* 15890–15892.

39. Sheldrick, W. S., In *The Chemistry of Organic Silicon Compounds*; Patai, S., Rappoport, Z., Eds.; Wiley: New York, 1989; Vol. 1, Chapter 3, and references therein.

40. a) Meltzer, A.; Praesang, C.; Milsmann, C.; Driess, M. *Angew. Chem.,Int. Ed.* **2009,** *48,* 3170-3173. b) Meltzer, A.; Praesang, C.; Driess, M. *J. Am. Chem. Soc.* **2009,** *131,* 7232-7233. c) Meltzer, A.; Inoue, S.; Praesang, C.; Driess, M. *J. Am. Chem. Soc.* **2010,** *132,* 3038-3046.

41. Tan, G.; Blom, B.; Gallego, G.; Driess, M.; *Organometallics* **2014,** *33,* 1, 363–369.

42. Watanabe, C.; Iwamoto, T.; Kabuto, C.; Kira, M.; *Angew. Chem. Int. Ed.* **2008,** *47,* 5386-5389.

43. a) Dupont, J.; Consorti, C. S.; Spencer, J.; *Chem. Rev.* **2005,** *105,* 2527-2572. b) Szabö, K. J. *Synlett* **2006,** 811. c) Selander, N.; Szabö, K. J.; *Dalton Trans.* **2009,** 6267-6279. d) Selander, K. J. Szabö, *Chem. Rev.* **2011,** *111,* 2048-2076. e) Zhang, H.; Lei, A.; *Dalton Trans.* **2011,** *40,* 8745-8754.

44. Wang, W.; Inoue, S.; Irran, E.; Driess, M.; *Angew. Chem. Int. Ed.* **2012,** *51,* 3691 –3694.

45. Corey, J. Y.; Braddock-Wilking, J.; *Chem. Rev.* **1999,** *99,* 175-292. b) Corey, J. Y.; *Chem. Rev.,* **2011,** *111,* 863-1071.

46. Nagendran, S.; Sen, S. S.; Roesky, H.W.; Koley, D.; Grubmüller, H.; Pal, A.; Herbst-Irmer, R.; *Organometallics* **2008,** *27,* 5459-5463.

47. Brück, A.; Gallego, D.; Wang, W.; Irran, E.; Driess, M.; Hartwig, J.F.; *Angew. Chem. Int. Ed.* **2012,** *51,* 11478 –11482.

48. Wang, W.; Inoue, S.; Enthaler, S.; Driess, M.; *Angew. Chem. Int. Ed.* **2012,** *51,* 6167-6171.

49. Gallego, D.; Brück, A.; Irran, E.; Meier, K.; Kaupp, M.; Driess, M.; Hartwig, J. F.; *J. Am. Chem. Soc.* **2013,** *135,* 15617−15626.

50. Tobita, H.; Matsuda, A.; Hashimoto, H.; Ueno, K.; Ogino, H. *Angew. Chem., Int. Ed.* **2004,**

43, 221−224.

51. Mesänen, T. T.; Gallego, G.; Szilvási, T.; Driess, M.; Oestreich, M.; *Chem. Sci*., **2015**, *6*, 7143-7149.

52. Gallego, D.; Inoue, S.; Blom, B.; Driess, M.; *Organometallics* **2014**, *33*, 6885–6897.

53. Zhou, Y.; Raoufmoghaddham, S.; Szilvási, T.; Driess, M.; *Angew. Chem. Int. Ed*. **2016**, *128*, 13060–13064.

54. a) Blom, B.; Tan, G.; Enthaler, S.; Inoue, S.; Epping, J. D.; Driess, M., *J. Am. Chem. Soc.* **2013**, *135*, 18108–18120. b) Kubo, H.; Hirano, M.; Komiya, S.; *J. Organomet. Chem.* **1998**, *556*, 89-95.

55. Lueke, M.; Porwal, D.; Kostenko, A.; Zhou, Y.; Yao, S.; Keck, M.; Limberg C.; Oestreich, M.; Driess, M.; *Dalton Trans*., **2017**, *46*, 16412–16418.

56. So, C. W.; Roesky, H. W.; Gurubasavaraj, P. M.; Oswald, R. B.; Gamer, M. T.; Jones, S. Blaurock, P. G.; *J. Am. Chem. Soc.* **2007**, *129*, 12049–12054.

57. Denk, M.; Lennon, R.; Hayashi, R.; West, R.; Belyakov, A. V.; Verne, H. P.; Haaland, A.; Wagner, M.; Metzler, N.; *J. Am. Chem. Soc.* **1994**, *116*, 2691–2692.

58. Schmidt, M.; Blom, B.; Szilvási, T.; Schomäcker, R.; Driess, M.; *Eur. J. Inorg. Chem.* **2017**, 1284–1291.

59. Wang, Y.; Kostenko, A.; Yao, S.; Driess. M.; *J. Am. Chem. Soc*. **2017**, *139*, 13499−13506.

60. Lücke, M.; Yao, S.; Driess, M.; *Chem. Sci*., **2021**, *12*, 2909-2915.

61. Chen, Xi.; Wang, H.; Du, S.; Driess, M.; Mo, Z.; *Angew. Chem. Int. Ed.* **2021**, *60*, e202114598.

62. a) Xiong, Y.; Yao, S.; Tan, G.; Inoue, S.; Driess, M.; *J. Am. Chem. Soc*. **2013**, *135*, 5004–5007. b) Xiong, Y.; Yao, S.; Inoue, S.; Berkefeld, A.; Driess, M.; *Chem. Commun*. **2012**, *48*, 12198–12200. c) Singh, A. P.; Roesky, H. W.; Carl, E.; Stalke, D.; Demers, J.-P.; Lange, A.; *J. Am. Chem. Soc*. **2012**, *134*, 4998–5003.

63. Zhou, Y.; Karni, M.; Yao, S.; Apeloig, Y.; Driess, M.; *Angew. Chem. Int. Ed*. **2016**, *55*, 15096 –15099.

64. Zhou, Y.; Karni, M.; Yao, S.; Apeloig, Y.; Driess, M.; *J. Am. Chem. Soc*. **2019**, *141*, 1655−1664.

65. Ishida, S.; Iwamoto, T.; Kabuto, C.; Kira, M.; *Nature* **2003**, *421*, 725−727.

66. Zhou, Y.; Karni, M.; Yao, S.; Kaushansky, A.; Apeloig, Y.; Driess, M.; *J. Am. Chem. Soc*. **2019**, *141*, 12916−12927.

67. Boom, D. H. A.; Jupp, A. R.; Nieger, M.; Ehlers, A. W.; Slootweg, J. C.; *Chem. Eur. J.* **2019**, *25*, 13299–13308.

68. Yao, S.; Szilvási, T.; Xiong, Y. Lorent, C.; Ruzicka, A.; Driess, M.; *Angew. Chem. Int. Ed.* **2020**, *59*, 22043 –22047.

69. Yao, S.; Kostenko, A.; Xiong, Y.; Ruzicka, A.; Driess, M.; *J. Am. Chem. Soc.* **2020**, *142*, 12608–12612.

70. Benedek, Z.; Szilvási, T.; *RSC Adv.,* **2015**, *5*, 5077–5086.

71. Wang, Y.; Szilvási, T.; Yao, S.; Driess, M.; *Nat. Chem.*, **2020**, *12*, 801-807.

72. Xu, J.; Dai, C.; Yao, S.; Zhu, J.; Driess, M.; *Angew. Chem.Int. Ed.* **2022**, *61*, e202114073.

73. Wang, W.; Kostenko, A.; Hadlington, T. J.; Luecke, M.; Yao, S.; Driess, M.; *J. Am. Chem. Soc.* **2019**, *141*, 626−634.

74. Luecke, M.; Kostenko, A.; Wang, Y.; Yao, S.; Driess, M.; *Angew. Chem. Int. Ed.* **2019**, *58*, 12940–12944.

75. Xiong, Y.; Yao, S.; Szilvási, T.; Ruzicka, A.; Driess, M.; *Chem. Commun.*, **2020**, *56*, 747.

76. Luecke, M.; Pens, E.; Yao, S.; Driess, M.; *Chem.Eur.J.* **2020**, *26*, 4500 –4504.

77. Luecke, M.; Giarrana, L.; Kostenko, A.; Gensch, T.; Yao, S.; Driess, M.; *Angew.Chem.Int. Ed.* **2022**, *61*, e202110398.

CHAPTER 2

Synthesis of bis(chlorogermyliumylidene) from a direct route in a PNNP ligand framework
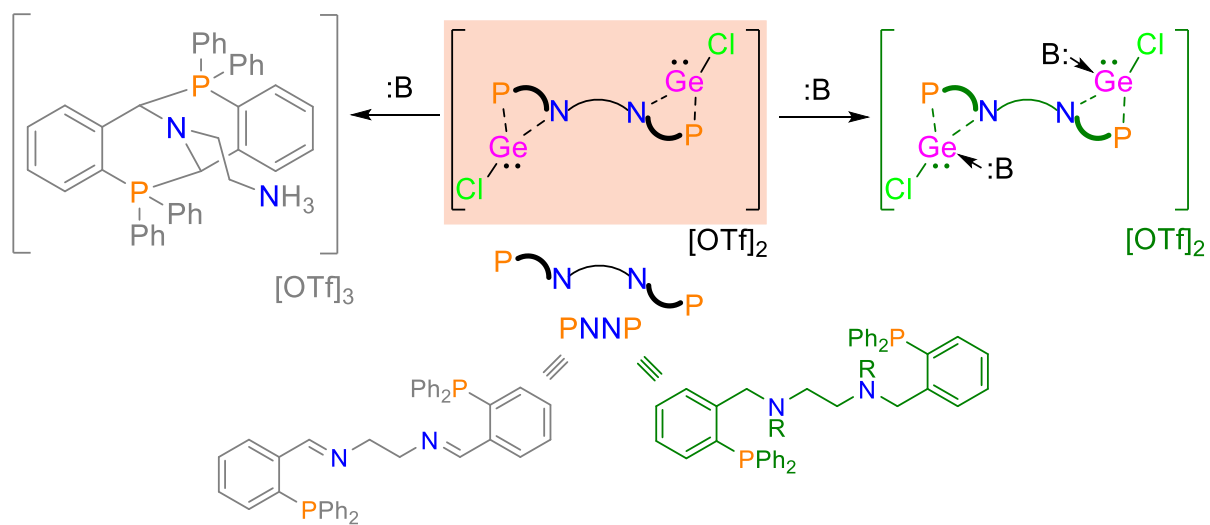
Abstract

Bis(chlorogermyliumylidene)s have been synthesized by a direct synthetic route by addition of *in-situ* generated germyliumylidene using $GeCl_2$.Dioxane and trimethylsilyl trifluoromethanesulfonate to a solution of three bulky ligands L_{Im}, L_{NH} and L_{Me}. The three bis(chlorogermyliumylidene)s **1**, **2** and **3** are crystallized from the solution directly by layering the solution with pentane. Complex **1** was found to be unstable at room temperature and rearranges into compound **4**. Compound 4 is obtained quantitatively when a solution of complex **1** is reacted with Lewis bases proving the instability of complex **1** towards Lewis bases. In presence of Lewis acid like $GaCl_3$ complex **1** rearranged to compound **5** due to the presence of Dioxane. However, Complexes **2** and **3** were found to be stable towards Lewis bases and their coordination with DMAP and PMe_3 was studied using NMR techniques. Further, DFT and NMR studies are done to elaborate the above-mentioned findings.

2.1. Introduction

Germyliumylidene species have been one of the sought-after group of molecules due to their versatility of acting both as a donor as well acceptor. This is achieved due to the presence of lone pair of electrons in one of the hybrid *p*-orbitals and an empty *p*-orbital respectively. The first germyliumylidene was reported by Jutzi et al. was a germanium (II) cation coordinated to Cp* ligand.[1] Since then, there are a huge number of reports of germyliumylidene stabilized kinetically or electronically.[2] However, only a few reports of bis(germyliumylidene)s have been seen in recent years. Müller et al. was the first to report a Ge^+-Ge^+ dication stabilized by phosphinomethanides (**A**).[3] Tobita et al. reported a dimetallodigermene-1,2-diylium ion (**B**) followed by Inoue et al. synthesizing an N-heterocyclic imine supported germylene-germyliumylidene (**C**) bearing some bis(germyliumylidene) character.[4,5] Again, Driess et al. reported bis(germyliumylidene) supported by borata-bis (N-Heterocyclic Carbene) (**D**) having a Ge-Ge bond.[6] Recently, a similar bis(germyliumylidene) stabilised by borata-bis (diphenylphosphine) ligand (**E**) was reported by Ragogna et al.[7]
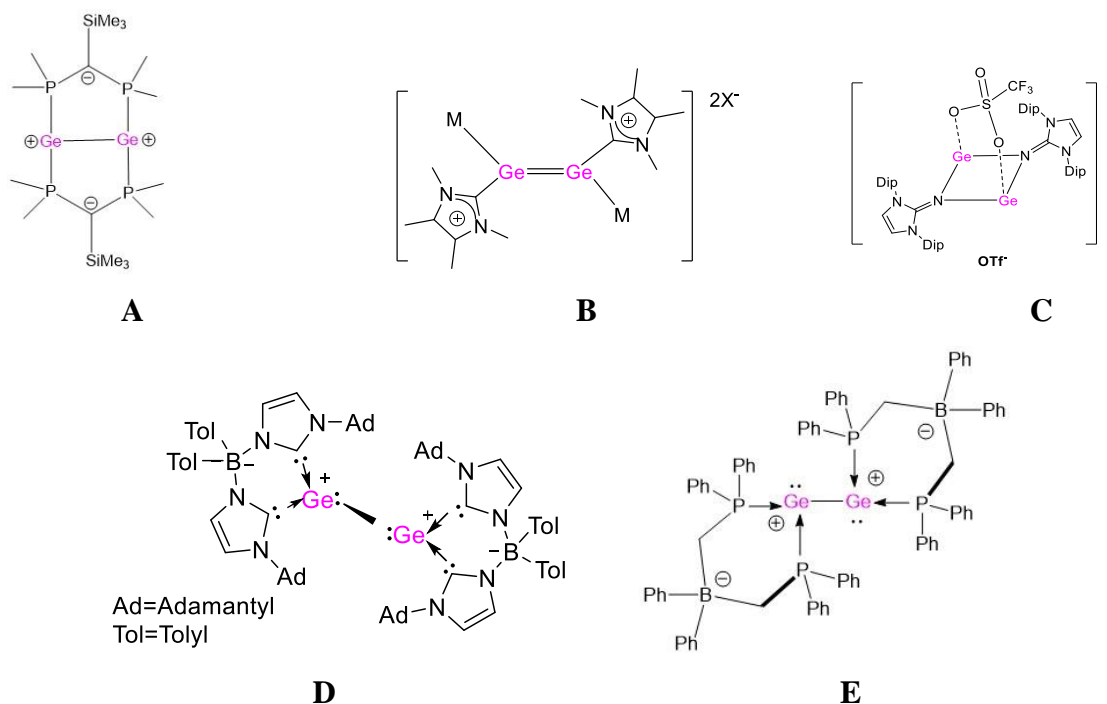
2.1.1 Previously reported examples of bis(germyliumylidene)s

2.2. Scope of workRecently, the very first bis(germyliumylidene) stabilised by a bis (α-iminopyridine) ligand was synthesised by Majumdar et al (Scheme 2.2.1).[8] The redistribution of chloride happens when the germanium (II) dication stabilised by the same ligand is reacted with GeCl$_2$.Dioxane leading to the formation of this species electrostatically favouring the monocation formation. However, unlike the previously reported complexes, this complex shows great flexibility in its backbone and hence gets canted by 99.32(4)° due to the coulombic repulsion between the two monocations.
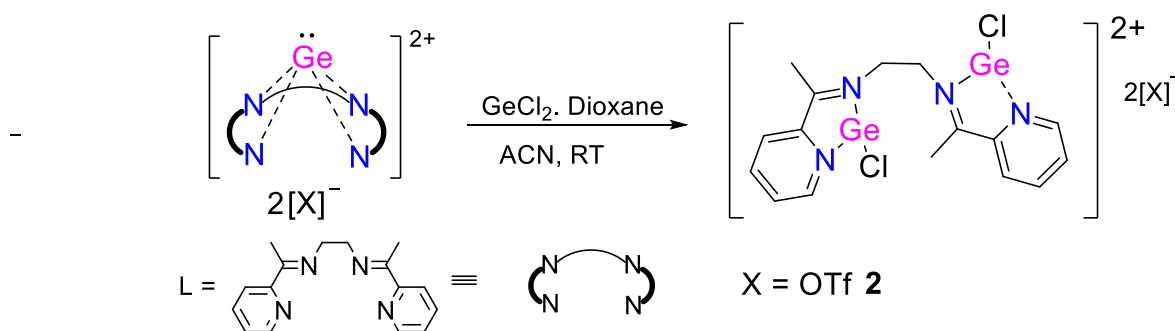
2.2.1 Synthesis of bis(chlorogermyliumylidene) from germanium(II) dication

The direct synthesis of such species can be achieved by introducing further bulk in the ligand. So, purposively placing ((2-diphenylphosphino)phenyl) group on the imino carbon

increases the desired bulk. Hence in presence of chloride abstracting agent the ligand coordinates with the monocation and directly yields the desired species. Also, more flexible amino phospine (N-H and N-Me) moieties have been used to carry out similar syntheses. Further, the the reactivity studies are carried to assess its potential as a donor or acceptor.

2.3. Results and Discussion

2.3.1. Bis(chlorogermyliumylidene)

The N, N'-bis [o- (diphenylphosphino)benzylidene]ethylenediamine (L_{im}) ligand was synthesised by performing Schiff base reaction between ethylenediamine and o-diphenylphosphinobenzaldehyde as reported previously.[9] Ligands L_{NH} and L_{NMe} were synthesized by modified literature procedures.[10] Bis(chlorogermyliumylidene) **1** was synthesized by addition of ligand L_{im} to the in-*situ* generated germyliumylidene species by reacting GeCl$_2$.Dioxane and TMSOTf in DCM at room temperature. The reaction mixture was allowed to stir for half an hour and was concentrated. The solution was layered with pentane and was allowed to stand overnight. Colourless crystals suitable for X-ray diffraction studies were obtained from the solution. Both the crystals and crude products were found to be insoluble in any polar and non-polar solvents. Hence, the *in-situ* samples were generated to perform the NMR experiments in CDCl$_3$ as the solvent. The *in-situ* NMR spectrum taken after two hours of reaction indicated a decomposed mixture. So, the NMR experiments were performed at low temperature. At -50°C, the sample gave reasonably well ^{1}H NMR spectrum. However, a ^{31}P NMR signal was not obtained. ^{1}H NMR spectrum showed downfield shifted peaks compared to the pure ligand NMR spectrum indicating the coordination of germyliumylidene species with the ligand. However, on increasing the temperature gradually by 10°C the NMR spectrum shows slow decomposition of the complex 1. ^{31}P NMR spectrum acquired immediately after attaining room temperature was found to have a peak at -1.48 ppm along with a subtly hidden peak at 3-4 ppm. After keeping the sample for 24 hours, the NMR spectrum was recorded. ^{1}H NMR spectrum depicted a complete decomposition of complex **1**. However, ^{31}P NMR spectrum showed new peaks at 4.53, 3.80, -2.13 and -3.81.

The L_{NH} and L_{NMe} supported bis(chlorogermyliumylidene) **2** and **3** were synthesized in a similar manner. The solutions were concentrated and layered with pentane at room temperature. On standing overnight they gave colourless crystals suitable X-ray diffraction studies. Again, the crude solids and the crystals, both were found to be insoluble in any polar or non-polar solvent. So, the *in-situ* NMR spectrum were generated in CDCl$_3$. The ^{1}H NMR

spectrum for both complexes showed downfield shifted peaks compared to free ligand conforming the complexation of germyliumylidene species with the respective ligands. ^{31}P NMR spectrum showed single peaks at -12.83 and -11.48 ppm respectively. These peaks are upfield shifted in comparison to complex **1** indicating stronger electron donation from P to Ge in case of complexes **2** and **3**.
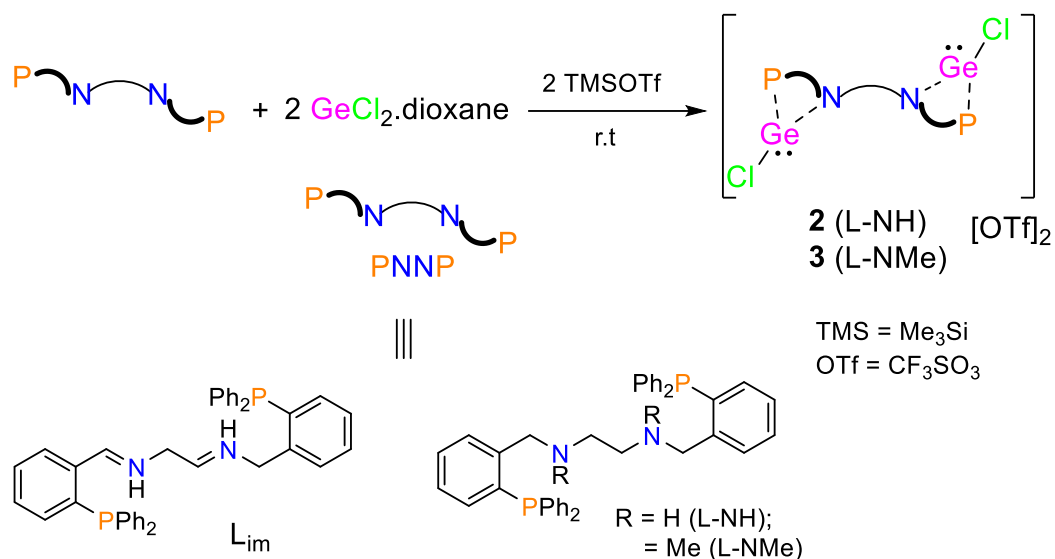
2.3.1. Synthesis of bis(chlorogermyliumylidene)s

2.3.2. Crystal structure

The three complexes **1**, **2** and **3** were characterized by single crystal X-ray crystallography technique. Single crystals were obtained by layering concentrated DCM solution of reaction mixture by pentane and letting the solution stand overnight at room temperature.

Figure 2.3.2.1. Molecular structure of the di-cationic part of **1** in the solid state (thermal ellipsoids at 30%, H atoms, solvent molecules and triflate counter anions omitted for clarity). Selected bond lengths [Å] and angles [°]: Ge1-N1 2.258(3), Ge1-P1 2.440(9), Ge1-Cl1 2.271(9); N1-Ge1-P1 78.81(7), N1-Ge1-Cl1 94.75 (7), P1-Ge1-Cl1 88.59 (3).

Colourless crystals of Complex **1** crystallizes in *P*-1 space group. The two Germyliumylidene units are coordinated by N_{imine} and -*P*Ph$_2$ of the ligand and the two germyliumylidene units oriented at 180° opposite to each other. Each germanium cation is coordinated to the ligand in a six membered ring with the germanium resting in a distorted tetrahedral position, 1.22 Å above the P-C-C-C-N basal plane. The Ge1-P1 bond distance (2.440(9) Å) lies in the long range of the Ge-P single bond lengths (2.33-2.37 Å) but in the lower range of Ge-P dative bond lengths (2.44-2.52 Å).[11,12] The Ge1-N1 bond distance is 2.258(3) Å which is longer than the usually reported Ge-N bond distances. The bond distances show that there is a strong donation of electrons from P to Ge but there is weak donation of electrons from N to Ge. The O of the triflate is found close to Ge (Ge1---O1 = 2.523(3) Å) which then results in a longer S-O bond length of the triflate (1.459(2) Å). The Ge1-Cl1 bond distance is found to be 2.271(9) Å which lies in the usual range of Ge-Cl bond lengths.[13] Due to the presence of lone pair on the germanium center considerable pyramidalization is observed and hence the sum of bond angles around Germanium atom is found to be $\Sigma = 262°$. The two Germanium centres of the germyliumylidene units were found to be separated by 6.680(9) Å (Figure 2.3.2.1).

Figure 2.3.2.2. Molecular structure of the di-cationic part of **2** in the solid state (thermal ellipsoids at 30%, H atoms and triflate counter anions omitted for clarity). Selected bond lengths [Å] and angles [°]: Ge1-N1 2.125 (7), Ge1-P1 2.500 (3), Ge1-Cl1 2.258 (3); N1-Ge1-P1 89.6 (2), N1-Ge1-Cl1 88.1 (2), P1-Ge1-Cl1 97.18 (9).

Complex **2** gives white crystals which crystallize in *P*-1 space group. Each unit contains two molecules having marginally different parameters. The germyliumylidene unit is coordinated by amine *N* atom and phosphine *P* atom forming a six membered puckered ring. The Ge1-P1 and Ge1-N1 bond distances are 2.500(3) Å and 2.125(7) Å respectively. The Ge2-P2 and Ge2-N2 bond distances are 2.479(3) Å and 2.073(8) Å respectively. The Ge1-O1 and

Ge2-O6 distances are 2.906(6) Å and 3.231(6) Å respectively. The two germyliumylidene units are separated by 6.57 Å and form a dihedral angle of 180° (Figure 2.3.2.2).
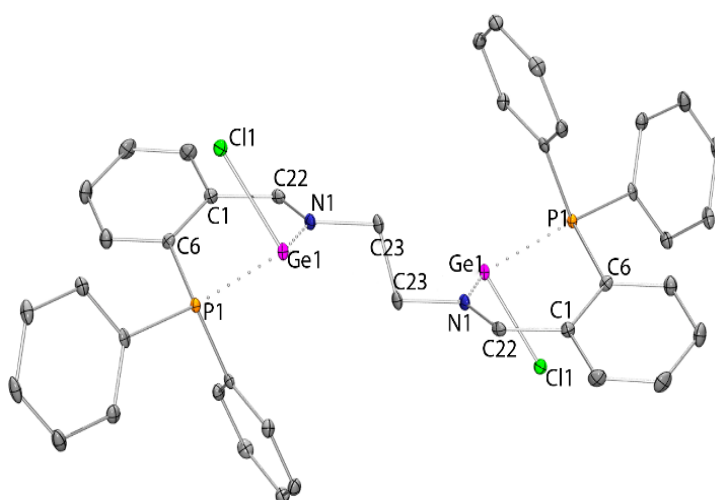

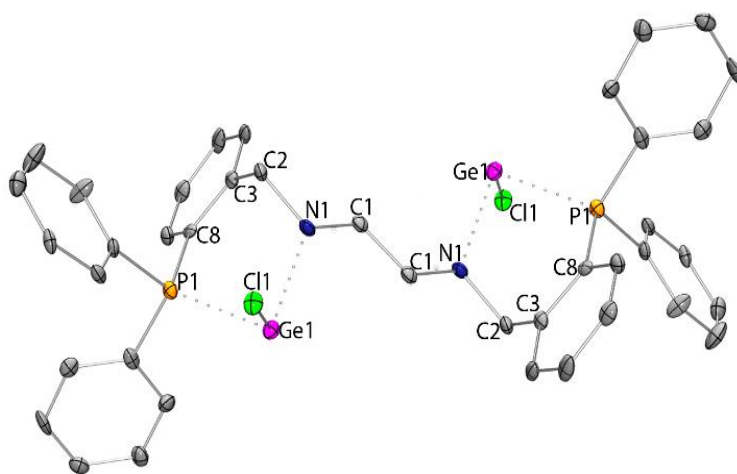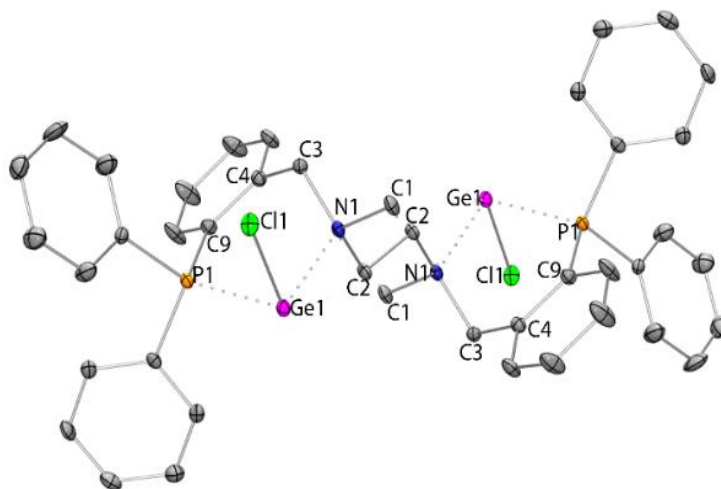**Figure 2.3.2.3.** Molecular structure of the di-cationic part of **3** in the solid state (thermal ellipsoids at 30%, H atoms, solvent molecules, disordered solvent and triflate counter anions omitted for clarity). Selected bond lengths [Å] and angles [°]: Ge1-N1 2.173 (5), Ge1-P1 2.4993 (18), Ge1-Cl1 2.2646 (18); N1-Ge1-P1 88.95 (15), N1-Ge1-Cl1 91.70 (15), P1-Ge1-Cl1 90.06 (6).

Complex **3** forms white crystals and crystallizes in $P2_1/c$ space group. Complex **3** exhibits similar bond parameters as complex **2**. The Ge1-O1 separation is found to be 2.646(5) Å with the germyliumylidene units separated by 7.25(11) Å (Figure 2.3.2.3).

2.3.3. DFT Studies

The DFT calculations were carried out at the B3LYP level using 6-31G(d,p) as the basis set. The triflate anions were omitted and optimized geometries **1'**, **2'** and **3'** were used in place of complexes **1**, **2** and **3** satisfactorily. Due to removal of the triflates the Ge-N bond distances in **1'** were found to be 2.123 Å which are shorter than the Ge-N bond distances reported for complex **1**. The lone pairs of the germanium centres contribute maximum to the HOMO and HOMO-1 orbitals of **1'**. HOMO- 18 to HOMO-21 shows the interaction between the empty p-orbital of Ge and the lone pairs of N and P. LUMO and LUMO+1 of **1'** resides in the ligands $\pi^*_{C=N}$ orbitals making them the reactive centres of the molecule.
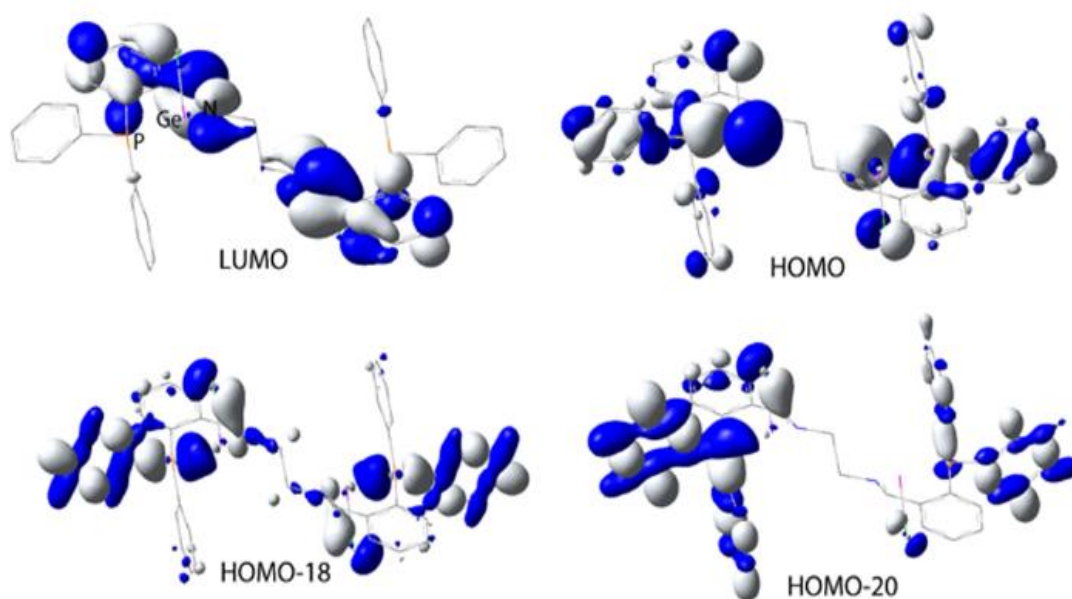
Figure 2.3.3.1. Relevant contour plots of **1'** at an isovalue of 0.03 au.

2' and **3'** exhibit similar electronic feature except in case of **2'** and **3'** the LUMO and LUMO +1 resides on the vacant p-orbitals of Ge and the σ^*_{P-C} orbitals. These findings confirm the formation of anticipated donor -acceptor complex. The Wiberg bond index for Ge-N and Ge-P bonds are 0.35 and 0.65 respectively. This indicates a strong Ge-P bond. Natural bond analysis of Ge-P bond shows that the bond is approximately 75% P-based with high p-character on the P lone pair. The Mulliken charges on Ge in all three structures is approximately 0.25.
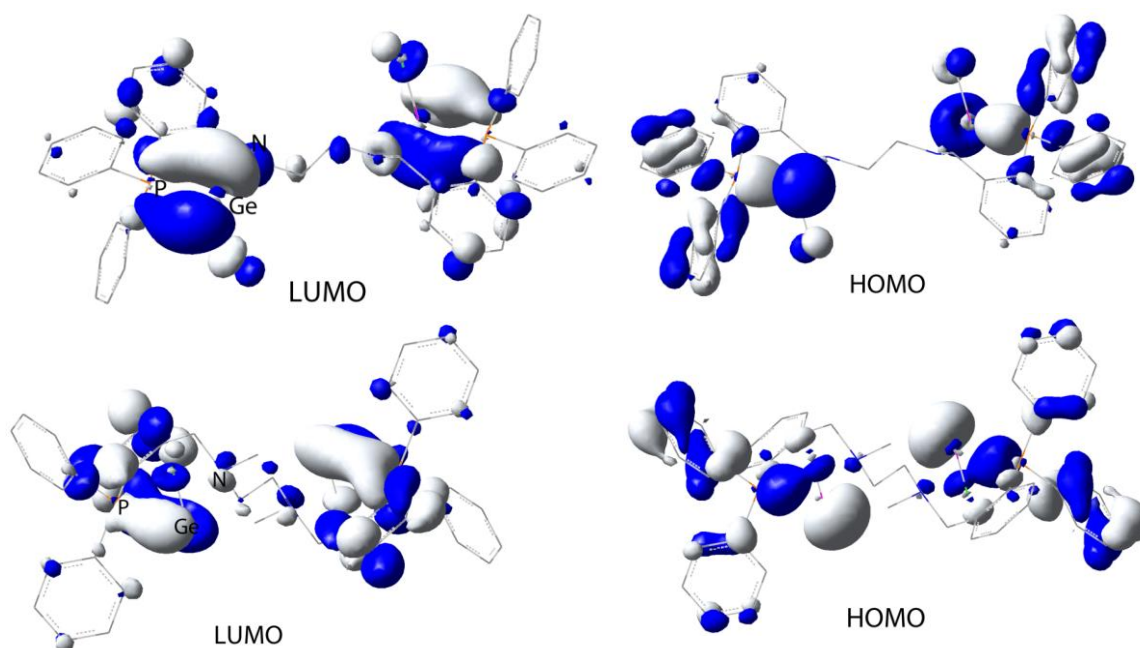
Figure 2.3.3.1. Relevant contour plots of **2'** and **3'** at an isovalue of 0.03 au.

2.3.4. Reactivity studies

Complex **1** was found to be unstable in presence of donor molecules and it rearranges to compound **4**. NMR studies already reflects this fact. So, crystals of complex 1 are grown from concentrated DCM solution layered with pentane. Excess pentane forces out the complex 1 in the form of white crystals. The same solution on standing for several days yields white crystals of **4**. On addition of DMAP to the reaction mixture of **1** in DCM and layering the reaction mixture with pentane, crystals of **4** are obtained quantitatively. ^{1}H NMR spectrum of compound **4** in THF-d_8 confirmed the formation of one of the diastereomers of **4**. The ^{31}P NMR spectrum of the compound **4** showed two peaks, one at +3.94 ppm and another in 3-4 ppm range. The first peak is attributed to crystallized diastereomer of **4** and the other peak is attributed to the other diastereomer. The second diastereomer also appears in the decomposed ^{31}P NMR spectrum of complex **1** taken in CDCl$_3$. Other peaks appearing in the ^{31}P NMR spectrum of complex **1** are probably of the undetermined tricoordinate phosphorus centres. The apparent reason for the rearrangement of complex **1** in presence of Lewis bases is that the donor centres of the Lewis base attack the imino carbons of the complex **1** facilitating the displacement of germyliumylidene units from the complex and leading to the formation of compound **4**. The polar protic solvent acts as the proton source for the formation of **4**. However, the ligand does not rearrange in the presence of Lewis bases. On reacting complex **1** with Lewis acids like GaCl$_3$ compound **5** was formed. Compound **5** was found to have a similar structure to compound **4** with the GaCl$_3$ coordinated to the pendant like -NH$_2$ group of the rearranged compound **5**. The possible reason for the rearrangement of complex **1** in presence of GaCl$_3$ is the dioxane present in the reaction mixture. The complex rearranges in presence of dioxane and then coordinates with the Lewis acid.
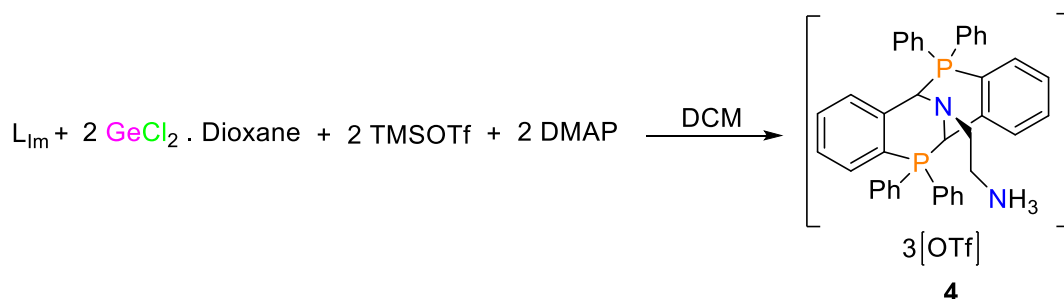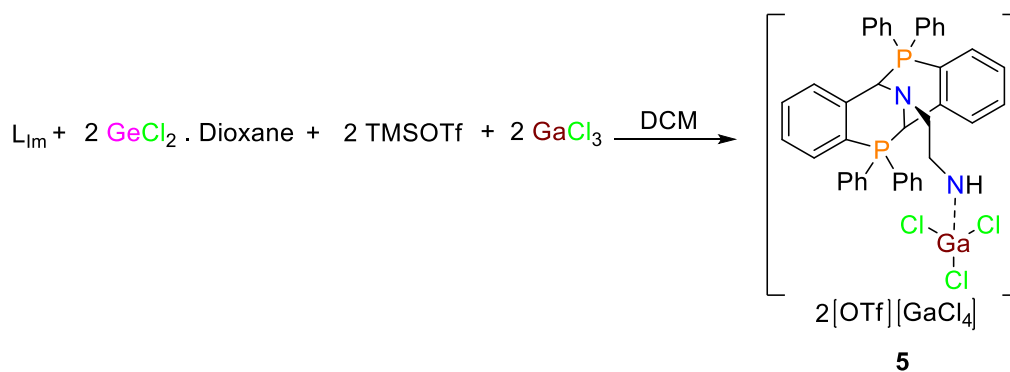
Scheme 2.3.4.1. Reactivity of **1** with coordinating solvents and Lewis base.

Complexes **2** and **3** show strong coordination with Lewis bases such as DMAP and PMe$_3$. NMR studies are carried out to study the coordination of such bases. In case of DMAP, ^{1}H NMR spectrum showed an upfield shift of signals while in case of PMe$_3$, ^{31}P NMR showed a downfield shift of peak for PMe$_3$ and upfield shift of -*P*Ph$_2$ confirming the coordination of Lewis bases to the germanium (II) centres.
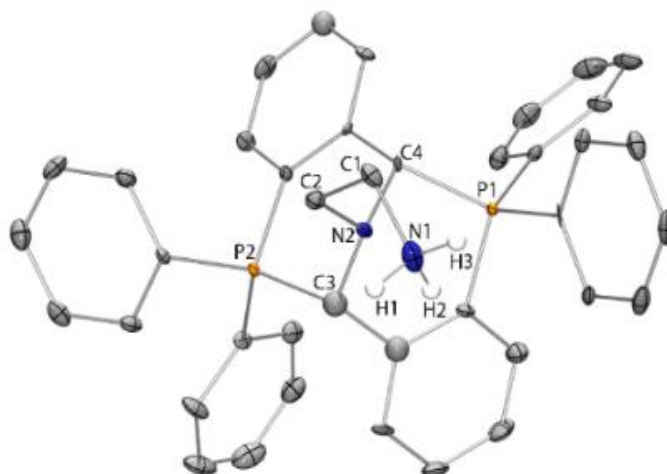
Figure 2.3.4.1. Molecular structure of the tri-cationic part of **4** in the solid state (thermal ellipsoids at 30%, H atoms and triflate counter anions omitted for clarity). Selected bond lengths [Å]: P1-C4 1.844 (5), P2-C3 1.873 (5), N2-C3 1.457 (7), N2-C4 1.446 (7), N2-C2 1.475 (7), N1-C1 1.486 (8).
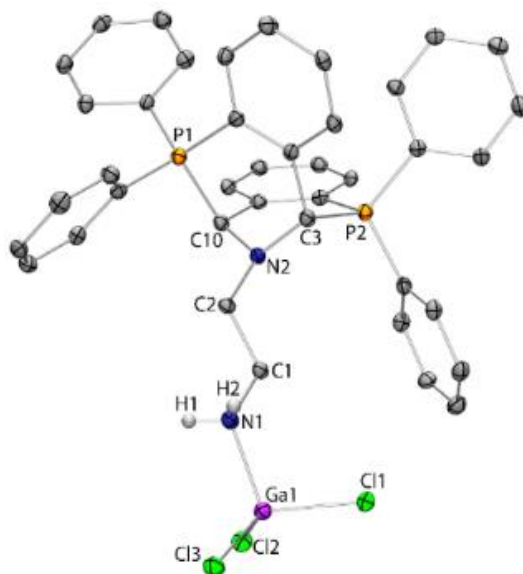
Figure 2.3.4.2. Molecular structure of the di-cationic part of **5** in the solid state (thermal ellipsoids at 30%, H atoms, solvent molecules and counter anions omitted for clarity). Selected bond lengths [Å]: P1-C10 1.866 (8), P2-C3 1.836 (8), N2-C10 1.451 (9), N2-C3 1.461 (9), N2-C2 1.477 (9), N1-C1 1.488 (10), N1-Ga1 1.977 (7).

2.4. Conclusion

In conclusion, bis(chlorogermyliumylidene)s were synthesized by stabilizing the germyliumyidene units in the PNNP framework. There is a strong donation of electrons from P to Ge which along with a weaker N to Ge donation supports the [:GeCl]$^+$ units. Complex 1 was found to be unstable due to reactive imino ligand backbone hence rearranges in presence of Lewis bases. However, complex 2 and 3 are fairly stable and shows strong coordination with PMe$_3$ and DMAP.

2.4. Experimental

2.4.3. General Remarks

All manipulations were carried out under a protective atmosphere of argon applying standard Schlenk techniques or in a dry box. Tetrahydrofuran was refluxed over sodium/benzophenone. Dichloromethane and Chloroform-d was stirred and refluxed over calcium hydride and kept over molecular sieves. All solvents were distilled and stored under argon and degassed prior to use. All chemicals were used as purchased. Chloroform-d was provided with the Trimethylsilane as internal standard. ^{1}H and ^{13}C{^{1}H} NMR spectra were referenced to external SiMe$_4$ using the residual signals of the deuterated solvent (^{1}H) or the solvent itself (^{13}C). ^{19}F

NMR was referenced to external $C_6H_5CF_3$ (TFT). NMR spectra were recorded on Bruker AVANCE III HD ASCEND 9.4 Tesla/400 MHz and Jeol 9.4 Tesla/400 MHz spectrometer. Melting points were determined under argon in closed NMR tubes and are uncorrected. Elemental analyses were performed on Elementar vario EL analyzer. Single crystal data were collected on Bruker SMART APEX four-circle diffractometer equipped with a CMOS photon 100 detector (Bruker Systems Inc.) with a Cu Kα radiation (1.5418 Å).

2.4.4. Ligand Synthesis

2.4.4.1. Characterization of Ligand L_{im}

^{1}**H NMR (400 MHz, CDCl$_3$, TMS)** δ 8.78 (d, $^4J_{P\text{-}H}$ = 4.8 Hz, 2H, HC$_{im}$); 7.91 (ddd, $^3J_{H\text{-}H}$ = 7.6 Hz, $^4J_{H\text{-}H}$ = 3.6 Hz, $^5J_{HH}$ = 1.2 Hz, 2H, HC-2); 7.36-7.30 (m, 15H, Ar-H); 7.28-7.22 (m, 10H, Ar-H); 6.86 (ddd, $^3J_{H\text{-}H}$ = 7.6 Hz, $^4J_{H\text{-}H}$ = 4.8 Hz, $^5J_{H\text{-}H}$ = 1.2 Hz, 2H, HC-5); 3.54 (s, 4H, -CH2-CH2-) ppm.

^{13}**C{1H} NMR (101 MHz, CDCl$_3$, TMS)** δ 160.27 (d, C_{im}, $^3J_{P\text{-}C}$ =20.80 Hz); 138.66 (d, C-6, $^2J_{P\text{-}C}$ =17.37 Hz), 136.52 (d, C-1, $^1J_{P\text{-}C}$ =19.69 Hz); 135.77 (d, C-2, $^2J_{P\text{-}C}$ = 9.69 Hz); 133.17 (d, ArC_{ipso}, $^1J_{P\text{-}C}$ =19.99 Hz); 132.43 (s, Ar-CH); 129.25 (s, Ar-CH); 127.95 (s, Ar-CH); 127.86 (s, Ar-CH); 127.70 (d, ArC_o, $^2J_{P\text{-}C}$ = 7.171 Hz); 126.87 (d, ArC_m, 3JP-C = 4.141 Hz); 60.49 (s, -CH2-CH2-) ppm.

^{31}**P{1H} NMR (162 MHz, CDCl$_3$, H$_3$PO$_4$)** δ = -13.00 ppm.

2.4.4.2. Synthesis and Characterization of Ligand L_{NH}

Ligand L_{im} (1 g, 1.65 mmol) and LiAlH$_4$ (0.282 g, 7.44 mmol) were taken in 50 mL of diethyl ether and stirred at room temperature for 24 hours. The mixture was quenched with 15mL water and extracted in (10 X 3mL) DCM. The organic layer was separated and dried over anhydrous Na$_2$SO$_4$. The solvent was evaporated under vacuum to obtain a pale-yellow sticky solid yielding 0.58 g (57.62%) of L_{NH}.

^{1}**H NMR (400 MHz, CDCl$_3$, TMS)** δ 7.45 (ddd, J=7 Hz, 4.8Hz, 0.8 Hz, 2H, HC-2); 7.34-7.24 (m, 22 H, Ar-H); 7.16 (dt, J = 7.6 Hz, 0.8 Hz, 2H, HC-4); 6.90 (ddd, J = 7.6Hz, 4.4Hz, 1.2 Hz, 2H, HC-5); 3.92 (s, 4H, Ar-CH_2-NH); 2.50 (s, 4H, -CH_2-CH_2-); 1.55 (br s, 2H, NH) ppm.

^{13}**C NMR (101 MHz, CDCl$_3$, TMS)** δ 144.84(d, C-1, J=23.81 Hz); 136.94 (d, C-6, J=10.15 Hz), 135.81(d, ArCipso, J=13.75Hz); 134.06 (d, ArCo, J=19.81Hz); 133.66 (C-5); 129.17 (d, ArCm, J=5.48); 129.02 (ArCp); 128.79 (C-3); 128.67 (d, C-2, J=6.96 Hz); 127.23 (C-4); 52.41 (d, N-CH$_2$, J=21.16Hz); 48.68 (-CH2-CH2-) ppm

31P NMR (162 MHz, CDCl3, H3PO4) δ = -15.41 ppm

Elemental Analysis: Calcd. for $C_{40}H_{38}N_2P_2$: C, 78.93; H, 6.29; N, 4.60. Found: C, 78.91; H, 6.43; N, 4.55

2.4.4.2. Synthesis and Characterization of Ligand L_NMe

Ligand L_{NH} (0.58 g, 0.952 mmol) was dissolved in 30 mL THF and the solution was cooled to -78°C. To this solution n-BuLi (1.31 ml, 2.09 mmol, 1.6 M in Hexane) was added and the mixture was thawed to room temperature, and it was further stirred for 30 min. To, the resultant mixture Methyl Iodide (1.048 ml, 2.09 mmol, 2 M in Methyl tert-butyl ether) was added at room temperature. The mixture was stirred for 24 hrs. The mixture was quenched with 15 mL water and extracted with hexane (10 X 3mL). The organic layer was separated and dried over anhydrous Na_2SO_4. The solution was evaporated to obtain a white solid yielding 0.48 g (79.12%) of L_{NMe}.

1H NMR (400 MHz, CDCl3, TMS) δ 7.45 (m, 2H, HC-2); 7.29-7.26 (m, 16H, Ar-H); 7.23-7.19 (m, 8H, Ar-H); 7.13 (t, J = 7.2 Hz, 2H, HC-4); 6.87 (ddd, J = 7.6Hz, 4.4Hz, 0.8Hz, 2H, HC-5); 3.62 (s, 4H, Ar-CH_2-NH); 2.23 (s, 4H, -CH_2-CH_2-); 1.93 (s, 6H, NCH_3) ppm

13C NMR (101 MHz, CDCl3, TMS) δ 144.48 (d, C-1, J=22.82 Hz); 137.74 (d, C-6, J=10.40 Hz), 136.45(d, ArCipso, J=15.04 Hz); 133.86 (d, ArCo, J=19.79 Hz); 133.81 (C-5); 129.06(d, ArCm, J=5.25 Hz); 128.54 (ArCp); 128.35 (d, C-2, J=6.17 Hz); 128.29 (C-3); 126.90 (C-4); 60.91 (d, N-CH_2, J=18.98 Hz); 54.54 (-CH_2-CH_2-); 41.74(N-CH_3) ppm

31P NMR (162 MHz, CDCl3, H3PO4) δ = -15.17 ppm.

Elemental Analysis: Calcd. For $C_{42}H_{42}N_2P_2$: C, 79.22; H, 6.65; N, 4.40. Found: C, 79.31; H, 6.45; N, 4.31.

2.4.5. Complex Synthesis

2.4.5.1. Synthesis and Characterization of Complex 1

Ligand L_{im} (0.3 g, 0.496 mmol) and $GeCl_2$.dioxane (0.23 g, 1.00 mmol) were dissolved in 30mL DCM and stirred at room temperature. Subsequently Trimethylsilyl triflate (0.18 g, 1.00 mmol) was added. The mixture was stirred for 30 minutes; concentrated to 10mL and layered with 5mL pentane. Colourless Crytals of **1** were obtained. Crystallization yield 0.306 g (55.15%) (Decompostion Temp.:142°C- 144°C).

1
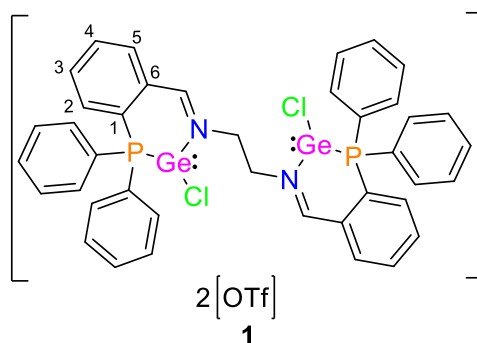
¹H NMR (400 MHz, CDCl₃, TMS) δ = 9.04 (s, 2H, N-CH), 8.03-8.13 (m, 5H, Ar-H), 7.72-7.74(m, 17H); 7.75-7.65(m, 29H); 7.48-7.52(m, 21 H); 7.38-7.42(m, 17H); 7.14-7.16 (m, 6H); 3.87 (s, 4H, -CH_2-CH_2-) ppm.

¹³C NMR (101 MHz, CDCl₃) δ =136.49; 136.24; 135.20; 135.05; 133.94; 132.73; 132.50; 130.05 ppm.

**³¹P NMR (162 MHz, H₃PO₄)** δ = 4.53; 3.80; -2.13; -3.81 ppm.

¹⁹F NMR (377 MHz, TFT) δ = -77.56 ppm.

Elemental Analysis: Calcd. For $C_{42}H_{36}Cl_2F_6Ge_2N_2O_6P_2S_2$: C, 45.08; H, 3.06; N, 2.50. Found: C, 44.98; H, 3.20; N, 2.56.

2.4.5.2. Synthesis and Characterization of Complex 2

Ligand L_{NH} (0.3 g, 0.492 mmol) and GeCl₂.dioxane(0.229 g, 0.991 mmol) were dissolved in 50mL DCM and stirred at room temperature. Subsequently trimethylsilyl triflate (0.22 g, 0.992 mmol) was added to the reaction mixture. The solution was stirred for 30 minutes The solvent was then removed completely under vacuum yielding 0.40 g (72%) of (Decomposition Temp.: 122-124⁰C). Colourless single crystals were obtained by layering *in situ* generated **2** taken in DCM with pentane.

2
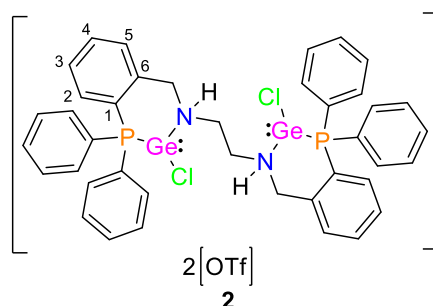
¹H NMR (400 MHz, CDCL₃, TMS) δ = δ 7.70 (s, 2H, HC-2); 7.54-7.34 (m, 26H, Ar-H); 7.06 (t, J = 7.2 Hz, 2H, HC-4); 5.93 (br s, 2H, NH); 4.34 (s, 4H, Ar-CH_2-NH); 3.34 (s, 4H, -CH_2-CH_2-) ppm.

¹³C NMR (101 MHz, CDCl₃, TMS) δ 137.77; 134.77; 134.02; 132.92; 131.61 (br); 130.76

(br); 129.49; 120.87, 117.70 (*C*F$_3$SO$_3$); 52.34 (N-*C*H$_2$); 48.76 (-*C*H$_2$-*C*H$_2$-) ppm.

^{31}P NMR (162 MHz, CDCl$_3$, H$_3$PO$_4$) δ = -12.83 ppm.

^{19}F NMR (377 MHz, CDCl$_3$, TFT) δ = -77.65 ppm.

Elemental Analysis: Calcd. For C$_{42}$H$_{38}$Cl$_2$F$_6$Ge$_2$N$_2$O$_6$P$_2$S$_2$: C, 44.92; H, 3.41; N, 2.49. Found: C, 44.98; H, 3.50; N, 2.38.

2.4.5.3. Synthesis and Characterization of Complex 3

Ligand **L**$_{NMe}$ (0.05 g, 0.078 mmol) and GeCl$_2$.dioxane (0.036 g, 0.157 mmol) were dissolved in 50mL DCM and were stirred at room temperature. Subsequently, trimethylsilyl triflate (0.035 g, 0.157 mmol) was added. The mixture was stirred for 30 minutes. The solvent was then removed completely under vacuum yielding 0.06 g (65%) of **3** (Decomposition Temp.: 128-130°C)**.** Colourless single crystals were obtained by layering *in situ* generated **3** taken in DCM with pentane.
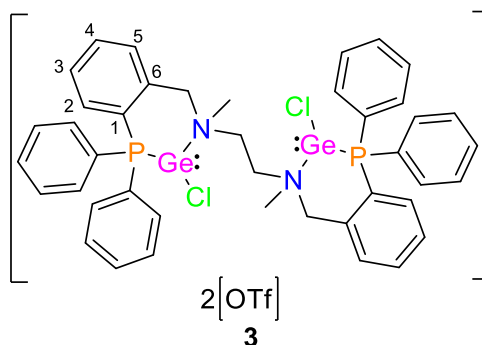
^{1}H NMR (400 MHz, CDCl$_3$, TMS) δ 7.73 (m, 2H, *H*C-2); 7.58-7.40 (m, 20.H, Ar-*H*); 7.32-7.28 (m, 4H, Ar-*H*); 7.07 (t, *J*=7.6, 7H, *H*C-4); 7.07 (t, 2H, *H*C-5); 4.27 (s, 4H, Ar-C*H*$_2$-NH); 3.44 (s, 4H, -C*H*$_2$-C*H*$_2$-); 2.54 (s, 6H, NC*H*$_3$) ppm.

^{13}C NMR (101 MHz, CDCl$_3$, TMS) δ 136.95; 134.83; 133.93; 133.84; 132.26; 131.79; 131.52; 130.56; 129.80; 129.59; 121.02, 117.86 (*C*F$_3$SO$_3$); 61.45 (N-*C*H$_2$); 55.08 (-*C*H$_2$-*C*H$_2$); 43.14 (N-*C*H$_3$) ppm.

^{31}P NMR (162 MHz, CDCl$_3$, H$_3$PO$_4$) δ = -11.48ppm.

^{19}F NMR (377 MHz, CDCl$_3$, TFT) δ = -77.71 ppm

Elemental Analysis: Calcd. For C$_{44}$H$_{44}$Cl$_2$F$_6$Ge$_2$N$_2$O$_6$P$_2$S$_2$: C, 45.91; H, 3.68; N, 2.43. Found: C, 45.92; H, 3.72; N, 2.49.

2.4.6. Reactivity studies for complex 1

2.4.6.1. Reaction with DMAP

Complex **1** (0.092 g, 0.082 mmol) and DMAP (0.020 g, 0.165 mmol) were taken in 10 mL

DCM and stirred for 30 min. The solution was then concentrated and layered with 5mL pentane. After 24 hrs colourless block crystals of the rearranged ligand **4** were obtained.

^{1}H NMR (400 MHz, THF-d_8, TMS) δ 8.11 (s, 3H, Ar-*H*); 7.90-7.74 (m,10H, Ar-*H*); 7.64-7.52 (m, 7H, Ar-*H*); 7.37-7.18 (m, 5H, Ar-*H*, N*H*$_3^+$); 7.06 (br., 2H, Ar-*H*); 6.90 (br., 2H, Ar-*H*); 6.76-6.57 (m, 2H, Ar-*H*); 3.58 (t, $^3J_{H\text{-}H}$ = 6 Hz, 2H, N-C*H2*-CH2-NH$_3^+$); 2.91 (s, 2H, P-C*H*); 1.74 (p, $^3J_{H\text{-}H}$= 6 Hz, 2H, N-CH2-C*H2*-NH$_3^+$) ppm.

^{31}P{1H} NMR (162 MHz, THF-d_8, H3PO4) δ = +3.94 ppm.

Elemental Analysis: Calcd. For $C_{42}H_{42}N_2P_2$: C, 79.06; H, 6.14; N, 4.61. Found: C, 79.00; H, 6.10; N, 4.65

2.4.6.2. Reaction with GaCl₃

Ligand L_{im} (0.050 g, 0.082 mmol)**,** GeCl₂.dioxane (0.038 g, 0.165 mmol) and trimethylsilyl triflate (0.036 g, 0.165 mmol) were added in 15mL DCM and kept for 10 minutes. GaCl₃ (0.029 g, 0.165 mmol) was added to the mixture in DCM and was stirred for 30 min. The solution was then concentrated and layered with 5mL pentane. After 24 hours colourless block crystals of the rearranged ligand **5** were obtained.

2.4.7. NMR scale reaction of complex 3

2.4.7.1. Reaction with DMAP

In an NMR tube L-NMe (0.02 g, 0.031 mmol)**,** GeCl2.dioxane (0.014 g, 0.062 mmol) and trimethylsilyl triflate (10.5 μL, 0.062 mmol) were added 0.6 mL CDCl₃. After dissolution of all the contents DMAP (0.0076 g, 0.062 mmol) was added to the tube in CDCl₃ and was left for 24 hours. After 24 hours the NMR data was obtained.

2.4.7.1. Reaction with PMe₃

In an NMR tube L-NMe (0.02 g, 0.031 mmol)**,** GeCl₂.dioxane (0.014 g, 0.062 mmol) and trimethylsilyl triflate (10.5 μL, 0.062 mmol) were added in CDCl₃. After dissolution of all the contents PMe₃ (6 μL, 0.062 mmol) was added to the tube in CDCl₃ and was left for 24 hours. After 24 hours the NMR data was obtained.

2.5. NMR Data
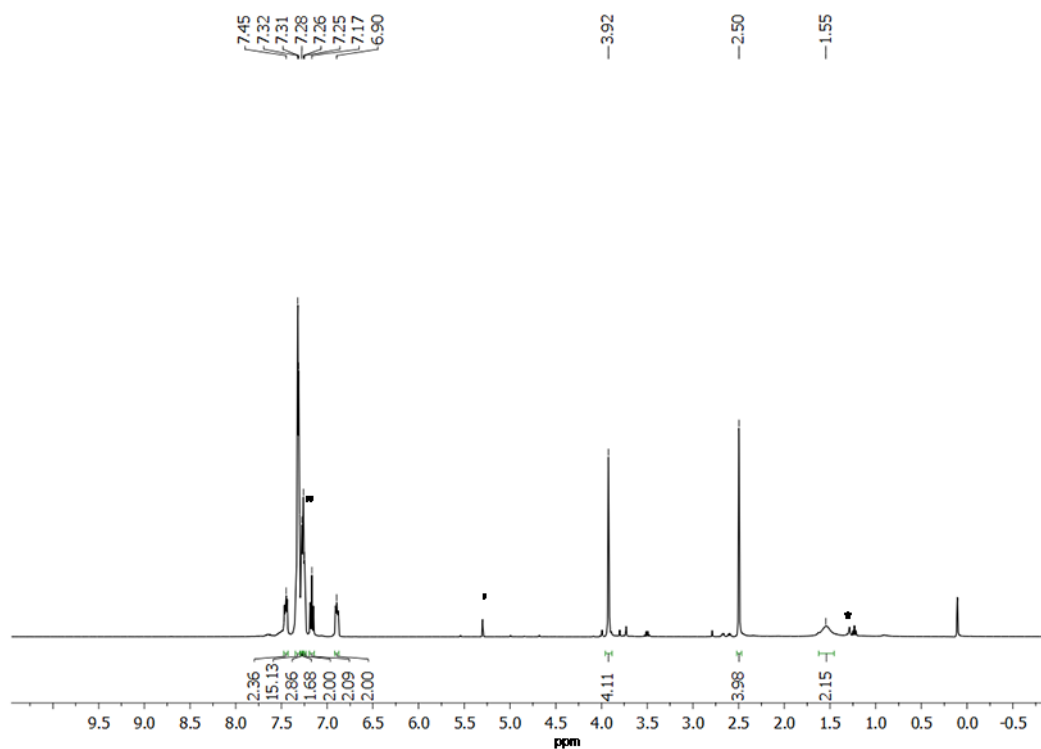
Figure 2.5.1. ^{1}H NMR of $\mathbf{L_{NH}}$ in CDCL$_3$ ("= solvent peak;'=DCM; *=impurity)
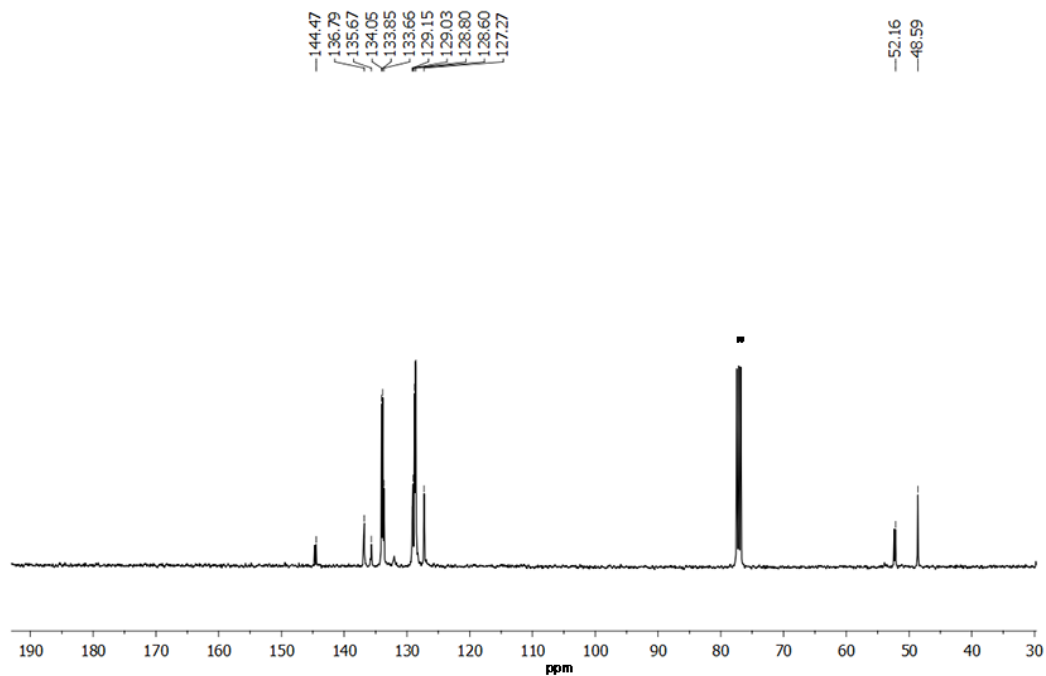
Figure 2.5.2. ^{13}C NMR of $\mathbf{L_{NH}}$ in CDCL$_3$ ("= solvent peak)

70
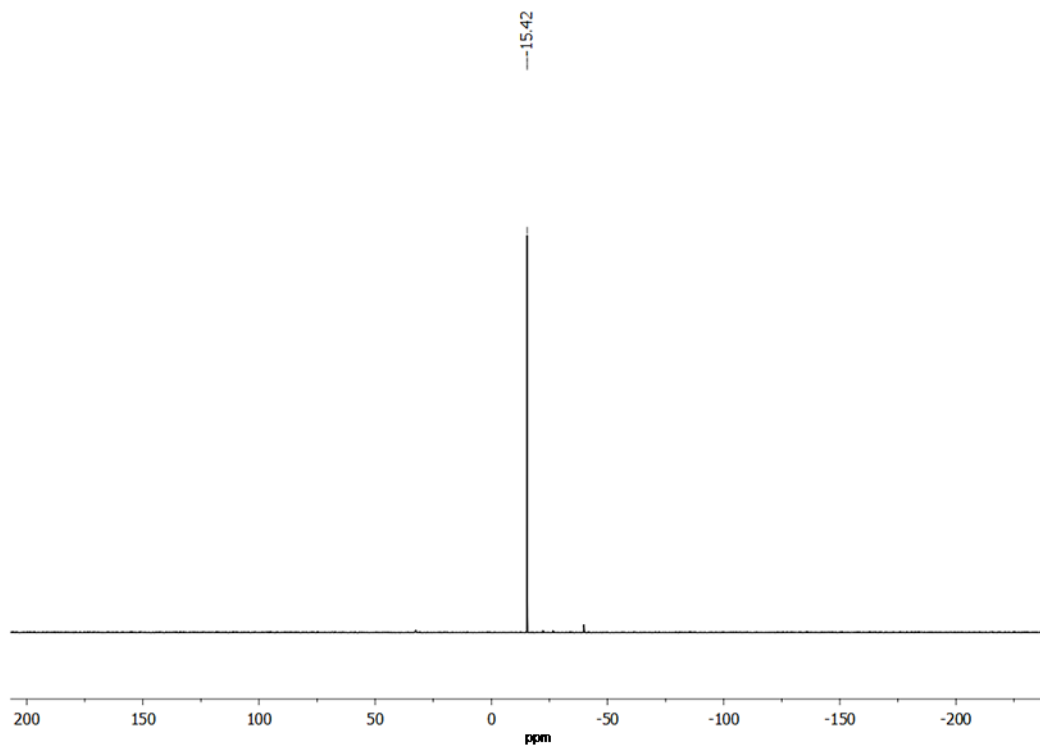
Figure 2.5.3. ^{31}P NMR of L_{NH} in CDCL$_3$
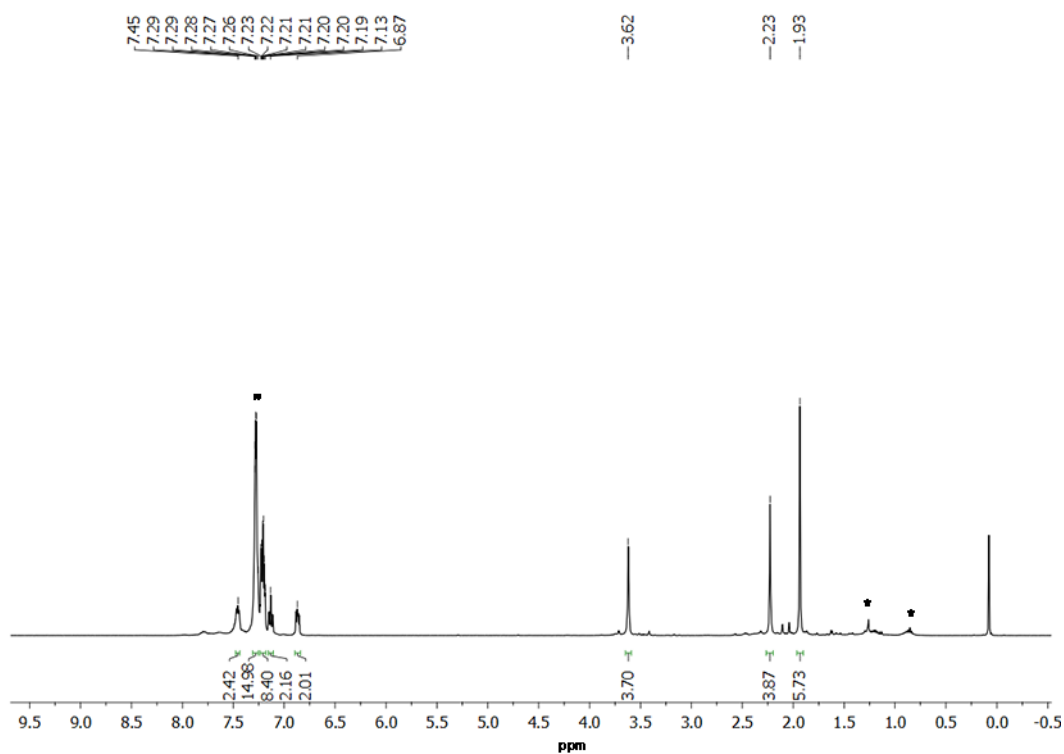
Figure 2.5.4. ^1H NMR of L_{NMe} in CDCL$_3$ ("= solvent peak; *=impurity)
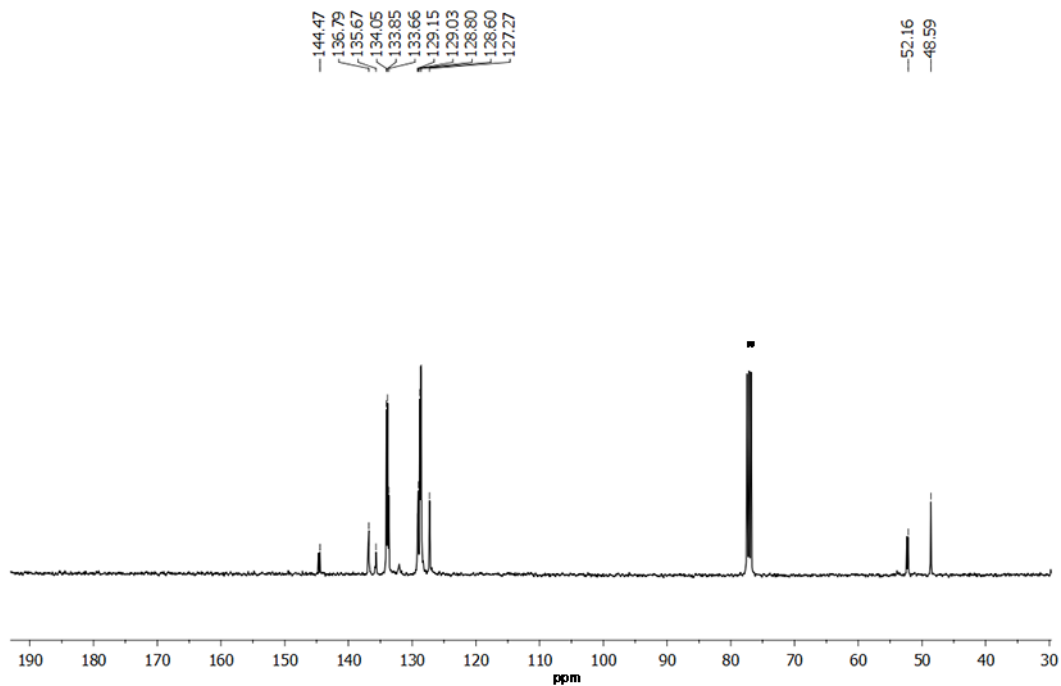
Figure 2.5.5. ^{13}C NMR of **L**$_{NMe}$ in CDCL$_3$ ("= solvent peak)
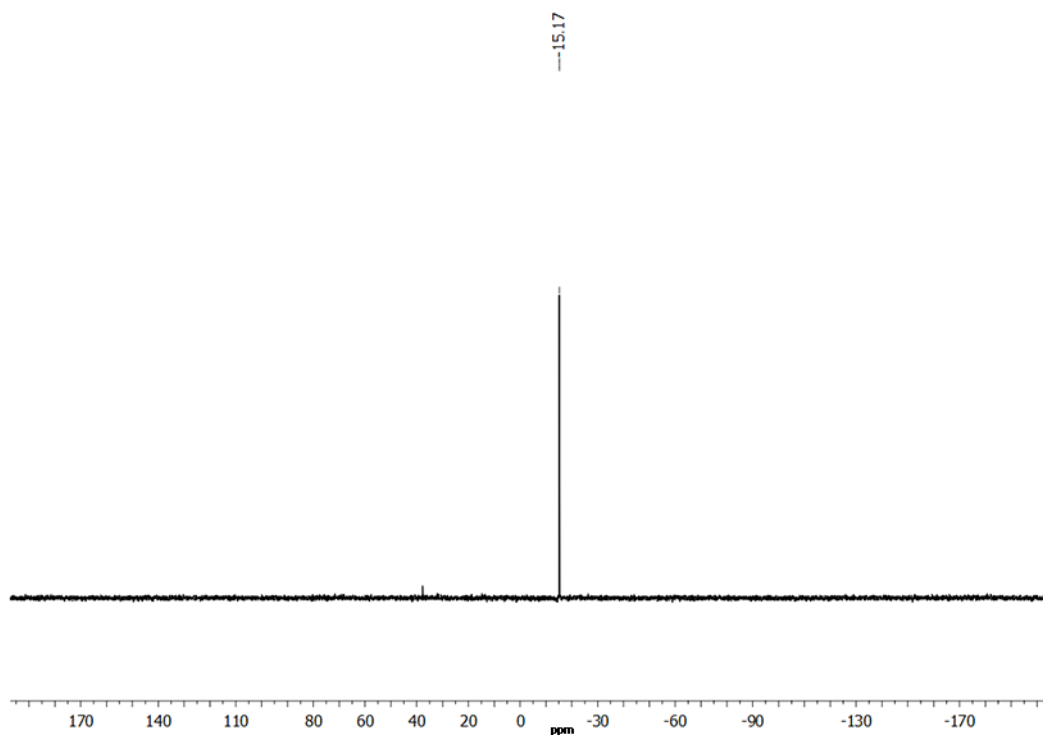
Figure 2.5.6. ^{31}P NMR of **L**$_{NMe}$ in CDCL$_3$
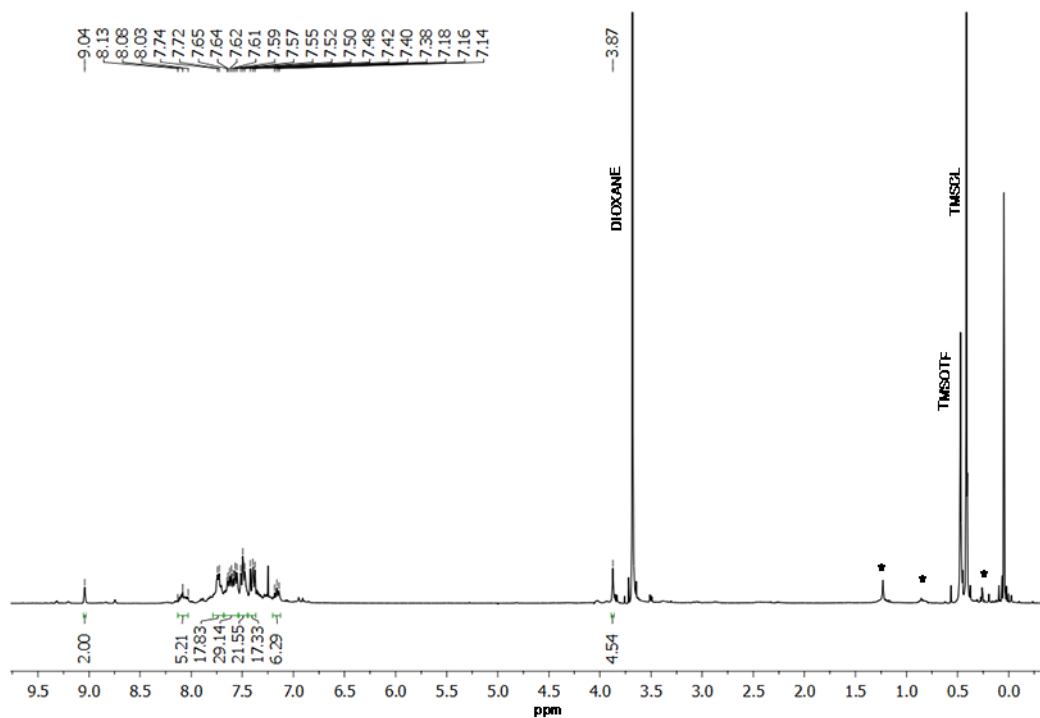
Figure 2.5.7. ^{1}H NMR of **1** in CDCl$_3$ ("= solvent peak; *=impurity)
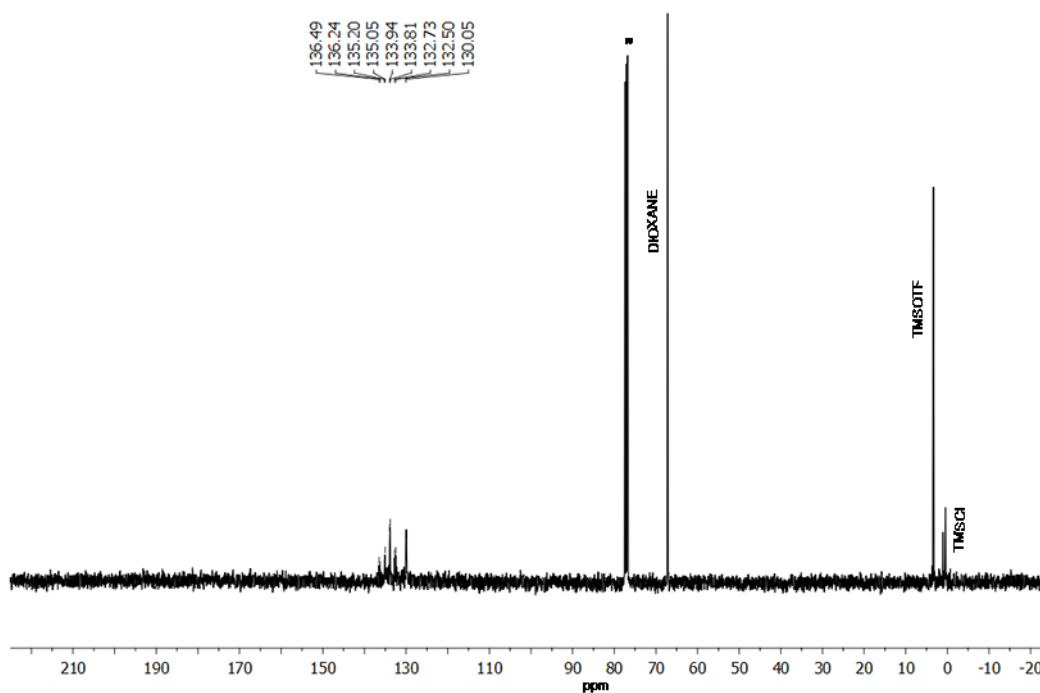
Figure 2.5.8. ^{13}C NMR of **1** in CDCl$_3$ ("= solvent peak)
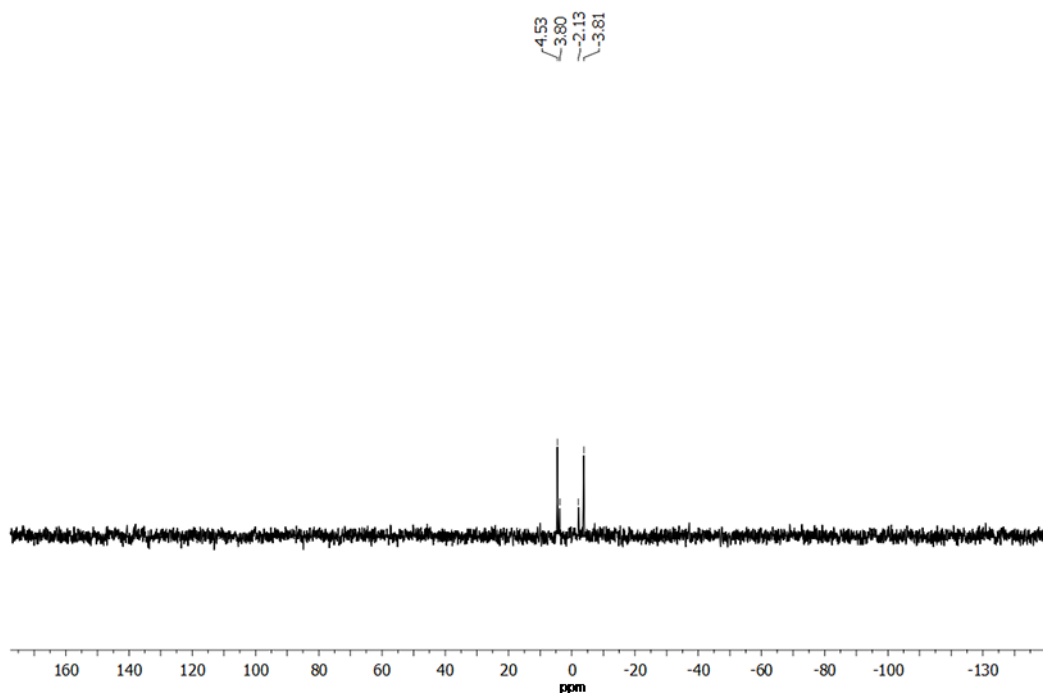
Figure 2.5.9. ^{31}P NMR of **1** in CDCl$_3$
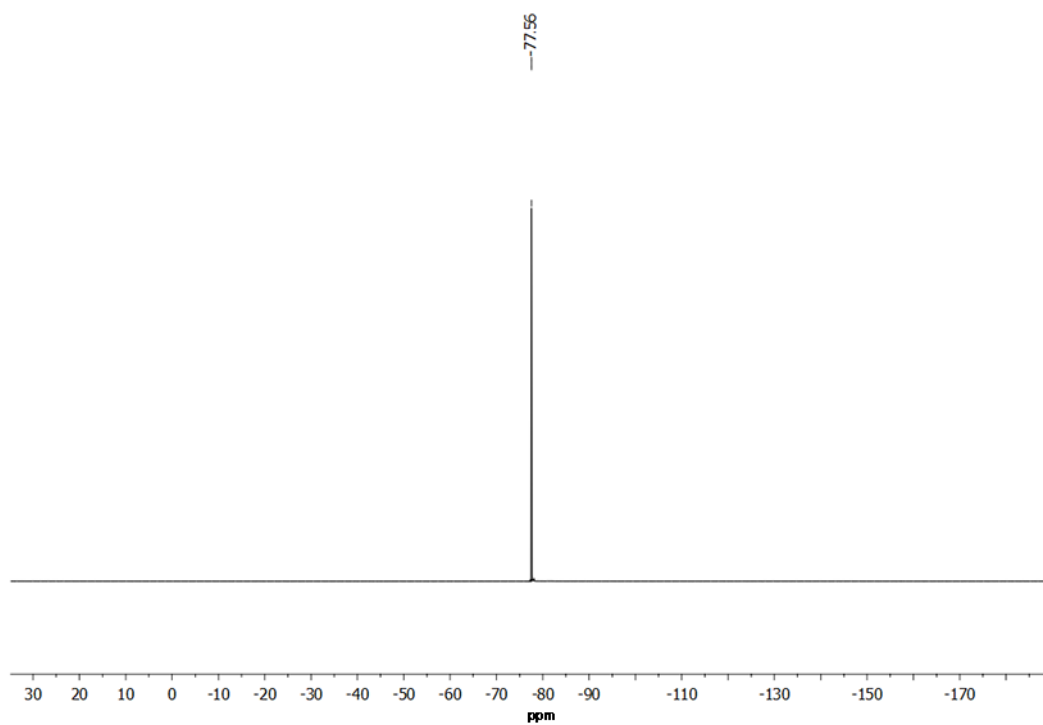
Figure 2.5.10. ^{19}F NMR of **1** in CDCl$_3$
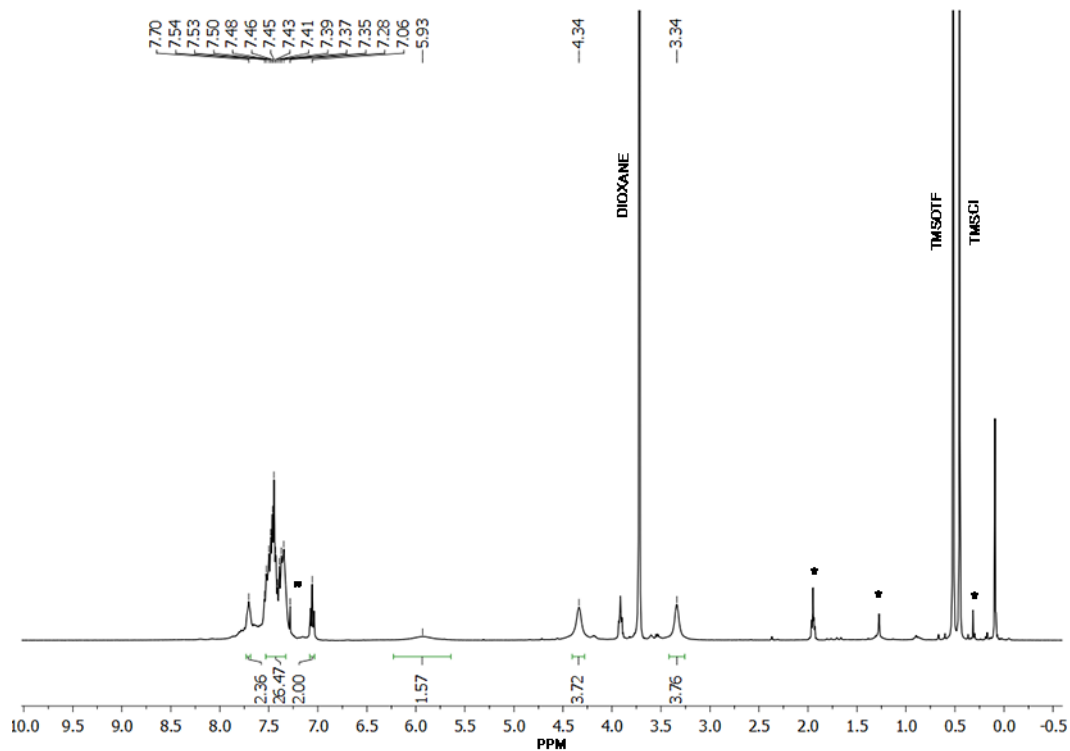
Figure 2.5.11. ^{1}H NMR of **2** in CDCl$_3$("= solvent peak; *=impurity)
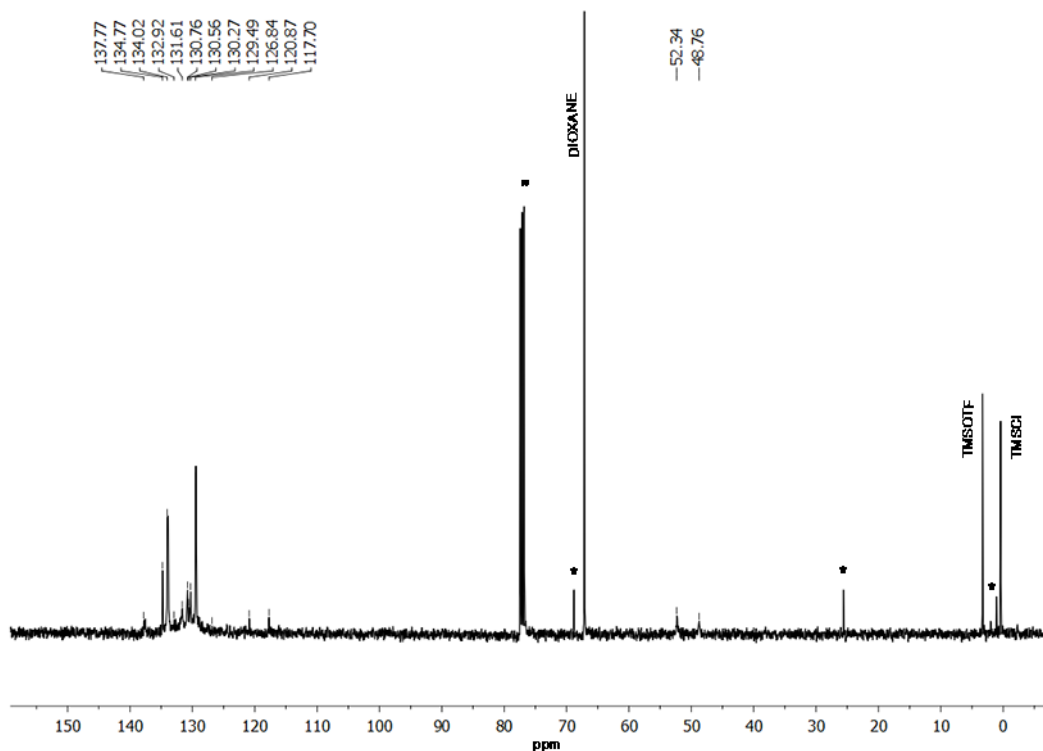
Figure 2.5.12. ^{13}C NMR of **2** in CDCl$_3$ ("= solvent peak; *=impurity)

‒‒12.83

170   140   110   80   60   40   20   0   -30   -60   -90   -120   -150   -180

ppm
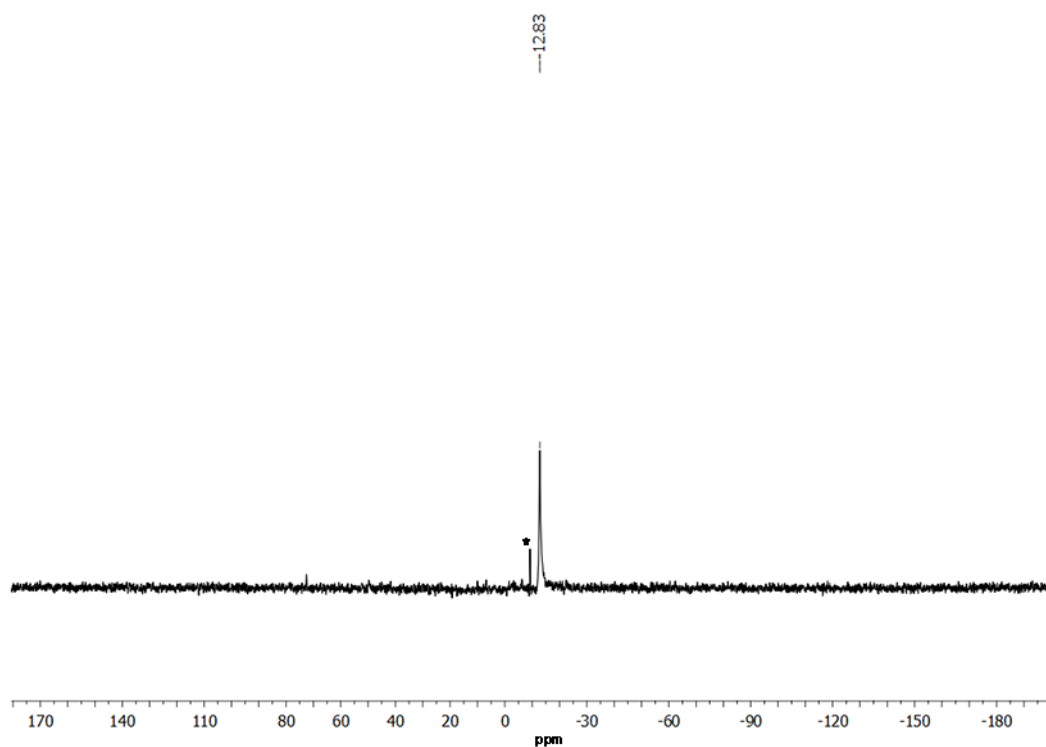
Figure 2.5.13. ^{31}P NMR of **2** in CDCl$_3$ (*=impurity)

‒‒77.65

10   0   -10   -20   -30   -40   -50   -60   -70   -80   -90   -100   -110   -120   -130   -140   -150   -160

ppm
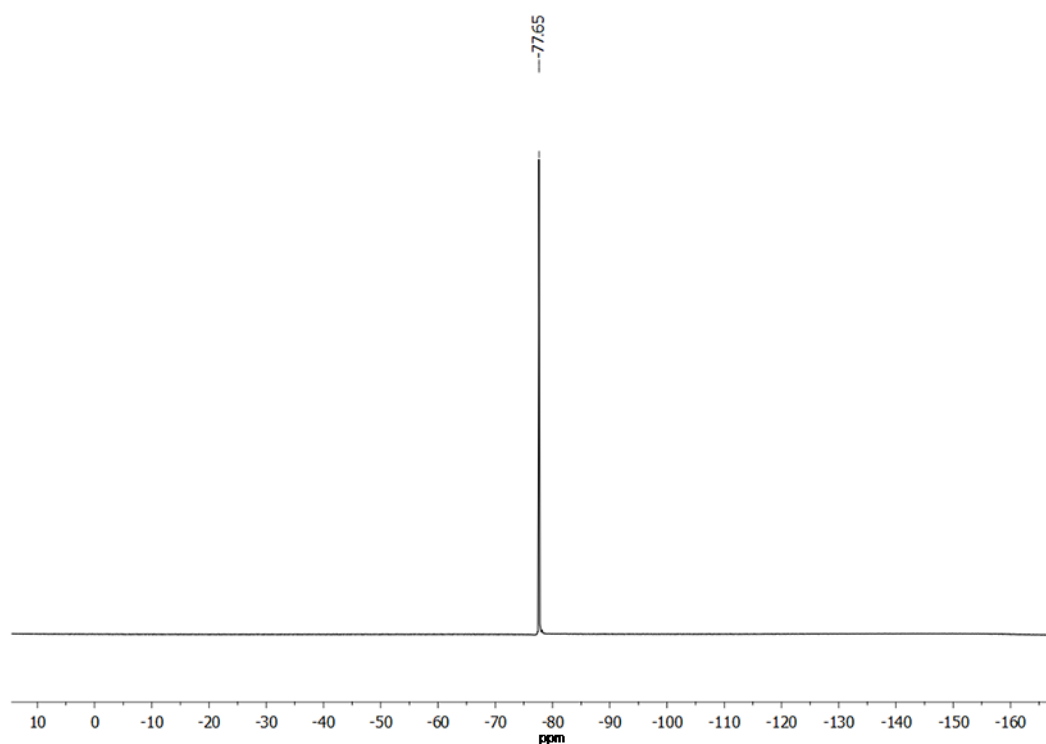
Figure 2.5.14. ^{19}F NMR of **2** in CDCl$_3$
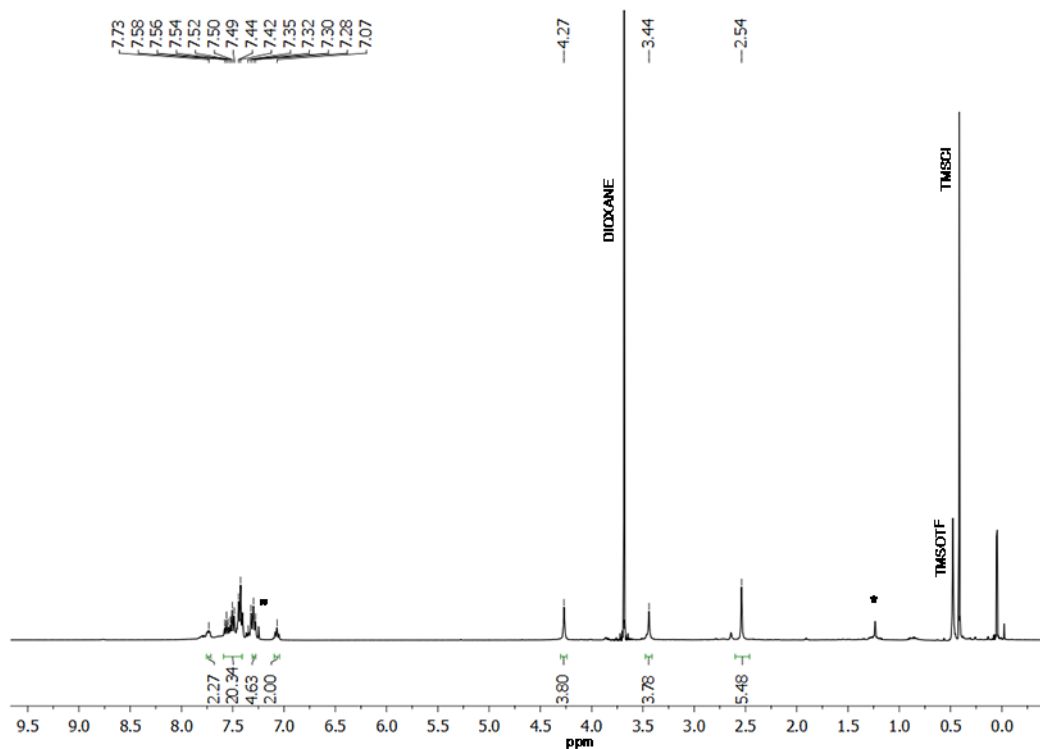
Figure 2.5.15. ^{1}H NMR of **3** in CDCl$_3$ ("= solvent peak; *=impurity)
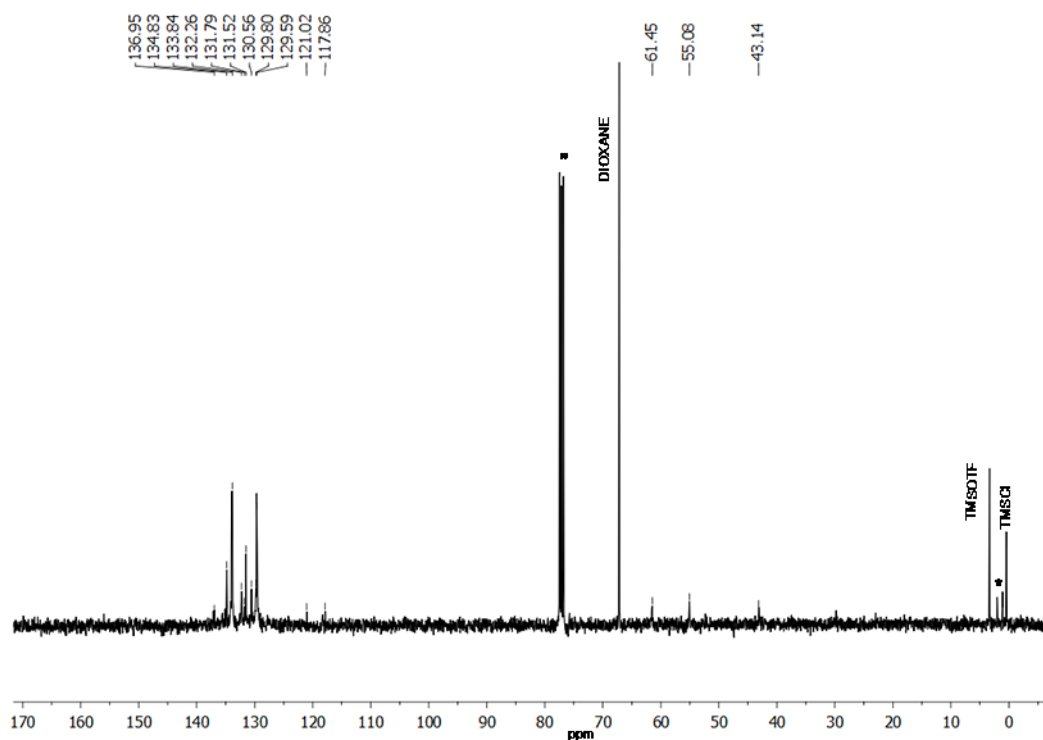
Figure 2.5.16. ^{13}C NMR of **3** in CDCl$_3$ ("= solvent peak; *=impurity)
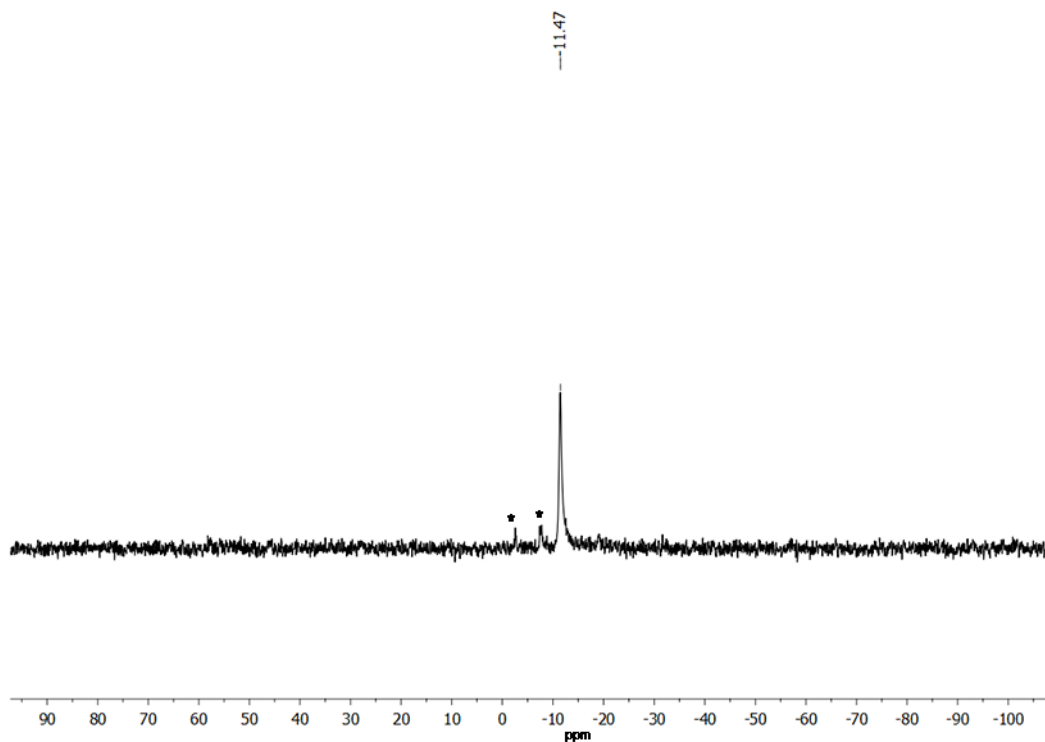
Figure 2.5.17. ^{31}P NMR of **3** in CDCl$_3$ (*=impurity)
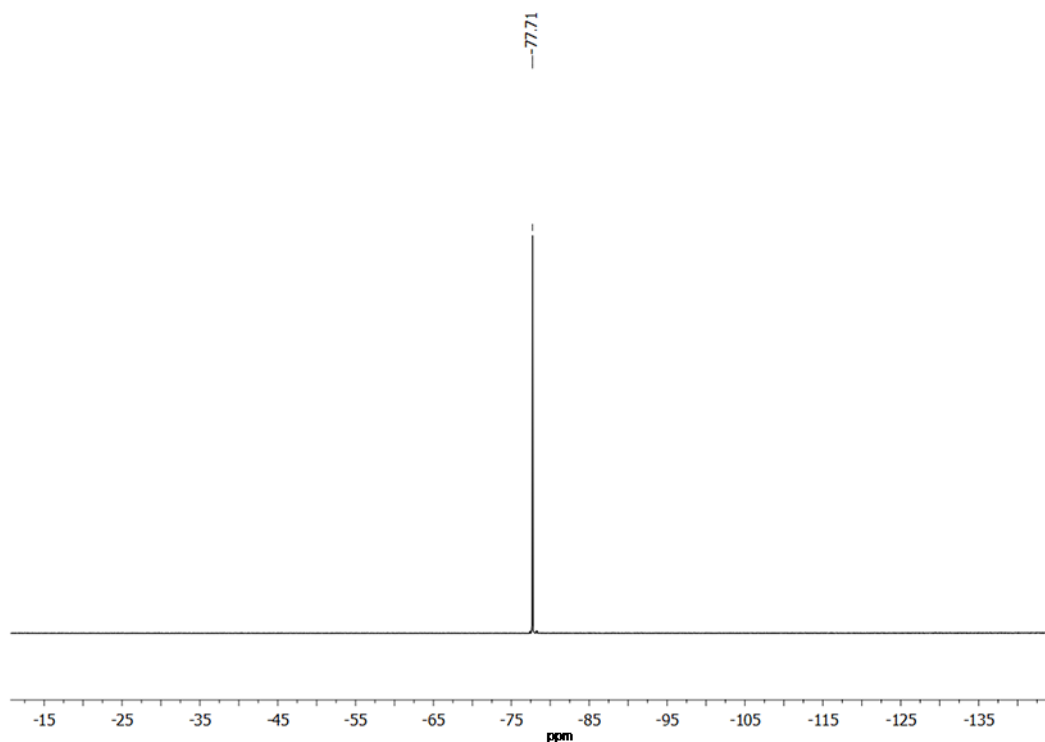
Figure 2.5.18. ^{19}F NMR of **3** in CDCl$_3$

Reaction of Bis-Monocation **3** with 4-Dimethylaminopyridine (DMAP):
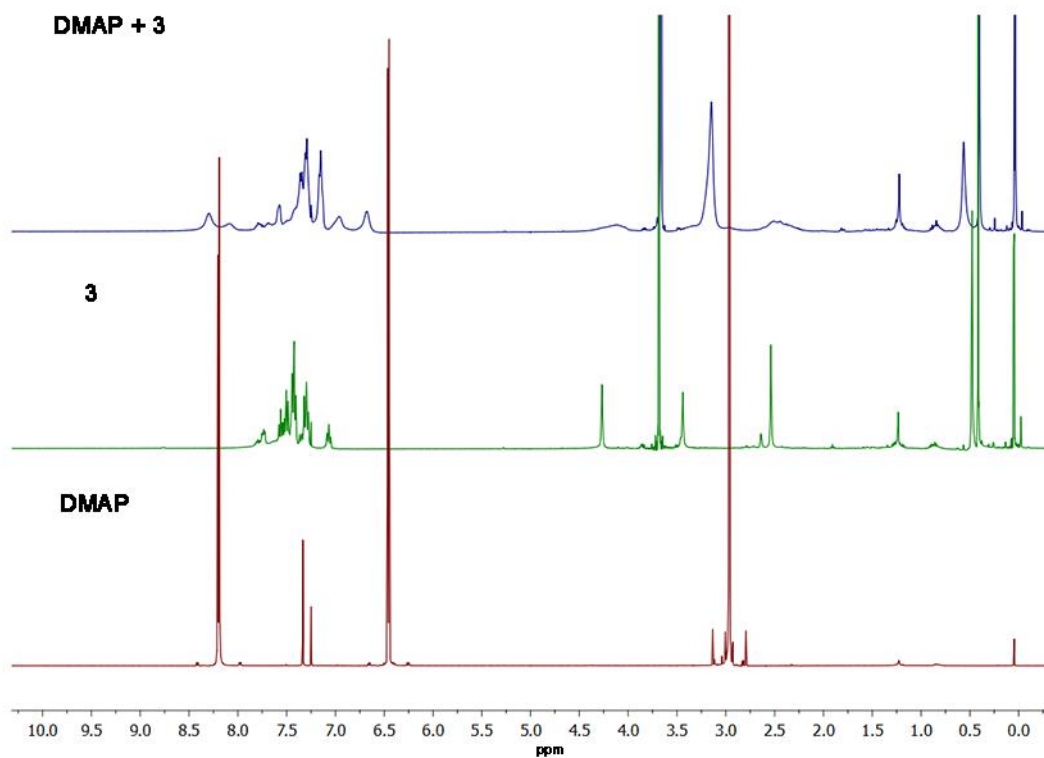
Figure 2.5.20. ^{1}H NMR in CDCl$_3$
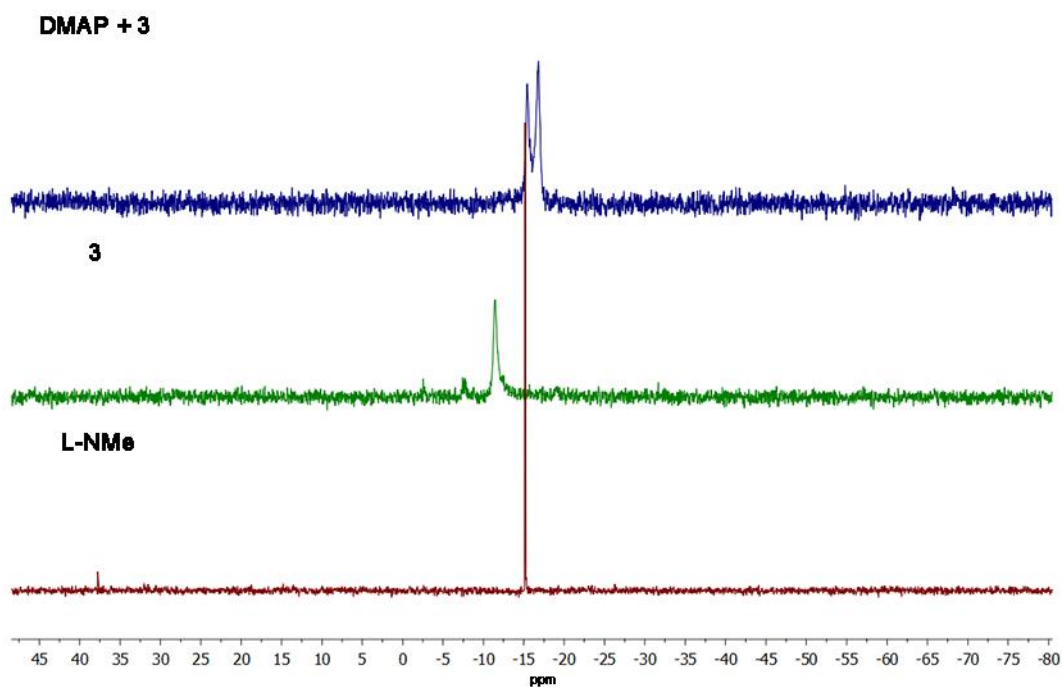
Figure 2.5.21. ^{31}P NMR in CDCl$_3$

Reaction of Bis-Monocation 3 with Trimethylphosphine (PMe₃):
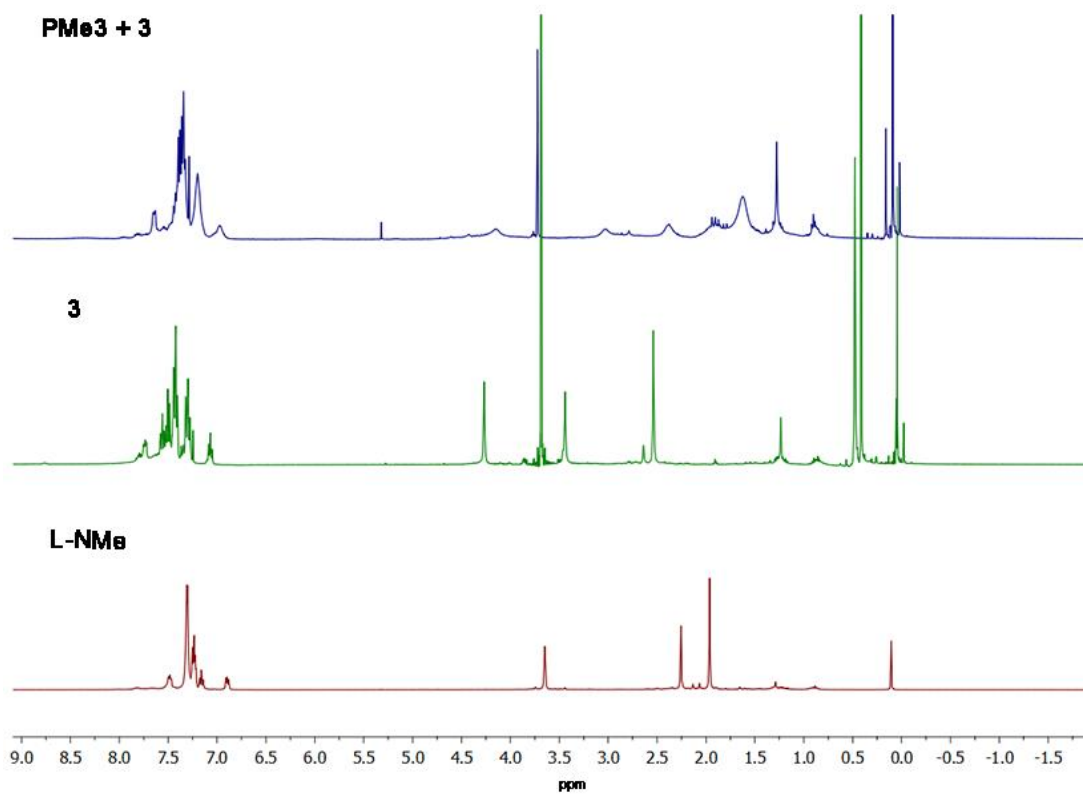
Figure 2.5.22. ^{1}H NMR in CDCl$_3$
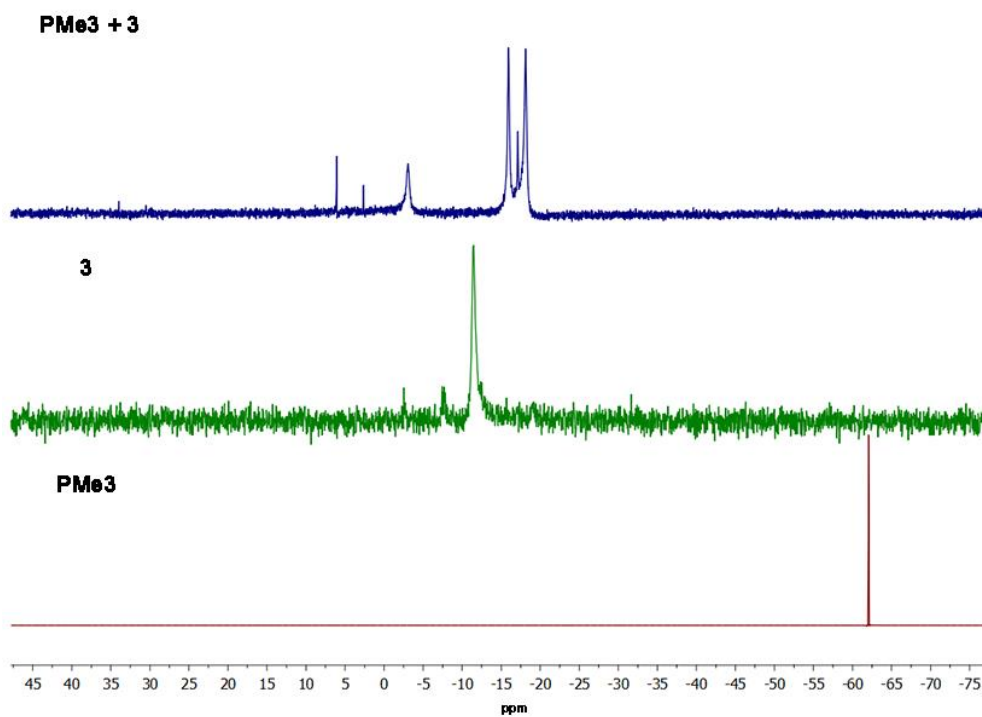
Figure 2.5.23. ^{31}P NMR in CDCl$_3$

2.6. Crystal data table
Table 2.6.1. Crystal data and structure refinement for **1**.

Empirical formula	C46 H42 Cl10 F6 Ge2 N2 O6 P2 S2
Formula weight	1458.55
Temperature	100(2) K
Wavelength	1.54178 Å
Crystal system	Triclinic
Space group	P-1
Unit cell dimensions	a = 11.0330(10)Å α = 62.303(3)°.
	b = 12.4374(11) Å β = 71.710(3)°.
	c = 13.1345(12) Å γ = 64.929(3)°.
Volume	1430.0 (2) Å^3
Z	1
Density (calculated)	1.694 Mg/m^3
Absorption coefficient	7.398 mm^{-1}
F (000)	730
Crystal size	0.56 x 0.45 x 0.38 mm^3
Theta range for data collection	3.84 to 66.87°.
Index ranges	-13<=h<=13, -14<=k<=14, -15<=l<=15
Reflections collected	16149
Independent reflections	5029 [R(int) = 0.0388]
Completeness to theta = 66.868°	98.9 %
Absorption correction	multi-scan
Max. and min. transmission	0.046 and 0.060
Refinement method	Full-matrix least-squares on F^2
Data / restraints / parameters	5029 / 0 / 344
Goodness-of-fit on F^2	1.081
Final R indices [I>2sigma (I)]	R1 = 0.0388, wR2 = 0.1026
R indices (all data)	R1 = 0.0443, wR2 = 0.1055
Largest diff. peak and hole	0.736 and -0.553 e.Å^{-3}

Table 2.6.2. Crystal data and structure refinement for **2**.

Empirical formula	C42 H38 Cl2 F6 Ge2 N2 O6 P2 S2
Formula weight	1122.88
Temperature	100(2) K
Wavelength	1.54178 Å
Crystal system	Triclinic
Space group	P-1
Unit cell dimensions	a = 12.9761(12) Å α = 85.400(6)°.
	b = 13.6739(14) Å β = 86.134(6)°.
	c = 13.7965(12) Å γ = 70.497(6)°.
Volume	2297.9(4) Å^3
Z	2
Density (calculated)	1.623 Mg/m^3
Absorption coefficient	4.832 mm^{-1}
F (000)	1132
Crystal size	0.09 x 0.08 x 0.06 mm^3
Theta range for data collection	3.22 to 66.15°.
Index ranges	-15<=h<=15, -16<=k<=16, -16<=l<=16
Reflections collected	26902
Independent reflections	8073 [R(int) = 0.0829]
Completeness to theta = 66.597°	99.4 %
Absorption correction	multi-scan
Max. and min. transmission	0.171 and 0.258
Refinement method	Full-matrix least-squares on F^2
Data / restraints / parameters	8073 / 0 / 577
Goodness-of-fit on F^2	0.999
Final R indices [I>2sigma (I)]	R1 = 0.0829, wR2 = 0.1585
R indices (all data)	R1 = 0.1784, wR2 = 0.1965
Largest diff. peak and hole	1.074 and -1.008 e.Å^{-3}

Table 2.6.3. Crystal data and structure refinement for **3**

Empirical formula	C23 H23 Cl3 F3 Ge N O3 P S
Formula weight	660.39
Temperature	100 (2) K
Wavelength	1.54178 Å
Crystal system	Monoclinic
Space group	P 21/c
Unit cell dimensions	a = 10.8139(5) Å $\quad$ $\alpha = 90°$.
	b = 17.6150(9) Å $\quad$ $\beta = 90.808(3)°$.
	c = 14.8147(8) Å $\quad$ $\gamma = 90°$.
Volume	2821.7(2) Å^3
Z	4
Density (calculated)	1.555 Mg/m^3
Absorption coefficient	5.730 mm^{-1}
F (000)	1332
Crystal size	0.33 x 0.21 x 0.10 mm^3
Theta range for data collection	3.90 to 66.95°.
Index ranges	-12<=h<=11, -21<=k<=20, -17<=l<=17
Reflections collected	16690
Independent reflections	5025 [R (int) = 0.0733]
Completeness to theta = 66.894°	99.7 %
Absorption correction	multi-scan
Max. and min. transmission	0.001 and 0.004
Refinement method	Full-matrix least-squares on F^2
Data / restraints / parameters	4915 / 90 / 353
Goodness-of-fit on F^2	0.973
Final R indices [I>2sigma (I)]	R1 = 0.0733, wR2 = 0.1698
R indices (all data)	R1 = 0.1094, wR2 = 0.1893
Largest diff. peak and hole	1.714 and -1.402 e.Å^{-3}

Table 2.6.4. Crystal data and structure refinement for **4**

Empirical formula	C43 H37 F9 N2 O9 P2 S3
Formula weight	1054.86
Temperature	100 (2) K
Wavelength	1.54178 Å
Crystal system	Monoclinic
Space group	P 21/n
Unit cell dimensions	a = 14.1906(5) Å $\quad$ α = 90°.
	b = 19.4217(7) Å $\quad$ β = 101.035(2)°.
	c = 16.8932(6) Å $\quad$ γ = 90°.
Volume	4596.8(3) Å^3
Z	4
Density (calculated)	1.533 Mg/m^3
Absorption coefficient	2.987 mm^{-1}
F (000)	2160
Crystal size	0.09 x 0.06 x 0.05 mm^3
Theta range for data collection	3.50 to 66.65°.
Index ranges	-16<=h<=13, -23<=k<=23, -20<=l<=20
Reflections collected	56035
Independent reflections	8084 [R (int) = 0.1015]
Completeness to theta = 66.922°	99.4 %
Absorption correction	multi-scan
Max. and min. transmission	0.249 and 0.321
Refinement method	Full-matrix least-squares on F^2
Data / restraints / parameters	8084/ 150 / 686
Goodness-of-fit on F^2	1.069
Final R indices [I>2sigma (I)]	R1 = 0.1015, wR2 = 0.2399
R indices (all data)	R1 = 0.1529, wR2 = 0.2693
Largest diff. peak and hole	0.962 and -0.600 e.Å^{-3}

Table 2.6.5. Crystal data and structure refinement for **5**.

Empirical formula	C42 H38 Cl9 F3 Ga2 N2 O3 P2 S
Formula weight	1228.23
Temperature	100(2) K
Wavelength	1.54178 Å
Crystal system	Monoclinic
Space group	P21/n
Unit cell dimensions	a = 10.8764(4) Å $\quad$ $\alpha = 90°$.
	b = 37.6034(12) Å $\quad$ $\beta = 104.849(2)°$.
	c = 12.6639(4) Å $\quad$ $\gamma = 90°$.
Volume	5006.4(3) Å^3
Z	4
Density (calculated)	1.630 Mg/m^3
Absorption coefficient	7.177 mm^{-1}
F (000)	2464
Crystal size	0.56 x 0.48 x 0.32 mm^3
Theta range for data collection	2.35 to 66.48°.
Index ranges	-12<=h<=12, -44<=k<=44, -13<=l<=15
Reflections collected	48512
Independent reflections	8803[R (int) = 0.0746]
Completeness to theta = 66.859°	99.1%
Absorption correction	multi-scan
Max. and min. transmission	0.045 and 0.101
Refinement method	Full-matrix least-squares on F^2
Data / restraints / parameters	8803/ 0 / 578
Goodness-of-fit on F^2	1.039
Final R indices [I>2sigma (I)]	R1 = 0.0746, wR2 = 0.1900
R indices (all data)	R1 = 0.1182, wR2 = 0.2195
Largest diff. peak and hole	0.758 and -0.702 e.Å^{-3}

2.7. References

1. Jutzi, P.; Mix, A.; Rummel, B.; Schoeller, W. W.; Neumann, B.; Stammler, H. –G.; *Science*, 2004, **305**, 849-853.

2. Swamy, V.S.V.S.N.; Pal, S.; Khan, S.; Sen, S. S.; *Dalton Trans.,***2015**, *44*, 12903-12923.

3. Karsch, H.H.; Deubelly, B.; Riede, J. Muller, G.; *Angew. Chem. Int. Ed.,* **1987**, *26,* 673-674.

4. Inomata, K.; Watanabe, T.; Tobita, H.; *J. Am. Chem. Soc.,* **2014**, *136*, 14341-14344.

5. Ochiai, T.; Szilvási, T.; Franz, D. Irran, E.; Inoue, S.; *Angew. Chem. Int. Ed.,* **2016**, *55,* 11619-11624.

6. Xiong, Y.; Yao, S.; Szilvási, T.; Martínez, E. B.; Grützmacher, H.; Driess, M.; *Angew. Chem. Int. Ed.,* **2017**, *56*, 4333-4336.

7. Vanessa, B.A.; Wang, Z.; Macdonald, C.L.B.; Sham, T.; Ragogna, P. J.; *Chem. Eur. J.*, **2019**, *25*, 14790-14800.

8. Majumdar, M.; Raut, R. K.; Sahoo, P.; Kumar, V.; *Chem. Commun.* **2018**, *54*, 10839-10842.

9. Jeffrey, J.C.; Rauchfuss, T.B.; Tucker, P. A.; *Inorg. Chem.* **1980**, *19,* 3306-3315.

10. Williams, D. B. G.; Pretorius, M.; *J. Mol. Catalysis A: Chemical,* **2008**, *284,* 77-84.

11. Izod, K.; Stewart, J.; Clark, E. R.; Clegg, W.; Harrington, R. W.; *Inorg. Chem.* **2010**, *49*, 4698-4707; Yao, S.; Brym, M., Merz, K.; Driess, M.; *Organometallics,* **2008**, *27*, 3601-3607; Brym, M.; Francis, M. D.; Jin, G.; Jones, C.; Mills, D. P.; Stasch, A.; *Organometallics,* **2006**, *25*, 4799-4807; Tam, E. C. Y.; Maynard, N. A.; Apperley, D. C.; Smith, J. D.; Coles, M. P.; Fulton, J. R.; *Inorg. Chem.* **2012**, *51*, 9403-9415.

12. Cheng, F.; Hector, A. L.; Levason, W.; Reid, G.; Webster, M.; Zhang, W.; *Inorg. Chem.* **2010**, *49*, 752-760; Davis, M. F.; Levason, W.; Reid G.; Webster, M.; *Dalton Trans.* **2008**, 2261-2269; Garcia, J. M.; Ocando-Mavárez, E.; Kato, T.; Coll, D. S.; Briceño, A.; Saffon-Merceron, N.; Baceiredo, A.; *Inorg. Chem.* **2012**, *51*, 8187-8193; Del Rio, N.; Baceiredo, A.; Saffon-Merceron, N.; Hashizume, D.; Lutters, D.; Müller, T.; Kato, T.; *Angew. Chem. Int. Ed*. **2016**, *55,* 4753-4758.

13. Su, B.; Ganguly, R.; Li, Y.; Kinjo, R.; *Angew. Chem. Int. Ed.*, **2014**, *53*, 13106-13109; Xiong, Y.; Yao, S.; Tan, G.; Inoue S.; Driess, M.; *J. Am. Chem. Soc.*, **2013**, *135*, 5004-5007; Singh, A. P.; Roesky, H. W.; Carl, E.; Stalke, D.; Demers J. –P.; Lange, A.; *J. Am.Chem. Soc.*, **2012**, *134*, 4998-5003; Li, J.; Schenk, C.; Winter, F.; Scherer, H.; Trapp, N.; Higelin, A.; Keller, S.; Pöttgen, R.; Krossing, I.; Jones, C.; *Angew. Chem. Int. Ed.*, **2012**, *51,* 9557-9561.

CHAPTER 3

## Synthesis of unique bimetallic gold-germanium complexes
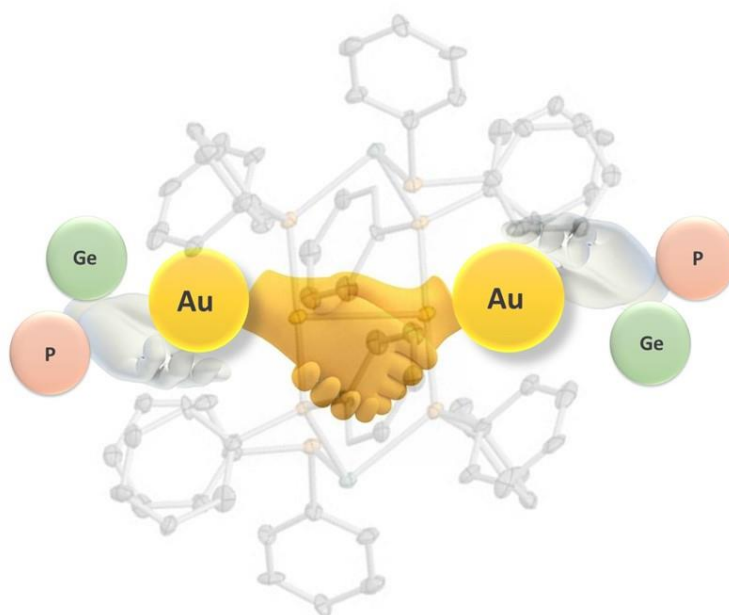
Abstract

The Ligand L_{im} on reaction with AuCl. SMe_2 led to the formation of Complex **1** and **2**. Complex is a monometallic complex with the imino Ns uncoordinated. Complex **2** is bimetallic complex with the two gold centres attached to the individual P-centres of the ligand. Both the complexes were characterized by NMR and Single Crystal X-ray diffraction techniques. Complex **1** was hence chosen for further reactivity studies. It was observed that the reaction of $GeCl_2$.Dioxane with Complex **1** led to the formation of complex **3** which indicates the lability of the chloride of complex **1**. Complex **3** was characterized by Single Crystal X-ray diffraction technique. Hence, the chloride was replaced with a less labile $-PPh_2$ group to form complex **4** which was characterized by NMR studies. Complex **4** was further reacted with $GeCl_2$.Dioxane which led to the formation of aurophilic complex **5**.

3.1. Introduction

The cationic group 14 species (Si-Pb) are well known for their catalytic applications.[1] Owing to the empty p-orbitals and a lone pair of electrons, germyliumylidene show ambiphilic nature.[2] This property can be utilised as they can act as an L-or Z-type ligand to the transition metal complexes.[3] A few examples of group 13 complexes and hypervalent group 15 complexes have been used as a Z-type ligand (**A-D**).[4,5] These complexes act as Lewis acidic center making the transition metal more electrophilic enhancing the catalytic activity of the bimetallic complexes. In comparison, there are lesser-known complexes of group 14 acting as Z-type ligands.[6] Mostly they have been used as L-type ligands.[7] Very recently, Gabbai et.al have synthesised a carbenium assisted gold complex which acts as a Z-type ligand (**E**).[8]

A

B

E=Al, Ga, In
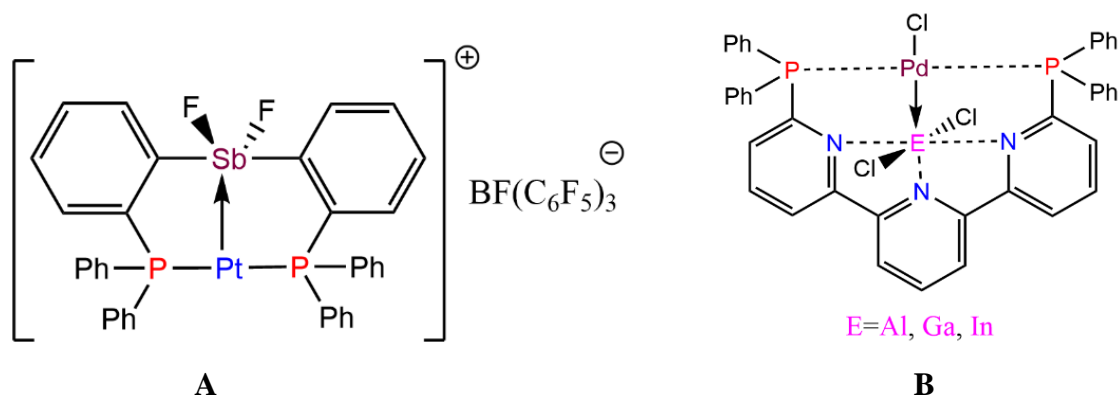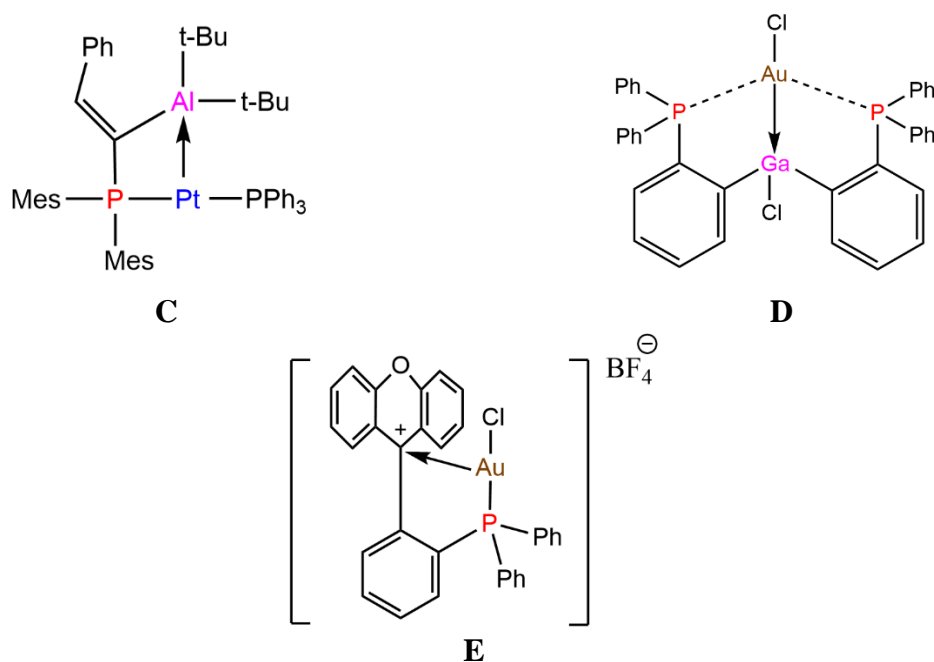
3.1.1 Previously reported examples of Z-type ligand complexes

3.2. Scope of the work

Recently, Majumdar et al. reported a germyliumylidene supported by the two imino nitrogens of the α-iminopyridine ligand (Scheme 3.2.1).[9] That provided the evidence for attempting the synthesis of a germyliumylidene species supported by L_{Im} ligand leaving the two phosphine phosphorus centres available for coordination with transition metal centres. However, on addition of one equivalent of $GeCl_2$.Dioxane along with one equivalent of trimethylsilyl trifluoromethanesulfonate the sole product obtained is bis(chlorogermyliumylidene). Hence, the coordination of transition metal centres was attempted first. Gold(I) chloride provided promising results with the synthesis of a monometallic and a bimetallic complex. The monometallic complex provided an open coordination site which was further exploited for the coordination of germanium metal center. However, it led to the formation of a different germanium-gold bimetallic complex. So, on replacing the chloride moiety bonded to the gold center with a -PPh_2 group, leads to formation of a different gold-germanium complex on reacting further with $GeCl_2$.Dioxane.
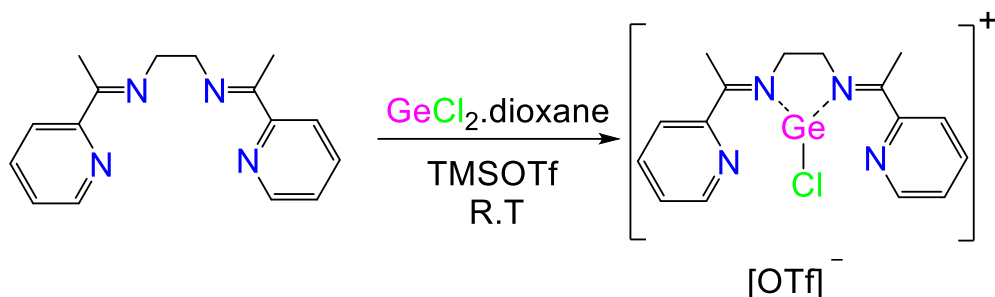
3.2.1 Chlorogermyliumylidene supported by α-iminopyridine ligand

3.3. Results and discussion

3.3.1. The Gold complexes

The ligand L_{Im} on when reacted with one equivalent of Gold(I) chloride in THF at room temperature gave a white solid on evaporation. The solid was redissolved in THF, was concentrated and layered with hexane. The solution was kept at -35°C to obtain white crystals of complex **1**. Similarly, on reacting two equivalents of Gold(I) chloride with the ligand in THF at room temperature gave another white solid. This solid on redissolving in THF, concentrating and layering with hexane gave white crystals of complex **2** at -35°C (Scheme 3.3.1). Both the complexes **1** and **2** were characterised by single crystal X-ray diffraction technique and NMR technique. The ^{31}P NMR spectrum was found to be downfield shifted in comparison that of ^{31}P NMR spectrum of the ligand. Worth mentioning is that the reaction of one equivalent of GeCl$_2$.Dioxane in presence of one equivalent of trimethylsilyl trifluoromethanesulfonate with the ligand L_{Im} only produced the bis(chlorogermyliumylidene). The expected product of monochlogermyliumylidene coordinated to the two imino nitrogens was not obtained.
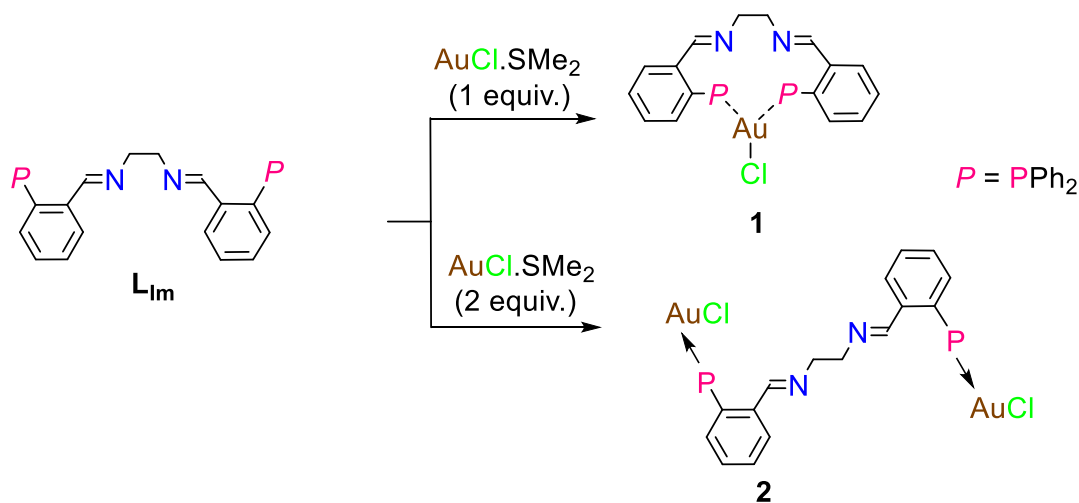
3.3.1. Synthesis of gold complexes **1** and **2**

90

3.3.2. The Gold-germanium complexes

Complex **1** as characterised by single crystal X-ray diffraction technique points out a free coordination site between the two imino nitrogens as the gold center binds to the two phopshine centres of the ligand. In attempt to use this free pocket, Complex **1** was reacted with one equivalent of GeCl₂.Dioxane in THF at room temperature. A white solid was obtained which was redissolved in THF and kept for crystallisation at -35°C (Scheme 3.3.2). White crystals of complex **3** were obtained. The complex was characterised by single crystal X-ray diffraction technique. Complex **3** shows that the chloride group of the complex **1** is highly labile so the germanium preferably goes for an oxidative addition with the chloride making an ionic complex with the gold rather than coordinating with the imino nitrogens.
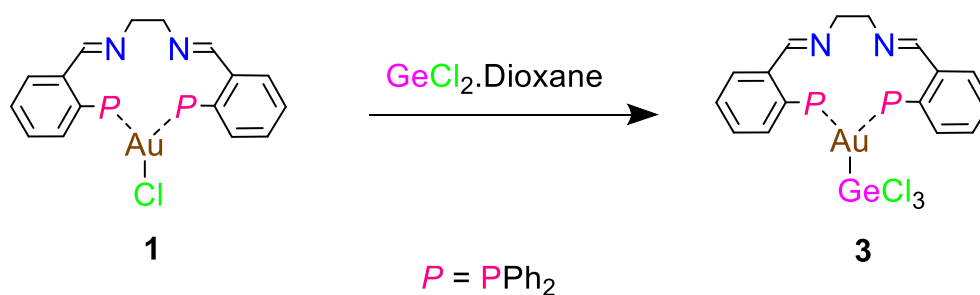
3.3.2. Synthesis of gold germanium complex **3**

So, an attempt was made to replace the chloride with a non-Labile group such as -PPh₂ to achieve the target molecule. Complex **1** was reacted with PPh₂Li to replace the chloride moiety. PPh₂Li is easily synthesised *in situ* by reacting lithium with a solution of PPh₂Cl in THF at room temperature which gives a bright orange-red coloured solution of PPh₂Li.[10] The solution of an excess of PPh₂Li was added directly to complex **1** in THF at room temperature. The solution was stirred overnight and then evaporated. The solid was extracted with toluene to remove the LiCl generated in the reaction and then the toluene solution was evaporated to obtain a pink crystalline solid of complex **4**. Complex **4** was characterised by NMR spectroscopy. The ³¹P NMR spectrum indicated two peaks at -14.36 ppm and -40.17 ppm. The peak at -40.17 ppm corresponds to the phosphine moiety of ligand and the other peak at -14.36 ppm corresponds to the phosphine group attached to Au center. Complex **4** has a similar coordinating site as complex **3**. So complex **4** was further reacted with one equivalent of GeCl₂.Dioxane in THF at room temperature. The colour of the solution changed from pink to orange within 12 hours. The solution was concentrated and kept at -35°C. After a few weeks, orange crystals of complex **5** are obtained (Scheme 3.3.3). Complex 5 is unique in its structure

as it has an Au-Au bond with the gold centres coordinated by phosphines which are further coordinated to a germylene. The complex was characterised by single crystal X-ray diffraction technique. The probable cause of formation of Complex 5 maybe the excess PPh_2Li that remains in the reaction mixture. This excess PPh_2Li reacts with $GeCl_2$.Dioxane which leads to the *in-situ* formation of a germylene supported by PPh_2 groups. The phosphine groups of the germylene further coordinates with the Au-PPh_2 moiety which losses the ligand L_{Im} to form complex **5**. The germylene is highly unstable so it accepts electron from the PPh_2 group of another gold center and gives rise a cyclic dimer.
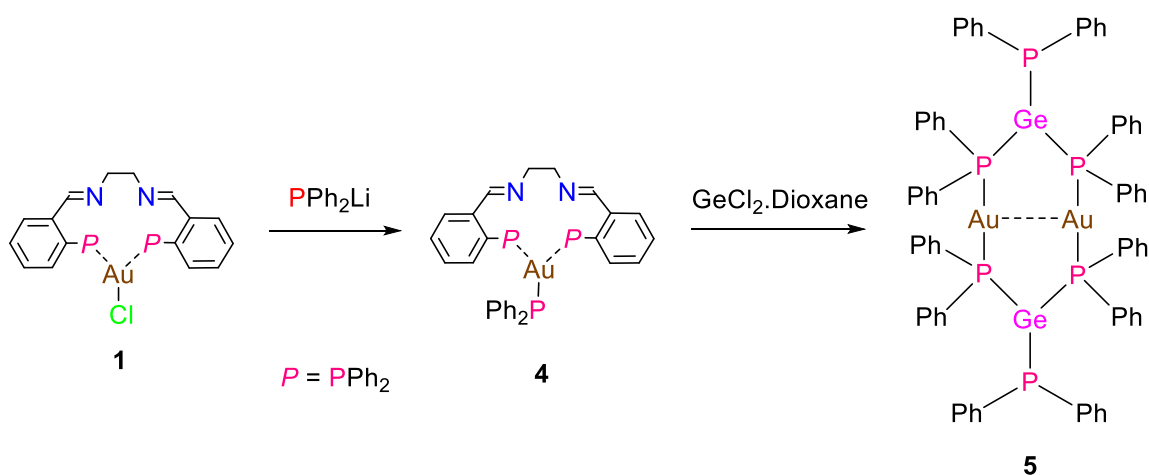
3.3.3. Synthesis of gold-germanium complex **5**

3.3.3. Crystal Structure

Complex **1** crystallised in the space group P-1 having a THF molecule in the asymmetric unit. The molecular structure shows the coordination of the two phosphorus atoms of the ligand P1 and P2 coordinated the AuCl moiety replacing the labile SMe_2 groups. The Au1-P1 bond distance is found to be 2.309(11) Å and the Au1-P2 distance is found to be 2.292(12) Å which comes in the range of previously reported Au-P complexes.[11] The two imino nitrogens are not coordinated by any metal center which creates a coordinating pocket for main group metal center. The Au1, P1, P2 and Cl1 all lie in the same plane. The summation of bond angle around Au(1) center is 359.95° (Figure 3.3.1).
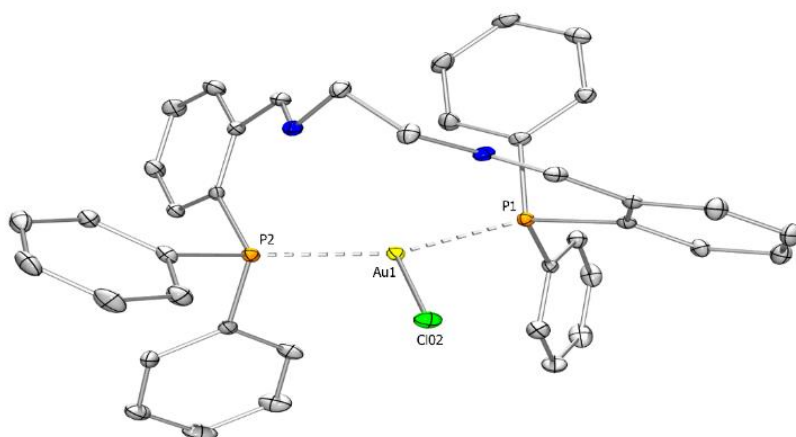
Figure 3.3.1. The molecular structure of compound **1** in the solid state (thermal ellipsoids at 30%, H atoms and tetrahydrofuran solvent molecule omitted for clarity). Selected bond lengths [Å] and angles [°]: Au1-P1 2.309(11), Au1-P2 2.292(12), Au1-Cl02 2.588(12); P1-Au1-P2 143.16(4), Cl02-Au1-P2 109.48(4), Cl02-Au1-P1 107.31(4).

Complex **2** crystallises in orthorhombic system with the space group Pna2$_1$ space group. The two Phosphorus centres coordinate to two gold centres independently having bond distances Au1-P2= 2.230(2) and Au2-P1= 2.333(2) Å. The average P-Au-Cl bond angle is 175.72° showing an almost linear geometry at the coordination site (Figure 3.3.2).

Figure 3.3.2 The molecular structure of compound **2** in the solid state (thermal ellipsoids at 30%, H atoms omitted for clarity). Selected bond lengths [Å] and angles [°]: P2-Au1 2.230(2), Au1-Cl1 2.292(2), P1-Au2 2.233(2), Au2-Cl2 2.279(2); P1-Au2-Cl2 176.75(8), P2-Au1-Cl1 174.70(7).

Complex **3** crystallises in monoclinc space group P2$_1$/n. The GeCl$_3$ group is bonded to the gold center with the two phosphorus donating electron to the gold center having bond

distances of Au1-P1= 2.331(5) and Au1-P2= 2.348(2) Å. The distance between gold and the germanium center is found to be 2.512(3) Å which is found to be longer than the range of Au-Ge bond distances.[12] The average Ge-Cl bond distance was found to be 2.232 Å. The GeCl$_3$ moiety was found to be pyramidal with the germanium at the apex coordinated to the gold center. The summation of bond angles around Au1 was found to be 359.3° depicting the planarity of Au1, P1, P2 and Ge1 (Scheme 3.3.3).

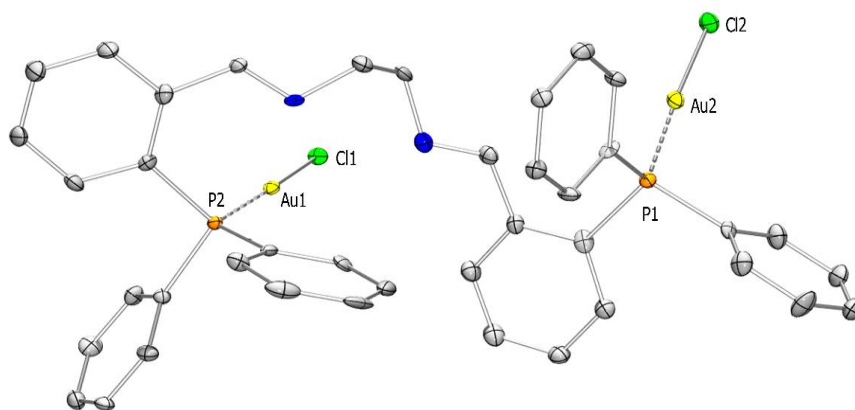**Figure 3.3.3** The molecular structure of compound **3** in the solid state (thermal ellipsoids at 30%, H atoms omitted for clarity). Selected bond lengths [Å]: P1-Au1 2.331(5), P2-Au1 2.348(2), Au1-Ge1 2.512(3).

Complex **5** crystallises in P-1 space group. The asymmetric unit contains germylene center with two -PPh$_2$ groups bonded with the germanium center. One of the phosphorus of the phosphine bonded to germanium is coordinated to the gold center which is bonded with a PPh$_2$ center. The complete molecule is a dimer of the moiety present in the asymmetric unit with the two gold having a bond distance of 3.074 Å which reflects a typical bond distance for aurophilic interaction.[13] The free phosphine group bonded to the gold center coordinates to the other germanium center in the other asymmetric unit. So, the two gold, two phosphorus and one germanium center each form a five membered ring which forms a puckered envelope like structure. Since the two gold centres are shared between the two five membered ring systems, together the two germanium, four phosphorus and two gold centres remain in a chair like configuration with the two germanium centres at the corners with a PPh$_2$ moiety bonded to them. The Au1-P1 and Au1-P2 bond distances are 2.312(4) Å and 2.315(6) Å. The Ge1-P2 and Ge1-P3 distances are 2.393(2) and 2.403(5) Å respectively. The P1-Au1-P2 bond angle is 167°

which slightly deviates from planarity and the bond angle of P2-Ge1-P3 is found to be 90.98° (Scheme 3.3.4).
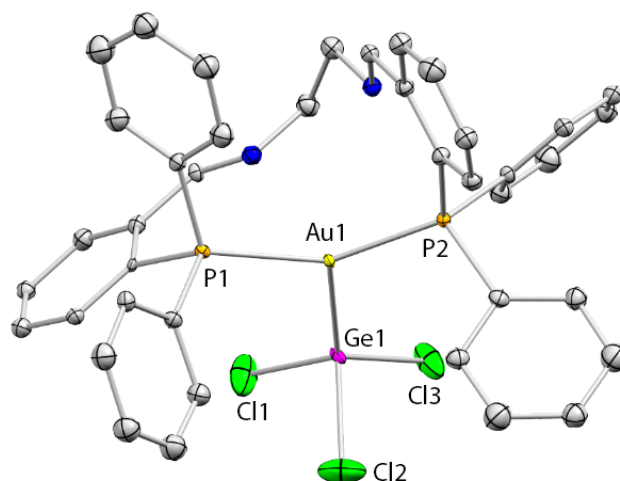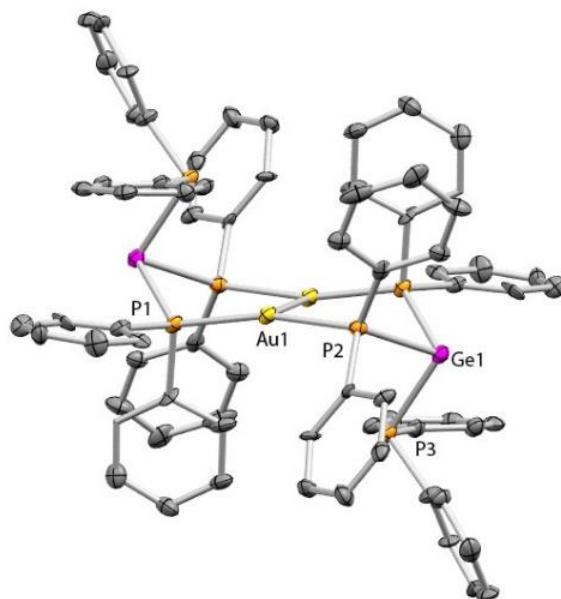

Figure 3.3.4 The molecular structure of compound **5** in the solid state (thermal ellipsoids at 30%, H atoms omitted for clarity). Selected bond lengths [Å] and angles [°]: Au1-P1 2.312(4), Au1-P2 2.315(6), Ge1-P2 2.393(2), Ge1-P3 2.403(5). P1-Au1-P2 167, P2-Ge1-P3 90.98.

3.4. Conclusion

In conclusion, an attempt was made to synthesize a Z-type complex with germyliumylidene as a ligand to gold(I) complex. So complex **1** and **2** were obtained on reacting AuCl.SMe$_2$ with ligand L$_{Im}$ in 1:1 and 1:2 ratios. Complex **1** is monometallic complex with an empty coordinating site between the two nitrogens. This fact was exploited by reacting it with GeCl$_2$.Dioxane which led to the formation of Complex **3**. To compensate for the labile chloride group of complex **1** it was reacted with PPh$_2$Li and complex **4** was obtained. Complex **4** on reaction with GeCl$_2$.Dioxane led to formation of the gold-germanium complex **5** which has a unique Au-Au bond supported by phosphine groups attached to the germylene.

3.5. Experimental

3.5.1. General Remarks

All manipulations were carried out under a protective atmosphere of argon applying standard Schlenk techniques or in a dry box. Tetrahydrofuran, hexane and pentane were refluxed over

sodium/benzophenone. All solvents were distilled and stored under argon and degassed prior to use. $CDCl_3$ were purchased from Sigma Aldrich and used as it is. Benzene-d_6 was purchase from Sigma Aldrich and was dried over potassium prior to use. All chemicals were used as purchased. The ligands L_{IM} was prepared according to literature procedure.[14] ^1H and $^{13}C\{^1H\}$ NMR spectra were referenced to external $SiMe_4$ using the residual signals of the deuterated solvent (^1H) or the solvent itself (^{13}C). $^{31}P\{^1H\}$ NMR was referenced to external 85% H_3PO_4. Elemental analyses were performed on Elementar vario EL analyzer. Single crystal data were collected on both Bruker SMART APEX four-circle diffractometer equipped with a CMOS photon 100 detector (Bruker Systems Inc.) with a Cu Kα radiation (1.5418 Å), and Bruker SMART APEX Duo diffractometer using Mo Kα radiation (0.71073 Å).

3.5.2. Synthesis and characterization of complex 1

Ligand L_{Im} (0.05 g, 0.08 mmol) and Chloro(dimethylsulfide)gold(I) (0.024 g, 0.082 mmol) were dissolved in 5 mL of THF and stirred overnight at room temperature. Single crystals were obtained by layering the reaction mixture with hexane and keeping overnight at -25 ºC. The crystals were isolated from the solution by filtration and drying under vacuum yielding 0.05 g (79 %) of **1** (Decomp. Temp. 183-185 ºC).

^1H NMR (400 MHz, CDCl$_3$, TMS): δ = 8.67 (s, 2H, N=CH); 7.99 (dd, J_{H-H} = 7.6 Hz, J_{H-H} = 1.2 Hz, 2H, Ar-H); 7.73 (t, J_{H-H} = 7.6 Hz, 2H, Ar-H); 7.57-7.41 (m, 22H, Ar-H); 6.90 (q, J_{H-H} = 6.5 Hz, 2H, Ar-H); 3.42 (s, 4H, -CH$_2$-CH$_2$-) ppm.

$^{13}C\{^1H\}$ NMR (101 MHz, CDCl$_3$, TMS): δ = 162.86 (s, N=CH); 138.05 (s, Ar-C); 135.29 (t, J_{C-P} = 3.74 Hz, Ar-C); 134.85 (d, J_{C-P} = 4.14 Hz, Ar-C); 133.87 (s, Ar-C); 133.79 (s, Ar-C); 132.13 (s, Ar-C); 131.72 (s, Ar-C); 130.51 (s, Ar-C); 130.21 (s, Ar-C); 129.35 (t, J_{C-P} = 5.76 Hz, Ar-C); 58.45 (s, -CH$_2$-CH$_2$-) ppm.

$^{31}P\{^1H\}$ NMR (162 MHz, CDCl$_3$, H$_3$PO$_4$): δ = -43.83 ppm

Elemental analysis: Calculated for $C_{40}H_{34}AuClN_2P_2$: C, 57.39; H, 4.09; N, 3.35. Found: C, 57.48; H, 4.04; N, 3.37.

3.5.3. Synthesis and characterization of complex 2

Ligand L_{Im} (0.05 g, 0.08 mmol) and Chloro(dimethylsulfide)gold(I) (0.048 g, 0.16 mmol) were dissolved in 10 mL of THF and stirred overnight at room temperature. Single crystals were obtained by layering the reaction mixture with hexane and keeping overnight at -25 ºC. The crystals were isolated from the solution by filtration and drying under vacuum yielding 0.06 g (72 %) of **2** (Decomp. Temp. 160-162 ºC).

¹H NMR (400 MHz, CDCl₃, TMS): δ = 8.39 (s, 2H, N=CH); 7.77 (ddd, J_{H-H} = 7.6 Hz, J_{H-H} = 4 Hz, J_{H-H} = 1.2 Hz, 2H, Ar-H); 7.59-7.49 (m, 14H, Ar-H); 7.44-7.40 (m, 8H, Ar-H); 7.33 (tt, J_{H-H} = 8 Hz, J_{H-H} = 1.6 Hz, 2H, Ar-H); 6.81 (dd, J_{H-H} = 13.2 Hz, J_{H-H} = 7.6 Hz, 2H, Ar-H); 3.33 (s, 4H, -CH₂-CH₂-) ppm.

¹³C{¹H} NMR (101 MHz, CDCl₃, TMS): δ = 160.14 (s, N=CH); 138.54 (s, Ar-C); 134.69 (d, J_{C-P} = 7.78 Hz, Ar-C); 133.99 (s, Ar-C); 133.82 (s, Ar-C); 132.94 (s, Ar-C); 131.49 (d, J_{C-P} = 2.02 Hz, Ar-C); 131.34 (d, J_{C-P} = 2.63 Hz, Ar-C); 130.48 (s, Ar-C); 129.89 (s, Ar-C); 129.13 (d, J_{C-P} = 12.02 Hz, Ar-C); 59.76 (s, -CH₂-CH₂-) ppm.

³¹P{¹H} NMR (162 MHz, CDCl₃, H₃PO₄): δ = -33.57 ppm

Elemental analysis: Calculated for $C_{40}H_{34}Au_2Cl_2N_2P_2$: C, 44.92; H, 3.20; N, 2.62. Found: C, 44.81; H, 3.24; N, 2.58.

3.5.3. Synthesis of complex 3

Complex **1** (0.05g, 0.06 mmol) was dissolved in 15 mL THF. To the solution GeCl₂.Dioxane (0.013g, 0.06 mmol) was added. The solution was stirred overnight and evaporated. A white solid was obtained which was redissolved in 5mL THF. It was concentrated and stored at -35°C for a week. White crystals of 3 were obtained. (Yield= 0.059g, 87%)

¹H NMR (400 MHz, CDCl₃, TMS): δ = 8.02(s, 2H, N=CH); 7.66 (m, 2H, Ar-H); 7.54 (m, 2H, Ar-H);7.46 (m, 3H, Ar-H); 7.36 (bs, 2H, Ar-H); 7.11 (m, 13H, Ar-H); 7.06 (m, 6H, Ar-H); 3.59 (s, 4H, -CH₂-CH₂-) ppm.

³¹P{¹H} NMR (162 MHz, CDCl₃, H₃PO₄): δ = -42.69 ppm

Elemental analysis: Calculated for $C_{40}H_{34}AuCl_3GeN_2P_2$: C, 49.01; H, 3.51; N, 2.88. Found: C, 48.89; H, 3.49; N, 2.86.

3.5.4. Synthesis of complex 4

PPh₂Li was synthesised by adding excess lithium granules to a solution of PPh₂Cl (0.026g, 0.1 mmol) in 10 mL THF. The reaction was stirred overnight to obtain a bright orange-red solution of PPh₂Li. The solution was filtered to remove excess lithium and it was added to a solution of Complex **1** (0.1g, 0.1 mmol) in 10 mL THF at -78°C. The reaction mixture was slowly allowed to thaw to room temperature and was stirred for 12 hours. After stirring is completed the solution is evaporated and extracted with toluene (10 X 3mL) to remove the LiCl generated. The toluene solution is evaporated and the pale yellow crystalline solid obtained is submitted for NMR studies. (Yield= 0.093g, 79%)

¹H NMR (400 MHz, CDCl₃, TMS): δ = 8.25 (s, 2H, N=CH); 7.69 (d, J_{H-H}= 7.8 Hz, 2H, Ar-H); 7.66 (m, J_{H-H}= 6.4 Hz, 2H, Ar-H); 7.47 (m, 7H, Ar-H); 7.37 (m, 23H, Ar-H); 6.90 (q, J_{H-H}= 6.4 Hz, 5.9 Hz, 7H, Ar-H,); 3.39 (s, 4H, -CH₂-CH₂-) ppm.

¹³C{¹H} NMR (101 MHz, CDCl₃, TMS): δ = 162.13 (s, N=CH); 138.51 (s, Ar-C); 134.91 (s, Ar-C); 134.34 (s, Ar-C); 133.71 (t, J_{C-P} = 8.6 Hz, Ar-C); 132.32 (s, Ar-C); 131.78 (s, Ar-C); 131.67 (s, Ar-C); 131.50 (s, Ar-C); 131.32 (s, Ar-C); 131.23 (s, Ar-C); 131.01 (s, Ar-C); 130.38 (s, Ar-C); 128.97 (t, J_{C-P} = 5.7 Hz, Ar-C); 128.49(s, Ar-C); 128.26 (s, Ar-C); 59.15 (s, -CH₂-CH₂-) ppm.

³¹P{¹H} NMR (162 MHz, CDCl₃, H₃PO₄): δ = -14.36 ppm, -40.17 ppm

Elemental analysis: Calculated for $C_{52}H_{44}AuN_2P_3$: C, 63.21; H, 4.56; N, 2.91. Found: C, 63.29; H, 4.49; N, 2.84.

3.5.5. Synthesis of complex 5

Complex **4** (0.1g, 0.1 mmol) is dissolved in THF. To the solution GeCl₂.Dioxane (0.023g, 0.1 mmol) was added. The solution was stirred overnight and evaporated. An orange solid was obtained which was dissolved in toluene and filtered to remove any insoluble solid. It was concentrated and stored at -35°C for 3-4 weeks. Orange crystals of **5** were obtained. (Yield= 0.093g, 56%)

¹H NMR (400 MHz, C₆D₆, TMS): δ = 7.55(m, 10H, Ar-H); 7.37 (m, 14H, Ar-H); 7.02 (m, 20H, Ar-H); 6.96 (m, 9H, Ar-H); 6.94 (m, 7H, Ar-H) ppm.

¹³C{¹H} NMR (101 MHz, C₆D₆, TMS): δ = 136.77 (s, Ar-C); 135.40 (s, Ar-C); 134.83 (s, Ar-C); 134.42 (s, Ar-C); 128.86 (s, Ar-C); 128.59 (s, Ar-C) ppm.

³¹P{¹H} NMR (162 MHz, C₆D₆, H₃PO₄): δ = -20.72 ppm, -46.40 ppm

Elemental analysis: Calculated for $C_{72}H_{60}Au_2Ge_2P_6$: C, 52.36; H, 3.70. Found: C, 52.40; H, 3.66.
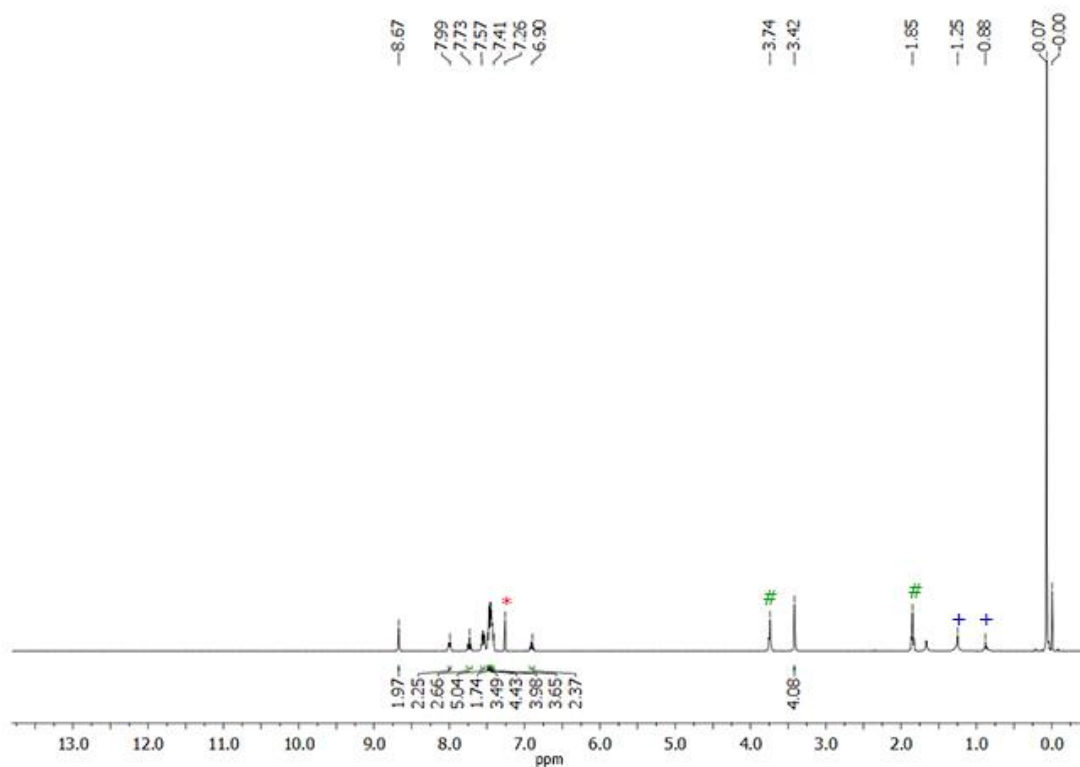
3.6. NMR Study

Figure 3.6.1. ^{1}H NMR of **1** in CDCl$_3$ (* = residual CDCl$_3$, # = THF, + = Hexane)
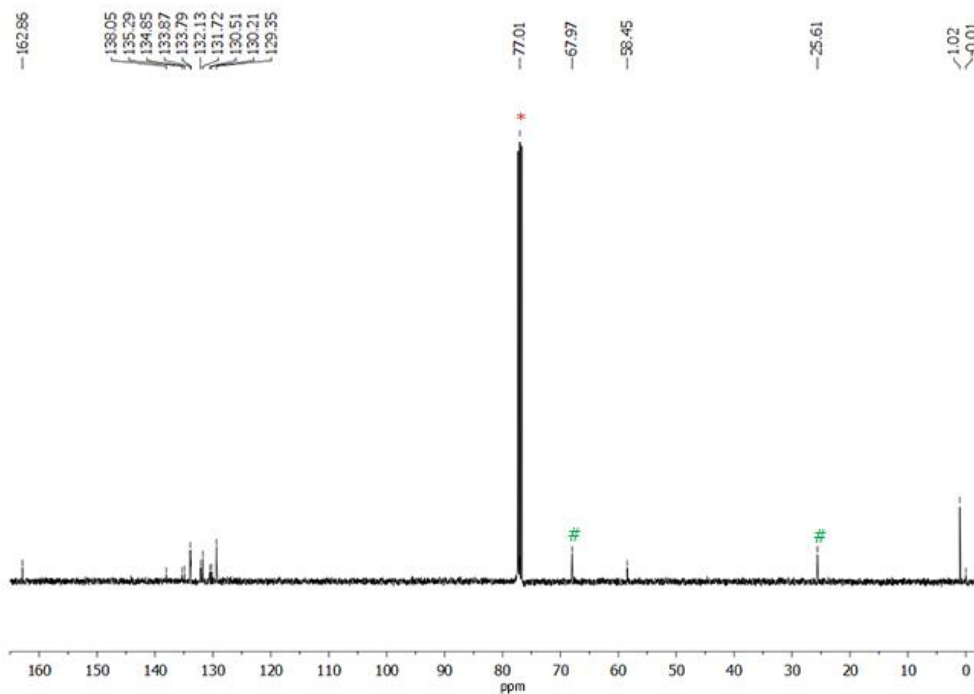
Figure 3.6.8. ^{13}C{^{1}H} NMR of **1** in CDCl$_3$ (* = CDCl$_3$, # = THF)
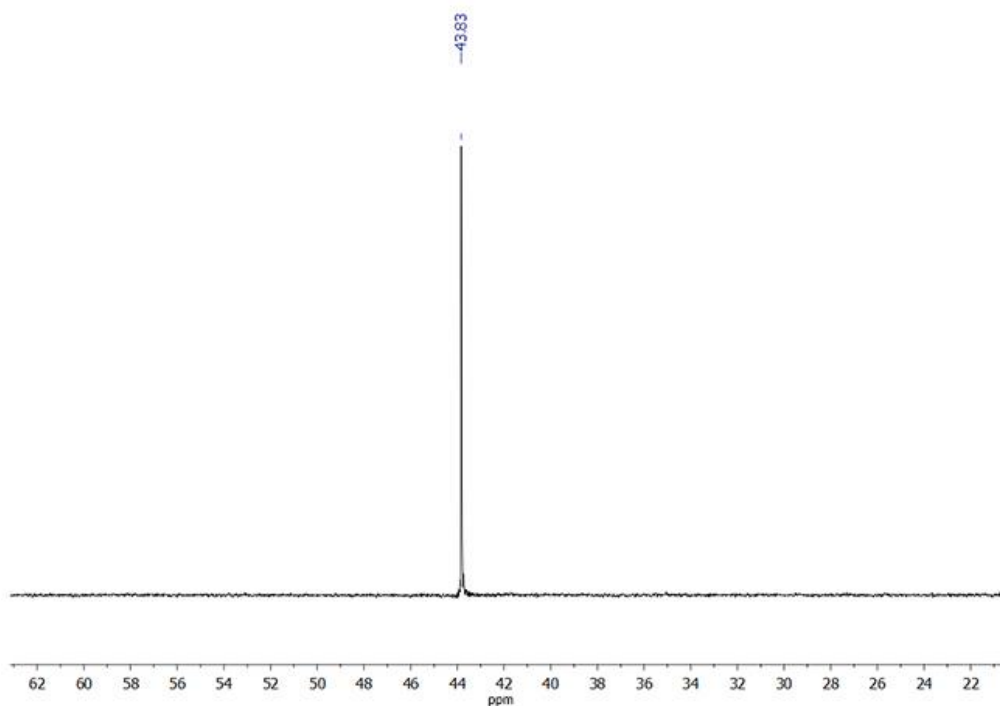
Figure 3.6.3. $^{31}P\{^1H\}$ NMR of **1** in CDCl$_3$
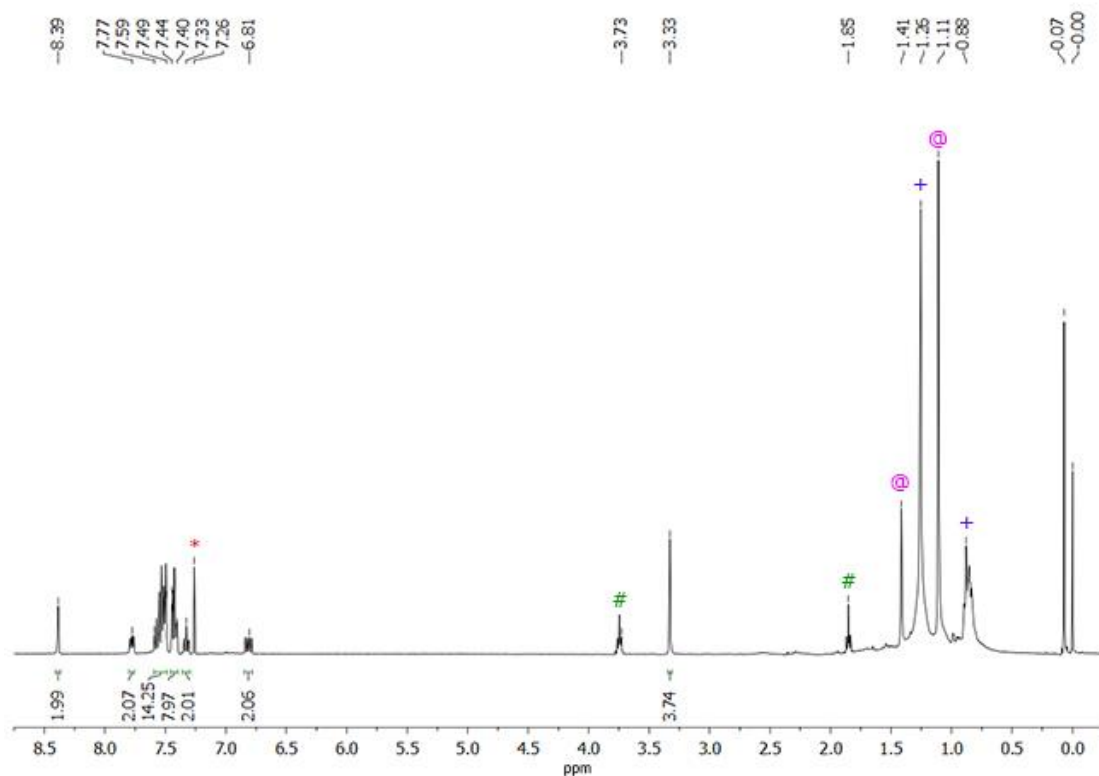
Figure 3.6.4. ^1H NMR of **2** in CDCl$_3$ (* = residual CDCl$_3$, # = THF, + = Hexane, @ = Impurity)
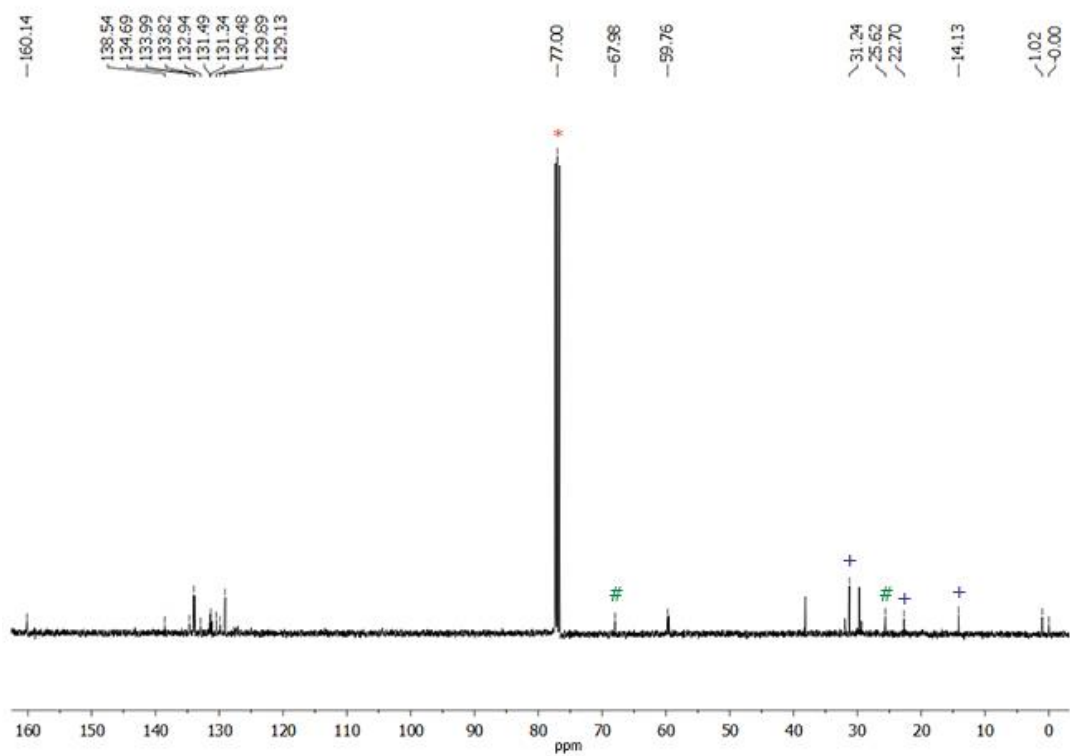
Figure 3.6.5. $^{13}C\{^1H\}$ NMR of **2** in CDCl$_3$ (* = CDCl$_3$, # = THF, + = Hexane)
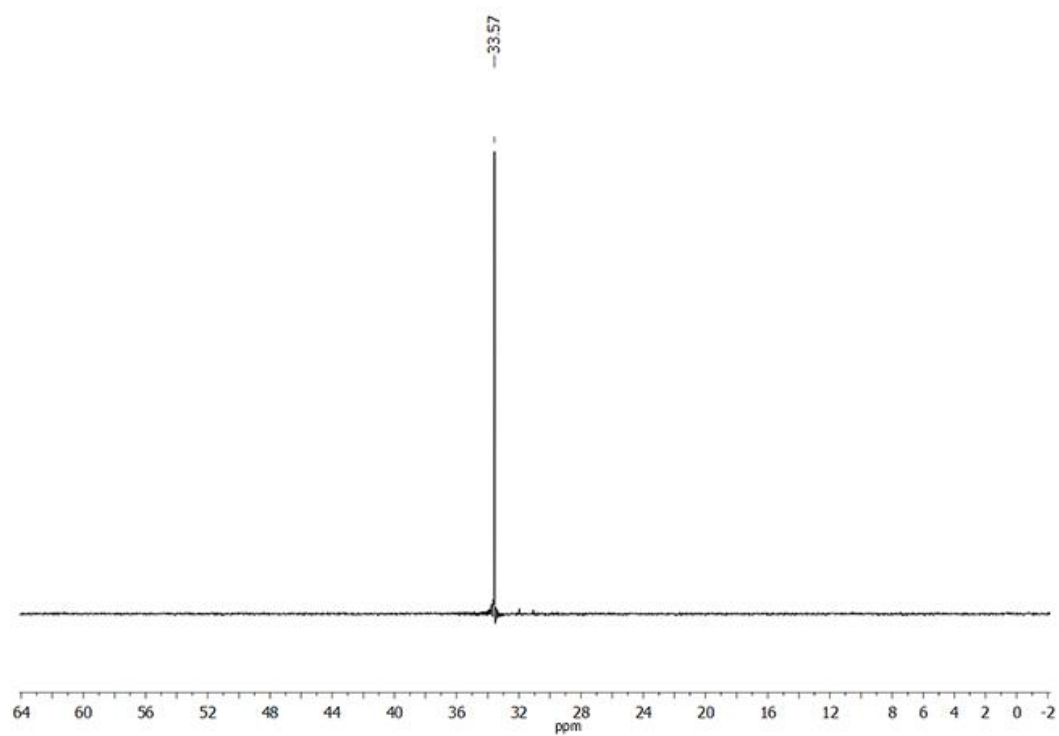
Figure 3.6.5. $^{31}P\{^1H\}$ NMR of **2** in CDCl$_3$
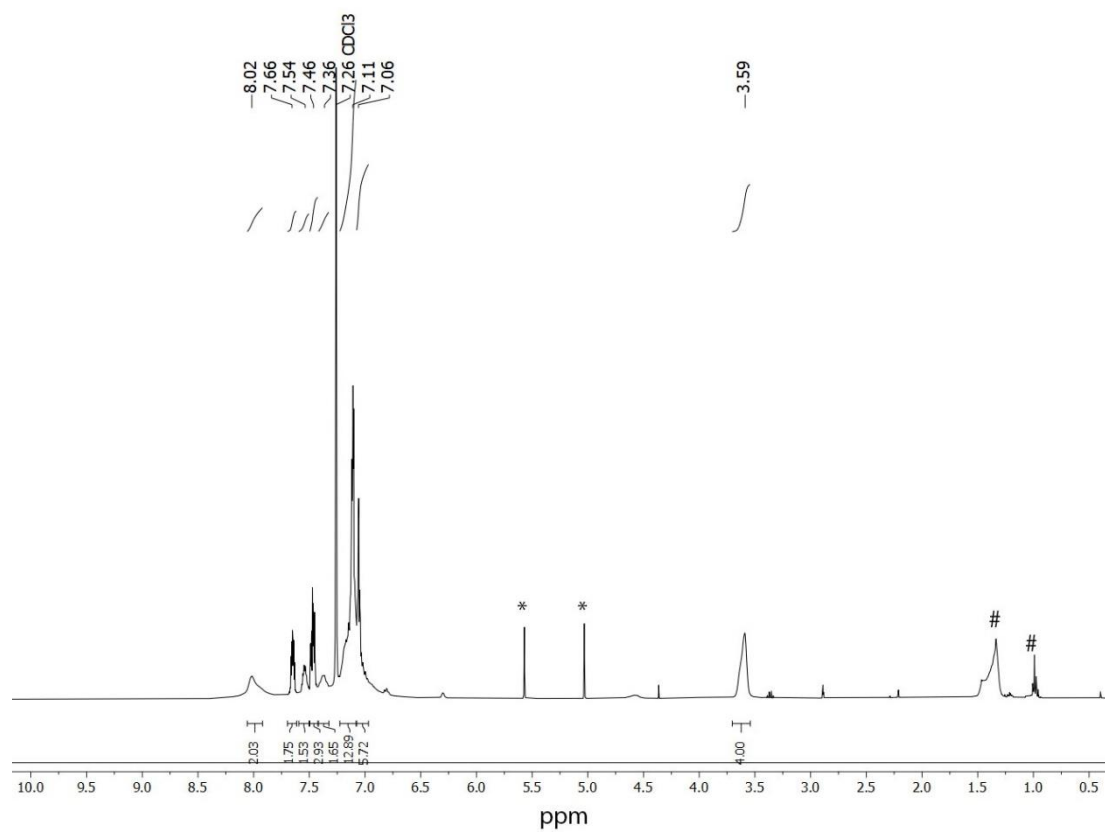
Figure 3.6.6. ^{1}H NMR of **3** in CDCl$_3$ (*= impurity, # = Hexane)
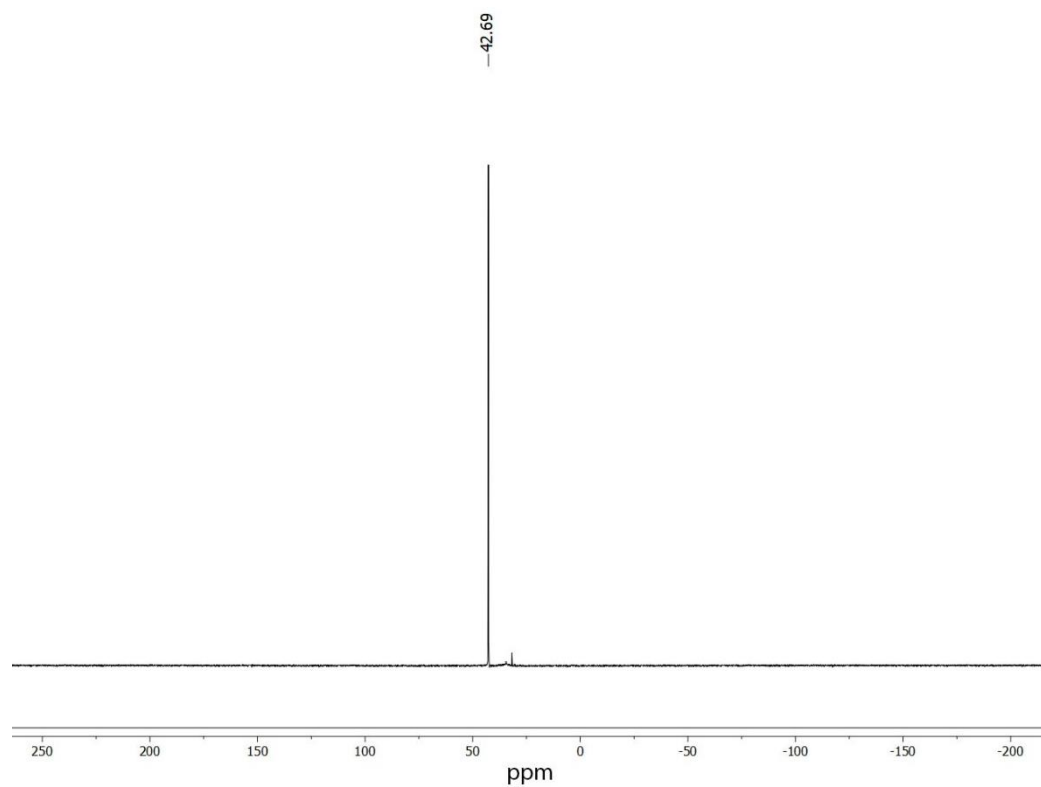
Figure 3.6.7. ^{31}P{^{1}H} NMR of **3** in CDCl$_3$
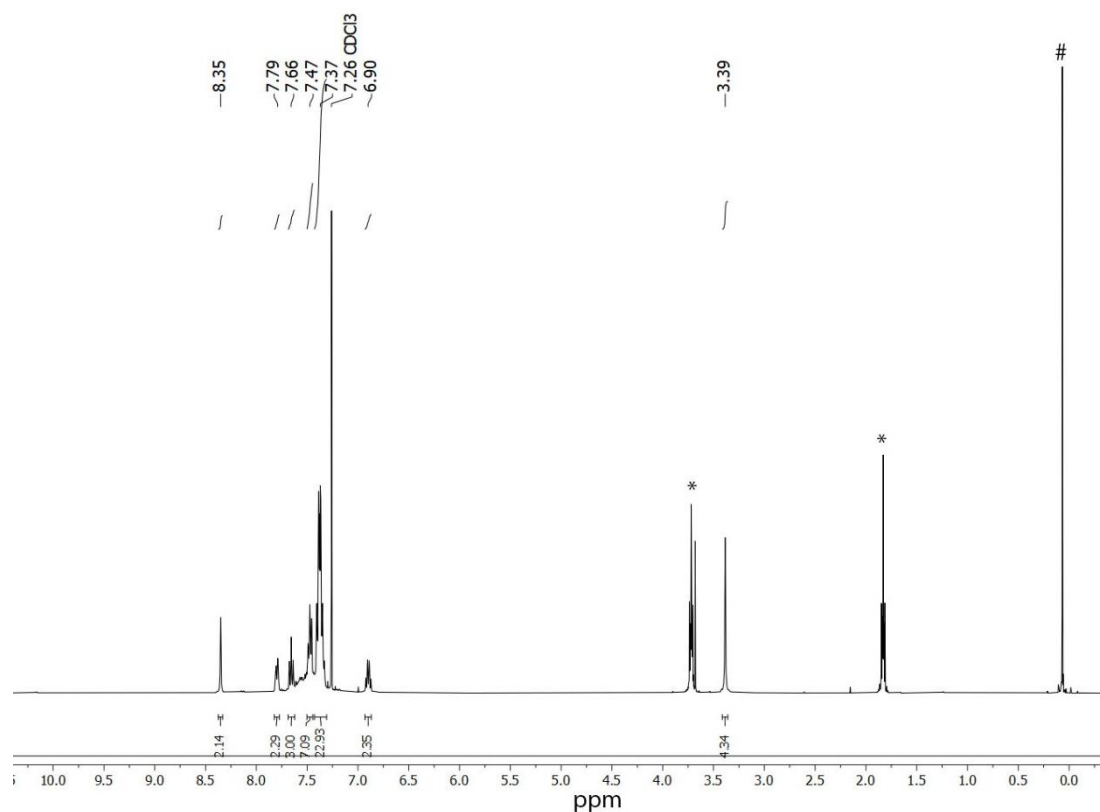
Figure 3.6.8. ^{1}H NMR of **4** in CDCl$_3$ (*= THF, #= TMS)
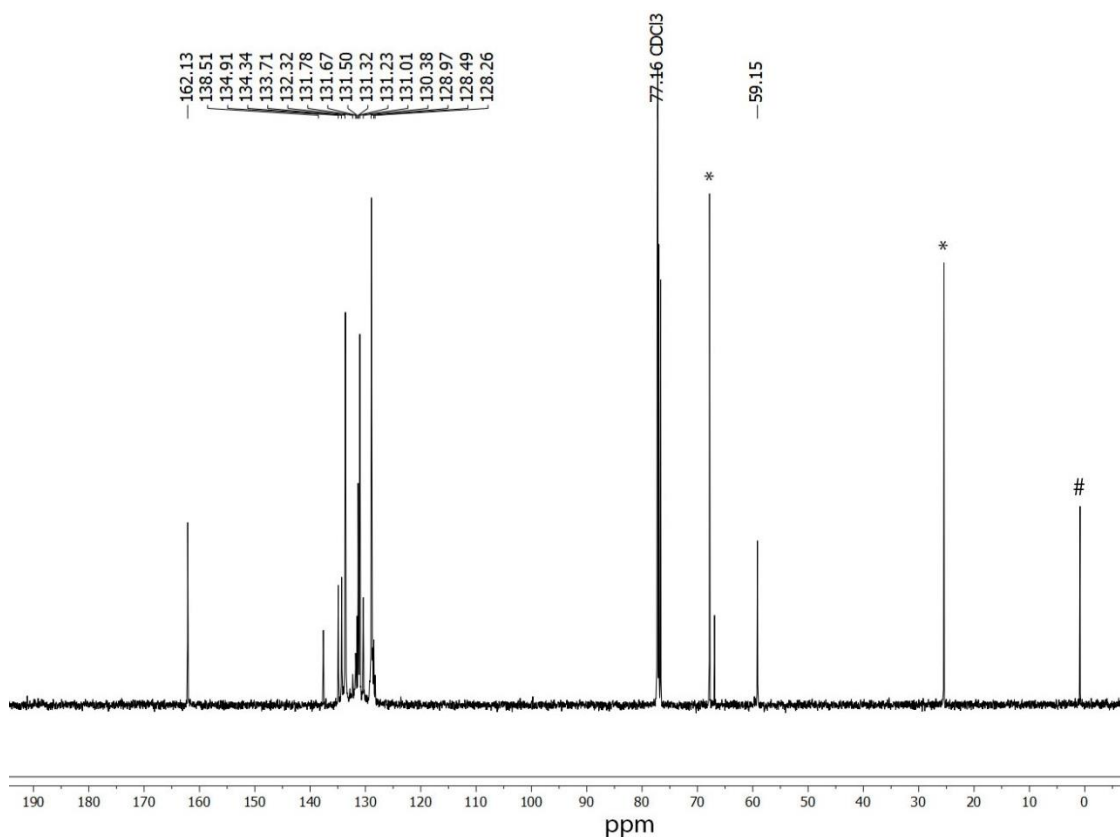
Figure 3.6.8. ^{13}C{^{1}H} NMR of **4** in CDCl$_3$ (*= THF, #= TMS)
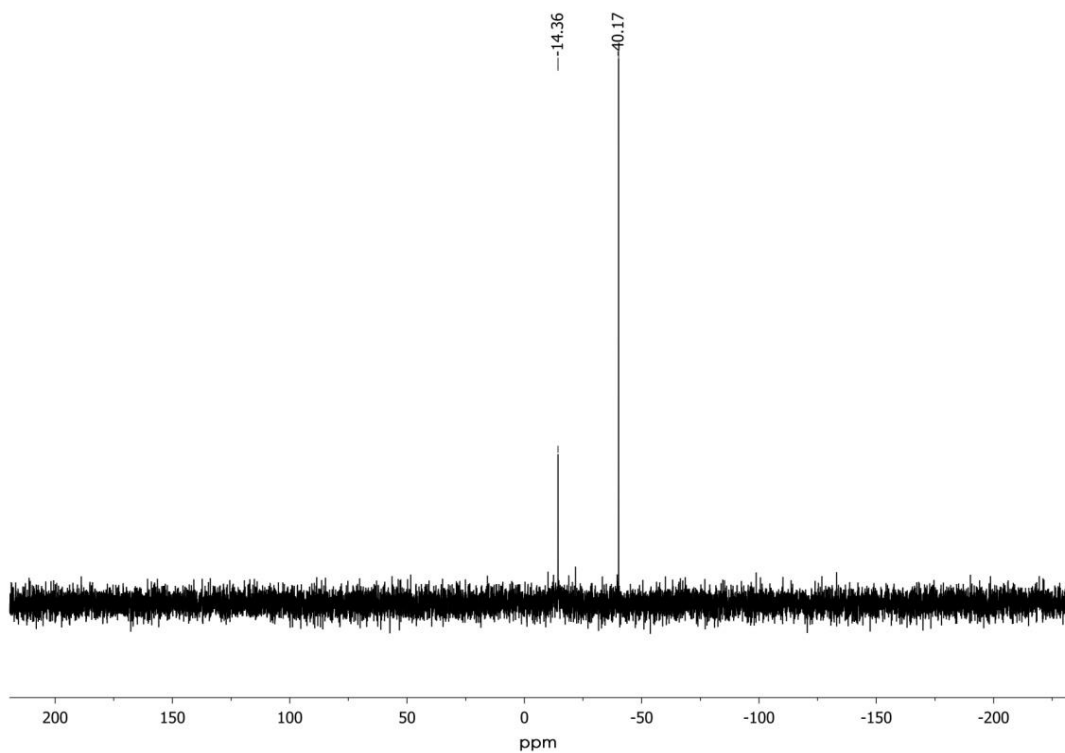
Figure 3.6.9. $^{31}P\{^{1}H\}$ NMR of **4** in C_6D_6
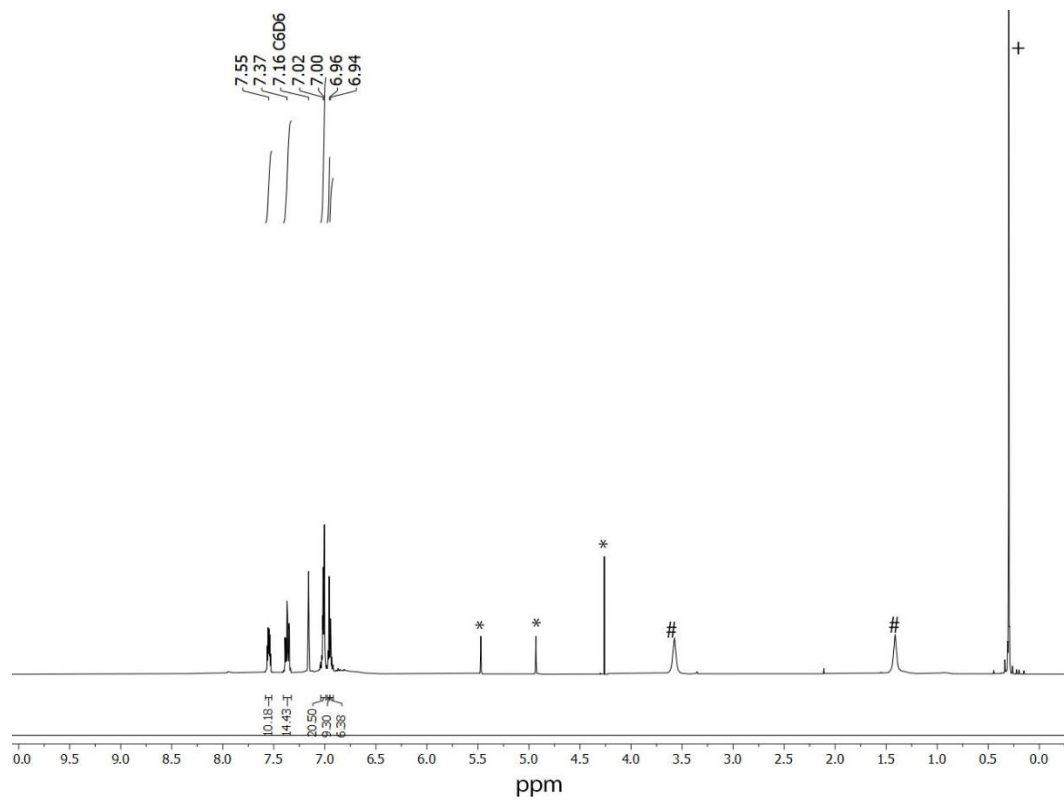
Figure 3.6.10. ^{1}H NMR of **5** in C_6D_6 (# = THF, + = TMS)
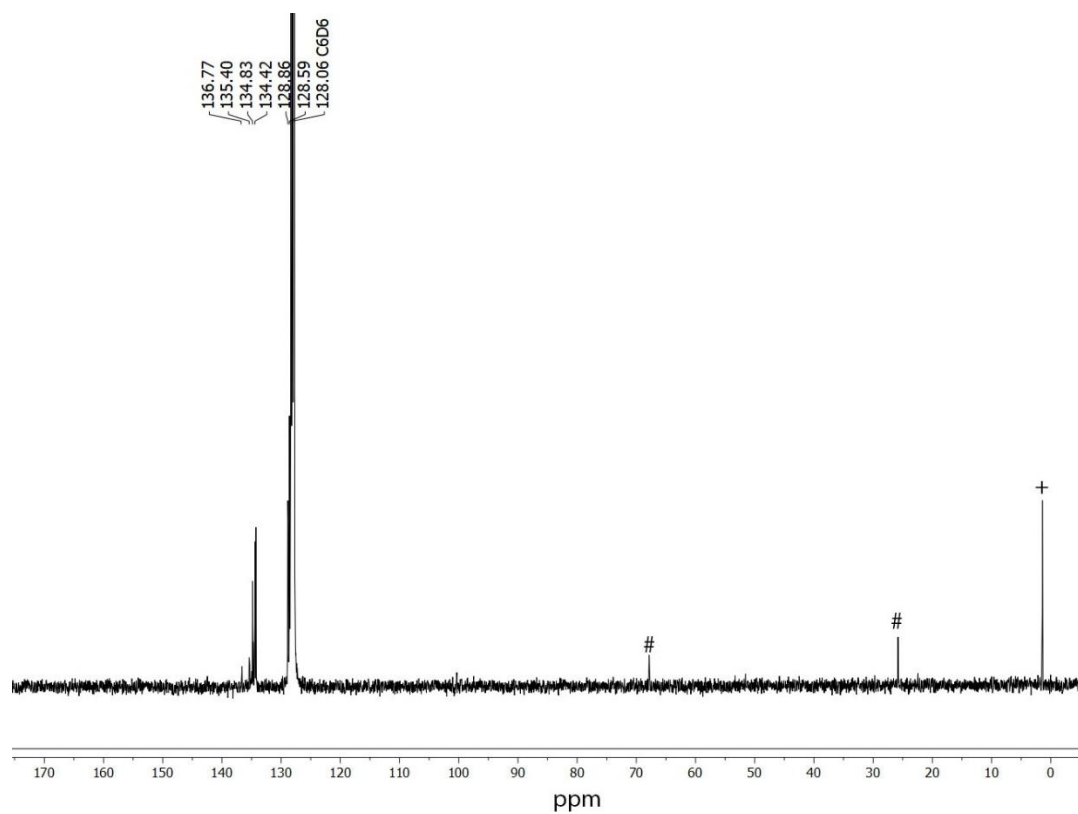
Figure 3.6.11. $^{13}C\{^1H\}$ NMR of **5** in C_6D_6 (# = THF, + = TMS)
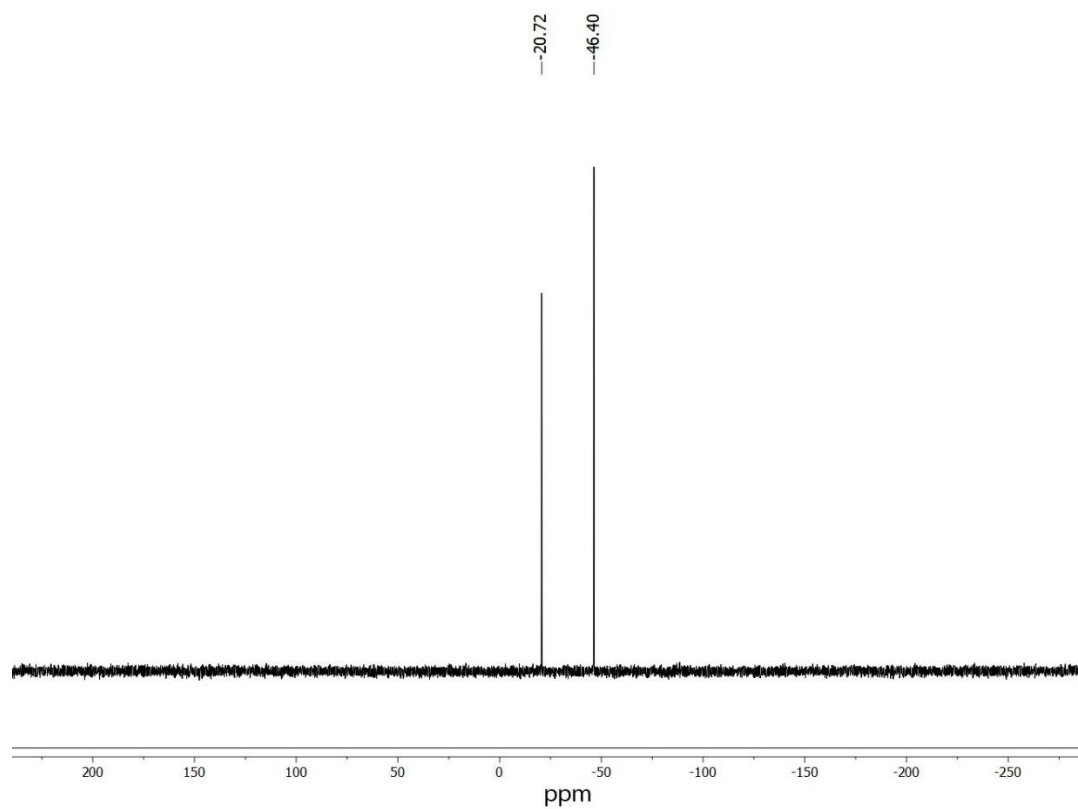
Figure 3.6.12. $^{31}P\{^1H\}$ NMR of **5** in C_6D_6

105

3.7. Crystal data table
Table 3.6.1. Crystal data and structure refinement for **1**.

Empirical formula	C40 H34 Au Cl N2 P2
Formula weight	909.15
Temperature	100(2) K
Wavelength	1.54178 Å
Crystal system	Triclinic
Space group	P-1
Unit cell dimensions	a = 9.111 (15)Å $\alpha = 87.173\ (4)°$.
	b = 12.410 (2)Å $\beta = 83.722\ (5)°$.
	c = 17.681 (3)Å $\gamma = 80.784\ (4)°$.
Volume	1960.6 (6)Å^3
Z	2
Density (calculated)	1.540 Mg/m^3
Absorption coefficient	3.938 mm^{-1}
F (000)	908
Crystal size	0.08 x 0.06 x 0.05 mm^3
Theta range for data collection	1.663 to 25.210°.
Index ranges	-10 < h < 7, -14 < k < 14, -21 < k < 21
Reflections collected	26288
Independent reflections	7011 [R(int) = 0.029]
Completeness to theta = 66.597°	99.6 %
Absorption correction	multi-scan
Refinement method	Full-matrix least-squares on F^2
Data / restraints / parameters	7011/ 0 / 460
Goodness-of-fit on F^2	0.905
Final R indices [I>2sigma (I)]	R1 = 0.029, wR2 = 0.065
R indices (all data)	R1 = 0.1284, wR2 = 0.1665
Largest diff. peak and hole	0.737 and -0.603 e.Å^{-3}

Table 3.6.2. Crystal data and structure refinement for **2**.

Empirical formula	C40 H34 Au2 Cl2 N2 P2
Formula weight	1069.47
Temperature	100(2) K

Wavelength	1.54178 Å	
Crystal system	Orthorhombic	
Space group	Pna21	
Unit cell dimensions	a = 14.874 (3)Å	α = 90°.
	b = 33.097 (7)	β = 90°.
	c = 9.015 (18)	γ = 90°.
Volume	4438.0 (16) Å^3	
Z	4	
Density (calculated)	1.601 Mg/m^3	
Absorption coefficient	14.361mm^{-1}	
F (000)	2040.0	
Crystal size	0.07 x 0.05 x 0.04 mm^3	
Theta range for data collection	2.670 to 72.521°.	
Index ranges	-18< h < 15, -40 < k < 40, -11 < k < 11	
Reflections collected	50899	
Independent reflections	8641 [R(int) = 0.0307]	
Completeness to theta = 72.521°	99.1%	
Absorption correction	multi-scan	
Refinement method	Full-matrix least-squares on F^2	
Data / restraints / parameters	8641 / 1 / 434	
Goodness-of-fit on F^2	0.967	
Final R indices [I>2sigma (I)]	R1 = 0.0307, wR2 = 0.081	
R indices (all data)	R1 = 0.1104, wR2 = 0.1365	
Largest diff. peak and hole	1.551 and -1.240 e.Å^{-3}	

Table 3.6.3. Crystal data and structure refinement for **3**.

Empirical formula	C160 H136 Au4Cl12Ge4N8P8
Formula weight	980.01
Temperature	100(2) K
Wavelength	1.54178 Å
Crystal system	Monoclinic
Space group	$P2_{1/n}$
Unit cell dimensions	a = 10.2371 (7)Å $\quad$ α = 90°.
	b = 17.6774 (12)Å $\quad$ β = 94.828 (4)°.
	c = 22.1530 (15)Å $\quad$ γ = 90°.
Volume	4008.75 (6)Å^3
Z	4
Density (calculated)	3.759 Mg/m^3
Absorption coefficient	53.30 mm^{-1}
F (000)	3925
Crystal size	0.05 x 0.05 x 0.02 mm^3
Theta range for data collection	2.499 to 64.977°.
Index ranges	-12 < h < 11, -20 < k < 20, -26 < k < 26
Reflections collected	44665
Independent reflections	6807 [R(int) = 0.0893]
Completeness to theta = 64.997°	99.4 %
Absorption correction	multi-scan
Refinement method	Full-matrix least-squares on F^2
Data / restraints / parameters	6807/ 294 / 444
Goodness-of-fit on F^2	1.072
Final R indices [I>2sigma (I)]	R1 = 0.0893, wR2 = 0.0996
R indices (all data)	R1 = 0.2243, wR2 = 0.2303
Largest diff. peak and hole	6.07 and -2.35 e.Å^{-3}

Table 3.6.4. Crystal data and structure refinement for **5**.

Empirical formula	C72 H60 Au2Ge2P6
Formula weight	1652.09
Temperature	100(2) K
Wavelength	0.71073 Å
Crystal system	Triclinic
Space group	P-1
Unit cell dimensions	a = 11.752 (6)Å $\quad$ α = 109.025 (15)°.
	b = 12.248 (6)Å $\quad$ β = 103.207 (13)°.
	c = 12.532 (6)Å $\quad$ γ = 96.410 (15)°.
Volume	1625.84 Å^3
Z	1
Density (calculated)	3.01 Mg/m^3
Absorption coefficient	32.71 mm^{-1}
F (000)	1680
Crystal size	0.06 x 0.05 x 0.04 mm^3
Theta range for data collection	1.663 to 25.210°.
Index ranges	-15 < h < 15, -16 < k < 15, -15 < k < 16
Reflections collected	28168
Independent reflections	7853 [R(int) = 0.0961]
Completeness to theta = 25.210°	99 %
Absorption correction	multi-scan
Refinement method	Full-matrix least-squares on F^2
Data / restraints / parameters	7853/ 0 / 371
Goodness-of-fit on F^2	0.966
Final R indices [I>2sigma (I)]	R1 = 0.0961, wR2 = 0.1125
R indices (all data)	R1 = 0.2202, wR2 = 0.2997
Largest diff. peak and hole	3.84 and -2.80 e.Å^{-3}

3.7. References

1. Engesser, T. A.; Lichtenthaler, M.R.; Schleep, M.; Krossing, I.; *Chem. Soc. Rev*. 2016, *45*, 789-899; Lee, V.Y.; Sekiguchi, A.; *Organometallic Compounds of Low-Coordinate Si, Ge, Sn and Pb, John Wiley & Sons Ltd., Chichester*. **2010**, pp. 1-44.

2. Bouhadir, G.; Bourrisou, D.; *Chem. Soc. Rev*. **2016**, *45*, 1065-1079.

3. Amgoune, A.; Bourissou, D.; *Chem. Commun.* **2011**, *47*, 859–871.

4. Kameo, H.; Yamamoto, J.; Asada, A.; Nakazawa, H.; Matsuzaka, H. Bourissou, D.; *Angew. Chem. Int. Ed.* **2019**, *52*, 18783-18787; J. Takaya, N. Iwasawa, *J. Am. Chem. Soc*. **2017**, *139*, 6074−6077; Devillard, M.; Declercg, R.; Nicolas, E.; Ehlers, A.W.; Backs, J.; Saffon-Merceron N.; Bouhadir, G.; Slootweg, J.C.; Bourissou, D.; *J. Am. Chem. Soc.*, **2016**, *138*, 4917−4926; Sircoglou, M.; Mercy, M.; Saffon, N.; Coppel, Y.; Bouhadir, G.; Maron, L.; Bourissou, D.; *Angew. Chem. Int. Ed*. **2009**, *48*, 3454-3457.

5. You, D.; Gabbaï, F. P.; *J. Am. Chem. Soc*. **2017**, *139*, 6843−6846; You, D.; Yang, H.; Sen, S.; Gabbaï, F.P.; *J. Am. Chem. Soc*. **2018**, *140*, 9644−9651; Yang, M.; Tofan, D.; Chen, C.; Jack, K. M.; Gabbaï, F. P.; *Angew. Chem. Int. Ed.*, **2018**, *57*, 13868-13872; Lao, Y.; Gabbaï, F.; *Angew. Chem. Int. Ed.*, **2019**, *58*, 10194-10197; Yang, H.; Gabbaï, F.; *J. Am. Chem. Soc*. **2015**, *137*, 13425−13432.

6. Gualco, P.;Lin, T.-P.; Sircoglou, M.; Mercy, M.; Ladeira, S.; Bouhadir, G.; Pérez, L. S.; Amogoune, A.; Maron, L.; Gabbaï, F. P.; Bourissou, D.; *Angew. Chem. Int. Ed.*, **2009**, *48*, 9892-9895; Gualco, P.; Mercy, N.; Ladeira, S.; Coppel, Y.; Maron, L.; Amogoune, A.; Bourissou, D.; *Chem. Eur. J.* **2010**, *16*, 10808-10817.

7. Frisch, P.; Szilvási, T.; Porzelt, A.; Inoue, S.; *Inorg. Chem.* **2019**, 58, 14931−14937; Yeong, H.-X.; Li, Y.; So, C.-W.; *Organometallics* **2014**, *33*, 3646−3648; Frisch, P.; Inoue, S.; *Chem. Commun.* **2018**, *54*, 13658-13661; Seow, C.; Bin Ismail, M. L.; Xi, H.; Li, Y.; Lim, K. H.; So, C.; *Organometallics* **2018**, *37*, 1368-1372.

8. Wilkins, L. C.; Kim, Y.; Litle E. D.; Gabbaï, F. P.; *Angew. Chem. Int. ed.*, **2019**, *58*, 18266-18270.

9. Raut, R.K.; Majumdar, M.; *Chem. Commun*. **2017**, *53*, 1467-1469.

10. Schwartz, R. H.; Filippo, J.S.; *J. Org. Chem.*, **1979**, *44*, 2705-2712.

11. Cooke, P. A.; Perera, S. D.; Shaw, B. L.; Thornton-Pett, M.; Vessey, J. D.; *J. Chem. Soc.*

Dalton Trans. **1997**, 435-438; Rampazzi, V.; Roger, J.; Amardeil, R.; Penouilh, M. –J.; Richard, P.; Fleurat-Lessard, P.; Hierso, J. –C.; *Inorg. Chem.* **2016**, *51*, 10907-10921; Cabeza, J. A.; Fernández, I.; García-Álvarez, P.; Laglera-Gándara, C. J.; *Dalton Trans*. **2019**, *48*, 13273-13280.

12. Hidalgo, N.; Bajo, S.; Moreno, J.J.; Navarro-Gilabert, C.; Mercado, B. Q.; Campos, J.; *Dalton Trans*., **2019**, *48*, 9127-9138; Hlina, J.; Arp, H.; Walewska, M.; Flörke, U.; Zangger, K.; Marschner, C.; Baumgartner, J.; *Organometallics* **2014**, *33*, 7069-7077; Bauer, A.; Schmidtbaur, H.; *J. Am. Chem. Soc.* **1996,** *118,* 5324-5325.

13. Schmidtbaur, H.; *Golden bulletin*, **2000**, *33*, 3-10.

14. Jeffrey, J.C.; Rauchfuss, T.B.; Tucker, P. A.; *Inorg. Chem.* **1980**, *19,* 3306-3315.

CHAPTER 4

A tin (II) macrocycle and its reactivity studies
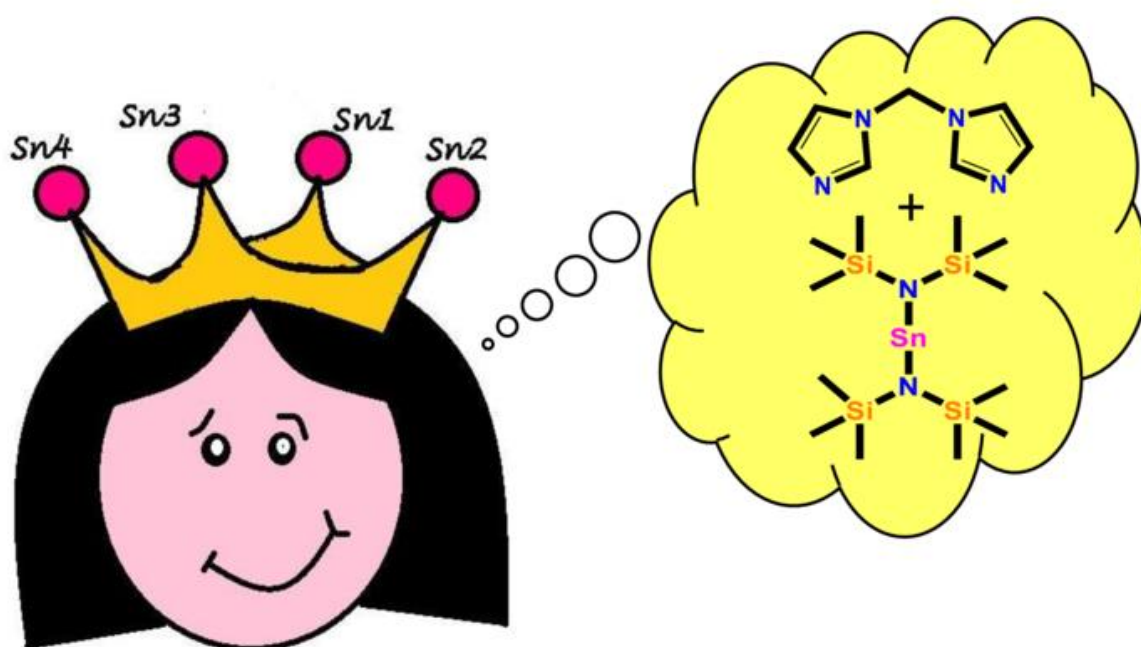
Abstract

The reaction of Sn[(NSiMe₃)₂]₂ and imidazole derivatives, bis(imidazolyl)methane and N-(Diisopropylphenyl)imidazole leads to the formation of complex **1** and complex **2** respectively. Complex **1** is a cyclic zwitterionic macrocycle of Sn(II) which has two different types of tin centres depending on the position of the tin centres. Complex **2** is a dimer of imidazole stabilised stannylene which also remains in a cuclic form. Both the complex are characterised by NMR and Single crystal X-ray data. DFT studies of complex **1** confirmed the zwitterionic form of the complex.

4.1. Introduction

The tin(II) chemistry began with the discovery of Sn[(NSiMe₃)₂]₂ by Lapper et al.[1] Since then, transamination reaction of Sn[(NSiMe₃)₂]₂ and suitable amines have led to the formation of different stannylenes.[2] Recently, transamination reaction with diaminopyridines, diiminopyridines, bis(α-iminopyridine), bis(diamine)s and imidazolin-2-imine have led to the formation of various monostannylenes as well polystannylenes (**A-C**).[3] As stannylenes are known to have a lone pair and an empty p-orbital they are ambiphilic in nature and hence used in coordination chemistry, small molecule activation and catalytic cycles.[4] On, the other hand a very few stannyliumylidenes have been reported till date (**D-F**).[5] The first report of stannyliumylidene was reported by Jutzi et al.[6] Most of these stannyliumylidenes have been synthesised by halide abstraction from the stannylene center or by Lewis base mediated autoionization.[7] The first report on autoionization employed 2,6-diacetylpyridinebis(2,6-diisopropylanil) as the Lewis base, which led to the isolation of low-valent Sn(II) species comprising of [:SnCl]⁺ and SnCl₃.[8] Since then there are many reports of a [:SnCl]⁺ stabilized by a variety of ligands.[9]

A   B   C
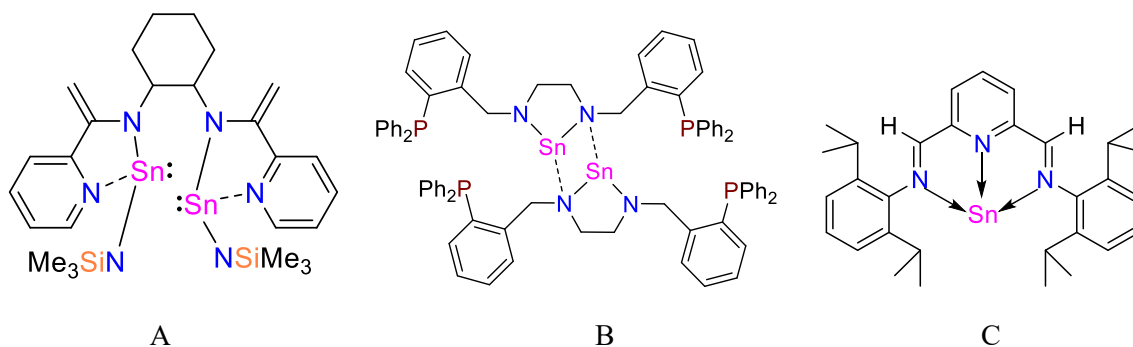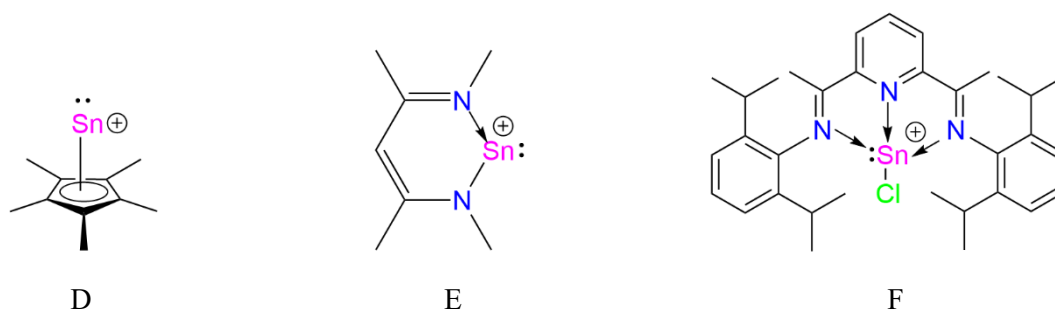
Scheme 4.1.1. Previously reported examples of stannylene synthesized from Sn[(NSiMe₃)₂]₂ (A-C) and stannyliumylidenes (D-F).

4.2. Scope of the work

Although there are significant numbers of reports of [:SnCl]$^+$ stabilized in a ligand framework however there are very few examples of stabilization of [:Sn-NSiMe₃]$^+$.[9] Inoue et al. reported the synthesis of a four membered stannacycle supported by imidazolin-2-iminato ligand in which the tin(II) center remains as the cation. The complex is synthesized from Sn[(NSiMe₃)₂]₂ as the Sn(II) precursor in two steps (Figure 4.2.1).[10] Also there are no reports on the reaction of the Lappert's tin(II) reagent with N-substituted imidazole. However, one related example is the reaction of imidazolium chloride with E[N(SiMe₃)₂]₂ (E = Ge, Sn) which gave rise to intramolecularly stabilized tetrylene having NHC∧amido chelate and chloride ligands (Figure 4.2.2).[11] Similarly an 1,4,2,5-diazaborinine has been reported which synthesized by reduction of imidazol-2-yl-chlorophenylborane with excess of KC₈.[12] Also, redox tautomerisaton of azoles at C2-H position by metal precursors led to metal complexation supported by N-heterocyclic carbene.[13] These reports led to the direct reaction of Lappert's tin(II) reagent with bis(imidazolyl)methane and N-(diisopropylphenyl)imidazole. These reactions led to the formation of a 12-membered tin(II) macrocyle complex **1** and a dimeric stannylene complex **2**. Further, Complex **1** was reacted with metal centres like Zn and Ag to obtain a 4-membered cyclic complex **3**.
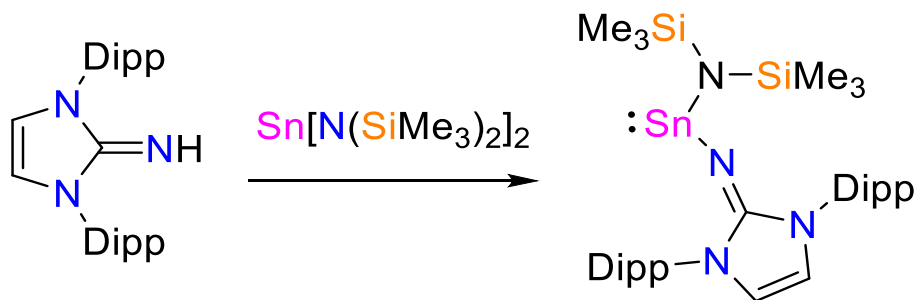

Figure 4.2.1. Synthesis of Stannylene supported by imidazolin-2-iminato ligand
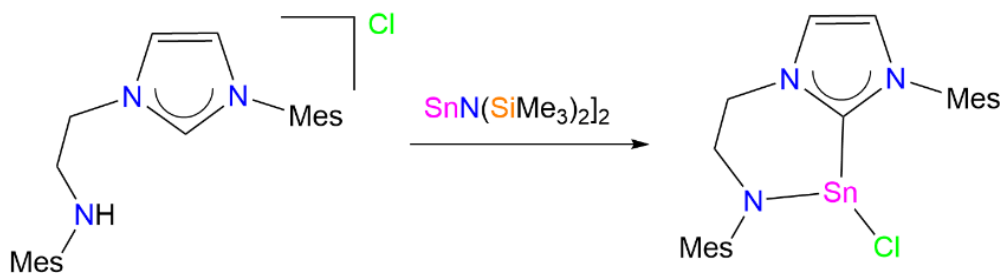
Figure 4.2.2. Synthesis of Stannylene supported by NHC∧amido chelate ligand

4.3. Results and Discussion

### 4.3.1. Synthesis of tin (II) Complexes

Complex **1** was synthesized by reacting one equivalent of bis(imidazolyl)methane and two equivalents of Sn[(NSiMe$_3$)$_2$]$_2$ in THF. The mixture was stirred for 24 hours at room temperature. After the reaction was complete the solvent was removed and the solid was dissolved in toluene leading to precipitation. The suspension was filtered, concentrated and kept at -35°C. After a few weeks crystals of complex **1** were obtained with a low yield of 15% (Scheme 4.3.1). Also, redissolving the dried-up toluene extract in diethyl ether to obtain single crystals did not improve the yield much. Other methods like dilution, slow addition of reactants, temperature variations did not increase the yield of the macrocycle. A similar example with multiple heavier Group 14 metals as coordination sites in a macrocycle was reported by Zabula et.al.[14] NMR spectra was obtained by dissolving the isolated crystals in THF-d_8. The crystals were not dried prior to NMR sample preparation as they usually dry-up into a white solid which is insoluble in any polar or non-polar solvent. So, the peaks for the small amount of bis(trimethylsilyl)amine were observed in the ^{1}H NMR spectrum. The probable cause of insolubility of the dried-up crystals is the removal of solvent molecules from the crystal lattice and crumbling of the lattice which renders it insoluble. The ^{1}H NMR spectrum depicts the disappearance of the C2-H protons of the two imidazole rings and there is a downfield shift of peaks for backbone protons of the ligand. The methylene protons are found to be magnetically inequivalent and appear as two doublets at 6.68 and 5.85 ppm. The anionic imidazol-2-yl carbon peak appears at 179.5 ppm in the ^{13}C NMR spectrum. The [119] Sn NMR depicts two peaks at -143 and -284 ppm for the two chemically inequivalent tin centres. The two signals appear with satellites due to tin-tin coupling in the solution state with a coupling constant of 842 Hz.[15] Both the ^{119}Sn NMR signals are significantly upfield shifted compared to that of the Sn[N(SiMe$_3$)$_2$]$_2$ precursor (δ ([119]Sn) = +767 ppm).[16] Correspondingly, the ^{29}Si NMR spectrum

exhibits two peaks at 2.14 ppm and 1.01 ppm due to two different environments around Si. The overall structure shows that the molecule is a zwitterionic complex with two tin centres identify as stannate with the anionic tin center tricoordinated to two carbon centres and a nitrogen center. The other two tin centres identify as stannyliumylidene centres stabilized by donor-acceptor interactions with the unsubstituted bis(imidazolyl) Ns.

R=Trimethylsilyl
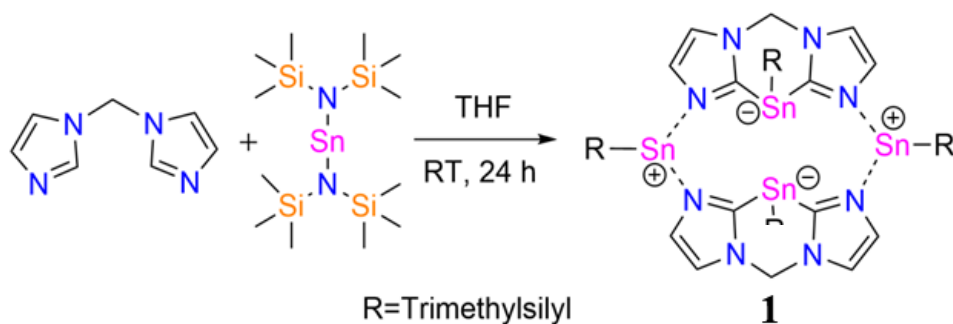
Scheme 4.3.1. Synthesis of Complex **1**

Complex **2** is synthesized by reacting one equivalent of N-(diisopropylphenyl)imidazole with 1.2 equivalents of Sn[(NSiMe$_3$)$_2$]$_2$ in THF. The reaction is stirred for 24 hours and evaporated. It was extracted with toluene and washed with hexane. Due to the similar solubility of complex **2** and the starting material N-(diisopropylphenyl)imidazole, the small amounts of unreacted N-(diisopropylphenyl)imidazole was removed by fractional crystallization. Colorless single crystals of **2** were grown from a concentrated toluene solution giving a crystallization yield of 74% (Scheme 4.3.2). Alternately, single crystals of compound **2** could be grown from hot hexane extract. Complex **2** was characterised using NMR techniques and Single crystal X-ray diffraction technique. It was found that the complex remains as dimer both in solid state as well as solution state. The crystals of complex **2** were dissolved in THF-d_8 for the NMR studies. ^{1}H NMR spectrum shows two different septet peaks at 2.50 and 2.79 ppm corresponding to (CH$_3$)$_2$CH- protons which infers their magnetic inequivalence due to the steric congestion created by the -N(SiMe$_3$)$_2$ groups in close vicinity. The 13C NMR spectrum depicts the peak of the anionic imidazolyl carbon at 184.4 ppm. As mentioned earlier the peaks of N-(diisopropylphenyl)imidazole were also found in the ^{1}H NMR spectrum. The ^{119}Sn NMR spectrum shows a resonance signal at δ = - 47 ppm which is significantly up-field shifted compared to Sn[N(SiMe$_3$)$_2$]$_2$ (δ (^{119}Sn) = +767 ppm).[16]
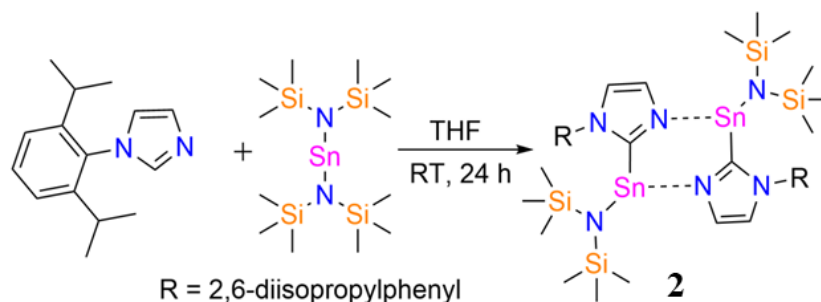
Scheme 4.3.2. Synthesis of Complex **2**

4.3.2. Crystal data

Complex **1** crystallised in triclinic space group P-1. The asymmetric unit contains two molecules of complex **1** and a diethyl ether molecule. The molecular unit shows a 12-membered carbon-nitrogen heterocycle with Sn(II) occupying the 1,4,7,10 positions. Two of the Sn(II) centres (Sn1, Sn3) are alternately placed and proximally positioned having a distance of 4.405(10) Å between them. The other two tin centres (Sn2, Sn4) are similarly alternately placed and are distally located at a distance of 6.837(10) Å. Each of the three-coordinate proximal tin centres Sn1 and Sn3 are bonded to two imidazol-2-yl carbon centres of the bis(imidazole) and to the nitrogen of the -N(SiMe$_3$)$_2$ group, thereby adopting a trigonal-pyramidal environment. The Sn-C bond lengths in **1** are Sn1-C1 = 2.271 (14) Å, Sn1-C10 = 2.233 (13) Å, Sn3-C4 = 2.266 (12) Å and Sn3-C7 = 2.293 (14) Å. Notably, the Sn$\cdots$C dative bond distances are of much higher values as observed in the reported cases of carbene-stannylene adducts.[17] So, it proves that the above-mentioned Sn-C bonds are covalent in nature. The Sn1-N9 and Sn3-N11 bond lengths are 2.163 (12) Å and 2.173 (12) Å respectively. The sum of bond angles around the two tin centres are ΣSn1 = 267.9° and ΣSn3 = 270.3° which comes in the range of bond angles for stannate ions.[18] Hence these two centres are identified as stannate(II) centres.

The distal tin centres Sn2 and Sn4 are bonded to the -NSiMe$_3$ group and to the two nitrogens of two different unsubstituted imidazole units from the bis(imidazolyl)aminostannate(II) units. The Sn-N$_{amino}$ covalent bond lengths in **1** are Sn2-N10 = 2.099 (11) Å and Sn4-N12 = 2.127 (13) Å. These values fall in the range of Sn-N bond distances for cyclic Sn(II) cations. The Sn$\cdots$N dative bond distances at Sn2 (Sn2-N2 = 2.196 (12) Å, Sn2-N4 = 2.227 (12) Å) and at Sn4 (Sn4-N6 = 2.257 (13) Å, Sn4-N8 = 2.263 (11) Å)

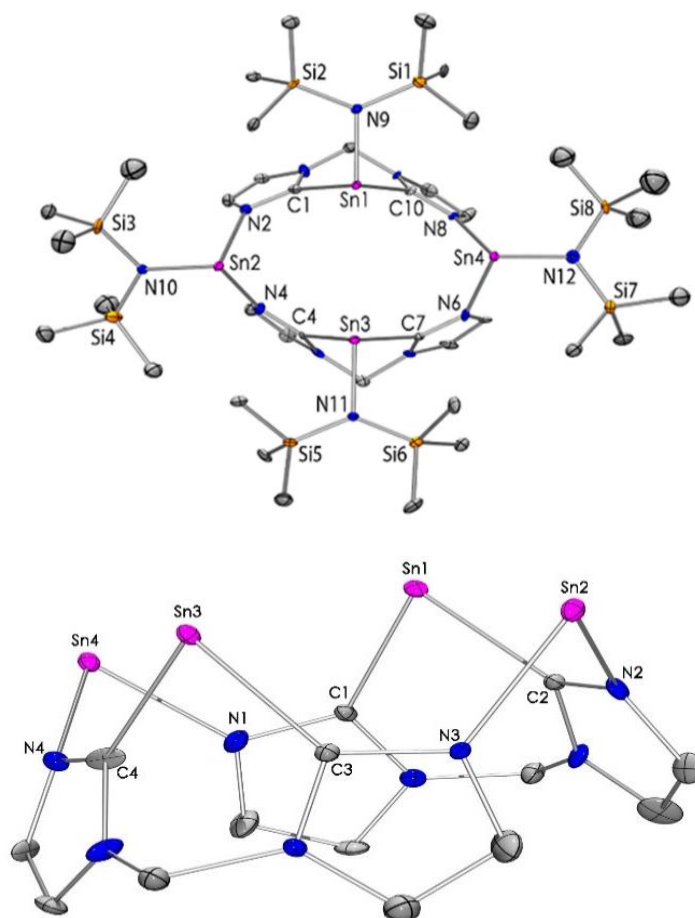in **1** are in the range of reported Sn···N dative bond distances (Figure 4.3.1).[8,10]

Figure 4.3.1. Molecular structure of 1 in the solid state (thermal ellipsoids at 30%, H atoms, solvent molecule omitted for clarity). (a) top view and (b) side view (-N(SiMe$_3$)$_2$ groups omitted for clarity). Selected bond lengths [Å]: Sn1-C1 2.271(14), Sn1-C10 2.233(13), Sn1-N9 2.163(12), Sn2-N2 2.196(12), Sn2-N4 2.227(12), Sn2-N10 2.099(11), Sn3-C4 2.266(12), Sn3-C7 2.293(14), Sn3-N11 2.173(12), Sn4-N6 2.257(13), Sn4-N8 2.263(11), Sn4-N12 2.127(13).

Complex **2** crystallised in P-1 space group. Complex **2** can be depicted as a dimer with monomeric unit of stannylene bonded to nitrogen of -NSiMe$_3$ group and anionic carbon centre of the N-(Diisipropylphenyl)imidazole. The unsubstituted nitrogen of imidazole attacks the Sn(II) centre of the other monomer which leads to the dimerization. The dimerization gives rise to chair conformed six membered C$_2$N$_2$Sn$_2$ ring. The Sn1-C1 bond length is 2.244(6) Å which is analogous to the values reported for Sn-C covalent bonds.[19] The Sn1-N2 has a bond length of 2.142(5) Å which falls within the higher end of Sn-N covalent bonds. The Sn1···N1

bond length is 2.251(4) Å, conferring to the lower range of Sn···N dative bond distances (Figure 4.3.2).[2,3]
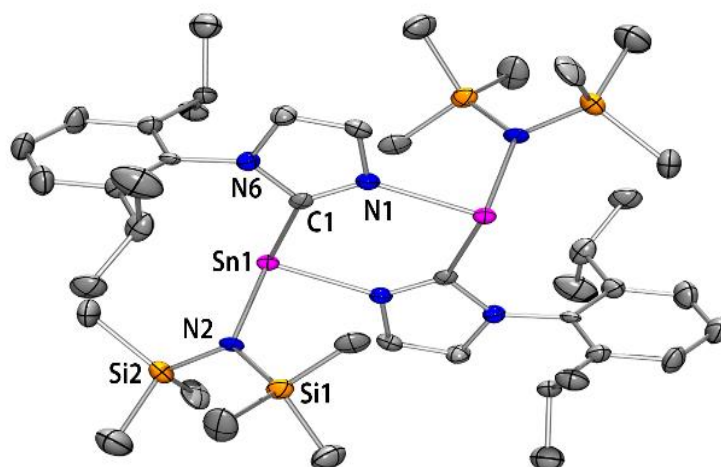

Figure 4.3.2. Molecular structure of **2** in the solid state (thermal ellipsoids at 30%, H atoms omitted for clarity). Selected bond lengths [Å]: Sn1-C1 2.244(6), Sn1-N2 2.142(5), Sn1-N1 2.251(4), C1-N1 1.322(7), C1-N6 1.382(7).

4.3.3. DFT Studies

To understand the electronic properties of the complex **1** quantum chemical analyses were performed by optimizing the structure with Gaussian 16 using B3LYP-D3BJ/def2-TZVPP level of theory.[20] The optimized geometry **1o** is consistent with the X-ray structure of **1**. The bonding orbitals, natural charges on each atom of the molecule and Wiberg bond index (WBI) were computed based upon natural population analysis (NPA) by the NBO program embedded in the Gaussian 16 package, at the same level.[21] For Sn1 and Sn3, the nitrogens were found to be bonded in a highly polarized covalent bond. However, for Sn2 and Sn4 the full coordinated nitrogen orbitals were not observed. (**Table 4.3.1**). This observation indicates stronger boning of nitrogens to Sn1 and Sn2 sites.

	Sn1-C1	Sn1-C10	Sn1-N9
BD orbital	(15.16%)Sn1 sp$^{22.06}$ (84.84%)C1 sp$^{1.48}$	(15.14%)Sn sp$^{22.06}$ (84.86%)C10 sp$^{1.48}$	(10.11%)Sn1 sp$^{12.90}$ (89.89%)N9 sp$^{3.63}$
WBI	0.48	0.48	0.34
	Sn2-N2	Sn2-N4	Sn2-N10
BD orbital	-	-	-
WBI	0.22	0.22	0.28
	Sn3-C4	Sn3-C7	Sn3-N11
BD orbital	(14.97%)Sn3 sp$^{22.48}$	(14.96%)Sn3 sp$^{22.69}$	(9.97%)Sn3 sp$^{13.48}$

	(85.03%)C4 sp$^{1.47}$	(85.04%)C7 sp$^{1.47}$	(90.03%)N11 sp$^{3.67}$
WBI	0.48	0.48	0.34
	Sn4-N6	Sn4-N8	Sn4-N12
BD orbital	-	-	-
WBI	0.22	0.22	0.28

Table 4.3.1. Selected bonding orbitals and WBI in **1o**

For a better understanding of bonding natures in Sn2 and Sn4 environments, we performed atoms in molecule (AIM) calculation to find out bond critical points of Sn-N interactions.[22] The positive Laplacian values coupled with negative energy density indicate a partial covalent bonding with contribution of closed-shell interaction. The relatively higher electron density, Laplacian, and ellipticity values at the BCPs of Sn2-N10 and Sn4-N12 bonds are associated with stronger bonding as compared to Sn2-N2 and Sn2-N4. Therefore, the bonding situation in Sn2-N2 and Sn2-N4 is determined to be dative. The partial NBO charges on Sn atoms indicating higher positive charge accumulation on Sn2 and Sn4. All these calculations indicate a zwitterionic structure dominating the neutral counterpart.
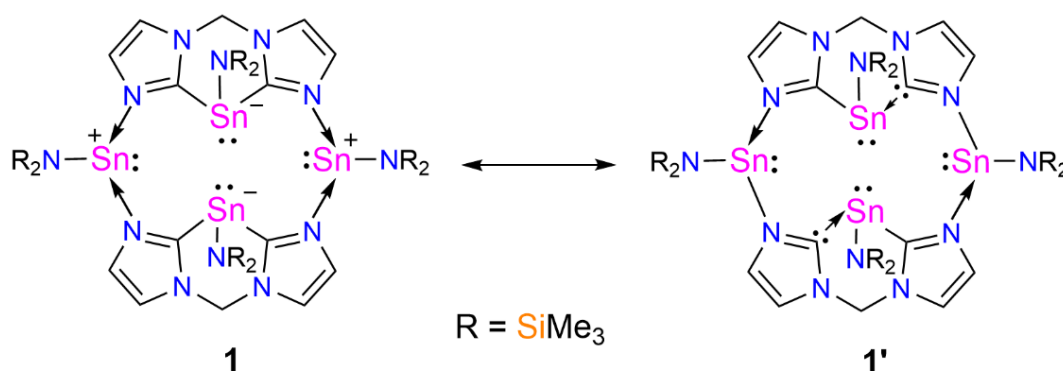

Figure 4.3.4. Canonical structures of complex **1**

The Fukui Calculations of **1o** also indicate the anionic Sn1 and Sn2 are more nucleophilic. The NO analysis shows that the HOMO and HOMO-1 resides on the tin lone pair. However, the experiments indicate a low reactivity. This can be attributed donor-acceptor (D-A) interactions of the corresponding LP and LP* orbitals on Sn and N atoms. The lone pair on Sn1 interacts with σ^* orbital of Sn3-N11 and the lone pair on Sn3 interacts with σ^* orbital of Sn1-N9 weaking the Sn-N bond. Also, the Sn1 and Sn3 lone pair interacts with the LP* of Sn2 and Sn4 decreasing their reactivity further. Low reactivity of cationic Sn2 and Sn4 stems from their strong donor-acceptor interaction with the lone pair orbitals of the adjacent N atoms
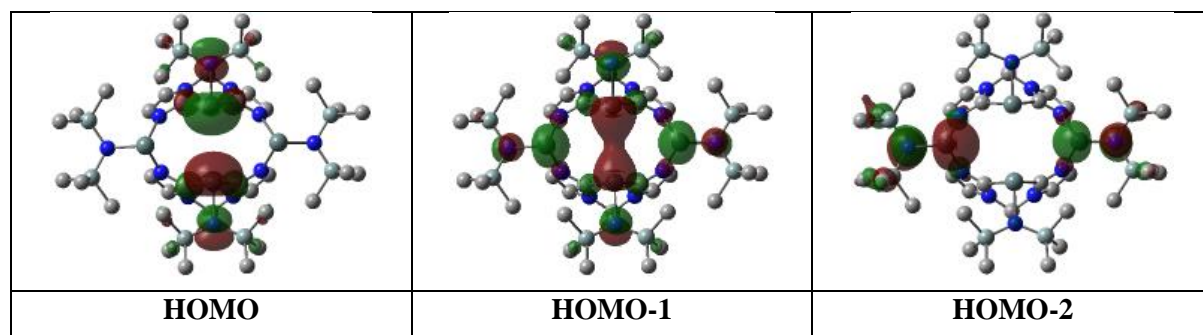
with LP* orbitals of Sn atoms.

| **HOMO** | **HOMO-1** | **HOMO-2** |

Figure 4.3.5. Selected frontier molecular orbitals of 1o (Isovalue = 0.03, H atoms omitted for clarity).

4.4. Conclusion

In conclusion, a tetrastanna(II) cycle complex **1** has been synthesised by deprotonating bis(imidazolyl)methane by Sn[(NSiMe$_3$)$_2$]$_2$ which acts as a base. The similar reaction with mono-imidazole led to dimer complex **2** formation. Experimental evidences and computational studies confirmed the zwitteronic form of the complex **1**. Two of the four Sn(II) centres are found to be stannates and the other two are stannyliumylidene moieties. Computational studies have shown that the proximal Sn(II) centres are more nucleophilic than the distal Sn(II) centres.

4.5. Experimental

4.5.1. General remarks

All manipulations were carried out under a protective atmosphere of argon applying standard Schlenk techniques or in a dry box. Tetrahydrofuran, toluene and hexane were refluxed over sodium/benzophenone. Chloroform-d was stirred and refluxed over calcium hydride and kept over molecular sieves. Benzene-d_6 was dried over potassium and Tetrahydrofuran-d_8 was used as purchased. All solvents were distilled and stored under argon and degassed prior to use. All chemicals were used as purchased. Chloroform-d was provided with tetramethylsilane as internal standard. Ligand precursors bis(imidazolyl)methane[23], N-(diisopropylphenyl)imidazole[24] and bis[bis(trimethylsilylamino)]tin(II)[25] were synthesized following the reported literature procedures. ^{1}H, ^{13}C{^{1}H} and ^{29}Si NMR spectra were referenced to external SiMe$_4$ using the residual signals of the deuterated solvent (^{1}H) or the solvent itself (^{13}C). ^{119}Sn NMR spectrum was recorded with SnCl$_4$ as a reference. NMR spectra

were recorded on Bruker AVANCE III HD ASCEND 9.4 Tesla/400 MHz and Jeol 9.4 Tesla/400 MHz spectrometer. Melting points were determined under argon in closed NMR tubes and are uncorrected. Elemental analyses were performed on Elementar vario EL analyzer. Single crystal data were collected on Bruker SMART APEX four-circle diffractometer equipped with a CMOS photon 100 detector (Bruker Systems Inc.) with a Mo Kα radiation (0.71073 Å) and a Cu Kα radiation (1.5418 Å).

4.5.1. Synthesis and characterization of Complex 1

Bis(imidazolyl)methane (50 mg, 0.33 mmol) and bis[bis(trimethylsilylamino)]tin(II) (297 mg, 0.67 mmol) were dissolved in 20 mL of tetrahydrofuran and was stirred at room temperature for 24 hours. The solvent was evaporated to obtain a sticky yellow solid. The mixture was extracted with 15 mL toluene and filtered. The filtrate was concentrated to 5 mL and stored at -35 °C. Colorless single crystals were obtained after a week. (Crystallization Yield = 70 mg (15%, 0.05 mmol). Single crystals of **1** were also grown by re-dissolving the dried-up toluene extract in diethyl ether giving similar yield. Decomposition Temp./ Melting Point: Above 180 °C.

^{1}H NMR (400 MHz, THF-d_8, TMS) δ 7.21 (s, 4H, C2-H); 7.11 (s, 4H, C1-H); 6.68 (d, $J_{\text{H-H}}$ = 12.7 Hz, 2H, -N-CH_2-N-); 5.85 (d, $J_{\text{H-H}}$ = 12.8 Hz, 2H, -N-CH_2-N-); 0.14 (s, 36H, -^{N}Si-CH); 0.05 (s, 36H, -^{C}Si-CH) ppm.

^{13}C {^{1}H} NMR (101 MHz, THF-d_8, TMS) δ 179.5 (-N$C_{carbanion}$N-); 126.1 (C2); 120.9 (C1); 60.1 (-NCN-); 6.9 (-^{N}Si-C-); 6.2 (-^{C}Si-C) ppm.

^{119}Sn {^{1}H} NMR (149.74 MHz, THF-d_8) δ -143 ppm ($^3J_{\text{Sn-Sn}}$= 842 Hz); -284 ppm ($^3J_{\text{Sn-Sn}}$= 842 Hz).

^{29}Si {^{1}H} NMR (79.53 MHz, THF-d_8) δ 2.1 ppm; 1.0 ppm.

Elemental analysis: calcd. for $C_{38}H_{84}N_{12}Si_8Sn_4$: C, 32.40; H, 6.01; N, 11.93. Found: C, 32.16; H, 5.99; N, 12.01.

4.5.2. Synthesis and characterization of Complex 2

N-(diisopropylphenyl)imidazole (1.00 g, 4.36 mmol) and bis[bis(trimethylsilylamino)]tin(II) (2.31 g, 5.23 mmol) were dissolved in 60 mL of tetrahydrofuran and was stirred at room temperature for 24 hours. The solvent was evaporated to obtain a sticky orange solid. The mixture was extracted with 25 mL toluene and filtered. The filtrate was evaporated to obtain an off white solid. The solid was washed with hexane yielding **2** in 1.64 g (74%, 1.62 mmol). Colorless single crystals were obtained from a concentrated toluene solution kept at room

temperature. Decomposition Temp./ Melting Point: Above 180 ºC.

^{1}H NMR (400 MHz, THF-d_8, TMS) δ 7.49 (t, J_{H-H} = 7.8 Hz, 2H, Ar$_{para}$-*H*); 7.43 (m, 2H, C8-*H*); 7.39 (d, J_{H-H} = 7.8 Hz, 2H, C7-*H*); 7.34 (m, 4H, Ar$_{meta}$-*H*); 2.79 (sept, J_{H-H} = 20.2, 13.5, 6.7 Hz, 2H, C5-*H*); 2.50 (sept, J_{H-H} = 19.4, 13.6, 6.8 Hz, 2H, C6-*H*); 1.40 (d, J_{H-H} = 6.8 Hz, 6H, C2-*H*); 1.34 (d, J_{H-H} = 6.8 Hz, 6H, C1-*H*); 1.16 (d, J_{H-H} = 6.7 Hz, 6H, C4-*H*); 0.98 (d, J_{H-H} = 6.7 Hz, 6H, C3-*H*); -0.09 (s, 36H, -Si-C*H*) ppm.

^{13}C {^{1}H} NMR (101 MHz, THF-d_8, TMS) δ 184.4 (-N*C*$_{carbanion}$N); 147.4 (*C*$_{ipso}$); 135.3 (*C*$_{ortho}$); 131.4 (*C*$_{para}$); 129.8 (*C*8); 125.3 (*C*7); 125.2 (*C*$_{meta}$); 29.4 (*C*6); 29.3 (*C*5); 27.1 (*C*3); 26.3 (*C*4); 24.4 (*C*2); 22.5 (*C*1); 7.0 (-*C*-Si-)ppm.

^{119}Sn {^{1}H} NMR (149.74 MHz, THF-d_8) δ −47 ppm.

Elemental analysis: calcd. for $C_{42}H_{74}N_6Si_4Sn_2$: C, 49.81; H, 7.36; N, 8.30. Found: C, 69.67; H, 9.68; N, 11.48. (Due to the presence of inseparable imidazole impurity).
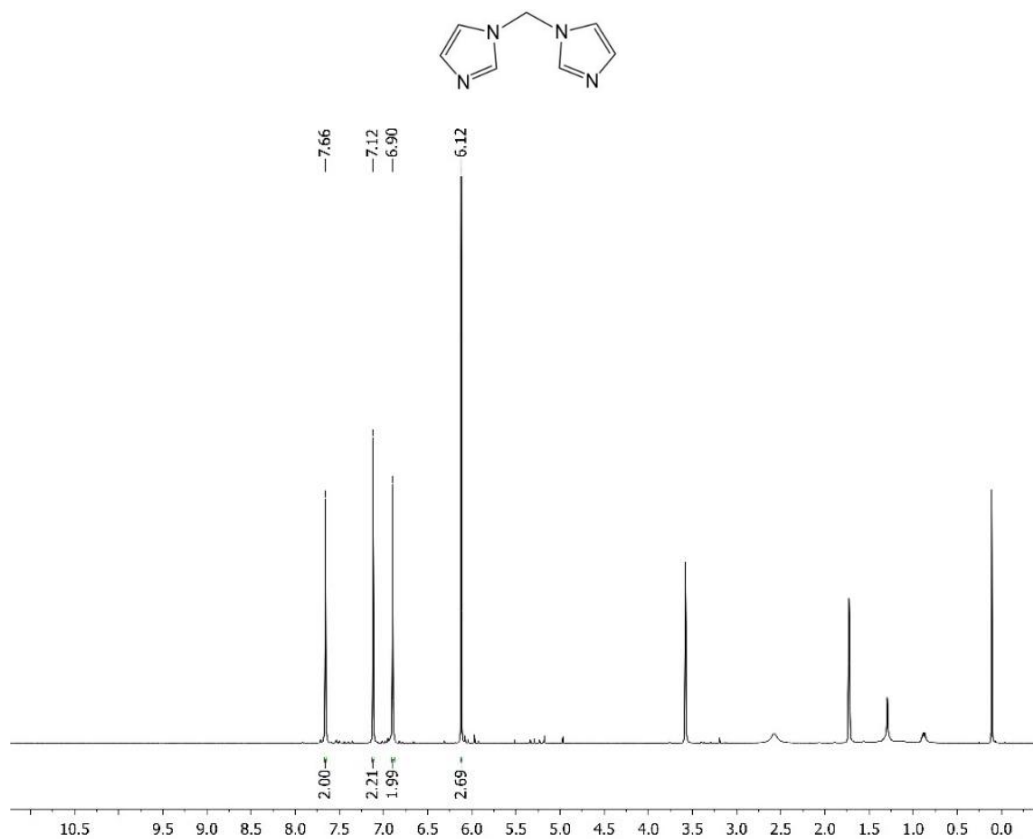
4.6. NMR Data

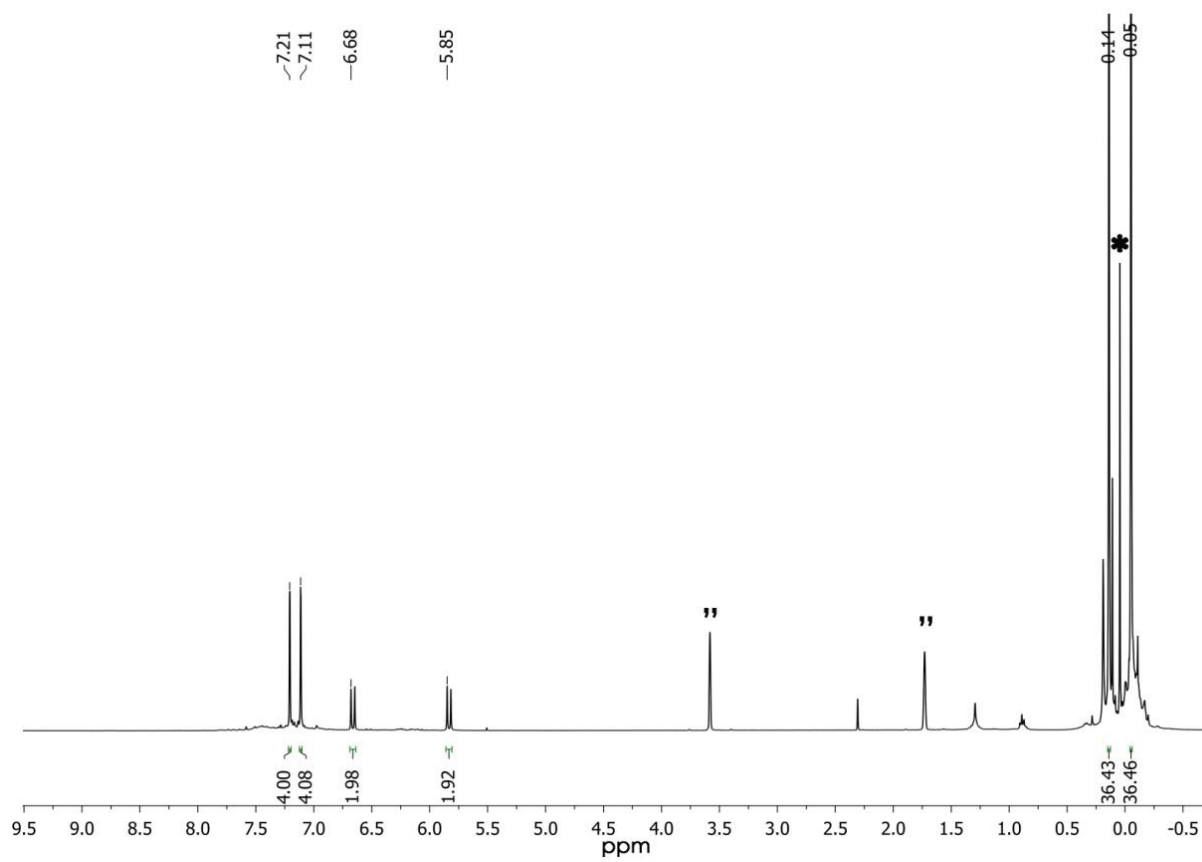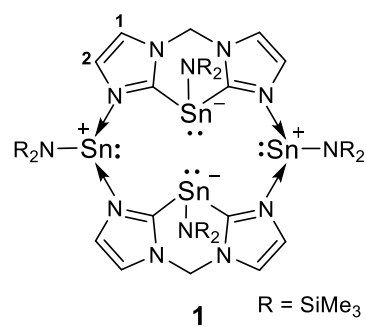Figure 4.6.1. ^{1}H NMR spectrum of bis(imidazolyl)methane in THF-d_8

Figure 4.6.2. ^{1}H NMR spectrum of **1** in THF-d_8 ("= THF-d_8, *= Bis(trimethylsilyl)amine)
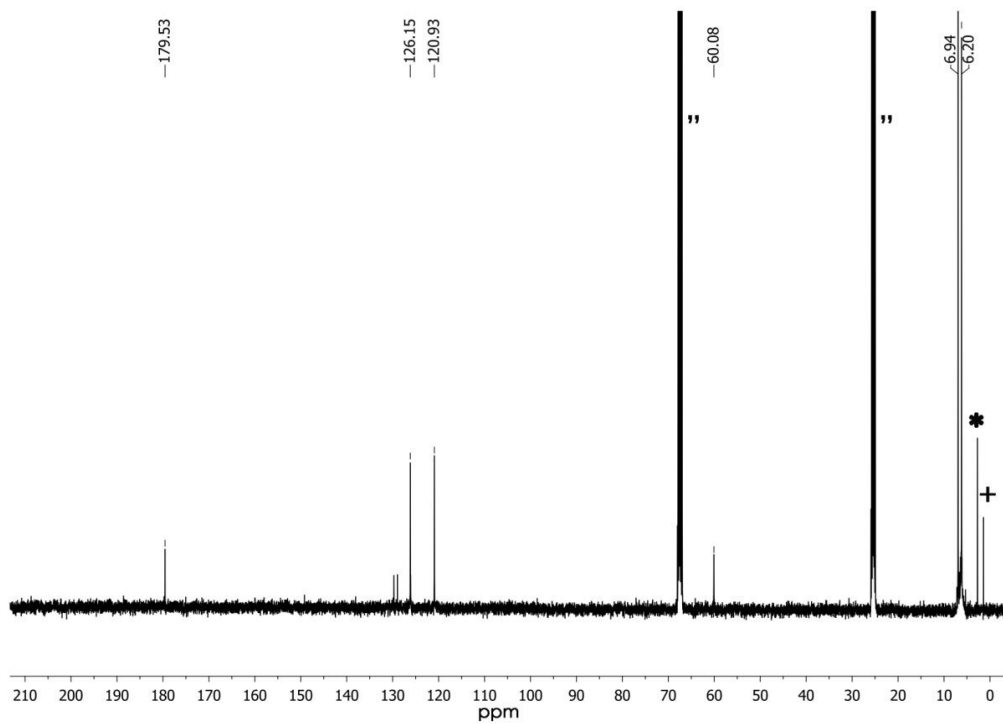
Figure 4.6.3. ^{13}C NMR spectrum of **1** in THF-d_8 ("= THF-d_8, *= Bis(trimethylsilyl)amine, +=
Tetramethylsilane)

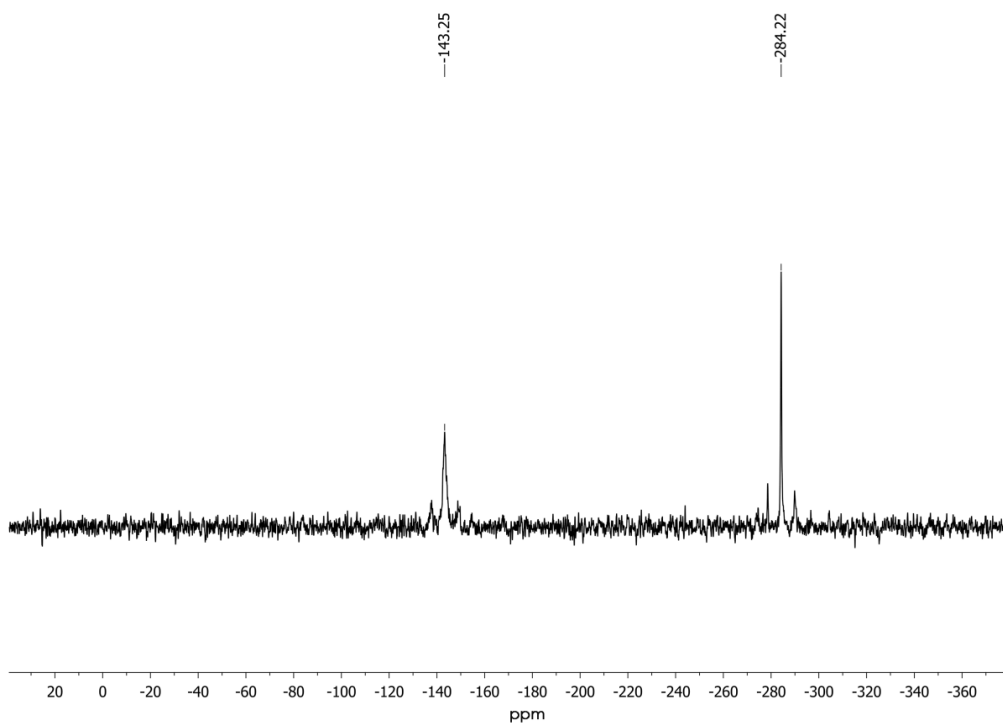Figure 4.6.4. ^{119}Sn NMR spectrum of **1** in THF-d_8
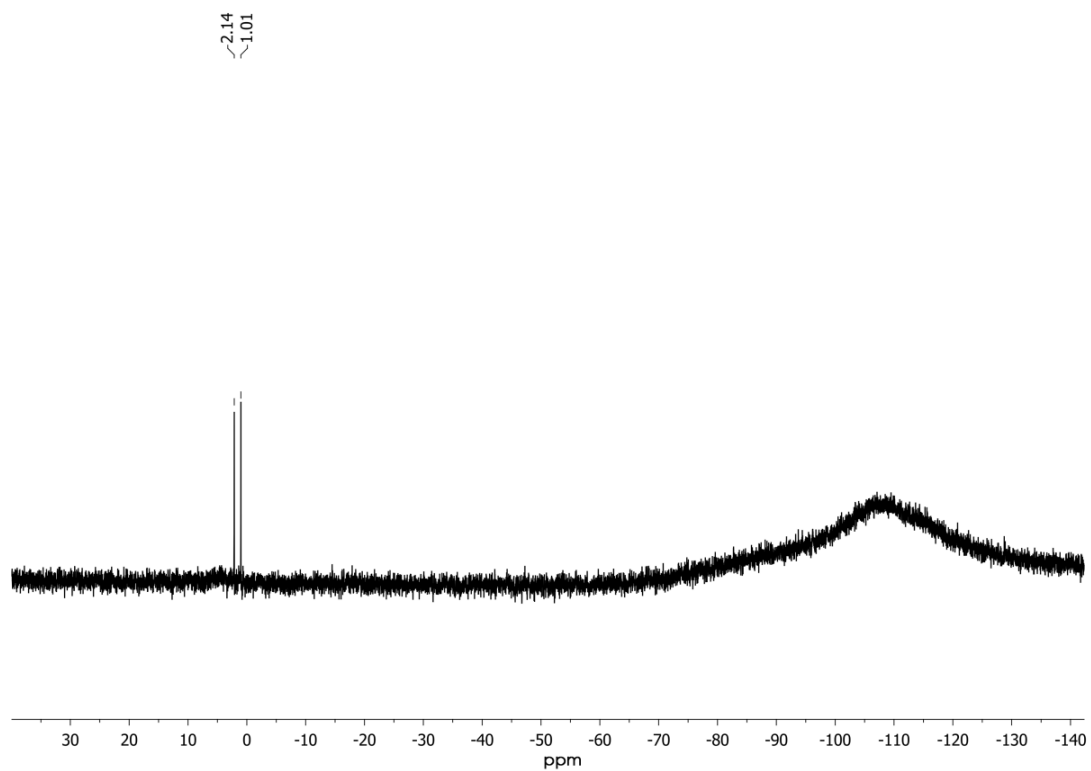
Figure 4.6.5. ^{29}Si NMR spectrum of **1** in THF-d_8
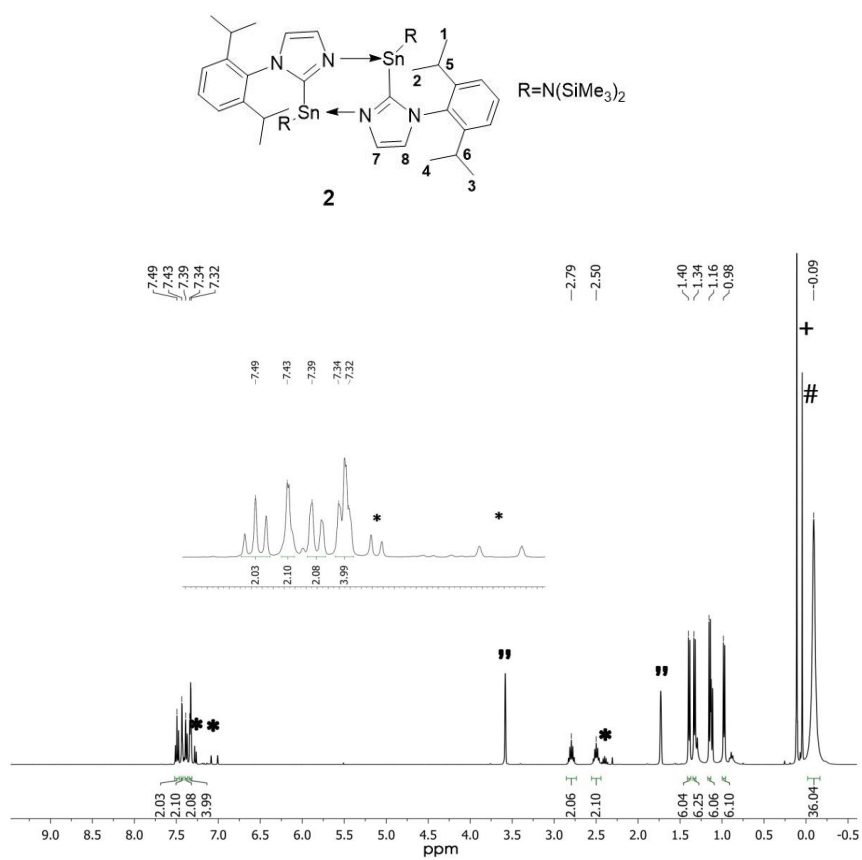

Figure 4.6.6. ^{1}H NMR spectrum of **2** in THF-d_8 ("=THF-d_8, *= N-(diisopropylphenyl)imidazole, +=

Bis(trimethylsilyl)amine, #=Tetramethylsilane)
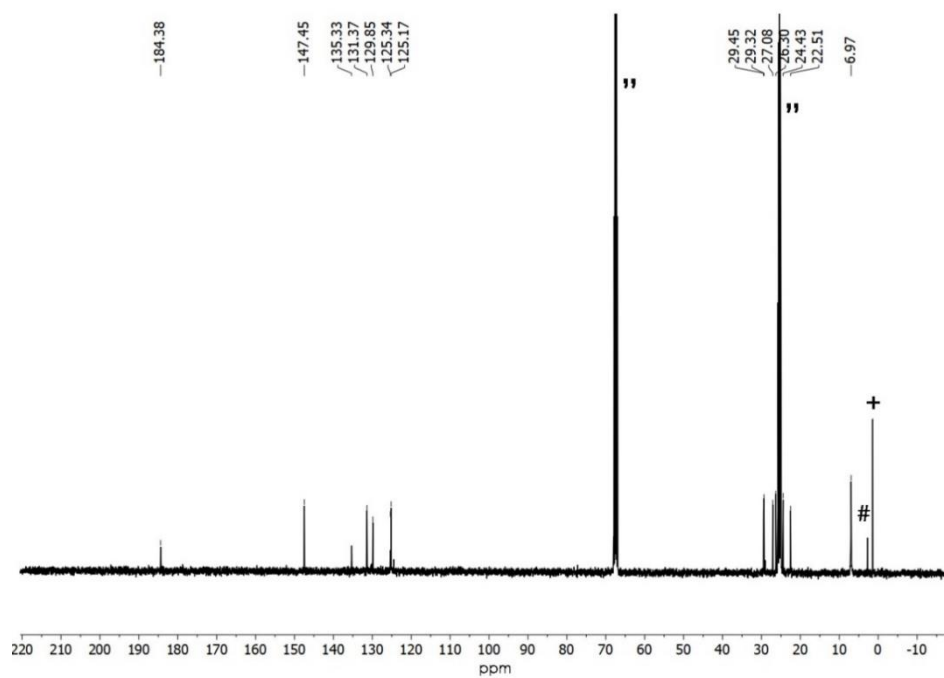

Figure 4.6.7. ^{13}C NMR spectrum of **2** in THF-d_8 ("=THF-d_8, +=Tetramethylsilane, #= Bis(trimethylsilyl)amine)
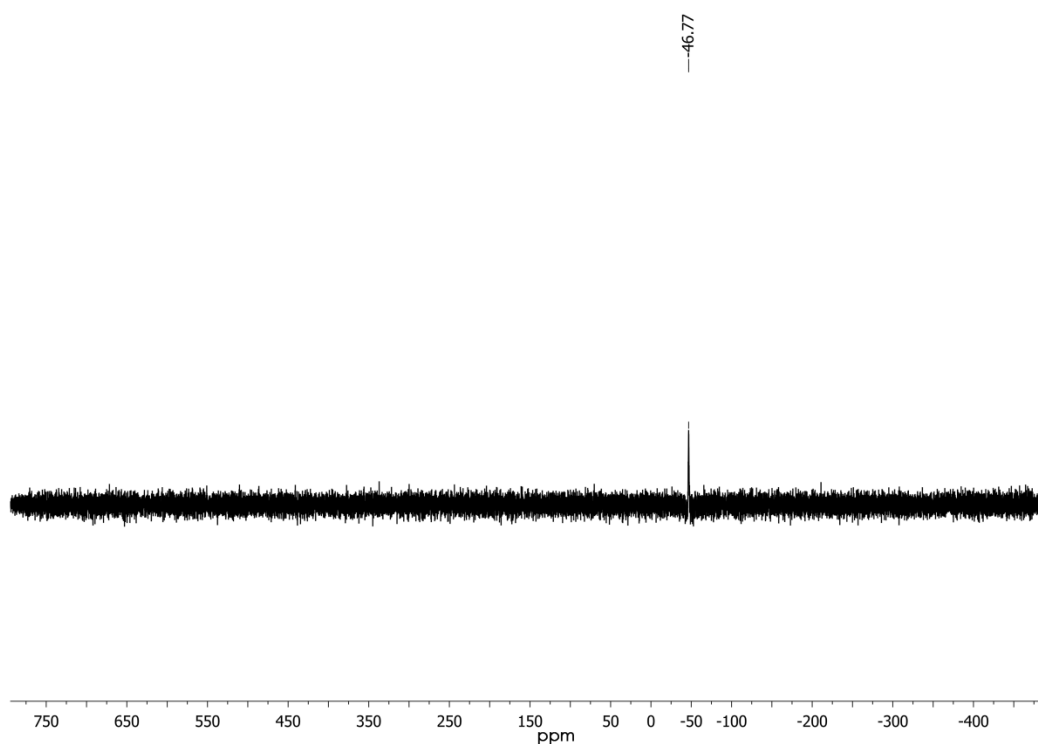

Figure 4.6.8. ^{119}Sn NMR spectrum of **2** in THF-d_8

4.7. Crystal Data

Table 4.7.1: Crystal data and structure refinement for **1**

Empirical Formula	$C_{76} H_{168} N_{24} Si_{16} Sn_8$
Formula Weight [g mol^{-1}]	2891.41
Crystal colour, shape	Colourless, thin plates
Crystal size (mm)	0.18 X 0.11 X 0.06
Crystal System	Triclinic
Space group	P-1
Formula Units	2
Temperature [K]	100(2)
Unit cell Dimensions [Å] and [°]	a=14.7687(8)
	b=15.4660(8)
	c=30.2361(17)
	α=91.181(3)
	β=102.645(3)
	γ=98.270(3)
Cell Volume [Å^3]	6659.0(6)
$\rho_{calc.}$ [g cm^{-3}]	1.442
μ (Cu K$_\alpha$)[mm^{-1}]	13.458
$\theta_{min}/\theta_{max}$ [°]	2.891-67.093
Reflections Measured	53392
Independent Reflections	23427 (R_{int}=0.1712)
Observed Reflections (I > 2σ(I))	12263
Number of parameters	1008
Number of restraints	0
R_1(I > 2σ(I))	0.0917
wR$_2$(all data)	0.2234

GooF	0.976
Largest diff. peak and hole[e Å^{-3}]	1.772/-1.884

Table 4.7.2: Crystal data and structure refinement for **2**

Empirical Formula	$C_{21}H_{37}N_3Si_2Sn$
Formula Weight [g mol^{-1}]	506.40
Crystal colour, shape	colourless, block
Crystal size (mm)	0.05 X 0.03X 0.02
Crystal System	Triclinic
Space group	P-1
Formula Units	2
Temperature [K]	100(2)
Unit cell Dimensions [Å] and [°]	a=10.579(9)
	b=11.026(9)
	c=11.823(10)
	α=84.19(2)
	β=82.09(3)
	γ=65.64(2)
Cell Volume [Å^3]	1242.9(18)
$\rho_{calc.}$ [g cm^{-3}]	1.353
μ (Mo K$_\alpha$)[mm^{-1}]	1.135
$\theta_{min}/\theta_{max}$ [°]	2.030-25.399
Reflections Measured	11756
Independent Reflections	4450 (R$_{int}$=0.0852)
Observed Reflections ((I > 2σ(I))	3248
Number of parameters	254
Number of restraints	0
R$_1$(I > 2σ(I))	0.0519
wR$_2$(all data)	0.1282
GooF	0.998
Largest diff. peak and hole [e Å^{-3}]	1.713 / -1.292

4.8. References

1. Harris, D. H.; Lappert, M. F.; *J. Chem. Soc. Chem. Commun.* **1974**, 895-896.

2. Zabula, A. V.; Hahn, F. E.; *Eur. J. Inorg. Chem.* **2008**, 5165–5179; Lappert, M.; Protchenko, A.; Power, P. P.; Seeber, A.; Weinheim: Wiley-VCH; Veith, M.; *Chem. Rev.* **1990**, *90*, 3-16.

3. Flock, J.; Suljanovic, A.; Torvisco, A.; Schoefberger, W.; Gerke, B.; Pöttengen, R.; Fischer, R.C.; Flock, M.; *Chem. Eur. J.* **2013**, *19*, 15504 – 15517; Raut, R.K.; Sahoo, P.; Chimnapure, D.; Majumdar, M.; *Dalton Trans.* **2019**, *48*, 10953-10961; Zabula, A. V.; Pape, T.; Hepp, A.; Hahn, F. E.; *Dalton Trans*. **2008**, 5886−5890; Ochai, T.; Inoue, S.; *Phosphorus, Sulfur, Silicon Relat. Elem.* **2016**, *191*, 624.

4. Mizuhata, Y.; Sasamori, T.; Tokitoh, N.; *Chem. Rev*. **2009**, *109*, 3479-3511.

5. Swamy, V. S. V. S. N.; Pal, S.; Khan, S.; Sen, S. S.; *Dalton Trans*. **2015**, *44*, 12903-12923.

6. Jutzi, P.; Kohl, F.; Krüger, C.; *Angew. Chem. Int. Ed. Engl*. **1979**, *18*, 59-60.

7. Raut, R. K.; Majumdar. M.; *J. Organomet. Chem.* **2019**, *887*, 18-23;

8. Singh, A. P.; Roesky, H. W.; Carl, E.; Stalke, D.; Demers, J. –P.; Lange, A.; *J. Am. Chem. Soc.* **2012**, *134*, 4998-5003.

9. Chai, Z. –Y.; Wang, Z. –X.; *Dalton Trans*. **2009**, 8005-8012.

10. Ochai, T.; Franz, D.; Irran, E.; Inoue, S.; *Chem. Eur. J.* **2015**, *21*, 6704-6707.

11. Paul, D.; Heins, F.; Krupski, S.; Hepp, A.; Daniliuc, C. G.; Klahr, K.; Neugebauer, J.; Glorius, F.; Hahn, F.E.; *Organometallics* **2017**, *36*, 1001-1008.

12. Wang, B.; Li, Y.; Ganguly, R.; Hirao, H.; Kinjo, R.; *Nat. Commun.* **2016**, *7***,** 11871-11881.

13. Kösterke, T.; Kösters, J.; Würthwein, E. –U.; Mück-Lichtenfeld, C.; Brinke, C. S.; Lahoz, F.; Hahn, F. E.; *Chem. Eur. J.* **2012**, *18*, 14594-14598.

14. Zabula, A.V.; Rogachev, A.Y.; West, R.; *Chem. Eur. J.* **2014**, *20*, 16652 – 16656.

15. Mitchell, T. N.; Reimann, W.; Nettelbeck, C.; *Organometallics* **1985**, *4*, 1044-1048.

16. Broeckaert, L.; Turek, J.; Olejník, R.; Růžička, A.; Biesemans, M.; Geerlings, P.; Willem, R.; Proft, F. D.; *Organometallics* **2013**, *32*, 2121-2134.

17. Katir, N.; Matioszek, D.; Ladeira, S.; Escudié, J.; Castel, A.; *Angew. Chem. Int. Ed.* **2011**, *50*, 5352-5355; Gehrhus, B.; Hitchcock, P. B.; Lappert, M. F.; *J. Chem. Soc. Dalton Trans.* **2000**, 3094-3099.

18. Zhao, H.; Li, J.; Xiao, X. –Q.; Kira, M.; Li, Z.; Müller. T.; *Chem. Eur. J.* **2018**, *24*, 5967-5973; Arp, H.; Baumgartner, J.; Marschner, C.; Müller. T.; *J. Am. Chem. Soc*. **2011**, *133*, 5632-5635; Yan, C.; Li, Z.; Xiao, X. –Q.; Wei, N.; Lu, Q.; Kira, M.; *Angew. Chem. Int. Ed*. **2016**, *55*,

14784-14787; Ochiai, T.; Franz, D.; Wu, X. –N.; Irran, E.; Inoue, S.; *Angew. Chem. Int. Ed.* **2016**, *55*, 6983-6987.

19. Kira, M.; Yauchibara, R.; Hirano, R.; Kabuto, C.; Sakurai, H.; *J. Am. Chem. Soc.* **1991**, *113*, 7785-7787.

20. Gaussian 16, Revision D.01, Frisch, M. J.; Trucks, G. W.; Schlegel, H. B.; Scuseria, G. E.; Robb, M. A.; Cheeseman, J. R.; Scalmani, G.; Barone, V.; Mennucci, B.; Petersson, G. A.; Nakatsuji, H.; Caricato, M.; Li, X.; Hratchian, H. P.; Izmaylov, A. F.; Bloino, J.; Zheng, G.; Sonnenberg, J. L.; Hada, M.; Ehara, M.; Toyota, K.; Fukuda, R.; Hasegawa, J.; Ishida, M.; Nakajima, T.; Honda, Y.; Kitao, O.; Nakai, H.; Vreven, T.; Montgomery, J. A. Jr.; Peralta, J. E.; Ogliaro, F.; Bearpark, M.; Heyd, J. J.; Brothers, E.; Kudin, K. N.; Staroverov, V. N.; Keith, T.; Kobayashi, R.; Normand, J.; Raghavachari, K.; Rendell, A.; Burant, J. C.; Iyengar, S. S.; Tomasi, J.; Cossi, M.; Rega, N.; Millam, J. M.; Klene, M.; Knox, J. E.; Cross, J. B.; Bakken, V.; Adamo, C.; Jaramillo, J.; Gomperts, R.; Stratmann, R. E.; Yazyev, O.;. Austin, A. J; Cammi, R.; Pomelli, C.; Ochterski, J. W.; Martin, R. L.; Morokuma, K.; Zakrzewski, V. G.; Voth, G. A.; Salvador, P.; Dannenberg, J. J.; Dapprich, S.; Daniels, A. D.; Farkas, O.; Foresman, J. B.; Ortiz, J. V.; Cioslowski, J.; Fox, D. J. Gaussian, Inc., Wallingford CT, 2016.

21. Wiberg, K. B. *Tetrahedron* **1968**, *24*, 1083–1096.

22. Lu, T.; Chen, F. *J. Comput. Chem.* **2012**, *33*, 580–592.

23. Haque, R.A.; Hasanudin, N.; Iqbal, M.A.; Ahmad, A.; Hashim, S.; Majid, A.A.; Ahamed, M. B. K. *J. Coord. Chem.* **2013**, *66*, 3211–3228.

24. Liu, J.; Chen, J.;Zhao, J.; Zhao, Y.; Li, L.; Zhang, H. *Synthesis*, **2003**, *17*, 2661–2666.

25. Han, J. H.; Chung, Y. J.; Park, B. K.; Kim, S.K.; Kim, H.; Kim, C.G.; Chung, T. *Chem. Mater.* **2014**, *26*, 6088-6091.